Technische Universität München
TUM School of Natural Sciences

REPPE ETHYNYLATION OF FORMALDEHYDE – CATALYST OPTIMIZATION AND STRUCTURE-ACTIVITY RELATIONSHIPS

Lingdi Kong

Vollständiger Abdruck der von der TUM School of Natural Sciences der Technischen Universität München zur Erlangung eines

Doktors der Naturwissenschaften (Dr. rer. nat.)

genehmigten Dissertation.

Vorsitz: **Prof. Dr. Lukas Hintermann**

Prüfende der Dissertation:

1. **Prof. Dr. Klaus Köhler**
2. **Hon.-Prof. Dr. Richard W. Fischer**

Die Dissertation wurde am 25.11.2024 bei der Technischen Universität München eingereicht und durch die TUM School of Natural Sciences am 10.12.2024 angenommen.

Die vorliegende Arbeit entstand im Zeitraum vom 01.04.2021 bis 31.10.2024 an der Technischen Universität München (TUM), TUM School of Natural Sciences, Department Chemie, und am Zentralinstitut für Katalyseforschung (CRC), Professur für Anorganische Chemie, Prof. Dr. Klaus Köhler.

The work was created from 01.04.2021 to 31.10.2024 at the Technical University of Munich, TUM School of Natural Sciences, Department of Chemistry, and the Central Institute for Catalysis Research (CRC), Professorship of Inorganic Chemistry, Prof. Dr. Klaus Köhler.

My special thanks go to my academic teacher

Prof. Dr. Klaus Köhler

for your excellent supervision and great interest in the success of this research work,

for your unconditional support, trust, guidance, and the freedom to perform the work

“道生一 一生二 二生三 三生萬物 萬物負陰而抱陽 沖氣以為和”

(Tao produced One; One produced Two; Two produced Three; Three produced All things. All things that carry Yin will go towards Yang and are harmonized with the moderation by Qi.)

——《道德經》Tao Te Ching (The Classic of the Tao and Its Virtue), Lao-Tzu, 6th century BC

“一陰一陽之謂道 繼之者善也 成之者性也”

(The movement of successive alternation between Yin and Yang constituted the Tao. One who follows its principles will achieve greatness. One who makes its principle will return to one’s true nature.)

——《易經》I Ching (The Classic of Changes), 9th century BC

- *Tao: the way (the rule, the principle); One: the nothingness; Two: Yin and Yang (plus and minus, active and reactive; positive and negative, Earth and Heaven); Three: Yin, Yang, and Qi (Earth, Heaven, and People).*

ACKNOWLEDGMENT

*First, I would like to express my sincere thanks to **Prof. Dr. Klaus Köhler**. I'm so proud to be part of your research team. I am deeply inspired and encouraged by your tremendous enthusiasm for scientific research, teaching and mentoring young scientists and students, and your consistently highest-standard daily hard work. You always provide me with the utmost freedom, trust, and support in academics, and always be there with your greatest encouragement, patience, and understanding. I would not have been able to accomplish my academic studies and present my work here without you. An additional thank you for the ice creams and donuts, as well as many of your jokes, fun stories, and experience sharing.*

*I would also like to thank **Clariant Produkte (Deutschland) GmbH** and **TUM MuniCat** for providing this incredible academic-industry partnership project on Reppe Chemistry and for the financial support. I am so grateful to be involved in the team, which is so supportive, cooperative, and effective, focusing on real scientific research, willing to solve real problems, and bringing the achievement into real applications. It is my pleasure to see my hard work and knowledge to be taken seriously in the industry.*

*I would like to take the opportunity to thank all my colleagues from MuniCat and Clariant at Heufeld and Shanghai. My special appreciation goes to **Prof. Dr. Richard Fischer** and **Dr. Dennis Beierlein** for your review of my reports, presentations, and dissertation, for your kind introduction and guidance, and for advice on my work and myself throughout the project. I would like to thank you for the coordination between TUM and Clariant to make everything smooth, effective, and achievable. I would also like to mention **Dr. Frank Grossman**, **Dr. Roman Bobka**, **Dr. Andreas Reitzmann** from Clariant Produkte (Deutschland) GmbH, **Dr. Yongwu Lv**, **Dr. Edmund Xu**, **Dr. Mingmin Wang**, **Dr. Shizhong Zhao** from Clariant Chemicals Technology (Shanghai) Ltd for the many fruitful discussion and valuable comments.*

*I would like to express my gratitude to my colleagues in the Prof. Köhler research group. They are **Lea Kopietz**, **Patrick Schlachta**, **Franz Bannert**, **Jinjin Tie**, **Dr. Andrea Abram**, **Dr. Max Hiller**, **Dr. Hannah Augenstein**, **Dr. Tobia Bruhm**, **Dr. Oliver Thomys**, **Dr. Patrick Bretzler**, **Dr. Florian Boch**, **Dr. Christoph Gnad**, and **Dr. Xiaoqiao Zhang**. Thanks for welcoming me to the group and introducing and guiding me in the lab, experiments, and research. I'm grateful for all your guidance and collaboration, as well as the memorable times.*

A special thanks to Lea, Patrick, Franz, Jinjin, and Andrea. You are with me for the whole time until the last step to my accomplishment. You are always so lovely, welcoming, and friendly to help me; you are always so energetic and encouraging to motivate me to work hard and live hard; and we always have wonderful times together in the lab, in the kitchen, and at Weimar, Prague, and Lyon. I feel safe, peaceful, and enjoyable when you are around.

My deep appreciation goes to Dr. Bruhm, Dr. Thomys, and Dr. Abram. Thanks for your hard work in starting the Reppe project and amazing research ideas with setting up the test unit, implementing

the experimental procedures, discovering the analytical techniques, and publishing an inspiring and high-quality work on this topic. Without your contributions, I wouldn't have completed my research work and never achieved my accomplishment.

A particular thanks goes to Franz. You provided me with the maximal support at the beginning of my research. I couldn't have started so smoothly and would have been restricted in my research without your proactive motivations. We are not only helping each other with the scientific work, but I am also thankful for our talks about culture, history, lives, and everything.

My enormous gratitude goes to Max. You guided me through the start of my research, taught me all devices, troubleshooting, data analysis and evaluation methods, and consistently gave me valuable comments and suggestions. We always had nice and meaningful talks and discussions. Your capability in the lab really encouraged me, and I really feel everything can be solved if you are around.

For the successful dissertation, TUM School of NAT, CRC, MuniCat, and Clariant are acknowledged. I would like to thank ***PD Dr. Gregor Kieslich*** *for the XRD analysis and advice for single crystal structure synthesis. I would like to thank all staff at CRC, especially* ***Dr. Eliza Gemel****, for organizing the central analytics laboratory.*

Incredible contributions come from the students. They deserve my sincere gratitude. They are ***Heide Hussain****,* ***Junbo Zhao****,* ***Wei Chen****,* ***Malte Kubisz****,* ***Tobias Weng****,* ***Bennedict Ohmann****,* ***Xi Li****,* ***Tianyu Wang****,* ***Mohammad Alsuwaidi****,* ***Jiale Zhang****,* ***Aimilios Christidis****,* ***Lion Jofan****,* ***Aijia Sun****,* ***Yilan Wang****,* ***Jihong Zhai****,* ***Yiling Xia****,* ***Wenhuang Yao****, and* ***Yujie Chen****.*

Additionally, I thank ***Ms. Renate Schuhbauer-Gerl*** *for the bureaucratic work. I thank* ***Dr. Oksana Storcheva*** *and the entire CIW Praktika team for organizing the AC lab course. I thank* ***Dr. Markus Drees****, the TUM Graduate Center_NAT, and the Dean's office for managing the doctoral programs.*

Last but most importantly, I thank my parents. We know how many hard times and good times we had; we know how difficult it is to reach this point because we experienced them together and achieved this now together. I thank you for everything.

ABSTRACT

The catalytic Reppe ethynylation of formaldehyde employs coal-based acetylene to produce the industrially valuable 1,4-butynediol. The structurally complex polynuclear and explosive cuprous acetylide, Cu_2C_2, which is formed from supported copper(II)oxide under reaction conditions, is generally accepted as the active species in this reaction of formaldehyde and acetylene. The present study bridges the gap between the stable CuO pre-catalysts and catalysis by focusing on the active species "Cu_2C_2". Numerous catalytic experiments were performed by broadly varying catalyst preparation methods, supports, copper loadings, activation conditions, formaldehyde concentrations, and promoters.

Two sets of lab-scale catalytic performance test units were built to ensure safety and effectiveness. Standard experimental procedures were implemented to solve reproducibility problems and ensure the reliability of the results. The rate-limiting and influential parameters are eliminated to maximize the catalytic performance.

$CuO\text{-}Bi_2O_3/SiO_2\text{-}(MgO)$ synthesized by co-precipitation is the most effective ethynylation catalyst found among various promoters, carriers, and synthesis techniques by evaluating their catalytic structure-activity relationships. The silica carrier well-disperses copper and provides strong metal-support interaction. Bismuth shows its crucial role in inhibiting the over-reduction of copper and stabilizing the active copper(I) phase. Magnesia may further improve the catalytic behavior by enhancing the catalyst's surface properties. The often overlooked role of aqueous formaldehyde solution is emphasized. The pH value adjusted at 7 by a sodium-hydrogen phosphate buffer is optimal to retain the long-term catalytic activity and stability and prevent it from deactivation by leaching and structural deformation. This is also a suitable condition for storing the activated catalyst to maintain its activity.

The *in situ*-formed cuprous acetylide (Cu_2C_2) is found to be the catalytically active phase in ethynylation. This work studied Cu_2C_2 species, including the pure phase, which are synthesized via multiple pathways despite their highly explosive nature. The pure-phase Cu_2C_2 characteristic properties are identified by XRD diffractograms and Raman spectra. It is also differentiated from its derivatives like CuC_2 and $Cu\text{-}(C_2)_n\text{-}Cu$ and other impurities by optimizing the synthesis, post-treatment, and analytical conditions. The Cu_2C_2 is also quantitatively evaluated. Its actual composition and structure are predicted by analyzing the Cu-to-C-to-H ratios, determined by TGA/DSC-MS and CHN analysis techniques. Lastly, the explosion conditions of copper acetylides are assessed for safe handling and operation. It should limit its growth into large crystallite and avoid direct contact with strong oxidizing agents, ignition sources, and intense energy.

LIST OF ABBREVIATIONS

Chemicals	
ACN	*Acetonitrile*
BYD / BED / BDO	*1,4-Butynediol / 1,4-Butenediol/ 1,4-Butanediol*
FA / pFA	*Formaldehyde / Paraformaldehyde*
PA	*Propargyl alcohol*
PDO	*1,3-Propanediol*
Analytical and Synthesis Techniques	
AAS	*Atomic Absorption Spectroscopy*
AE	*Ammonia evaporation*
BET / BJH	*Brunauer-Emmett-Teller / Barrett-Joyner-Hallenda*
CHN(S)(O)	*Carbon-Hydrogen-Nitrogen-(Sulfur)-(Oxygen)*
CP	*Co-precipitation*
DFT	*Density Functional Theory*
DP-A	*Deposition-precipitation in ammonia (via ligand removal)*
DP-PP	*Direct-precipitation of pure-phase*
DP-U	*Deposition-precipitation in urea (via hydrolysis)*
EPC	*Electronic Pneumatics Control*
GC/GLC	*Gas (Liquid) Chromatography*
ICP-OES	*Inductively Coupled Plasma-Optical Emission Spectroscopy*
IR	*Infrared Spectroscopy*
IWI	*Incipient wetness impregnation*
MS	*Mass Spectrometry*
NMR	*Nuclear Magnetic Resonance*
PXRD	*Powder X-ray Diffraction*
TCD / FID	*Thermal Conductivity Detector / Flame Ionization Detector*
TGA-DSC	*Thermogravimetric Analysis-Differential Scanning Calorimetry*
TPR	*Temperature-Programmed Reduction*
Abbreviations	
a.u.	*Arbitrary Unit*
ICDD	*International Centre for Diffraction Data*
IS	*Internal Standard*
m/z	*Mass-to-charge ratio*
p/p_0	*Equilibrium pressure over saturation pressure*
P&ID	*Pipe and Instrumentation Diagram*
rpm	*Revolutions per minute*
S	*Selectivity*
S_{BET}	*BET Surface Area (m^2/g)*
t_R	*Retention time*
TOF	*Turnover frequency*
V_P	*Pore volume*
wt.% / v/v.%	*Weight Percentage / Volume Percentage*
X	*Conversion*
Y	*Yield*
θ	*Diffraction angle (Bragg angle)*
λ	*Wavelength*

TABLE OF CONTENTS

1

INTRODUCTION AND MOTIVATIONS

1.1 Introduction and Theory

1.1.1 History and Development of Acetylene

Acetylene and Its Discovery and History

Gas phase chemistry appeared in the 17th century when J.B. Van Helmont discovered different gaseous products from air, and Stephen Hales invented a pneumatic trough to isolate the pure gases [1-3]. A subclass of gaseous molecules is hydrocarbons, which consist only of hydrogens and carbons, namely alkanes, alkenes, and alkynes. The focus of the current work, acetylene (formula: C_2H_2, IUPAC nomenclature: ethyne), is the simplest alkyne and the third-found hydrocarbon [1, 3-4].

Acetylene was first reported by a British Scientist, Edmund Davy, in 1836 [5]. A further study was done by a French Scientist, Marcelin Berthelot, in 1860 [6]. Since the large-scale production of calcium carbide was developed by a Canadian scientist, Thomas Willson, in 1892 [7], the detailed investigation of acetylene chemistry and its applications became possible.

The colorless and odorless acetylene gas was synthesized accidentally by Davy in an experiment to produce potassium, who burnt potassium bitartrate ($KC_4H_5O_6$) and charcoal in an iron container [3-4]. A soft, dark substance is obtained, which has been identified as potassium carbide (K_2C_2). A vigorous reaction occurred when the substance was in contact with water and released an inflammable carbonaceous gas. The gas was named *bi-carburet of hydrogen*, with a formula 2C+H①. Davy reported its inflammable and explosive nature, which produces a bright flame and deposits carbon [3, 6, 8-10].

Berthelot rediscovered the gas without knowing Davy's work in 1860, who identified it as *hydrogen tetra carbide* with a formula C_4H_2 ① and named it *acétylène* [3, 5]. He initially synthesized the acetylene by introducing the organic gases through a hot tube. He later invented a device called Marcelin's d'œufélectrique (electric egg) in 1862 and developed an electric-arc method. The device allowed hydrogen feeding and electric discharge between two purified carbon rods, where half of the carbon rod was converted into acetylene, and the other half was dispersed into dust. The mixture of acetylene was trapped in an aqueous ammoniacal cuprous chloride solution as reddish copper acetylide precipitates. The precipitates were treated with hydrochloric acid to release the acetylene gas and then purified with potash. Berthelot successfully increased the acetylene production to 10-12 ml/min [3, 5, 9-13]. However, this is not enough for large-scale production.

① Before the 1860s, it was commonly known that the molecular mass of carbon was 6 rather than 12. Thus, the number of carbons doubled in the formulas proposed by Davy and Berthelot. This was finally corrected when the molecular formula system was developed over the century.

In 1892, Willson accidentally discovered a process to produce calcium carbide and acetylene in a commercial quantity. Willson initially planned to produce metallic calcium via the electrothermal reduction of lime and coal in a modified electric-arc furnace, which operates at higher temperatures, electric current, and voltage. However, the products ended up with heavy, brittle, and dark solids, which were later found to be calcium carbide. When the solid was discarded and in contact with water, extensive gas was released and was identified as acetylene. Willson soon patented his finding and sold it to several manufacturers [3, 14-17]. This allowed the rapid development of acetylene chemistry②.

Acetylene and Its Commercial Production

The thermodynamic studies of acetylene, the carbon-containing (coal, coke, soot, hydrocarbon gases, and petroleum) and calcium-containing (calcium oxide, calcium hydroxide, calcium carbide, and metallic calcium) feedstocks, intermediates, and by-products made the most significant contributions in the process design and development of the commercial-scale acetylene production [10, 16-22].

Initiated by Berthelot's and Willson's inventions, techniques with higher environmental, energy, cost, and safety efficiency have been developed over the years. The primary commercial acetylene production techniques are combustion cracking of hydrocarbons, partial oxidation of methane, electric-arc pyrolysis, and hydrolysis of calcium carbide.

The partial oxidation process was invented by Sachsse and Bartholomé from BASF in the 1950s [23-24]. The cracked gas stream heated up to 1600 °C and provided sufficient energy to oxidize methane into acetylene. The gas stream must be cooled down immediately by water or oil quenching to prevent thermodynamically favorable acetylene decomposition and to remove soot in the reaction chamber [10, 25]. The similar Montecatini process and Société Belge de l'Azote process were developed. Some features, such as the burning chamber, gas separator, quenching methods, and soot removal techniques, were modified [10, 25].

Compared to the combustion and oxidation methods, the electrothermic methods introduced electrical energy directly into the system, which showed higher production efficiency. Hüls, plasma, and coal electric-arc processes, invented by Hoechst and Chemische Werke Hüls AG, produced acetylene from gasified, liquid, and solid hydrocarbons, respectively. The processes operated at low pressures but made the high conversion of acetylene with high purity [10, 26].

② When Davy discovered acetylene in 1836, it was initially used as a cheap source for artificial gaslight due to its illumination ability. In 1903, French engineers Edmond Fouché and Charles Picard developed the oxyacetylene as an oxy-fuel, which can be burnt to 3500 °C. The oxyacetylene was then used in welding and cutting. The purified acetylene gas was also found to be effective as an inhalation anesthetic in medical field, reported by William S. Sykes in 1930.

The chemical reactions and parameters of some processes are shown in Scheme 1-1.

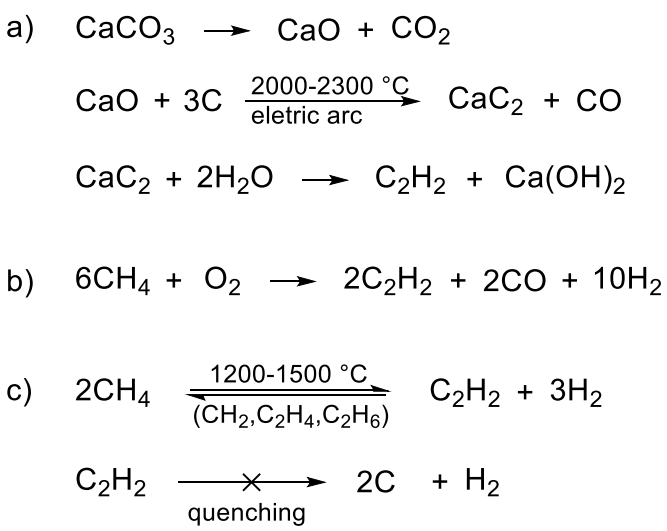

Scheme 1-1. The reaction mechanisms and parameters for three typical industrial acetylene production pathways since the 1910s [10, 17, 27-28]. (a). Limestone is calcined to decompose into lime and carbon dioxide, followed by electric-arc pyrolysis of lime with a carbon source (coke, tar, charcoal, etc.) to produce calcium carbide, the acetylene is produced by calcium carbide hydrolysis (b). Partial oxidation of methane to produce acetylene, carbon monoxide, and hydrogen; and (c). Thermal cracking (pyrolysis) of methane at 1200-1500 °C via bond breaking–forming mechanism with a catalyst, followed by immediate quenching to prevent thermodynamically favorable acetylene decomposition③. Hydrogen is added as a fuel to maintain the temperature and shift the equilibrium.

Acetylene Chemistry and Its Development

Many scientists made outstanding contributions to the development of acetylene chemistry [2-3, 10, 17, 29-31]. Berthelot started the investigation of polymeric acetylenes in 1866 [12, 16, 32]. With Berthelot's theory, solid acetylene and polyethylene were successfully prepared by Von Pechmann in 1898 [33]. In 1907, D. Mclntosh reported the physical properties of liquid and solid acetylenes [27]. E.R. Weaver developed acetylene's purification and colorimetric determination techniques in organic solvents in 1916 [34]. More details on the solubility and thermal properties of acetylene in organic solvents were patented by N.D. Scott and C. Roberts, from du Pont, in 1939 [35].

A tremendous achievement in acetylene chemistry was made in the early 20th century.

③ Acetylene production is highly endothermic; a tremendous amount of energy, either from heat or electricity, is required. Acetylene is thermodynamically stable compared to hydrocarbon gases at above 1230 °C; it is thermodynamically unstable and decomposed into carbon and hydrogen at room temperature, with slight pressure, and at above 3100 °C. The thermal cracking of natural gases may form carbon monoxide, hydrogen, carbon, and water vapor as intermediate or by-products.

Alexei E. Favorskii, from Russia, is considered the founder of acetylene chemistry, who made an outstanding contribution to the organic synthesis of acetylene and its derivatives. Favorskii invented vinylation, acetylene-allene isomerization, and acetylene zipper reaction. The famous *Favorskii rearrangement* involving acetylene is still widely applied as a powerful synthetic tool to produce a wide range of organic compounds [36-37].

Julius Nieuwland, from the United States, was the dominant scientist in this field since his Ph.D. thesis, *Some Reactions of Acetylene* [38], in 1904. Nieuwland and Richard Vogt published their book, *The Chemistry of Acetylene* [9], in 1945, which provided a great collection of insights into acetylene, from its production and industrial synthesis to its chemical properties, derivatives, and future applications.

Another dominant scientist, Walter Reppe, from Germany, published a book, *Neue Entwicklungen auf dem Gebiete der Chemie des Acetylens und Kohlenoxyds* (*New developments in the chemistry of acetylene and carbon oxide*), in 1949 [39]. Reppe and co-workers, who worked on acetylene at BASF since 1928, developed a series of crucial chemical processes using acetylene as the feedstocks to produce essential chemicals, which created an immense impact globally in the 1940s and 1950s [16, 25, 29, 40-43].

Following excellent scientific research, evaluations on the commercial purpose of acetylene chemistry were carried out in the 1940s. Extensive studies related to acetylene have been published and patented, led by giant chemical corporations, such as du Pont, GAF, Linde, and BASF [7, 10, 16, 25, 39]. Acetylene-related production in the chemical industry reached its peak in the 1960s and declined due to the domination of cheaper and safer petroleum- and gas-derived feedstocks④ [10, 17, 29, 43-44]. However, acetylene chemistry still showed its potential in a competitive role.

During that time, studies on the physical, chemical, thermal, and structural properties of acetylene and its derivatives were one of the hottest topics. The preparation of acetylene and metal acetylides using different techniques was discussed extensively. B. Dana [45] was among the first to report systematic preparation methods of metal acetylides and their properties in 1917. From the 1940s to the 1960s, Brameld *et al.* [46] and Nosetani *et al.* [47] reported the synthesis techniques of copper acetylides with aqueous copper(II) solution under an acetylene atmosphere, while Castro *et al.* [48] reported the reactions and the mechanisms of copper acetylides and their derivatives. Rutledge [49-50] investigated the properties and reactions of sodium acetylides. Other metal acetylides and polyacetylenes, such as lithium, potassium, mercury, silver, and gold acetylides, were also studied [10, 51-52].

④ The annual worldwide acetylene production reached a peak of 10 million metric tons in the 1960s. It dropped to half in the 1990s and continued to decline to several hundred thousand metric tons in the 2010s. It only increased in the recent decade due to the fluctuating petroleum price.

Glaser-Eglinton-Hay plays a significant role in acetylene-related organic synthesis for valuable chemicals in the industry [20]. Motivated by Carl Glaser [53], who invented the oxidative homo-coupling of terminal alkynes with the copper acetylide-based catalyst in 1869, Eglinton [54] and Hay [55] continued the investigation of the coupling reaction of acetylenes in the 1960s.

Catalytic processes involving acetylene and metal acetylides were another focus topic. Mainly developed by Reppe [39-40], vinylation, ethynylation, carbonylation, and cyclization reactions involving acetylene played an essential role in the 1950s. The details of *Reppe Chemistry* will be discussed in Chapter 1.1.2.

Safety Concerns of Acetylene and Its Derivatives

With deeper evaluations and commercial-scale productions, the safety inspection of the dangerous acetylene, its derivative species, and reaction processes has gained attention.

Since its discovery, Acetylene has been known as highly inflammable and explosive [6]. Davy and Berthelot both reported its explosion when mixed with oxygen and chlorine [5-6]. Davy also invented a method to keep the gas safe without decomposition under mercury for the long term [6, 8]. Tedeschi warned that the explosion of acetylene could happen at any time due to any minor mistake [17-18]. Detailed investigations of the thermal properties of acetylene were done by McIntosh, who evaluated the specific heat of acetylene in all phases and during the transaction states and explained the explosive nature of acetylene [27]. Nieuwland and Vogt agreed with McIntosh and discussed the highly endothermic character of acetylene [9].

During the *Symposium on Chemical Process Hazards* in 1960, Miller and Penny reported the hazards of handling acetylene in chemical processes [56]. Their research and experiments reported a wide range of the explosion limits of acetylene and metal acetylides under various temperatures and pressures. Several hazards were mentioned, such as internal and external flammation, sources of initiation of explosive acetylene decomposition, deflagration, detonation, etc. [56]. The relevant data and information can also be found from Gay *et al*., who experimentally determined the thermal decomposition of acetylene in shock waves [57], and Carver *et al.*, who reported the parameters and conditions of the explosion decomposition of acetylene in pipelines [58].

Hanford and Fuller, from GAF Corporation, emphasized the characteristic explosion of acetylene via the exclusive lab-scale explosion test in 1948. They suggested a safety factor of eight, by calculation, with respect to the pressure, temperature, and concentration of acetylene in the pipeline and vessel operations [29]. Chiddix reported the relationship between the pre-detonation distance of the pipeline and the pressure ratio of the acetylene. He concluded that the decomposition of acetylene may raise the temperature from 18 °C to 3000 °C with a 12-

folded pressure increase, and the denotation of acetylene may raise the pressure by 200 times the initial pressure [59-60].

The most significant contributions in developing the safety procedures to work with acetylene were made by Reppe and his co-workers from I.G. Farbenindustrie AG and BASF [10, 29-30, 39, 60-61]. By studying the deflagration and detonation properties, Reppe successfully developed methods to handle acetylene at high temperatures and pressures up to 200 °C and 20 bar, which wasn't possible at above 1.4 bar in the past [25, 29, 38-39]. Reppe suggested diluting acetylene in inert gases and adsorbing acetylene in organic solvents during the operations to avoid its decomposition and explosion⑤ [20-21, 44, 59, 62-64]. These inventions allowed Reppe to develop a series of organic syntheses and industrial processes involving acetylene [29-30, 39].

Economic and Environmental Concerns

Due to fluctuating petroleum prices and existing environmental issues, acetylene-based chemistry has gained industrial interest as a potential alternative chemical feedstock.

Chemical production via coal-based acetylene pathways, in comparison to environmentally friendly biomass and energy-efficient petroleum, has had no technical barrier since its leap-forward industrial development in the 1940s. Their industrial applications rely more on the economic, environmental, and geopolitical aspects, which differ country by country, such as the availability of raw materials, safety regulations on manufacturing, shipping, and storage, and the cost of energy and workforce [16, 22, 65].

The production of acetylene, as mentioned above, requires a tremendous amount of heat due to the high energy consumption by its triple bond, which makes the production much more expensive. The hydrocarbon by-products of acetylene, mostly ethylene, are sometimes valuable, but the purification and recovery processes can also be complex and costly, thus undesirable. In addition, the shipment of acetylene, either by pipeline or high-pressure containers, is comparably dangerous and expensive [10, 17, 22].

For example, countries like South Africa and China have rich coal reserves, limited petroleum, and relatively cheap electricity costs that favor acetylene production. China is the largest acetylene market and contributes roughly 80% of the manufacturing of vinyl chloride, butynediol, and acetylene-derived chemicals [17, 66].

⑤ The explosion limit of acetylene on ignition is between 2.5 vol.% and 82 vol.% in the acetylene-air mixture and extended to 93 vol.% in the acetylene-oxygen mixture. The pressure increase during deflagration and decomposition into carbon and hydrogen is up to 50-fold.

1.1.2 Reppe Chemistry

Walter Reppe and Reppe Chemistry

Since Davy discovered the acetylene and Willson allowed commercial-scale production, it wasn't possible to operate the thermodynamically unstable and highly explosive acetylene at a pressure above 1.4 bar [10, 25]. This limits the versatility of acetylene in organic synthesis and its commercial values in commodity applications.

The chemistry of acetylene is known as Reppe Chemistry in recognition of the German scientist Walter Julius Reppe's (1892 – 1969) remarkable achievement in developing the pressured acetylene reaction processes. Reppe joined BASF in 1921; he has focused on safely handling acetylene since 1928 and has successfully invented acetylene storage and transportation techniques. To restrict the explosion of acetylene due to its wide range of flammability limits and extremely low minimum ignition energy, Reppe and co-workers suggested diluting the acetylene with inert gases such as nitrogen, argon, or carbon dioxide. They also suggested filling the pipes, storage containers, or reaction vessels with packing materials [17, 19, 39, 67].

The most renowned technique is to achieve an acetylene pressure of up to 50 bar by dissolving acetylene in acetone and pressurizing it in steel tanks filled with monolithic porous mass, such as asbestos. This is because the acetylene solubility at 15 °C is raised from 25 mL of acetylene per mL acetone at ambient conditions to 300 mL/mL at 12 bar (1.2MPa) [9, 17, 39, 44, 68]. This allows the development of acetylene chemistry and the invention of the typical Reppe processes employing acetylene as a feedstock. Reppe was issued 97 US patents, mostly related to acetylene, found in the United States Patent and Trademark Office [10, 25, 69].

The acetylene handling specifications and techniques, initially developed by Reppe and co-workers, regulated by *Technische Regeln für Acetylenanlagen and Calciumcarbidlager (TRAC)* [70] and *Bundesanstalt für Materialforschung und -prüfung (BAM)* [71] of Germany and still applied up to today.

Typical Reppe Processes and Industry Applications

A wide range of industrial processes using coal-based acetylene as the feedstock was developed and applied in the 1940s, benefiting from acetylene's high reactivity and versatility, which mainly involves overall thermodynamically favored reactions and fewer processing steps. However, they have been replaced by petroleum-based chemical processes since the 1960s because of higher energy, cost efficiency, and safety reasons. Only a few typical Reppe processes, namely vinylation, carbonylation, cyclic polymerization, and ethynylation, as shown in Scheme 1-2, are still actively applied in the market, mainly in countries with rich coal resources and low energy costs, such as China and South Africa [10, 18, 22, 25, 39, 44, 60].

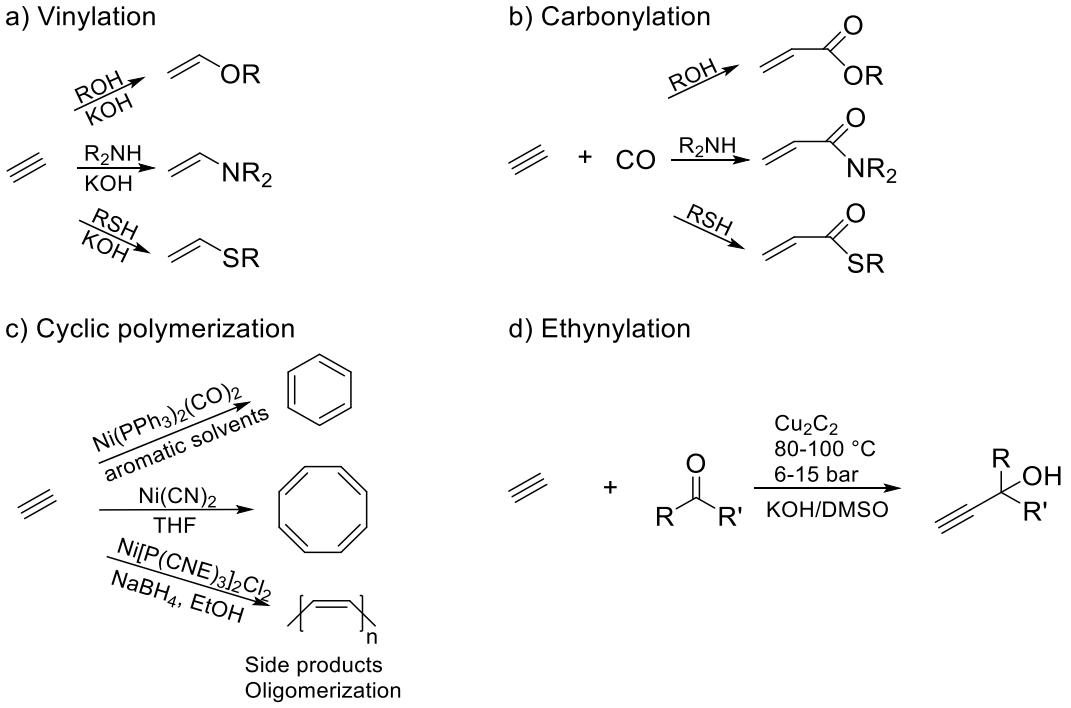

Scheme 1-2. The well-established reactions in the literature and industrial processes use acetylene as the starting material. Four of the typical Reppe processes include: a). vinylation, b). carbonylation, c). cyclic polymerization, and d). ethynylation.

The typical industrial Reppe processes invented in the 1940s are elaborated:

Vinylation is the nucleophilic addition of O-, S-, N-, (C-)containing compounds with a slightly acidic hydrogen atom, such as alcohols, thiols, and amines, to the vinyl group (CH_2=CH-) from the acetylene to produce monomer acetaldehyde, vinyl chloride, vinyl acetate, vinyl ethers, and esters; and subsequently to their corresponding value-added polymers [42, 44, 60].

Carbonylation is the reaction of acetylene with carbon monoxide, catalyzed by metal (e.g., Ni) carbonyls. Acetylene carbonylation is only performed in the liquid phase, such as in water, alcohol, and amines, where the corresponding esters and amides will be formed. The most interesting product is acrylic monomers and their derivatives [17, 44, 72].

Cyclic polymerization of acetylene yields a wide variation of products such as cyclic $C_{6\text{-}12}H_{6\text{-}12}$ (e.g., benzene, styrene, pyridine, cyclooctatetraene) and linear cuprene, which is mainly dependent on the catalysts synthesis conditions [73].

Ethynylation is the addition of alkynes to the carbonyls (aldehydes, ketones) to produce alkynols and diols under slight acetylene pressure [40-41, 74]. Ethynylation of formaldehyde to produce industrially valuable propargyl alcohol and 1,4-butynediol selectively with a copper-acetylide-based catalyst has gained increasing industrial attention recently. It is the focus of this research and will be discussed in detail.

1.1.3 Catalytic Ethynylation of Formaldehyde

The copper-catalyzed 3-phase Reppe ethynylation of formaldehyde in an aqueous medium selectively produces the intermediate product, propargyl alcohol (PA), and the desired product, 1,4-butynediol (BYD), under the slightly over-pressured acetylene atmosphere [40-41, 74]. The reaction scheme and parameters of the ethynylation are shown in Scheme 1-3.

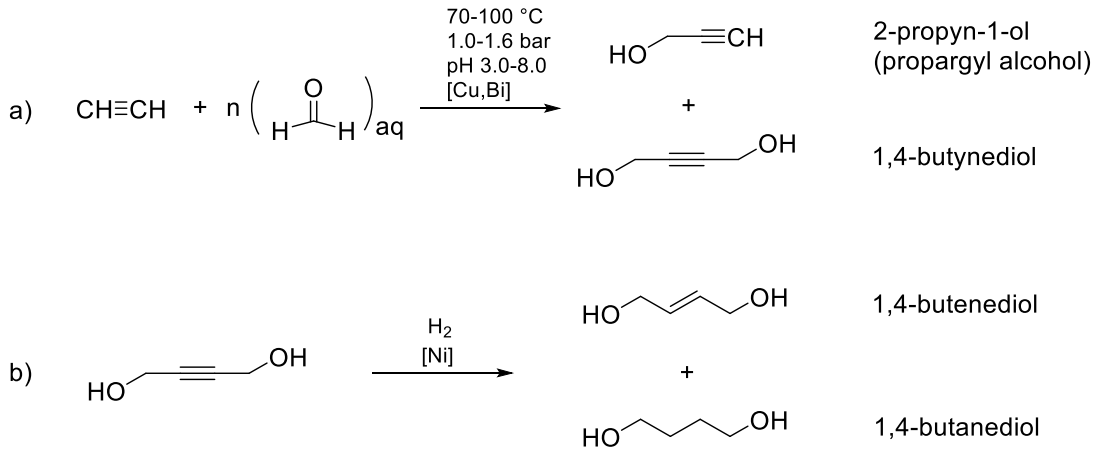

Scheme 1-3. The reaction of a). catalytic ethynylation of formaldehyde to propargyl alcohol (intermediate product) and 1,4-butynediol (desired final product), b) hydrogenation of the 1,4-butynediol into 1,4-butenediol and 1,4-butanediol, and applicable reaction parameters.

Propargyl Alcohol and 1,4-Butynediol

Since Reppe *et al.* [74] patented the *Production of Alkinols* in 1942, the process development, catalyst design, and industrial applications via Reppe ethynylation were well established in the 1940s to 1960s. The versatile products, PA and BYD, show high commercial values and increasing demands in many industrial processes. This is because their excellent chemical properties contributed from the electron-rich alkynyl group (-C≡C-) and the polar hydroxyl group (-OH). PA is an essential bioactive building block in organic synthesis. BYD is the intermediate that can be hydrogenated with a nickel catalyst to produce 1,4-butenediol (BED) and 1,4-butanediol (BDO) [75-79]. They serve as C-4 feedstock to synthesize value-added and biodegradable polymers, solvents, and chemicals, such as tetrahydrofuran (THF), γ-butyrolactone (GBL), and polybutylene succinate (PBS). PA, BYD, and their downstream products are widely used as corrosion inhibitors and cleansing agents and are applied in agrochemicals, pharmaceuticals, electronics, automotive, and textile industries [80-81]. The catalytic Reppe ethynylation process has recently regained recognition as an economical and energy-efficient pathway to produce large-scale PA and BYD [66, 82-83].

The selectivity of PA and BYD is process- and parameter-dependent. Following Reppe *et al.* [74], Suzuki extensively studied and reported the reaction kinetics and the optimal conditions to synthesize BYD and PA in 1954 [84-85]. He concluded that the continuous process might produce a high yield of BYD at 120 °C and 1 bar using a concentrated formaldehyde solution of pH 5 or higher [84]. PA, as the reaction intermediate, due to its reactivity and equilibrium, cannot be synthesized under this condition. Suzuki introduced tetrahydrofuran (THF) as the solvent (2-fold in the volume of aqueous formaldehyde) to produce a 30% space-time yield of PA. He further employed a static method to increase the yield to 50%, in which he suggested using a temperature below 100 °C, the highest possible pressure, and the lowest possible pH value that is safe to operate and would not damage the device or the catalyst [85]. Companies like du Pont de Nemours, GAF Corporation, and Allied Chemical Corporation recognized Suzuki's research. Their scientists, Shull [86], Graham *et al.* [87], Chidix *et al.* [88], Zak [89], Reiss *et al.* [90], W. Moore *et al.* [91], and G. Moore [92] patented the modified processes, devices, parameters, and post-treatments on BYD and PA synthesis in the 1960s. With the pioneers' contributions, this work continues to optimize the specific ethynylation processes and parameters to produce a high BYD yield and selectivity.

Aqueous Formaldehyde Solution

Formaldehyde (HCHO) is the simplest aldehyde and the most abundant carbonyl compound in the atmosphere. The formaldehyde in an aqueous solution is mainly applied as a preservative and fixative in pathology. It is also widely studied in atmospheric chemistry and as an essential C-1 building block in organic synthesis processes [93-96]. Formaldehyde saturated at 37 wt.% in water and stabilized with 8-15 wt.% methanol is known as formalin⑥. It is commercially available in different concentrations, additives, and pH values [93, 97-98]. The aqueous formaldehyde is highly reactive as an electrophilic species, making it challenging in analysis studies, especially quantitatively [99]. Some relevant reaction equilibria, which are affected mainly by the concentration of the monomeric formaldehyde, are shown in Scheme 1-4 [98, 100-101].

⑥ The commercial formalin solution, according to the product's MSDS and specifications, generally exists as soluble low polymer formaldehyde molecules with 2 to 8 units. Aqueous formaldehyde tends to polymerize at concentrations higher than 30 wt.%. Methanol between 10-15 wt% is commercially added as a stabilizer in aqueous formaldehyde solution, which generates hemiacetal (methylene hydrate, $HO\text{-}CH_2\text{-}OH$) that prevents formaldehyde polymerization. A buffer species, ranging from phosphate, acetate, citrate, and carbonate, are added to adjust and maintain the desired pH values of the formaldehyde solution.

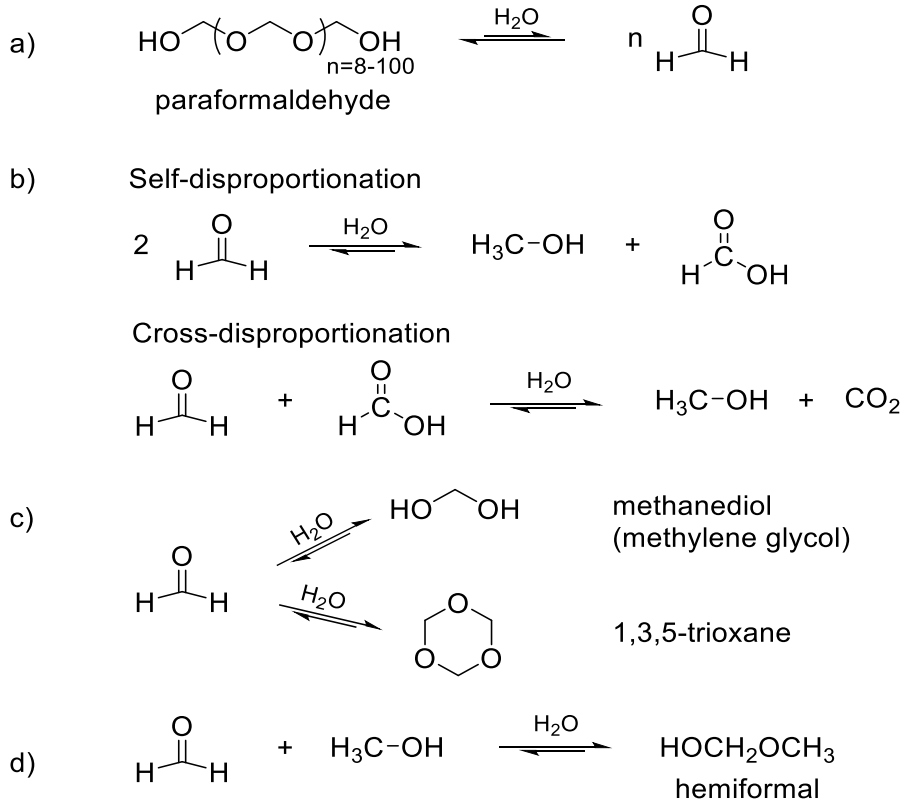

Scheme 1-4. The typical reactions involve formaldehyde in an aqueous solution and their reaction equilibria: a). equilibrium of dissolution of paraformaldehyde and polymerization of aqueous formaldehyde; b). self-disproportionation of formaldehyde in water to methanol and formic acid, and continued cross-disproportionation of formaldehyde and formic acid to methanol and carbon dioxide; c). equilibrium of formaldehyde in water to a hydration of formaldehyde, methylene glycol, or a stable cyclic trimer of formaldehyde, 1,3,5-trioxane; and d) equilibrium of formaldehyde and methanol to hemiformal.

Aqueous formaldehyde solution is the crucial component in the 3-phase Reppe ethynylation process. However, it has often been overlooked. Formaldehyde, not only as the starting material of the reaction but also as the reaction medium, is decisive in the acetylene gas solubility, the reaction kinetics, the active catalyst phase stability, and the catalytic performance.

Kiyama *et al.* [102-103] studied the reaction kinetics of acetylene with an aqueous formaldehyde solution in 1952. They concluded that BYD yield increases linearly with increasing formaldehyde concentration, while formaldehyde conversion decreases with increasing methanol content. With limited publications on the kinetics, Kale *et al.* [104] proposed 0.4 orders; Gupte *et al.* [105] and Change *et al.* [106] proposed 0.58 and 0.59 orders with respect to concentration in ethynylation. The effects of methanol content have not been revised. Methanol has different physical and chemical properties from formaldehyde and water, which is expected to affect the reaction mechanism by changing the formaldehyde equilibrium, gas solubilities, and catalyst activation.

pH values and the buffer species that adjust and maintain the pH of aqueous formaldehyde also play an essential role in ethynylation. It may affect the protonation in the catalytic reaction, change the yield and the selectivity of BYD and PA, affect the formation and stability of the catalytically active phase, and deactivate the catalyst [84, 102, 107].

Unfortunately, the relevant information, such as pH values, buffers, and the content of the additives, is mostly missing from the commercial formaldehyde solutions. It is necessary to self-prepare the aqueous formaldehyde solution and identify the exact data.

The list of the commercial formaldehyde solution and the details on the compositions and procedures of the self-prepared aqueous formaldehyde are shown in Chapters 5.1 and 5.3.2. The investigations on the effects of formaldehyde concentration, methanol contents, pH values, and buffer species in the Reppe ethynylation process will be discussed in this work.

Copper-Based Ethynylation Catalyst and Synthesis Techniques

The catalytic ethynylation employs a supported copper-based pre-catalyst, which can be activated in a reductive condition under an acetylene atmosphere. The cuprous acetylide (Cu_2C_2)-containing species was suggested by Reppe [74] and is commonly accepted as the catalytically active species in the ethynylation process.

Copper has a wide range of applications in catalysis and organic synthesis due to its unique chemical and physical properties as a versatile transition metal. Its oxidation states as metallic copper and copper(I)/(II) allow it to be easily involved in redox mechanisms, making it a suitable catalyst in oxidation, reduction, hydrogenation, and coupling reactions [52, 108-111].

Copper species, as a catalyst, has been thoroughly studied and characterized in the literature. Copper(I)/(II) oxides, hydroxides, chlorides, carbonates, and nitrates are the precursor phases in many catalytic reactions based on their chemical and thermal properties. Various carriers, such as silica, alumina, magnesia, and zinc oxide, are applied to adjust the catalyst's metal-support interactions that influence the catalytic activities [112]. It can also be easily prepared by most catalyst synthesis techniques, including co-precipitation, impregnation, sol-gel, and ammonia evaporation, which allow the tuning of the catalyst's morphology to study the structure-activity relationships. This, again, leads to copper as the most studied and industrially applied catalyst [113-114]. Another significant advantage of copper is its recyclability and cost-efficiency as an earth-abundant metal compared to noble metals of a similar function [115].

Taking the advantages mentioned, this work prepared a series of copper-based pre-catalysts of various compositions, carriers, synthesis techniques, and post-treatment conditions to investigate the catalytic performance in a highly complex 3-phase Reppe ethynylation process (Table 5-6 and Chapter 5.3.1).

1.1.4 Recent Development on Reppe Ethynylation

Reppe *et al.* published a series of papers on acetylene chemistry, titled *Production of Alkinols* [72] in 1942, *Chemie und Technik der Acetylen-Druck-Reaktionen* [39] in 1950 and *Äthinylierung* [41] in 1955. As proposed by Reppe, the silica-supported copper(II) oxide bismuth oxide ($CuO\text{-}Bi_2O_3/SiO_2$) as the catalyst precursor, the bismuth species as the promoter/inhibitor, and *in situ* formed cuprous acetylide (Cu_2C_2) species as the catalytically active phase in ethynylation of formaldehyde are well recognized.

It is still the most widely applied and effective catalyst in the industry. However, developing a new generation of ethynylation catalysts to improve catalytic performance has never stopped in academia and industry.

Silica supported Copper Oxide Catalyst in Ethynylation

The CuO pre-catalyst is a safe and low-cost precursor during storage and transportation, compared to the highly explosive active Cu_2C_2 phase in the ethynylation reaction.

Silica, in all phases and morphologies, is one of the most applied carriers in heterogeneous catalysis, as in ethynylation. The CuO/SiO_2 catalyst can be easily prepared by co-precipitation, ion exchange, impregnation, deposition precipitation, and ammonia evaporation [116-117]. Silica, as an inert carrier with a large specific surface area and abundant mesopores, effectively disperses and stabilizes the copper species [118-119]. The formation of a copper-phyllosilicate (Si-O-Cu) with the confinement effect that contributed to its unique fibrous nanotube structure has been repeatedly reported [116-117, 120-124]. It shows not only outstanding initial activity but also long-term stability due to the slow release of the stable Cu^+ centers [117]. The nanocrystalline CuO, confined into the well-structured SiO_2 network upon 650 °C heating, exhibits a high initial catalytic activity [125]. The core-shell catalyst with radially aligned mesoporous SiO_2 by the sol-gel method shows excellent catalytic stability [126].

Stabilizing the Cu^+ phase, which can be *in situ* transformed into the catalytically active cuprous acetylide species, is essential for the catalyst's activity and stability. However, it is challenging, especially under the reductive atmosphere with formaldehyde and acetylene [124].

Many researchers, since Reppe, have repeatedly investigated and reported the crucial role of bismuth species as the promoter and the inhibitor in the Reppe ethynylation process. The addition of Bi showed an electron synergistic effect with copper species, which weakened the CuO-support interaction. It allows a ready reduction of the Cu^{2+} precursor but inhibits the over-reduction into the inactive metallic Cu^0, which may catalyze the formation of polyacetylene and block the active sites [74, 119, 127-133].

Copper-Based Catalyst Precursor in Ethynylation

The recent research on the ethynylation of formaldehyde has mainly focused on the structures, properties, and interactions of copper-based pre-catalysts. This includes novel catalyst designs with different promoters and carriers that exist with specific catalysts' surface properties and metal-support interactions. Also, with the catalyst synthesis techniques that create unique morphology and structural features. The wide range of developments in the ethynylation catalyst has been mainly done in the past ten years by a few research groups.

G. Yang, as the first author, published a series of papers discussing the promotion of bismuth species and the supporting effects of different Cu-Si interactions of ethynylation catalysts.

Yang *et al.* [130, 134] employed an MCM-41 molecular sieve to support the $CuO\text{-}Bi_2O_3$ nanoparticle catalyst by facial impregnation. MCM-41 has one-dimensional mesoporous cylindrical structures that contain a large number of cross-linked silanol groups. It promotes a highly-dispersed copper species with silanols in its channels, proven by SEM and H_2-TPR. Yang *et al.* [124] also synthesized CuO/SiO_2 catalyst by hydrolysis precipitation methods, using ethyl orthosilicate as the silica source, and calcined at up to 450 °C. They successfully generated a large lamellar copper-phyllosilicate structure existing with a strong CuO and SiO_2 interaction, which contributes to a highly stable catalyst. Yang *et al.* [135] latest paper investigated the role of zinc in $CuO/ZnO/SiO_2$ catalysts synthesized via the deposition precipitation method, and by adding 15 wt.% zinc, the yield of BYD increased nearly 3-fold. At the same time, the activation energy of the reaction decreased to half.

The research group from Shanxi University has published a dozen papers covering multiple innovative catalysts with different promoters, carriers, and synthesis techniques.

Li *et al.* [117, 125] investigated CuO/SiO_2 catalysts synthesized by different methods and calcination temperatures. They reported a direct relationship among the smaller CuO particle sizes, higher CuO dispersion, more and stronger copper phyllosilicate structures, better initial catalytic activity, and longer stability. Wang *et al.* [118] studied the surface acidity and basicity effects of the binary nano $CuO\text{-}Al_2O_3$ and CuO-MgO catalysts in comparison to $CuO\text{-}SiO_2$. The alumina support creates acidic sites, which polymerize acetylene and cover the active Cu^+ sites that lower the activity. Magnesia provides basic sites that coordinate with Cu^+ and dissociate acetylene into $HC{\equiv}C^{\delta-}$ (deprotonation), which allows strong nucleophilic addition to the $C^{\delta+}$ of the electropositive formaldehyde carbonyl. As part of the nano-binary catalyst, Wang *et al.* [131] synthesized $CuO\text{-}Bi_2O_3$. They confirmed the promoting role of the Bi_2O_3 phase to disperse Cu and restrict over-reduction to metallic Cu^0 by stabilizing the Cu^+ valence, even without any other carriers. They also investigated the spinel $CuBi_2O_4$ phase formed at 700 °C calcination, where Cu^{2+} is gradually released from the spinel and transformed into the active phase, which shows low initial activity but long-term stability. Wang *et al.* [136] further studied

CuO/SiO_2-MgO catalyst with a Si-O-Mg structure that contains medium-strong basic sites. It enhances the copper interaction and dispersion, stabilizes the active Cu^+ valence, and facilitates the acetylene dissociation, which results in high catalytic activity in ethynylation. Introducing an appropriate amount of ZnO in CuO-xZnO [137], CuO/SiO_2-ZnO [135, 138], and CuO-$Zn_xMg_yAl_z$ layered double oxide (LDO) multicenter catalyst [139] shows a similar synergistic effect as MgO. It provides moderate basic sites that disperse and stabilize the active Cu^+ by electron transfer through the conducive CuO-ZnO interface. It also promotes, by the Lewis acid site of Zn^{2+} in the strongly interacted CuO-ZnO interlayer, the adsorption of the intermediate carbonyl oxygen (HCO*) and enhancing the electropositivity of $C^{\delta+}$ of formaldehyde activity [137, 139-140], hence improving the ethynylation rate and the catalysis.

In addition, the promoting effects of iron species in magnetic CuO [141] and CuO-Bi_2O_3 [142] on Fe_3O_4-SiO_2-MgO catalyst and composite Cu_xO-Fe_yO_z nanocatalyst [143] are investigated. The Fe_2O_3 and Fe_3O_4 species, similar to Bi_2O_3, are the electronic promoters that stabilize Cu_2O by electron transfer and inhibit the over-reduction by its unique redox features.

It is also interesting to explore the Cu_2O-based pre-catalysts since Cu^+ is the active phase in the ethynylation. Gao *et al.* [132] reported a chlorine-doped Cu_2O microcrystalline catalyst. It strengthens the Cu-O bonds and reduces the adsorbed oxygen by introducing Cl^- into the Cu_2O lattices, which regulates the Cu_2O morphology. Li *et al.* [144] and Wang *et al.* [144-145] studied Cu_2O/TiO_2 polymorphs catalysts, where titania can be prepared as a rutile and anatase structure. It was found that the rutile TiO_2 (110) has more exposure to strongly coordinate with Cu_2O, which enhances better dispersion and stabilizes the active Cu^+ valence.

The other developments of ethynylation catalysts that can be found in the literature in recent years include the regenerated kaolin (alumina silicate) support, patented by Zakharov *et al.* [146]; the HZSM-5 support (monoclinic H^+ modified SiO_2/Al_2O_3), patented by Lin *et al.* [147]; the activated alumina support, patented by Madhukar and Sidram [148-149] and Dai *et al.* [150]; and the magnesia support, published by Liu *et al.* [151]. Madon *et al.* [152] patented spray-drying methods to synthesize ethynylation catalysts with Cu-Bi and a wide range of carriers such as clay (hydrated aluminum phyllosilicate), talc (hydrated magnesium silicate), calcium silicate, kieselguhr (Si/Al/Fe/O), and activated carbon. The unsupported synthetic malachite [153-154] is also applied industrially as the catalyst, which shows high activity; however, as expected, it has poor stability and is difficult to separate from the slurry bed reaction of ethynylation.

With decades of serious investigation of the copper-based catalyst precursors, the transformation and stabilization of the so-called active Cu^+ phase, the commonly accepted catalytically active Cu_2C_2 phase, the exact activation mechanism, and the structure of the Cu_2C_2-containing species needs to draw more attention, also in this work.

Pre-reduction of Cu^{2+} Pre-Catalyst in Formaldehyde and Acetylene

As mentioned above, copper(II)-based pre-catalyst is the safest and most cost-effective catalyst. Thus, it is important to pre-reduce copper(II) species into active copper(I) sites and then convert them to the catalytically active Cu_2C_2-containing species by acetylene, as shown in Scheme 1-5 and performed in the catalytic ethynylation. The aqueous formaldehyde is suggested in the literature as the reducing agent according to the redox reaction shown in Scheme 1-6 [132, 155-157]. However, not enough investigation has been made.

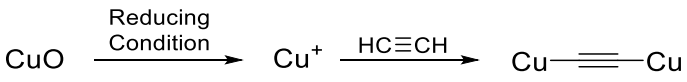

Scheme 1-5. The proposed catalyst activation pathways from cupric oxide to the cuprous oxide by reduction, and further transferred to cuprous acetylide in acetylene atmosphere.

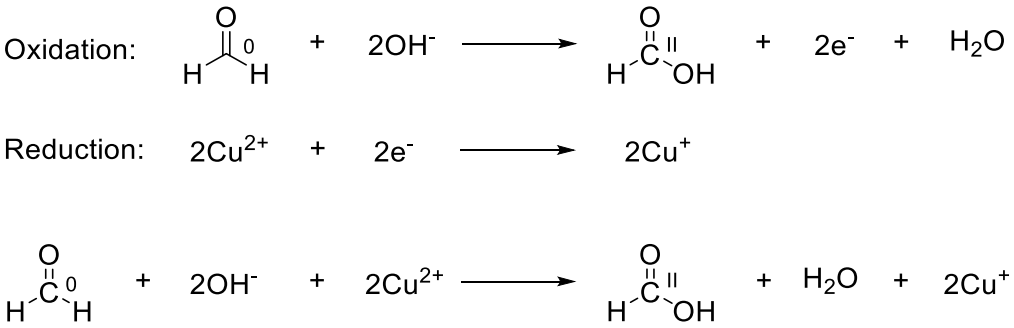

Scheme 1-6. The proposed redox reaction of copper in an aqueous formaldehyde solution in alkalic condition, where the cupric ion is reduced to cuprous ions, and formaldehyde is oxidized to formic acid.

Luo *et al.* [158] agreed with the function of formaldehyde, which ultimately reduced CuO into Cu_2O in a saturated formaldehyde solution at 90 °C under an N_2 atmosphere. However, the reduction is only made after 48 h, proven by XRD, and no reduction has taken place in the first 6 h. The converted Cu_2O is then activated into Cu_2C_2 with the introduction of acetylene.

Bruhm *et al.* [159] questioned the reduction role of the formaldehyde. They investigated the copper(II) species in a dissolved phase in solution and in a solid phase that attached at the interface, with EPR spectroscopy at up to 1.1 bar of acetylene absolute pressure and 100 °C. They concluded that acetylene, without formaldehyde, reduces the Cu^{2+} to Cu^{+} and simultaneously converts into Cu_2C_2 entirely within 45 min at 25 °C and in 2 min at 100 °C.

However, they accepted the synergistic effect of acetylene and formaldehyde in the activation of CuO under the typical ethynylation conditions, which is more practical and effective.

Brameld *et al.* [46] investigated the formation of acetylides from various cuprous solutions, cupric solutions, and on the surface of copper and its alloys in 1947. It is clear from their findings that both cupric and cuprous acetylides can be formed in an aqueous solution or on a moistened metal surface with the introduction of acetylene gas. However, the reducing agent is necessary for the cuprous solution to form the cuprous acetylide. Otherwise, cupric acetylide would be present. In addition, they emphasized the importance of the alkalinity of the solution, mainly the ammoniacal solution, which allows the immediate formation of the copper acetylides.

The pH effect for butynediol production has raised some attention, especially in the industrial Reppe ethynylation processes. Most of the industry manufacturers, such as GAF Corporation [87-88], du Pont [89, 160], and BASF [90, 119], since the 1960s, have tried to maintain the pH value of the aqueous solution during ethynylation at pH 5 – 8, and preferably at pH 6.0 – 7.0 by continuously adding metal hydroxide or carbonate salts solution dropwise. Stock *et al.* [161] investigated the abovementioned pH-adjusting agents. They claimed the ideal pH range is between 6.0 and 6.5 using an equivalent $NaOH/Na_2CO_3$ ratio of 2:1 – 3:1, based on the potential chemical reaction among the metals (Na, Mg, Ca, K), the hydroxides, the carbonates, and the formaldehyde.

However, to the best of the author's knowledge, no relevant literature reported on the sole effect of pH values and the pH-adjusting agents of formaldehyde on the *in situ* transformation of the catalytically active cuprous acetylides phase and subsequential influences on the yield and selectivity of BYD in the Reppe ethynylation process. This, again, meets one of the primary objectives of this work, which is to focus on the properties of the pH-adjusted aqueous formaldehyde solution in the catalytic ethynylation process.

Discovery of Catalytically Active Cuprous Acetylide Species

The catalytically active phase in ethynylation, copper acetylide, as a highly hazardous product, has been thoroughly studied in the industry for its formation conditions as a mandatory risk assessment and explosion prevention measure. However, due to its high explosivity, the exact structure, formation mechanisms, and influencing parameters are challenging to interpret. Several copper acetylide-containing structures have been reported in history. Some of the potentially existing structures that are related to the catalytic ethynylation of this work are shown in Scheme 1-7 [31-32, 159, 162-165].

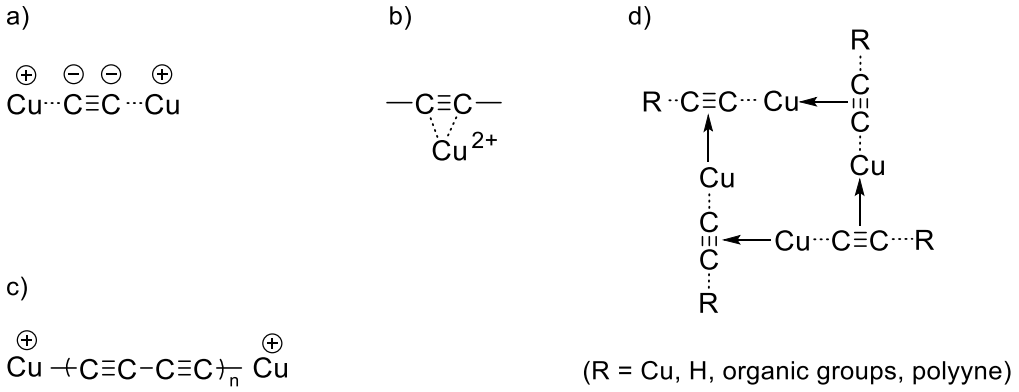

Scheme 1-7. Some of the typical copper-acetylide species and structures reported in the literature are potentially present in the catalytic ethynylation process: a). cuprous acetylide, Cu_2C_2; b). cupric acetylide, CuC_2; c). cuprous polyynide, $Cu_2(C{\equiv}C)_n$; and d). a possible structure of copper polyynide clusters.

Some of the copper acetylide-containing structures, including but not limited to the following:

Brameld et al. [46] synthesized cuprous and cupric acetylides from different copper salt solutions, such as nitrates, chlorides, and acetates, and on the metallic copper and copper alloy surfaces. Cataldo and co-workers [166-171] proposed the structures of dicopper diacetylide (Cu-C≡C-C≡C-Cu) and copper polyynides in which the polyynes are formed by oxidative coupling (e.g., Glaser coupling) of acetylene prior to contact with copper sources. The formation of metallic copper-catalyzed cuprene (polyacetylene, $-(HC{=}CH)_n-$) was also well-established in the literature [32, 133, 172-173]. Cataldo and co-workers investigated their structures and the molar concentration of each polyyne (C_6H_2 to $C_{16}H_2$) with HPLC, Raman, and FT-IR spectroscopies. Cataldo [166] also claimed that dicopper acetylide (Cu-C≡C-Cu) would initially convert to the superior homolog dicopper diacetylide (Cu-C≡C-C≡C-Cu) upon aging for weeks in air and then proceed to the longer chain formation via solid state coupling. Judai *et al.* [162, 174] studied copper acetylide nanoparticles deposited on the surface of metallic and semiconducting nanowires upon annealing. They proved the C_2Cu_2 existence by TEM and PXRD and provided the phase identification with density functional theory (DFT) calculations (refer to Figure 7-12). Rosenthal [165] proposed several types of bonding and coordination modes of metal (i.e., copper) acetylide ($[M]_2C_2$) and preferable polymetallic polyynides ($[M]_m(\mu_n\text{-}C_2)$) complexes, who claimed acetylide as the bridge between two metal centers and each C_2 unit may be complexed with up to eight metal centers. Makarem *et al.* [164] agreed with Rosenthal and synthesized copper acetylide clusters, namely the octacopper(I) hexaacetylide, via stoichiometry reaction of thermodynamically favored dicopper complex with an excess of air-sensitive acetylene cluster in non-acidic media and analyzed with NMR. A similar ideology with the linear polyacetylene chain is also interpreted by Liu *et al.* [175]. However, they focused on substituting the hydrogen atoms of the repeated acetylene units in organic synthesis instead

of replacing the terminal hydrogens with metals. The green and energy-efficient electro-organic synthesis of copper(I) acetylide on a copper-coated graphite electrode using a sacrificial copper anode was done by Seavill *et al.* [176-177].

Despite the limited number of publications on copper acetylide species, its varieties, the proposed structures, the synthesis techniques, the analysis, and applications are reported in detail. However, this work is more interested in identifying the *in situ*-formed Cu_2C_2 active phase from copper-based pre-catalyst under the ethynylation conditions. Bruhm *et al.* [159] are one of the very few who addressed this issue. Bruhm *et al.* experimentally tracked the activation progress from $CuO\text{-}Bi_2O_3/SiO_2$ pre-catalyst into the Cu_2C_2 phase in an aqueous formaldehyde solution at pH 7.0, 100 °C, and 1.2 bar of acetylene pressure. They observed the gradual existence of the vibrational signals corresponding to Cu-C bond and C≡C- bond in Raman spectra and the PXRD patterns corresponding to Cu_2C_2 over 5 h of activation. They also quantitatively identified the Cu_2C_2 structure by TG-MS analysis. Kirchner *et al.* [160, 178] aimed to reveal the cuprous acetylide complex structure, activated from a cupric compound catalyst in ethynylation, with the empirical formula. Kirchner proposed the general formula of $(Cu_2C_2/CuC_2)_w(CH_2O)_x(C_2H_2)_y(H_2O)_z$ by analyzing the atomic ratio of C/Cu, C/H, and C/O, based on Cu weight percent under various pH values, temperatures, and acetylene pressures (refer to Table 7-3).

It is helpful for this work to continue exploring the actual structures, formation mechanisms, and influential parameters, as much as possible, of the catalytically active cuprous acetylide phase in the Reppe ethynylation process to produce BYD.

1.2 Motivation and Objectives

Since petroleum and crude oil took over the dominant role of coal-based fuel and feedstock in the chemical industry in the 1960s, coal chemistry received little attention and showed a sign of stagnating for decades. Due to the recent worldwide conflicts, highly fluctuating oil prices, the potential petroleum and energy shortage, and global environmental issues, coal-based chemistry has regained the interest of the industry and academics [21, 44].

Acetylene is mainly produced from coal via electric-arc pyrolysis and calcium carbide hydrolysis. It can also be made from natural gas and biomass (Chapter 1.1.1). As a raw material, it has recently been accepted as a novel and reliable alternative to the petrochemical pathway in a wide range of industrial applications, such as the Reppe process (Chapter 1.1.2).

Catalytic Ethynylation of Formaldehyde

The catalytic synthesis of propargyl alcohol (PA) and 1,4-butynediol (BYD) via the Reppe ethynylation process is one of the most well-known industrial applications with acetylene. PA and BYD, as essential C-3 and C-4 feedstock produced from coal-based acetylene pathways, show high demand in many value-added processes (Chapter 1.1.3).

Despite millions of tonnes of annual PA-BYD production via the Reppe process all over the world in the past decades, optimizing the reaction units and the parameters, developing more active and stable catalysts, and maintaining the safe, sustainable, and economical- and environmental-friendly process remain the biggest concern of the industry.

In addition, the chemistry of this highly complex 3-phase catalytic reaction, such as the phase identification and characterization of the catalytically active species, investigation of reaction kinetics, the catalyst's structure-activity relationships, and catalytic reaction mechanisms, is still the black box that draws academic researchers' attention.

In this work, two sets of reaction units, a flexible glassware parallel reactor, and a six-fold Carousel reaction station were constructed for different applications (Table 5-8 and Chapter 5.3.3). The optimal catalytic ethynylation parameters and their influences, such as the pressure and temperature, stirring efficiency and catalyst-to-solution ratio, and the roles of the promoters, inhibitors, and carriers of the pre-catalyst, were investigated. The standard experimental procedures, including the catalyst activation, the catalytic ethynylation, the activated catalyst's separation and storage, and the spent catalyst's deactivation and disposal, were implemented and revised for safety reasons (Chapter 2.1).

Genesis of Active Cuprous Acetylide Species

The cuprous acetylide, Cu_2C_2, has been proposed as the catalytically active phase in the Reppe ethynylation process since the 1940s. However, the exact chemical structure and the characteristics of the Cu_2C_2 species have yet to be investigated due to its extraordinarily explosive and highly reactive nature. It is challenging to apply safe and suitable analytic techniques with appropriate analytical parameters (Chapter 1.1.4).

This work aims to experimentally identify the *in situ* activation of Cu_2C_2 from the copper(II)-containing pre-catalyst during ethynylation and correlate with the catalytic activity of the Cu_2C_2 species. Several analytical techniques were selected, along with careful safety inspection, to analyze the explosive Cu_2C_2 species (Chapter 5.3.4 and Table 5-5).

The qualitative analysis is focused on PXRD and Raman spectroscopy. A pure-phase Cu_2C_2 crystalline sample was synthesized by introducing acetylene in ammoniacal cuprous chloride solution. The analytical data of the pure-phase species is then served as a reference for phase identification. The quantitative analysis is studied by TGA/DSC-MS and elemental analysis methods like ICP-OES and CHN, where appropriate purification, drying, and storage techniques were implemented. The mass balance was then evaluated (Chapter 3.1).

Importance of the Aqueous Formaldehyde Solution

Aqueous formaldehyde is not only the starting material of this highly complex catalytic reaction but also the reaction medium. However, the crucial role of formaldehyde in this process has often been overlooked.

The formaldehyde dissolves the acetylene gas under slight overpressure. It also acts to some extent as a reducing agent to reduce the copper(II)-containing pre-catalyst into copper(I) and then activate and stabilize to the active cuprous acetylide phase with the dissolved acetylene. Furthermore, formaldehyde also provides an optimal condition to allow the nucleophilic addition of the cuprous-activated acetylide anions to the electrophilic carbonyls in the solution to produce the desired products.

This work uses both commercially available formalin and self-prepared formaldehyde solutions to prove its decisive role. The formaldehyde solution, prepared by dissolving paraformaldehyde in a water-methanol mixture, is pH-adjusted to the desired pH range by adding conjugated acid-base buffer species, such as sodium-hydrogen phosphates, NaH_2PO_4 and Na_2HPO_4. The influences of its properties, like its concentration, pH values, and pH buffer species, were investigated on the rate of the active cuprous acetylide formation and the catalytic activity in the ethynylation (Chapter 2.3).

2

CATALYTIC ETHYNYLATION OF FORMALDEHYDE

2.1 Implementation of Experimental Procedures

Catalytic Reppe ethynylation of formaldehyde to produce propargyl alcohol as the intermediate product and 1,4-butynediol as the desired product is a highly complex 3-phase reaction that multiple factors can easily influence.

Many patents and publications have reported the reaction parameters and procedures of catalytic ethynylation. However, each of the studies has its specific objectives.

For example, industrial manufacturers value safety and economic and environmental efficiency. It is essential to modify the reaction process to exhibit better long-term stability and sustainability by employing catalysts with better stability and lifespan rather than initial activity. They also tend to operate under milder reaction parameters with a higher factor of safety and increase batch sizes to prolong the turnovers by applying (semi-)continuous processes to overcome the rate-limiting parameters. On the other hand, the researchers are mainly interested in laboratory-scale reactions that can interpret the initial catalytic activity, selectivity, and conversion precisely. It is essential to identify the influences of each parameter and investigate their optimal values. There is also great attention to exploring the activation and ethynylation mechanisms with complex kinetic studies and structure-activity relationships. In addition, the separation and regeneration of the spent catalysts and the purification of the desired products are the main concerns of the manufacturers but not the researchers. These make a difference in the selection of the experimental procedures and parameters.

This section implements and optimizes various reaction parameters and procedures to meet multiple research objectives and motivations. Chapter 2.1.1 focuses on implementing two sets of testing units to perform the catalytic reactions with higher capacity and better reproducibility. It also interprets setting up the special units to conduct tests, synthesis, and sample preparations under specific conditions. Chapter 2.1.2 develops flexible experimental procedures and reaction processes for different studies. Chapter 2.1.3 investigates the influences of catalyst activation and ethynylation conditions and determines the rate-limiting parameters. The optimized experimental parameters and procedures will be applied for the respective experiments in this work.

2.1.1 Installation of Catalytic Performance Test Units

The complex 3-phase ethynylation process obtains a brownish slurry during the reaction that consists of volatile, toxic, and pungent aqueous formaldehyde, a highly flammable and easily decomposable acetylene gas, and a highly sensitive and explosive cuprous acetylide catalytically active species. Thus, implementation and optimization of a safe, easy-operate, and reliable test unit for the catalytic performance of ethynylation is the pre-priority step.

General Considerations in the Test Unit Design

In the beginning, several test units and accessories were discussed and trial-tested. Some examples, as shown in Figure 7-1, are the autoclave reactor, which consists of a digital temperature controller and an electric-controlled pneumatic agitation system. Accessories for maintaining strict conditions and improving consistency, like an electronic heating-cooling jacket, a mechanical overhead stirrer, electronic mass flow controllers (MFCs), a pressure regulation system and safety pressure relief valves, a pH-monitored automatic titrator, etc.

However, most of the suggestions are not practical for this unique catalytic Reppe ethynylation test. This is mainly due to the safety and effectiveness of the successful experiments.

One consideration is the possibility of unexpected pressure build-up in the system due to sampling, refilling, and solid-liquid phase (catalyst from the reaction mixture) separation. Acetylene has wide explosion limits from 2.5 wt.% to 85 wt.% in the air and easily explodes in the presence of oxygen or under absolute pressures as low as 1.4 bar [56].

The perfectly sealed stainless steel autoclave reactor has multiple connection ports. Despite its ability to stand high pressures and temperatures of up to 30-100 bars and 150-400 °C, the decomposition of acetylene may raise the temperature to 3000 °C and 200-fold the initial pressure during explosion [59-60]. It may cause severe and irreversible damage. Another risk is the potential deposition and accumulation of hazardous explosive Cu_2C_2 particles in the pipelines and connections. Additionally, cleaning the autoclave reactor can also be challenging, as the contaminants cannot be easily removed. This may cause a pipeline explosion [58], corrode the metal parts, and damage the reaction system over time.

On the other hand, the installation of additional accessories, especially electronic devices like the pH-electrode, automatic titrator, and mechanical overhead stirrer, may create potential risks of hot spots, sparks, and electric shock that may ignite the explosive acetylene. It also makes the system more challenging to install, troubleshoot, and maintain daily routine tasks.

Consider the safety and simplicity of the test unit design; with the excessive inspections of safe and practical operations, a simple but effective test unit consisting of two to three two-necked

round-bottom glassware flasks connected in parallel was applied. To increase the testing capacity of the catalytic performance tests, the homogeneity of the reaction parameters, and the comparability of the testing results, a Carousel 6PLUS Reaction Station™ was installed.

Parallel Test Unit

The parallel test unit, as demonstrated in Figure 2-1, was implemented and used for the catalytic ethynylation performance test. Two to three glassware flasks are connected in parallel as the reactor can be chosen flexibly in sizes and shapes.

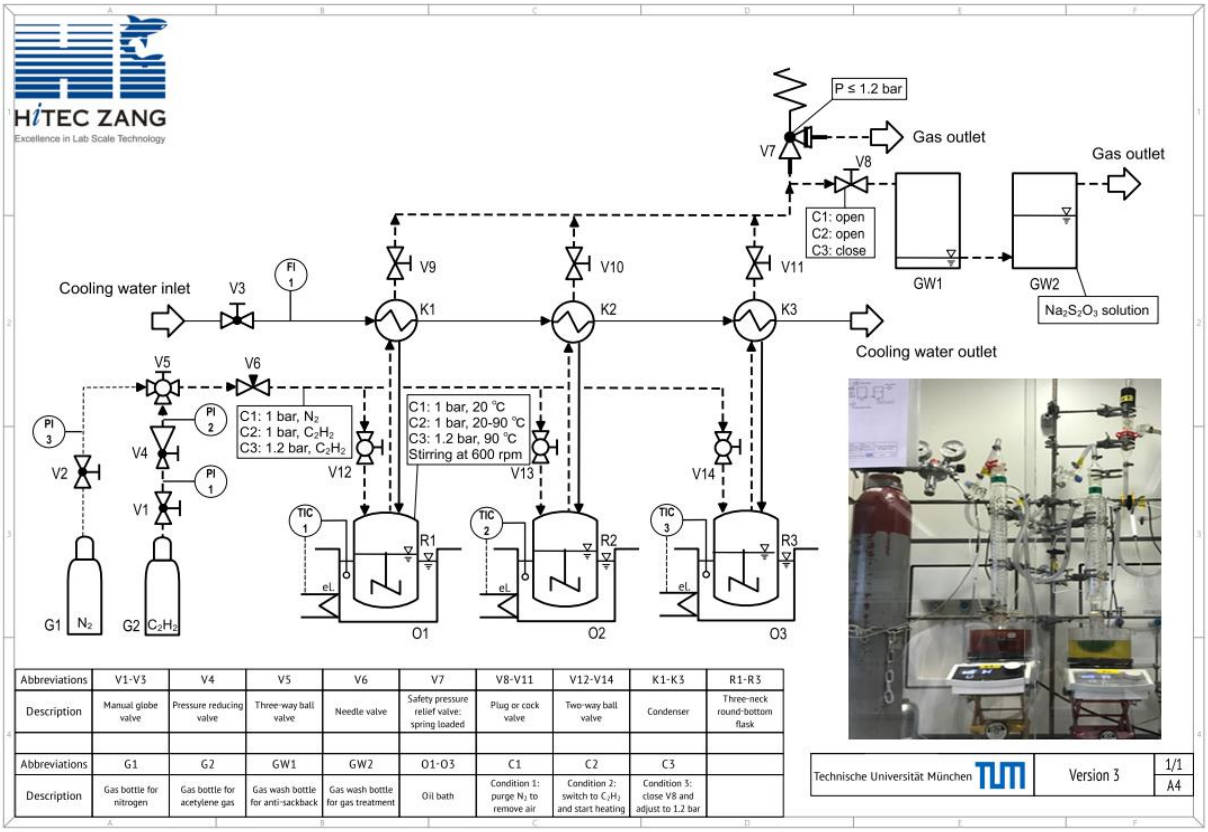

Abbreviations	V1-V3	V4	V5	V6	V7	V8-V11	V12-V14	K1-K3	R1-R3
Description	Manual globe valve	Pressure reducing valve	Three-way ball valve	Needle valve	Safety pressure relief valve: spring loaded	Plug or cock valve	Two-way ball valve	Condenser	Three-neck round-bottom flask
Abbreviations	G1	G2	GW1	GW2	O1-O3	C1	C2	C3	
Description	Gas bottle for nitrogen	Gas bottle for acetylene gas	Gas wash bottle for anti-sackback	Gas wash bottle for gas treatment	Oil bath	Condition 1: purge N_2 to remove air	Condition 2: switch to C_2H_2 and start heating	Condition 3: close V8 and adjust to 1.2 bar	

Figure 2-1. The demonstration P&ID and picture of the parallel glassware reactors for the Reppe ethynylation process. Two or three flasks are connected in parallel with the gas flow and cooling water systems. Each flask has two sidearms, sealed with rubber septa, which are connected to a reflux condenser, heated in an oil bath, and stirred with a magnetic stirring bar by a digital magnetic stirring hotplate. Nitrogen for purging and acetylene gas for ethynylation reaction, controlled by a three-way valve, can be introduced into the reactors through one of the sidearms; sample taking can be done via another sidearm. An overhead safety pressure relief valve is installed and will be activated automatically when the pressure in the system is above the designated pressure. A washing bottle containing sodium sulfite solution is connected to the gas outlet stream, which traps toxic formaldehyde gas released from the reaction mixture during heating and purging for safety reasons.

The glassware parallel test unit has several significant advantages in lab-scale research compared to complex reactors like the autoclave. One is simply its transparency, which is essential to gaining hands-on experience about the entire ethynylation process. It allows direct visual observation. For example, the color changes from blueish, greenish, or black pre-catalysts into the reddish-brownish active copper acetylide phase during the initial activation stage, and the stirring efficiency with the magnetic stirring bar when the reaction mixture gets more viscous over time. It is also beneficial for cleaning, where the leftover hazardous substances can be visually seen and then cleaned thoroughly.

Furthermore, considering its effectiveness as a reactor for the performance test of the catalytic ethynylation, several parameters and reaction conditions have to be taken into account. The selection of the setups and accessories must not affect the performance, and its influences must be proven experimentally, as shown in the following chapters.

First of all, catalytic ethynylation is carried out at mild reaction conditions between 80 to 120 °C and 1.0 to 1.3 bar absolute acetylene pressure. The glassware reactor has excellent corrosion resistance and is chemically inert. All parts of the reaction system are copper-free to avoid the formation of explosive copper acetylides. With pure and saturated aqueous formaldehyde as the solvent and reactant, the glassware reactor is perfect since even the stainless steel can still be corroded if the temperature rises above 120 °C [179].

Secondly, catalytic ethynylation is performed between pH 4.0 to 8.0. The reaction mixture, mainly the reactive aqueous formaldehyde solution at the beginning, tends to be acidic due to the self-disproportionation reactions in water to form formic acid (Scheme 1-4). It is necessary to keep a constant pH value during ethynylation for optimal catalytic performance. Most Reppe ethynylation processes and publications, for instance, the recent development patented by BASF [119], suggested continuously adding diluted NaOH to maintain the pH value. In this case, a pH electrode and a liquid inlet stream, controlled by an automatic pH titrator, must be connected to the reaction system. This brings a lot more complications to the test unit design and operations. An alternative using a pH-buffered formaldehyde solution was investigated. It was tested effectively to maintain the desired pH values and enhance the catalytic performance. The challenges of preparing a suitable formaldehyde solution instead of using the commercially available ones and the investigation of the influences of catalytic performance by differently pH-buffered formaldehyde are extensively discussed in Chapter 2.3. In this case, it is no longer necessary to have additional ports to place the pH electrode and titrator in the reactor.

Next, the stirring efficiency, which is especially crucial for the 3-phase system and influences the mass transport limitation, was considered. The efficient and professional stirring devices include an overhead digital pneumatic agitator and a KPG stirrer shaft with different types of blades. However, the simple magnetic stirring bar was finally selected.

Another factor is the acetylene gas flow rate and pressure. Both flowing acetylene bubbled through the reaction mixture and static pressurized acetylene atmosphere for the catalytic ethynylation are reported in the literature. Each reaction system has its advantages and limitations. The experimental objectives and the operation process will influence the selection.

The flowing acetylene system is particularly suitable for continuous processes in which the reaction inputs and outputs can be easily added and withdrawn. The acetylene gas bubbles through the reaction mixture may show a synergistic effect with the stirring efficiency to overcome the mass transport limitation of the 3-phase reaction system. However, the flowing system requires the connection of a recycling stream and a purification unit for acetylene gas to reduce wastage and lower the acetylene discharged into the surroundings for safety reasons.

On the other hand, the static pressurized acetylene atmosphere is suitable for a batch process where there is no addition of inputs or withdrawal of outputs during the reaction, except for a small amount of sample taking. It operates at a slight over-pressure of acetylene, which may speed up the chemical kinetics of the ethynylation by increasing the acetylene gas solubility in the liquid phase reaction mixture. The adverse effect is the potential pressure build-up in any part of the system, which is difficult to predict in case of failure, such as pipeline blockage. Hence, a sensitive pressure relief valve is installed.

With the abovementioned considerations, the static pressurized acetylene condition and batch process reactor are chosen for the performance test of catalytic ethynylation with the glassware parallel test unit. These factors are not only discussed based on theoretical research but also proved experimentally. The investigations are shown in the following chapters.

Carousel 6PLUS Reaction Station™

Carousel 6PLUS Reaction Stataion™, as shown in Figure 2-2, is introduced to increase the testing capacity and improve the reproducibility of the catalytic ethynylation performance test.

The Carousel unit has setups and accessories similar to those of the parallel test unit that assemble six flasks in an integral Carousel flask holder with a built-in gas and cooling water system on a single magnetic stirring hotplate.

The Carousel test unit saves space in the fume hood, reduces the number of devices and equipment, and, more importantly, ensures synchronized reaction conditions like heating rate, stirring rate, and pressure. The unit is used for abundant catalyst tests, benefiting from its 6-fold testing capacity and identical reaction conditions. It speeds up the testing progress and makes a large sample pool for comparison possible. It significantly improves the reproducibility of the catalytic testing results, which is crucially important in catalysis. It also provides reliability when comparing the results among different testing batches.

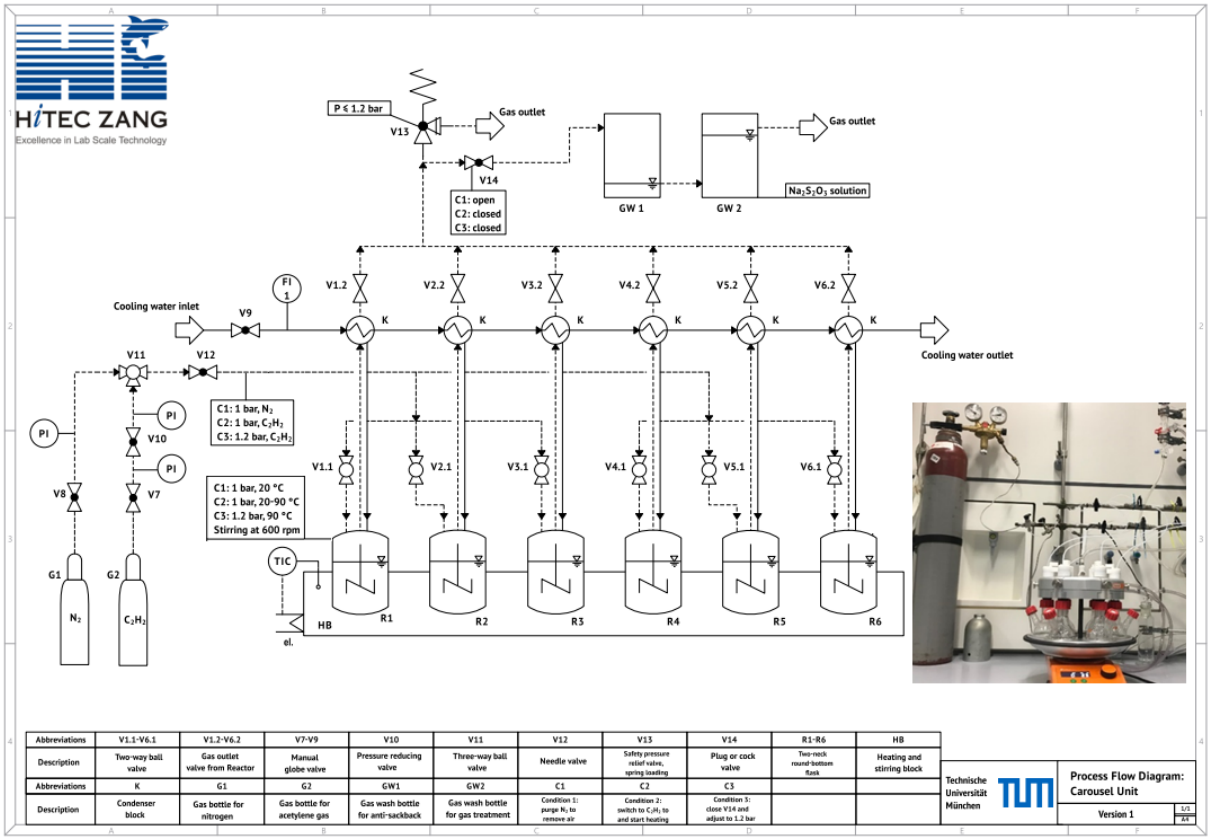

Figure 2-2. The demonstration P&ID and picture of the Carousel 6PLUS reaction station for the Reppe ethynylation process. Six flasks are placed firmly on an integral Carousel flask holder on a single magnetic stirring hotplate. The reflux condenser connected to the flask is assembled with the metal lock to the upper part of the Carousel holder, which provides a built-in cooling water system. The cap to the reflux condenser is sealed with a gas outlet stream, which is also built-in, and the gas is discharged via a pipeline connected to the pressure relief valve (activated at 1.2 bar) and the washing bottle (sodium sulfite solution to trap gaseous formaldehyde) before being released into the atmosphere. The gas inlet pipe is also inserted via a septum on the cap. Each flask has one sidearm, sealed with a septum cap, for sample taking by a needle and syringe.

In general, the parallel and the Carousel test units sufficiently fulfill the requirements of daily routine catalytic performance tests and investigations. The parallel test unit provides flexibility in the reaction conditions in which the temperature and stirring rate can be set differently. A flask of different shapes, like a beaker or a Schlenk line tube, and in case an additional stream or a pH electrode needs to be connected for specific experiments, can be applied. However, the Carousel unit provides highly unified and synchronized conditions and allows unique round-bottom flasks due to the standard Carousel sample holder.

The detailed standard experimental procedures for the catalytic performance test of Reppe ethynylation using the glassware parallel test unit and the Carousel 6PLUS Reaction Station™ are shown in Chapter 5.3.3.

Specially Designed Test Unit

Besides the supported copper-based pre-catalysts that are activated *in situ*, the cuprous acetylide-containing synthesized by direct precipitation or by deposition precipitation on carriers are prepared and tested for catalytic performance. As shown in Scheme 1-7, multiple copper acetylide species can be formed in a generous synthesis condition and environment. For instance, the cupric acetylide is favored where the copper +2 oxidation state is more stable in aqueous conditions due to its electronic configurations. In contrast, the presence of metallic copper, which is over-reduced from Cu^{2+} or formed by the self-disproportionation reaction of Cu^{+} in an aqueous solution, will catalyze the polymerization of acetylene and form copper polyynides. As a result, maintaining a strict oxygen-depleted environment is a priori for the synthesis of the pure-phase cuprous acetylide, and a specially customized setup is implemented, as shown in Figure 2-3.

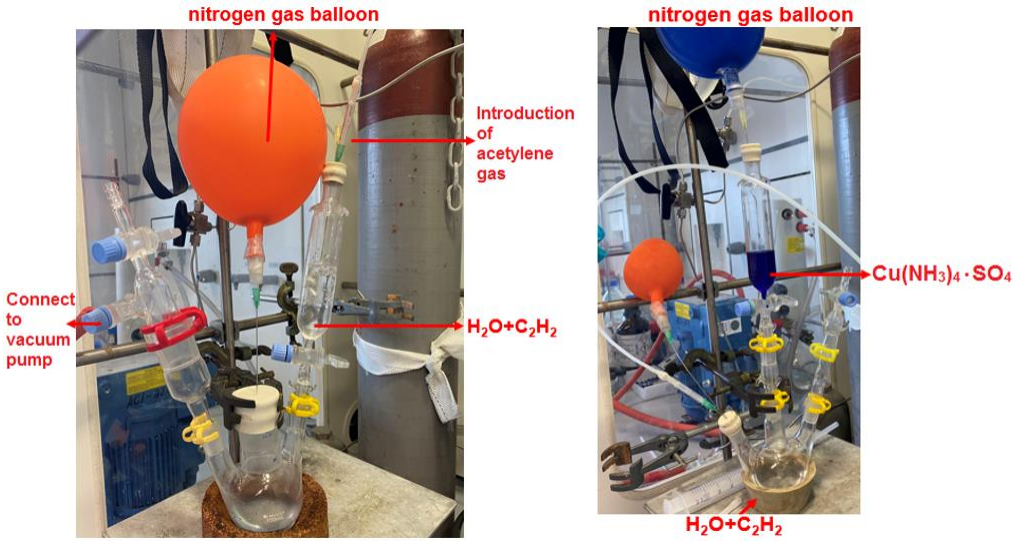

Figure 2-3. The demonstration picture of the specially designed setup for the synthesis of pure-phase cuprous acetylide under an oxygen-depleted environment. The setup consists of a three-port flask adjustably connected to the Schlenk line tubes, a vacuum pump, a backflash stream of inert gas that can be switched between N_2 and Ar, a nitrogen gas balloon, a cannula filtration tube, and an inlet stream of dropwise addition of reaction medium. The oxygen-depleted environment is monitored by the vacuum pump and the purging of the inert gases. The addition and withdrawal of the reaction medium are driven by the slight pressure difference created by the pump or the gas balloon. The obtained pure-phase cuprous acetylide is then separated, washed, and purified using the Schlenk line technique. Then, the catalytic performance in ethynylation can be tested following standard operation procedures.

Maintaining the oxygen-depleted environment for pure-phase cuprous acetylide synthesis is challenging. Using the Schlenk line and operating in the glove box is the option for most experiments requiring oxygen-free and inert conditions. However, they are not eligible for the

synthesis of cuprous acetylide. This is because the reaction involves a gas phase of acetylene or the pressure-sensitive dissolved acetylene in an aqueous solution and the highly versatile ammonia-containing solution. Another challenge is difficulty in identifying and differentiating the copper acetylide species, none of which are recorded in the analytical database, such as the XRD and Raman spectra. This makes it questionable when tracking the role of oxygen and investigating the effect of the synthesis conditions in the formation of cuprous acetylide. Additionally, maintaining the conditions has to be considered during the synthesis, purification, and analytical stages, which are highly challenging and time-consuming.

The setup shown in Figure 2-3 was customized and optimized with the abovementioned considerations. It performed effectively based on the current analytical results. Its catalytic performance was tested with parallel test units, in which the flask reactor is pre-purged to prevent re-oxidation and deactivation. The detailed investigations and discussion on the genesis and identification of pure-phase cuprous acetylide are shown in Chapter 3.1.

2.1.2 Development of Flexible Experimental Processes

After a successful implementation of the reaction test units, the reaction processes to meet the different Reppe ethynylation research objectives are investigated.

In heterogeneous catalysis, the air-stable catalyst precursors need to be activated into their catalytically active phase under preliminary conditions. Both the catalyst precursor and the activated phase are well characterized. However, in the 3-phase Reppe ethynylation process, the catalytically active phase is believed to be the highly explosive cuprous acetylide-containing species, which appears as a brownish slurry. It is generated under the acetylene atmosphere in a formaldehyde solution. It is difficult to characterize due to its appearance and chemical and thermal properties. Furthermore, separating the activated slurry catalyst and its purification and storage are even more challenging, which is ideally done under the acetylene or inert atmosphere to prevent the potential catalyst deactivation and decomposition.

These unique properties and difficulties in handling the activated catalysts underscore the feasibility of the experiment design. Hence, it makes a reasonable debate for the lab-scale experiments to perform the catalytic ethynylation. That is, whether to perform a one-step batch process with the pre-catalyst that activated *in situ* under identical reaction conditions or a two-step process with a pre-activation step followed by the actual ethynylation with the activated catalyst. Besides those, there is another proposal for a specially designed industrial-like semi-continuous process for the specific catalytic ethynylation tests, such as the leaching and deactivation studies, and for investigating the *in situ* formation of the active phase.

The deep investigation of the performance and suitability of the catalytic Reppe ethynylation process, whether it's the one-step batch process, the two-step process, or the industrial-like process, is significant. Each process has its own set of strengths and limitations. In addition, the selection of different combinations of the reaction processes and setups, as mentioned in Chapter 2.1.1, is crucial to allow optimal compatibility to achieve the desired research objectives and outcomes. The detailed and finalized standard operation procedures and their applications to each process in this framework are shown in Chapter 5.3.3 and Table 5-8.

An example as a preview of two runs of catalytic performance tests on reproducibility is given in Figure 2-4. The catalytic performance tests use the identical Cu-Bi/SiO_2 (CBS) pre-catalyst and aqueous formaldehyde (FA) solution under identical experimental procedures and parameters. The results show the most significant difference in the yield of BYD in the one-step process, also known as the activation step of the two-step process. However, after separating and purifying the activated catalyst and performing the second step of the ethynylation reaction with the activated catalyst, a highly reproducible result in terms of the yield of BYD is obtained. The same trends are observed in most of the similar tests performed with different catalysts, formaldehyde solutions, and reaction conditions, as elaborated later.

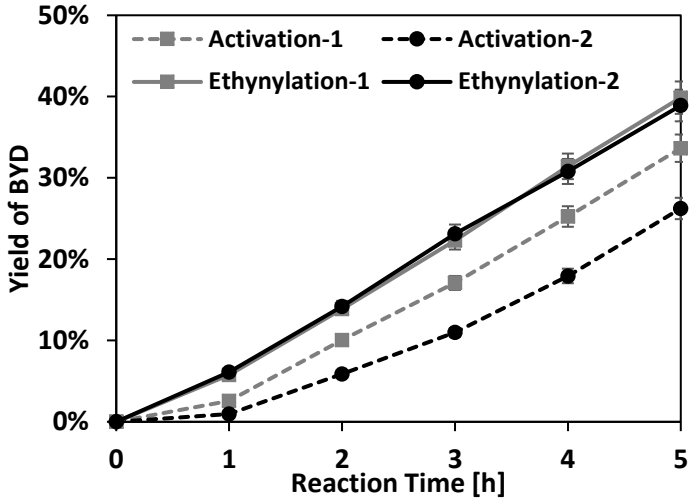

Figure 2-4. The graph illustrates the reproducibility of two runs of catalytic performance tests (the orange and blue lines, respectively). The plots show the yield of BYD over 5 h of reaction time. The yield of BYD is calculated based on the theoretical 100% FA conversion into BYD, with a stoichiometric of 2:1 for FA-to-BYD. The identical Cu-Bi/SiO_2 pre-catalyst, formaldehyde solution, and the reaction conditions are applied. The pre-catalyst is activated for 5 h; this is a one-step process. The activated catalyst, after 5 h, is separated, purified, and performed for another 5 h for the ethynylation. Both the activation and ethynylation are considered a two-step process.

One-Step Batch Ethynylation Process

The advantage of the one-step batch process is its simplicity and safety in operation. It uses the chemically stable pre-catalyst at the beginning. The spent catalyst is deactivated and disposed of immediately after the reaction, which brings no risk. This process is best for the catalytic performance test that focuses only on the short-term catalytic activity, selectivity, and deactivation. On the adverse side, it is less convincing but more complicated to interpret the reaction mechanisms, kinetics, and catalyst activation and deactivation behaviors. This is because there are too many parameters that may interfere with each other, creating synergistic effects in this holistic batch reaction. It is more helpful to study the sole impact of each factor instead, as systematically investigated in Chapter 2.1.3, which seems more challenging but is necessary for a deeper understanding of the catalytic ethynylation process.

On the other hand, the one-step process tends to show poor initial activity and reproducibility, as shown by the activation curves in Figure 2-4. This is because the five to seven-hour catalytic performance test is considered the initial stage. It has been proven experimentally, based on the increasing reaction rate represented by an upward curve, that the activation of pre-catalysts is generally just about completed. Thus, the difference in the reaction kinetics for the catalyst activation and the catalytic ethynylation has been taken into account. This argument, which is believed to be the reason for the irreproducible results of the catalytic activity and the yield of BYD, leads to the implementation of the two-step process.

Two-Step Activation-Ethynylation Process

The two-step process consists of an activation step of the pre-catalyst and a separated ethynylation step of the activated catalyst. The implementation of the two-step process initially aims to solve the problem of reproducibility, which is crucial for catalytic performance tests of extensive catalysts with different compositions and properties, as investigated in Chapter 2.2.1.

The activation rate is dependent on the reducibility of the metal salt precursors, metal-support interactions, surface properties, and intermolecular bonding forces, which are commonly investigated and interpreted in heterogeneous catalysis studies. The catalytic reaction rate with the activated catalysts, when all pre-catalysts are fully converted into the catalytically active phase, should be constant over time until the rate-limiting parameter appears or the catalyst starts deactivating. The constant reaction rate is directly related to the catalytic activity, represented by the constant TOF or the linearly increased yield of BYD, as the different gradients of the slopes for the activation and ethynylation curves are shown in Figure 2-4.

However, one of the challenges is that the 3-phase catalytic ethynylation, which differs from most of the other heterogeneous catalysis processes, requires identical conditions for the catalyst's activation as for the actual ethynylation. Hence, the gradually *in situ*-formed active Cu_2C_2-containing catalysts readily undergo catalytic ethynylation to yield BYD simultaneously. It is shown in Figure 2-4, where BYD is formed at the very first hour, even with the pre-catalyst. The rate of BYD formation continuously increases while more of the catalysts are activated. This brings uncertainty and nonlinearity in the initial reaction rate and makes the investigation of reaction kinetics complex. It is largely affected by the catalyst activation process that consists of the reduction of copper(II) into copper(I) active phase and the transformation into the catalytically active cuprous acetylide. This also supports the necessity of separating the activation and catalytic ethynylation steps in specific studies.

Applying the two-step process is convincing in achieving reproducibility. It also helps in reducing the variable factors of the complex catalytic Reppe ethynylation process to study the sole impacts of each parameter. However, the process also brings additional difficulties during the implementations and operations. That is the most challenging and unavoidable transition step in between the activation and ethynylation steps, which is the separation of the activated catalyst slurry from the reaction mixture, washing and purifying the catalyst, and storing it safely to prevent it from explosion, decomposition, and deactivation. The detailed investigations of the transition steps, storage effects, and deactivation behaviors are shown in Chapter 2.4.

In addition, studying the kinetics of the activation and ethynylation steps separately provides an opportunity to reveal hidden information regarding the catalytically active cuprous acetylide phase and eventually provide the information to propose the activation mechanism of the cuprous acetylide formation and the ethynylation mechanism involving the active phase.

One-step Industrial-like Semi-continuous Ethynylation Process

The relevant data and results obtained from the lab-scale research of the catalytic ethynylation process will eventually be transferred into industrial applications and productions. Hence, it is reasonable to simulate a process similar to those in the industry to understand real-world problems and provide referable and reliable solutions. Thus, a long-term, one-step, semi-continuous process with a single glassware reactor was implemented.

The catalytic performance test is conducted to investigate the advantages and limitations of the long-term and one-step process. It is also expected to determine the limiting reagent and estimate the appropriate parameters, such as the reaction time and the amount of catalyst and FA solution to be used, that may eliminate the rate-limiting parameters of the process. The tests are carried out with the standard CBS pre-catalysts, which are gradually activated *in situ* during the initial activation stage in saturated aqueous FA solution. The evaluation is based on the yield of BYD and the conversion of FA, as shown in Figure 2-5.

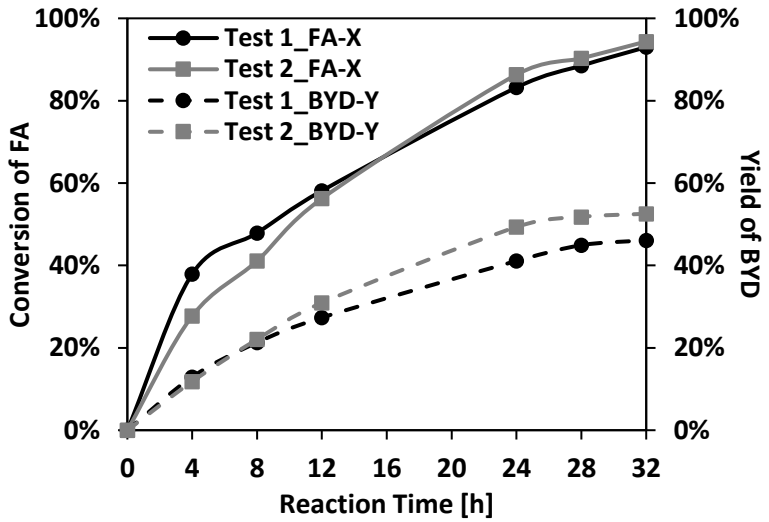

Figure 2-5. The graphs illustrate two runs of long-term catalytic performance tests with saturated aqueous formaldehyde solutions in the conversion of FA (solid lines) and the yield of BYD (dotted lines) over 32 h of reaction time. An identical Cu-Bi/SiO_2 (CBS) pre-catalyst is applied under the standard experimental procedures and parameters.

It is expected that the highest formation rates of BYD correspond to the highest conversion rates of FA, and the formation rates of BYD and conversion rates of FA will be reduced while FA is consumed over time. From the graph, two tests show good reproducibility. The decreasing curves for both BYD yield and FA conversion are observed, which meets the expectation. When the FA conversion reaches 80% after 24 h, little increase in BYD yield is observed. While the FA is further consumed to more than 90% after 28 h, there is nearly no

more increase in the yield of BYD. This is because the concentration of FA is too low in the reaction system to continue forming the product. Hence, FA is concluded to be the limiting reagent that limits the rate of the long-term catalytic reaction.

From the experimental results, it is suggested that the reaction time should be ideally within 20 h, and FA conversion should not exceed 75%. It is also necessary to increase the amount of FA solution to ensure sufficient FA is available to maintain the constant catalytic reaction rate. The appropriate amount of catalyst and FA can be estimated. Additionally, applying the long-term, one-step ethynylation process minimizes confusion due to the difference in BYD formation rate and eliminates the complex transition steps. Also, the possibility of catalytic activity as the rate-limiting parameter is evaluated. However, the pre-request is that no other factors will limit the reaction rate. Hence, this will be discussed in the next chapter when the optimization of reaction setups and experimental procedures.

In contrast to the pseudo-batch process, where acetylene is continuously added into the static system to ensure the constant acetylene pressure during ethynylation, the semi-continuous process is established as the periodic addition of fresh formaldehyde solution and the catalyst. This systematic approach ensures the reliability and stability of the process, as it overcomes the rate-limiting parameter. Another circumstance for refilling the formaldehyde and catalyst is when a large amount of the reaction mixture is extracted for analysis.

Handling of the Activated Catalyst and Deactivation

Handling the activated catalyst, which contains the explosive catalytically active cuprous acetylide species, is challenging. The transition step in the two-step process involves separation, purification, and storage of the activated catalyst, which is unavoidable and decisive in determining accurate catalytic performance in ethynylation. This step is also applied to the multi-cycle experiments and sample preparations for the catalyst's active phase identification and characterizations.

The stepwise development of the optimal separation techniques took place with tremendous care for safety. Several difficulties were encountered, and few references can be found in the literature for the practical handling steps of the cuprous acetylide-containing species relevant to this application. In this circumstance, the down-scaled trial explosivity tests and inspections under various conditions were performed. The literature states that the cuprous acetylide is explosive when dried in air. It has been experimentally proven by the explosion tests that the supported catalyst containing cuprous acetylide is stable when dried but may catch fire or react vigorously with impact, spark, and strong oxidizing agents and acids. The details are presented in Chapter 3.2.3.

Separation of Activated Catalyst Slurry

The separation tests of the experimental scale of activated catalyst were carried out using four proposed typical separation techniques: rotary evaporation, Schlenk line technique, vacuum filtration, and centrifugation.

Rotary evaporation separates the organic solvents by different volatilities and boiling points under elevated temperatures and reduced pressures. It is not possible in this case where the highly viscous aqueous-organic mixtures contain a large variety of compounds with boiling points ranging from 65 °C to 238 °C. It has low separation efficiency when drying out the catalyst slurry, and it is highly time-consuming.

The Schlenk line technique, while excluded for the same reason, has a unique advantage in the operation with multiple flasks under inert operation conditions, allowing long-term storage that can be transferred to the glove box. This makes it highly relevant, but preferably for down-scaled experiments. This technique is also ideal when synthesizing the pure-phase cuprous acetylide species and preparing test samples for analysis.

Vacuum filtration is a suitable process that effectively separates the activated catalyst slurry from the reaction mixture through filter paper. This is achieved with a pore size of 8-13 µm, allowing a relatively easy and quick washing but inefficient transferring process. The separated catalyst has a higher degree of purity and dryness. Still, it is relatively challenging to transfer the catalyst residues, as illustrated in Figure 2-6, causing a loss of the amount of catalyst. The traces and the leached active species during washing will be filtered away and cause more loss of active sites. Additionally, vacuum filtration is conducted in an open atmosphere, which could lead to catalyst deactivation by oxidation and decomposition.

Figure 2-6. The vacuum filtration technique efficiently separates the activated catalyst slurry from the reaction mixture via filter paper and at a higher purity and dryness after the activation step of the two-step Reppe ethynylation process. The filtrates are decanted. The residual catalysts (left) are washed and purified using the same methods. The purified residual catalysts are then transferred into the reactors for the ethynylation reaction. The leftovers that remain on the filter paper (right) are the loss of the active site of the catalyst in the process.

Centrifugation is also a suitable but more effective technique that separates the activated catalyst slurry from the reaction mixture in a centrifuge tube. The liquid layer supernatant solution can be easily decanted while the catalyst slurry is retained. It can later be washed and purified using the same procedures. On the other hand, the centrifugation force can disrupt the catalyst's structure, forming a layer of dark brownish residue of the active species at the bottom and a layer of white species of the carriers (i.e., silica) at the surface, refer to Figure 2-7. This leads to desorption and agglomeration of the active species. Moreover, The solid-phase catalyst retains a significant amount of moisture, which may contain impurities. The washing and separation steps may also unintentionally remove the traces of the activated catalyst particles and the leached active cuprous species, resulting in a permanent loss of the active sites. This is a source of catalyst deactivation from both separation techniques.

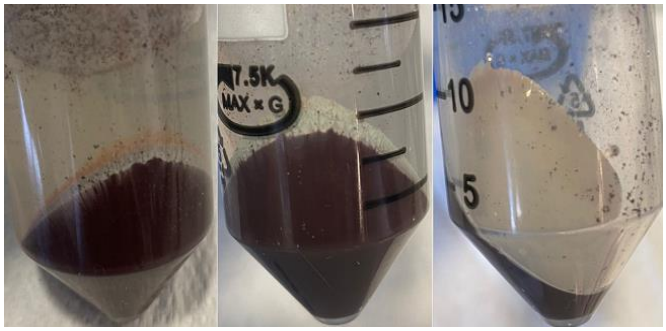

Figure 2-7. The centrifugation technique separates the activated catalyst slurry from the reaction mixture in a centrifuge tube after the activation step of the two-step Reppe ethynylation process. The liquid layer supernatant solution is decanted, while the solid layer catalyst slurry is retained (left). It is then washed and purified using the same methods. However, the retained catalyst slurry after centrifugation contains a relatively large amount of moisture. It may reduce the purity of the catalyst. Additionally, the centrifugation force may also potentially destroy the catalyst's metal-support structure, which causes the leaching of active species (dark brownish residue at the bottom) from the supporting material (white species on the top layer at the surface of the interface).

Washing and Purification of Activated Catalyst Slurry

Washing with an appropriate washing agent is crucial to remove the impurities from the activated catalyst. The impurities, such as the polymeric products from the dissolved formaldehyde and acetylene, might be deposited or adsorbed on the catalyst's surface, causing deactivation. The separation and purification efficiency of the activated catalyst is analyzed by GC-TCD, which measures the residual FA and BYD contents before the ethynylation step. As depicted in Figure 2-8, neither vacuum filtration nor centrifugation methods can completely remove the impurities from the activated catalysts by separation itself. The signals are significantly reduced after one time of washing and nearly disappear after the second washing.

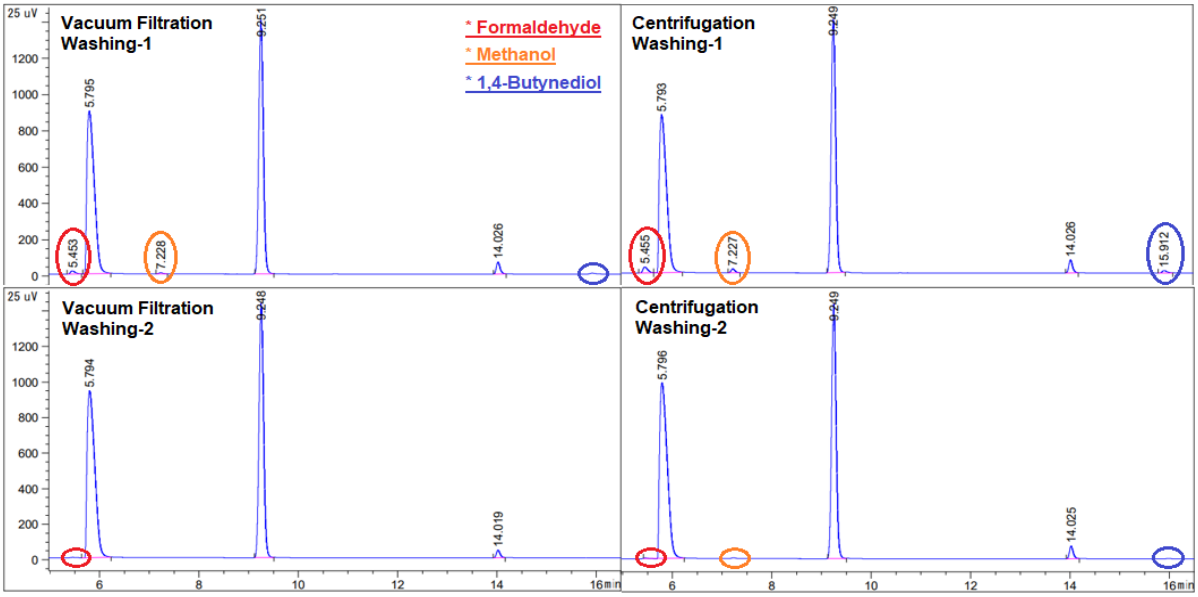

Figure 2-8. The GC-TCD analysis of the supernatant solutions from the washing and purification of the activated catalyst slurries. The chromatogram plots the intensity of a substance's thermal conductivity against its retention time before reaching the detector. The catalysts are separated after washing with water by vacuum filtration (left) and centrifugation (right), respectively, two times. The supernatant solutions obtained after washing are collected and diluted with acetonitrile (MeCN, signals at ~9.5 min). The internal standard (IS), 1.3-propanediol (PDO, signals at ~14.0 min), is added for the quantification. The signals for formaldehyde (red), methanol (orange), and 1,4-butynediol (blue) from each GC chromatogram are marked. The water signal at ~5.8 min can also be identified.

After washing with water for one time, the remaining FA, MeOH, and BYD can be detected, as circled in the top two chromatograms. However, vacuum filtration shows slightly higher separation efficiency than centrifugation due to the smaller signals after calculation with respect to the amount of IS from GC analysis. After the second washing, both chromatograms at the bottom show no detectable signals of remaining substances. There are slightly more observable signals from the one with the centrifugation method as circled. However, the non-detectable signals have to be neglected due to the detection limit.①

The implementation of the proper washing and purification steps eliminates several sources of errors during experiments and analysis, ensuring the accurate determination of the catalytic performance tests in terms of the TOF, BYD yield, and FA conversion. The standardized experimental procedures play a crucial role in allowing reliable and convincing comparisons among the results. It further helps with the investigation of the kinetic studies on the activation and ethynylation rates and potentially of the corresponding reaction mechanisms.

① GC-TCD analysis is able to quantitatively determine FA, MeOH, PA, and BYD with the addition of an internal standard. The oligomeric impurities from formaldehyde, methanediol and trioxane (2-3 units of FA), obtained only at a high concentration of FA, can also be identified in GC. However, the polymeric products, which are mainly formed as a solid phase that deposits on the catalyst surface, will be filtered out before the GC measurement, and thus cannot be identified in GC-TCD. They have to be removed.

Based on the catalytic performance results in Chapter 2.4 and the activated catalysts' analytical data in Chapter 3.1, it has been proven effective and necessary to wash the activated cuprous acetylide-containing catalyst slurry with water two times. It is suggested that the catalyst be washed with methanol once if it needs to be dried for further storage and analysis.

This series of experiments indicates sufficient separation efficiency by centrifugation and the necessity of washing and purifying steps in the two-step process. Another series of experiments on the effect of storage conditions leads to the discussion of the last section of this crucial transition step, which is the storage conditions.

Storage Conditions for Activated Catalyst Slurry

The catalytically active cuprous acetylide-containing species in the Reppe ethynylation process is rarely reported and discussed in the literature regarding its storage methods and conditions. This active species is highly sensitive and explosively decomposed due to the $C{\equiv}C^{2-}$ structure. The cuprous species readily undergoes oxidation to copper(II), which may form a catalytically inactive phase, and a reduction to metallic copper, which may catalyze the polymerization of acetylene and is hazardous to this catalytic reaction. Furthermore, the unavoidable liquid-solid separation, washing, and purification steps of this process bring additional influencing factors that may affect the catalytic performance.

As a consequence, it is worth implementing a systematic investigation to study the effects on storage conditions for the activated catalysts. The proposed catalyst storage conditions include storing in wet slurry form in water, methanol, and formaldehyde solution and dried form in air, acetylene, and an inert atmosphere. To enhance the effects for easy comparison, storage for one-, three-, and seven-day is carried out. The detailed discussion is reported in Chapter 2.4.1.

Based on the experimental results, storing the purified activated catalyst slurry under fresh formaldehyde solution is optimal. It shows excellent catalyst performance and consistency with respect to the yield of BYD. Moreover, it is also the most convenient way for the activated catalyst since the formaldehyde solution will be used directly, without additional treatments, in the catalytic ethynylation step, making the process more manageable and less complex.

In conclusion, the difficulty in the judgment of the separation, purification, and storage efficiency of the activated catalyst slurry, which contains the explosive cuprous acetylides, is the limitation of the precise analysis qualitatively and quantitatively in all steps of the Reppe ethynylation process. The influences can only be partially concluded based on the changes in catalytic activity from the multi-cycle performance tests and the corresponding storage and aging effect tests. The related analysis was further studied at a later stage, as elaborated in Chapter 3.1.

2.1.3 Investigation of Experimental Parameters

The investigation of the experimental parameters for the 3-phase ethynylation process is often overlooked. A deep understanding of their influences is crucial and decisive for different research objectives and to validate the testing results and findings. This work applies a systematic approach to investigate several critical parameters in consideration of the reaction's kinetic and thermodynamic properties and to finalize the standardized reaction conditions of the catalytic Reppe ethynylation process.

The most essential factors are operational safety and simplicity, which are already emphasized during the implementation of the catalytic performance test units and experimental processes. The other of equivalent importance are catalytic activity and reproducibility, which makes the determination of the rate-limiting parameter necessary. Additionally, this section focuses only on the sole effect of each reaction parameter that minimizes the impact other than the catalysis itself. Thus, the catalytic structure-activity relationships can be studied without interference from the effects of experimental procedures and parameters in Chapter 2.2. However, the finalized parameters do not aim to find the optimal values but are the most appropriate ones that compromise all the considerations for sustainable and prosperous research.

In this chapter, unless stated otherwise, the standard pre-catalyst with 35 wt.% copper loading and 4 wt.% bismuth loading supported on silica (CBS) is used. This standard catalyst is synthesized via the co-precipitation (CP) method and calcined (c) at 450 °C. The catalyst 35CuO-4Bi_2O_3/SiO_2_CP-c450 is denoted as CBS-CP-c. The formaldehyde (FA) solution is the self-prepared pH-buffered saturated aqueous solution at pH 7.0. The solution contains 10 wt.% methanol (M), 6 wt.% disodium hydrogen phosphate-sodium dihydrogen phosphate, Na_2HPO_4-NaH_2PO_4 buffer (P), and 37 wt.% paraformaldehyde dissolved in water. The aqueous formaldehyde is denoted as FA-P7.

Grain Size of Pre-catalyst

The grain size of the pre-catalyst may influence the efficiency of the mass transport of the 3-phase ethynylation. In heterogeneous catalysis, the reactants undergo external interphase diffusion through the boundary layer of the bulk phase to the catalyst, followed by intraparticle diffusion through the pores to the inner catalytic surface. They are then adsorbed to the catalytic active sites and form the products of the catalytic reaction. Next, the products are desorbed and diffused out in the same sequence.

The catalyst’s grain size may affect the mass transfer of the internal diffusion in the pores of the catalyst. This is not the sole effect but in combination with factors like stirring efficiency, gas solubility, temperature- and pressure-dependent diffusion coefficient, and concentration

gradients, according to Fick's Laws of diffusion. The direct influence of the grain size is pore diffusion. The larger grain size is more difficult to diffuse homogeneously due to the distance, retention time, and driving force, which limits the catalytic reaction rate.

A series of experiments are performed with a standard catalyst ground and sieved from below 50 µm to up to 1000 µm. The catalytic performance tests of varying catalyst grain sizes in terms of the BYD yield after 5 h and 7 h are depicted in Figure 2-9.

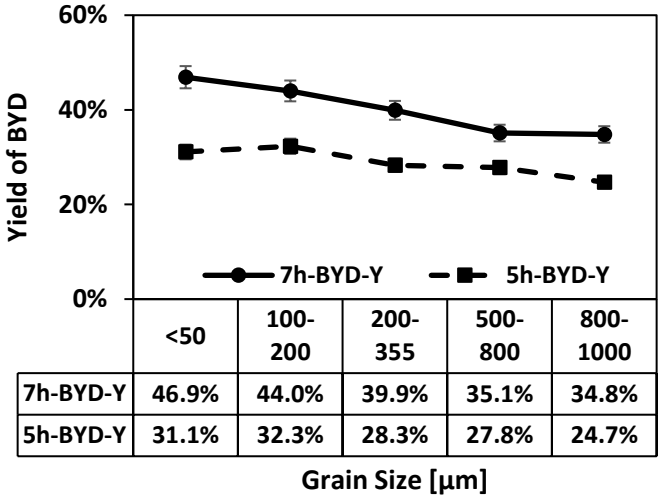

	<50	100-200	200-355	500-800	800-1000
7h-BYD-Y	46.9%	44.0%	39.9%	35.1%	34.8%
5h-BYD-Y	31.1%	32.3%	28.3%	27.8%	24.7%

Figure 2-9. The graph depicted the influences of the grain size of the per-catalyst on the catalytic performance of ethynylation. The yield (Y) of BYD is plotted after 5 h and 7 h of the one-step batch catalytic Reppe ethynylation process with the catalyst's grain sizes below 50 µm, 100-200 µm, 200-355 µm, 500-800 µm, and 800-1000 µm.

A clear trend is obtained that smaller catalyst grain sizes produce higher BYD yields. The results agree with the expectation regarding the limitation of mass transport for internal diffusion through the pores of the catalyst. Based on the results, the optimal grain size is below 50 µm. However, a practical concern is that a grain size that is too small may bring extra challenges in solid-liquid separation and washing of this ethynylation process. It can also be tricky to weigh and transfer the fine catalyst particles. As a result, the catalyst grain size of 100-300 µm is selected as the standard size.

Reaction Temperature and Pressure

The most critical aspect of thermal catalysis is the temperature and pressure of the reaction. It is particularly vital for the Reppe ethynylation process. This series of experiments aims to obtain the best catalytic performance while considering the safety factors and explosion limits associated with acetylene and acetylides. As summarized from the recent publications of the

catalytic ethynylation process in Chapter 1.1.4, the reaction temperature is preferably between 70 to 110 °C, and the acetylene gas pressure is between 1.0 to 1.4 bar.

The experimental results, shown in Figure 2-10, compared the catalytic performance in terms of the BYD yield (Y) in %, the FA conversion (X) in %, and turnover frequency (TOF) in $mol_{BYD} \cdot mol_{Cu}^{-1}\ h^{-1}$ of the standard Reppe ethynylation process at temperatures of 80 °C, 90 °C, and 100 °C and static acetylene pressures of 1.1 bar and 1.2 bar, respectively. The conditions were chosen in the preferred ranges to avoid unnecessary repeating work that the pioneers had already studied and concluded.

The experiments were conducted using a one-step process with a two-flask parallel test unit. This allows the elimination of possible interfering factors, like the complicated transition step.

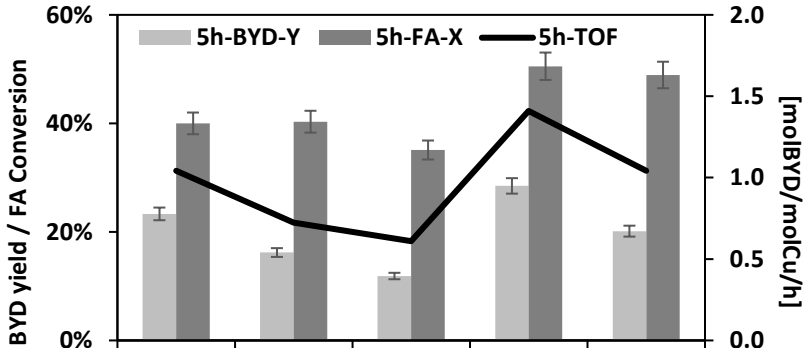

	1.1 bar, 90°C	1.1 bar, 100°C	1.2 bar, 80°C	1.2 bar, 90°C	1.2 bar, 100°C
5h-BYD-Y	23.3%	16.2%	11.9%	28.5%	20.1%
5h-FA-X	40.0%	40.3%	35.1%	50.5%	48.9%
5h-TOF	1.042	0.724	0.610	1.410	1.042

Figure 2-10. The graph depicted the influences of reaction temperatures of 80 °C, 90 °C, and 100 °C and static acetylene gas pressures of 1.1 bar and 1.2 bar on the catalytic performance of ethynylation. The yield of BYD is plotted after 3 h and 5 h of the one-step batch catalytic ethynylation process.

From Figure 2-10, based on the BYD yield, FA conversion, and TOF after 5 h of the catalytic ethynylation process, the optimal ethynylation condition at a temperature of 90 °C and absolute acetylene pressure of 1.2 bar shows the best performance. These conditions are applied as the standard experimental procedure of this work.

The conclusion drawn from the experimental results can also be explained theoretically. The Arrhenius equation and Henry's Law, as shown in Equation 2-1, practically implicate the correlations of reaction temperature and pressure with the chemical kinetics, respectively, in general thermal catalysis reactions, which can be used to explain the phenomena from the catalytic Reppe ethynylation process.

$$k = A*\exp[-E_a/RT] \quad (1)$$

$$C = k*P_{gas} \quad (2)$$

Equation 2-1. (1). Arrhenius equation shows the relation between the rate of reaction and the absolute temperature, where k is the rate constant, A is the pre-exponential factor, E_a is the activation energy in Joule per mole, R is the universal gas constant in Joule per Kelvin per mole, and T is the absolute temperature in Kelvin. (2) Henry's Law equation shows the relation between gas solubility and the partial pressure of the gas, where C is the solubility of gas at a fixed temperature in a particular solvent in the mole of gas per liter, k is Henry's law constant in mole per Atmosphere, and P_{gas} is the partial pressure of the gas in Atmosphere.

The Arrhenius equation formulates that the rate of the chemical reaction is exponentially proportional to the absolute temperature. This means that increasing the temperature provides additional energy to overcome the activation energy barrier and allow the catalytic reaction to take place, thereby increasing the rate of reaction. This applies to the catalyst performance results at 80 °C and 90 °C at 1.2 bar, where the temperature at 80 °Cis not sufficient. However, it doesn't seem to apply to ones at 90 °C and 100 °C for both series of experiments at 1.1 bar and 1.2 bar, in which a higher reaction temperature gives a lower yield and conversion.

Therefore, Henry's Law is considered, which formulates that the amount of gas dissolved in the liquid phase is directly related to the partial pressure of the gas above the liquid. The increasing pressure from 1.1 bar to 1.2 bar is crucial for both series of experiments at 90 °C and 100 °C, as it allows a higher concentration of dissolved acetylene gas in the aqueous solution to be involved in the catalytic ethynylation process. The amount of dissolved acetylene, due to its considerably low solubility, is potentially the rate-limiting reagent, as the other source of limitations, such as the amount of formaldehyde and active sites and the mass transport efficiency, can be easily eliminated by changing the respective parameters.

The conflicts in the results on the effects of the reaction temperature and acetylene pressure once again highlight the highly complicated reaction kinetics that are to be revealed of the 3-phase catalytic ethynylation. It is also suggested that another factor exhibits a dominating effect against the effects of temperature, which is proposed to be gas solubility, as is discussed below.

Acetylene Gas Solubility

Acetylene gas solubility in the reaction mixture is particularly crucial in the 3-phase catalytic ethynylation process. Acetylene is the catalyst activation agent that forms the catalytically active cuprous acetylide from the copper-based pre-catalyst and is the starting material of the catalytic reaction that forms the products PA and BYD with formaldehyde. Understanding the factors that affect acetylene gas solubility, namely temperature, acetylene pressure, and the composition and concentration of the reaction mixture, is necessary for further studies.

Throughout the static ethynylation process in this work, the temperature and acetylene pressure remain constant. However, the composition of the reaction mixture changes over time. The saturated FA at the beginning slowly consumed and produced BYD, significantly altering the composition of the reaction mixture. This may potentially affect the acetylene gas solubility.

Acetylene solubility in water is reported in *Aqueous Solutions* [180], as shown in Table 2-1. The data was cited by the *Handbook of Aqueous Solubility Data* [181] in 2010, which claims it is an *"extensive compilation of published data for the solubility."* It shows that acetylene solubility decreases by more than half when the temperature rises from 20 °C to 60 °C. No data is found at temperatures above 60 °C. The solubility of acetylene in donor solvents [182], in polar and non-polar solvents [183], and alcohols and ketones [184] are also reported.

Table 2-1. The solubility of acetylene gas at respective temperatures according to *Aqueous Solutions* [180] and *Handbook of Aqueous Solubility Data* [181].

Temperature [°C]	***Solubility [g/L]***
0	*2.30*
20	*1.20*
60	*0.51*

Jadkar and Chaudhari [185] studied the acetylene solubility in formaldehyde and 2-butyne-1,4-diol solutions from 7 °C to 55 °C with a self-modified apparatus in 1980. Their findings show that the acetylene solubility is inversely proportional to the temperature based on the Arrhenius plot, corrected to 1 atm vapor pressure according to Henry's Law, which agrees with the data shown above. This provides a strong argument for the decision to perform ethynylation at a lower temperature of 90 °C instead of 100 °C. Furthermore, they concluded that the solubility of acetylene in an FA solution is the same as that in water where the FA concentration is below 6.57 M (approximately 19 wt.%). In contrast, acetylene solubility increases by about 32% at 20 °C with increasing FA concentration to 12.78 M at saturation (37 wt.%). Similarly, the acetylene solubility remains unchanged when BYD concentration is below 3 M. It increases by about 48% when BYD concentration rises to 9.2 M.

Based on the catalytic ethynylation performance tests in general, the initial FA concentration is at about 12.8 M and reduces to 6.4 M (~50% FA conversion) after approximately 8-20 h. At the same time, the BYD concentration reaches 3 M (approximately 15% yield and 70% selectivity of BYD). This concludes that the acetylene solubility remains low but constant since the relatively minor changes in solubility offset each other due to the reduction in FA concentration but the rise in BYD concentration throughout the ethynylation process. To avoid acetylene solubility becoming the rate-limiting parameter, it is essential to apply the static acetylene absolute pressure of 1.2 bar during the ethynylation, as supported by Henry's Law and experimentally from Figure 2-10.

Stirring Efficiency

Stirring efficiency is also a key factor and directly influences acetylene pressure and solubility in the 3-phase reaction. Effective stirring helps to speed up the catalytic reaction by reducing the mass transport limitation in the bulk liquid phase, where the dissolved acetylene and the formaldehyde molecules can be homogeneously dispersed to the catalyst interface and further diffuse to the active sites to proceed with the catalytic reaction. Many factors can influence stirring efficiency, such as the type of reaction flasks (size, shape, baffles), the type of magnetic stirrers, and the stirring rate. It may create different stirring patents, like the vortex, axial- and radial-turbulent, that change the homogeneity of the mixture and the mass transport efficiency.

This series of experiments uses 18 mm oval-shaped magnetic stirrers at 400 rpm, 700 rpm, and 1000 rpm to perform the one-step ethynylation process, as shown in Figure 2-11.

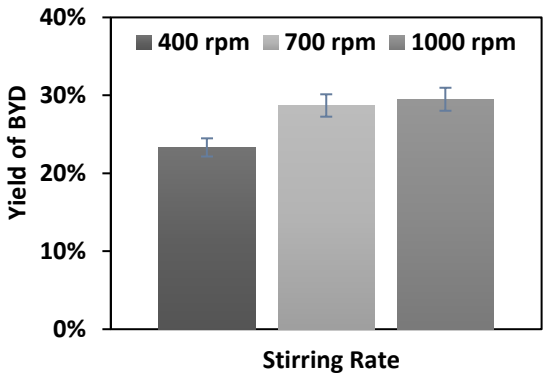

Figure 2-11. The graph depicted the influences of the stirring rate of an oval-shaped magnetic stirrer in a 100 mL round bottom flask on the catalytic performance of ethynylation. The yield of BYD is plotted after 3 h and 5 h of the one-step batch catalytic Reppe ethynylation process in the parallel test unit. The stirring rates are set at 400 rpm, 700 rpm, and 1000 rpm.

The yield of BYD is proportionally related to the stirring rate, which agrees with the assumption that the higher stirring rate overcomes the mass transport limitation in the 3-phase catalytic reaction, thus increasing the reaction rate and resulting in a higher yield of BYD.

However, the stirring capacity is considered. This is because the suspension slurries from the ethynylation reaction can be highly viscous, so the magnetic stirrer may not be able to stir consistently, especially in the Carousel unit. For example, the pre-catalyst contains magnesia, which is difficult to separate after activation, and the reaction mixture shows high viscosity. The magnetic force is not sufficient to stir the reaction mixture effectively at above 600 rpm in the Carousel unit. The inconsistency in stirring is sometimes also found when higher amounts of catalysts are used and in long-term ethynylation experiments. Thus, to ensure the standardization of the reaction parameters, the best stirring rate by the magnetic stirring device for the Carousel is between 400-600 rpm and between 700-1000 rpm for the parallel test unit.

The lack of stirring capacity by magnetic stirring creates the major challenge of producing comparable, reliable, and reproducible catalytic performance results. It also created troubles during the transition step when handling the activated catalyst slurry. These problems initiate the necessity to investigate the appropriate catalyst-to-solution ratio of catalytic ethynylation, which may potentially be beneficial in ensuring the consistency and sufficiency of stirring.

Catalyst-to-Solution Ratio

A series of ethynylation performance tests with 0.5 g, 1.0 g, 2.0 g, 3.0 g, 5.0 g, and 6.0 g of CBS pre-catalyst in 50 mL of aqueous FA solution were performed, as shown in Figure 2-12.

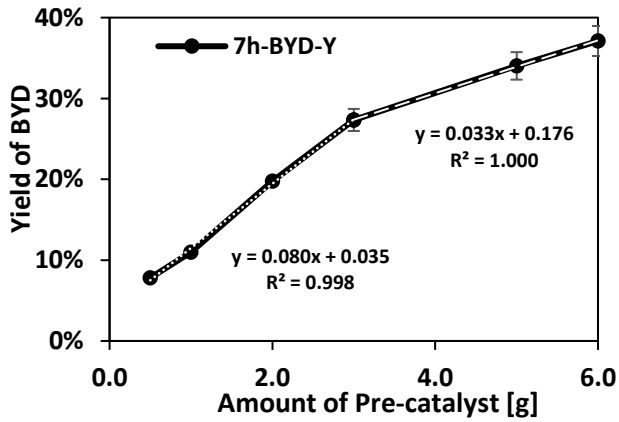

Figure 2-12. The graph depicted the influences of the catalyst-to-formaldehyde ratio on the catalytic performance of ethynylation. The yield of BYD is plotted after 7 h of the one-step ethynylation process.

The appropriate catalyst-to-solution ratio is essential to ensure stirring efficiency and to analyze the limiting reagent of the catalytic reaction. Since the acetylene gas solubility in the reaction mixture is unchangeable under the ethynylation condition at static 1.2 bar and 90 °C. It is necessary to eliminate another potential source of the rate-limiting parameters, either the limited formaldehyde concentration or the catalytic activity and the number of active sites.

The curve can be divided into two parts, with significant differences in the gradient of the slopes, at the turning point corresponding to 3.0 g of pre-catalyst, as labeled with two trendline equations in Figure 2-12. This shows that with a higher amount of pre-catalysts from 0.5 g to 3.0 g, the yield of BYD increases linearly. However, further increasing the pre-catalyst to 5.0 g and 6.0 g does not increase the BYD yield at the same rate. This represents the amount of pre-catalyst, which is also assumed to be the equivalent amount of catalytically active copper phase, becoming the excess reagent that no longer affects the rate of the catalytic reaction. As a result, it is appropriate to use the catalyst-to-formaldehyde between 0.5 g-3.0 g to 50 mL. This is finalized at 2.0 g catalyst to 40 mL formaldehyde at the standard parameters.

2.2 Optimization of Catalyst Characteristics and Structure-Activity Relationships

The catalytic structure-activity relationships in heterogeneous catalysis are also of interest in the catalytic ethynylation process. Recent publications have reported the new generations of copper-based ethynylation catalysts derived from the one proposed by Reppe in the 1940s. These reported catalysts, whether synthesized with functional promoters or carriers or employing innovative catalyst synthesis and post-treatment methods, bring specific characteristics to the catalyst to enhance the catalytic performance in terms of activity and stability. The newly generated pre-catalysts have been extensively characterized using a large variety of characterization techniques and then tested in the Reppe ethynylation reaction.

In this chapter, the catalytic structure-activity relationships in the catalytic ethynylation of formaldehyde are studied using standard experimental procedures and parameters. Abundant catalysts of different components and compositions, as shown in Chapter 2.2.1, by various synthesis and post-treatment methods, as shown in Chapter 2.2.2, are prepared and tested. The catalyst precursors are also characterized and analyzed by selected analytical techniques that are of direct necessity in this specific research work, as shown in Chapter 2.2.3.

The catalyst precursor, CBS-CP-c, is 35 wt.%CuO-4 wt.%Bi_2O_3 on SiO_2 synthesized by co-precipitation and calcined at 450 °C, and the aqueous formaldehyde solution, FA-P7 that is 37 wt% FA with NaH_2PO_4-Na_2HPO_4 buffer adjusted at pH7, is used as standard. Their catalytic performance and analytical results serve as the benchmark for reference of the new inventions. The catalyst, depending on different experiments, will be given specified denoted names. For comparison, commercial catalysts and formalin solutions with unknown properties and specifications are tested in several experiments to support the findings of the current research.

The catalytic activity defines the catalytic performance in terms of the yield and the selectivity of the desired product, BYD, and the conversion of the educt, aqueous FA solution. The absolute value, turnover frequency (TOF), in terms of the mole of BYD produced per unit mole of Cu^{2+} species in the pre-catalyst per hour of ethynylation ($mol_{BYD} \cdot mol_{Cu2+}^{-1} \cdot h^{-1}$), is applied.

2.2.1 Catalytic Performance Based on Catalyst Components and Compositions

From Reppe's invention in the 1940s, the conventional ethynylation catalyst precursor synthesized by the co-precipitation method contains copper species as the active phase, bismuth species as the promoter, and silica as the carrier. As detailed in Chapter 1.1.4, the stable copper(II) species in the pre-catalyst is reduced into copper(I) and activated *in situ* into catalytically active cuprous acetylide species in formaldehyde solution and acetylene atmosphere. The bismuth species, mostly Bi_2O_3, reduce the size of copper crystallites to improve copper dispersion, hence increasing the active surface. It also stabilizes the active copper(I) species by inhibiting the copper(II) over-reduction into metallic copper, which prevents the catalyst from deactivation. The silica, SiO_2, as an inert carrier with uniform mesoporous structures and a large specific surface area, will form a copper phyllosilicate structure with strong metal-carrier interaction, which provides high catalyst stability.

With these critical factors of the functional promoters and carriers, their functions to enhance the catalytic activities and catalyst stabilities in the ethynylation process by increasing the number and stabilizing the active copper(I) sites are investigated.

However, the exact structure of catalytically active cuprous acetylide species is challenging to identify and even more difficult to quantify. It is only assumed that the number of copper(II) sites is equivalent to that of the cuprous acetylide active sites if the complete conversion from copper(II) to the copper(I) active phase is achieved. Hence, this chapter only focuses on the catalytic structures of the pre-catalysts and their catalytic performance.

Therefore, several series of experiments are planned. First, the effects of different copper-loading from 15-55 wt.% in the pre-catalyst are investigated. Additionally, different copper(II) species, such as CuO, $Cu_2(CO_3)(OH)_2$, $Cu_2(NO_3)_2(OH)_2$, and $CuSiO_3$ or $CuBi_2O_4$ spinel, obtained by different thermal treatments, are also investigated. Next, the role of bismuth (Bi_2O_3) in reducing the crystallite size of copper by improving dispersion and stabilizing copper(I) is evaluated. The replacement or addition of new species as functional promoters and carriers is also studied. These include magnesia (MgO), alumina (Al_2O_3), zinc oxide (ZnO), and their combinations in molar ratios of 1-to-1.

All of the catalysts are synthesized by co-precipitation methods under the standard procedures and conditions, as elaborated in Chapter 5.3.1, unless stated otherwise.

Structural Effects of the Pre-catalyst by Thermal Treatments

The co-precipitated catalysts are dried at 80 °C overnight and then ground, sieved, and characterized. They can be applied directly as the ethynylation catalyst. However, drying at 80 °C is not able to decompose OH^-, NO_3^-, and CO_2^{2-} species from the catalysts. Hence, calcination at a higher temperature is necessary to standardize the pre-catalyst's composition by decomposing the impurities and oxidizing the copper species to CuO.

The suitable calcination temperature for the silica-supported Cu-Bi oxide (CBS) ethynylation pre-catalyst is experimentally determined at 450 °C. The photos in Figure 2-13 show the color of CBS-CP pre-catalysts calcined at 80 °C, 300 °C, 450 °C, and 700 °C. It also shows the color change of CBS-CP pre-catalysts containing 15 wt.% to 55 wt.% copper that are dried at 80 °C (d80) and calcined at 450 °C (c-450).

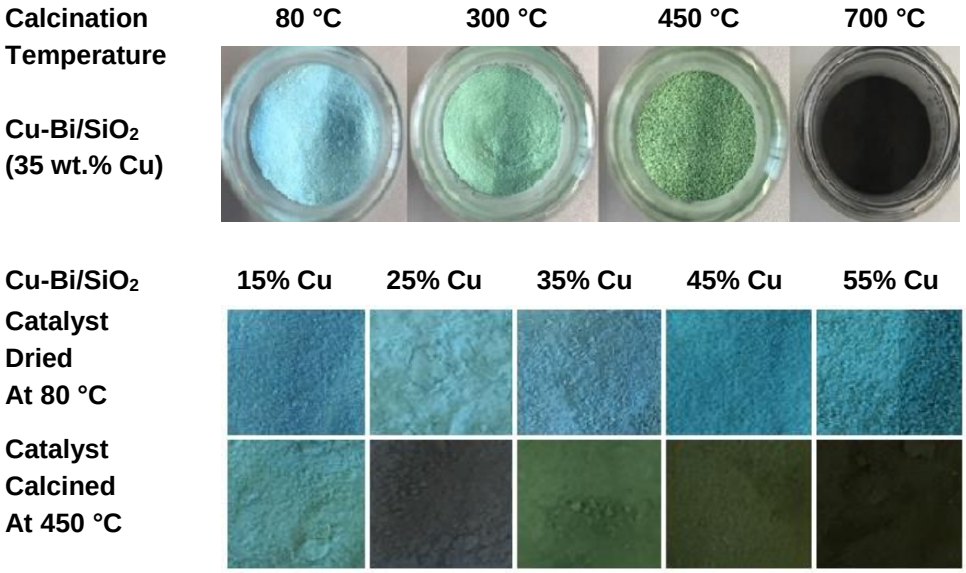

Figure 2-13. The photos of the powder Cu-Bi/SiO_2 catalysts synthesized by co-precipitation method. The colors of the pre-catalysts with 35 wt.% copper loadings are calcined at 80 °C, 300 °C, 450 °C, and 700 °C (top). The colors of the pre-catalysts with copper loading of 15 wt.%, 25 wt.%, 35 wt.%, 45 wt.%, and 55 wt.% are calcined at 80 °C and 450 °C (bottom).

The calcined pre-catalysts are analyzed by TGA/DSC-MS to determine the decomposition temperatures, the mass, and the decomposed species of the impurities present in the pre-catalysts (refer to Figure 2-24). The phase identification of the pre-catalysts is determined by PXRD (refer to Figure 2-21). The pre-catalyst compositions, like the actual copper loadings, are determined by ICP-OES, and the precatalyst's surface area and porous size are determined by N_2-physisorption via BET and BJH methods (refer to Table 2-2 and Table 2-3). Their catalytic ethynylation performance tests are shown in Figure 2-14 and Figure 2-15.

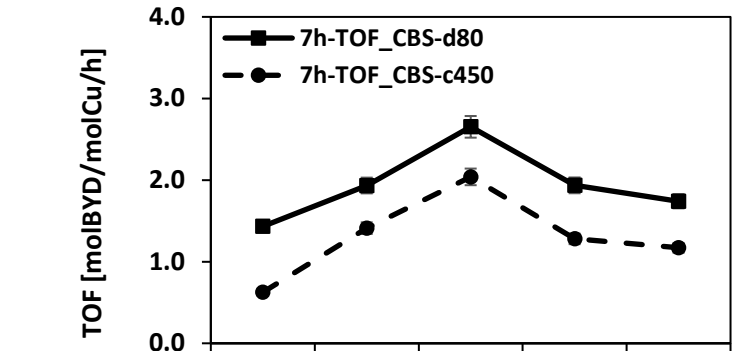

	15Cu	25Cu	35Cu	45Cu	55Cu
7h-TOF_CBS-d80	1.43	1.93	2.65	1.94	1.74
7h-TOF_CBS-c450	0.62	1.41	2.04	1.28	1.17

Figure 2-14. The graph depicted the catalytic performance in terms of TOF in $mol_{BYD} \cdot mol_{Cu2+}^{-1} \cdot h^{-1}$ of Cu-Bi/SiO_2 (CBS) pre-catalyst calcined at 80 °C and 450 °C with copper loading of 15 wt.%, 25 wt.%, 35 wt.%, 45 wt.%, and 55 wt.%, respectively, after 7 h of one-step batch Reppe ethynylation process. The exact copper loading in *wt.%* in the catalyst is determined by the ICP-OES technique; the amount of copper in *mmol* is then converted per *gram* of Cu-Bi/SiO_2 pre-catalyst, as shown in Table 2-2.

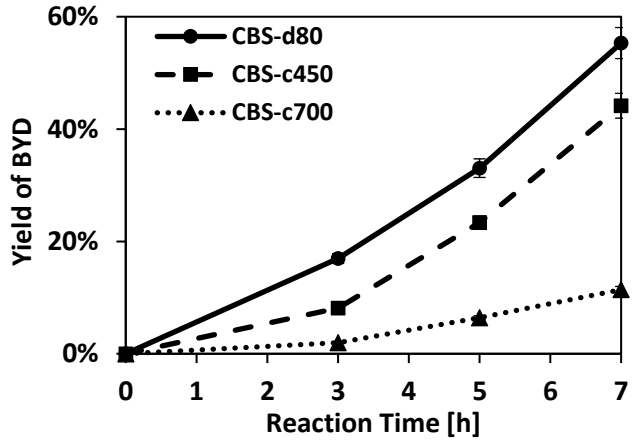

Figure 2-15. The graphs illustrate the catalytic performance test in yield of BYD over 7 h of the one-step batch ethynylation process with Cu-Bi/SiO_2 (CBS) pre-catalysts calcined at 80 °C, 450 °C, and 700 °C.

It can be seen in Figure 2-14 that CBS-d80 pre-catalysts show higher TOF after 7 h of ethynylation than the ones with CBS-c450, regardless of copper loadings. It is known that during the initial stage of one-step catalytic ethynylation, copper(II) species in different phases are activated gradually over time via reduction into copper(I) and conversion with dissolved acetylene into catalytically active cuprous acetylide species. It is then simultaneously produced BYD as the product in this catalytic reaction. However, it is expected that CuO in CBS-c450 has a different reducibility than the other copper(II) phases in CBS-d80. Thus, it can be

concluded that the initial activity of the catalyst in 7 h largely depends on the activation rate of the pre-catalyst instead of the catalytic activity of the activated catalyst. This argument is proven by the yield of BYD versus the time plot, as shown in Figure 2-15.

In the *BYD yield vs. time* graph, upward curves are observed in all three plots, including CBS-c700, which has a considerably low overall yield and a very gentle slope. It can also be seen that the gradients of the slopes, again, for all three plots, get steeper at a later time between 5-7 h, which represents an increasing reaction rate over time. This supports the argument that pre-catalysts are gradually activated at the beginning and gain catalytic activity by the growing number of active sites formed *in situ*. The catalytic performance in BYD yield then becomes constant when the pre-catalysts are completely activated. The curve will become linear. It will finally decline either when the catalyst deactivates or when the limiting reagent is used up. This is observed in the ethynylation step of the two-step process or the long-term performance test, such as the ones shown in Figure 2-4 and Figure 2-5 in the previous chapter.

Another compelling observation from the diagram as evidence is the increasing trends of the curves for CBS-d80 and CBS-c450. In the first 3 hours, the gradients of the two plots are clearly varied; it shows that the pre-catalysts are activated at different rates, thus showing a different yield of BYD corresponding to the number of active sites. However, from 3 to 7 hours, the gradients of the two plots are nearly the same, which means that both pre-catalysts are completely activated. The same amount of copper in the pre-catalysts is converted into the same number of active sites, which gives the same rates of the catalytic reaction to yield BYD.

On the other hand, as the objectives of this series of experiments, the significant differences in the BYD yield and the gradients of the slope (reaction rate) of the pre-catalysts calcined at different temperatures are discussed. This is, as proposed above, because of the differences in the activation rate of the copper species in the pre-catalysts. It has been found by PXRD and TGA/DSC-MS that the copper species in the pre-catalysts is mainly the Malachite (basic copper(II) carbonate, $Cu_2CO_3(OH)_2$) and Rouaite (copper(II) hydroxide nitrate, $Cu_2NO_3(OH)_3$) when calcined at 80 °C, depending on the co-precipitation conditions, whether nitric acid, sodium hydroxide, or sodium carbonate is added as the precipitation agent to maintain the constant pH value. When the pre-catalyst is calcined at 450 °C, the CuO is present, whereas at 700 °C, the $CuBi_2O_4$ spinel is present. Each copper species in the pre-catalysts exhibits different reducibility due to the bonding strengths of their structural and crystalline properties. It affects the rate of activation and, thus, the initial catalytic activities that yield BYD.

The low yield of CBS-c700 is believed to be due to the reducibility and slow release of copper(II) ions from the strongly bonded spinel structure, which limits the activation rate and results in poor initial activity. Nevertheless, the CBS-c700 may still be a potential ethynylation catalyst that shows excellent long-term stability and activity, but this is not the focus of the current work.

Based on the experimental results, CBS-d80 shows the best performance in ethynylation. However, it cannot be used at the standard pre-catalyst because it is difficult to determine the exact structure and composition of the copper species. It is highly probably a mixture of copper nitrates and copper carbonates composites that are composed of various amounts of hydroxides and water molecules, as determined by the TGA-MS. It is also not possible to be identified by PXRD due to its excellent copper dispersion on the silica support, which mainly exists as XRD amorphous. However, suppose the pre-catalyst is calcined at 450 °C; in this case, it can be sure that all the hydroxide, nitrate, and carbonate can be thermally decomposed, and all copper phases will be oxidized into CuO. For standardization, consistency, and reproducibility reasons, pre-catalyst calcined at 450 °C is preferred.

Effects of Copper Loading from 15-55 wt.% in the Pre-catalyst

After eliminating the mass transport and interface diffusion limitations by adjusting the stirring rate, catalyst grain size, and catalyst-to-formaldehyde ratio, the limitation due to the catalytic activity correlates to the number of active copper species that convert from the copper loading in the pre-catalyst is investigated.

The co-precipitated Cu-Bi/SiO_2 pre-catalysts contain 15 wt.%, 25 wt.%, 35 wt.%, 45 wt.%, and 55 wt.% of copper, respectively, are denoted as 15/25/35/45/55CBS-d80/c450. The actual copper loading is determined by ICP-OES, and the amount of copper in *mmol* in every *gram* of pre-catalyst is converted, as shown in Table 2-2. The catalytic performance of the catalysts in terms of TOF, calculated based on the actual copper amount that is assumed to be converted equivalently into the active phase, is also shown in Figure 2-14 above.

Table 2-2. The listed Cu-Bi/SiO_2 pre-catalysts were synthesized by co-precipitation with copper loading of 15 wt.%, 25 wt.%, 35 wt.%, 45 wt.%, and 55 wt.%. The catalysts are either dried at 80 °C or calcined at 450 °C. The exact copper loading in *wt.%* is determined by the ICP-OES technique; the amount of copper in *mmol* is then converted per 1 g of Cu-Bi/SiO_2 pre-catalyst.

Copper Loading in Cu-Bi/SiO_2	***Copper Loading Determined in ICP-OES***		***Copper Amount per 1g Catalyst [mmol]***	
	80 °C	***450 °C***	***80 °C***	***450 °C***
15 wt.%	*13.9%*	*14.4%*	*2.19*	*2.27*
25 wt.%	*23.0%*	*26.5%*	*3.62*	*4.16*
35 wt.%	*31.5%*	*32.8%*	*4.96*	*5.15*
45 wt.%	*39.0%*	*42.5%*	*6.13*	*6.69*
55 wt.%	*48.5%*	*54.4%*	*7.62*	*8.56*

From Figure 2-14, the TOF reaches the highest at 35CBS. It means that when the copper loading increases from 15 wt.% to 35 wt.%, the TOFs increase proportionally. When further

increasing to 45 wt.% and 55 wt.%, the TOFs cannot increase anymore but start to decline. This represents the active copper site becoming saturated and in excess. Too high copper loading will not contribute to improving the catalytic activity but adversely cause agglomeration of the active sites and the formation of crystallines of copper species, which causes deactivation. It is partially proven by the PXRD analysis of CBS pre-catalysts, for which 15, 25, and most of 35 show XRD-amorphous. Some of 35 and most of 45 and 55 show different degrees of XRD-crystalline with unique reflexes corresponding to CuO. It also shows that most of the co-precipitated CBS pre-catalysts are XRD-amorphous due to the high copper-bismuth dispersion on silica.

As a result, 35 wt.% of copper loading is selected for the co-precipitation of Cu-Bi/SiO_2 pre-catalyst for the Reppe ethynylation process for its best catalytic performance.

Role of Bismuth as Promoter in Catalytic Ethynylation

Bismuth plays a crucial role in Cu-Bi/SiO_2 ethynylation catalyst. The standard pre-catalyst contains 4 wt.% bismuth in the form of bismuth oxide (Bi_2O_3) and serves as a promoter and inhibitor. This dual function of bismuth significantly enhances the copper dispersion, thereby increasing the potential number of active sites. Moreover, it stabilizes the active copper(I) species by preventing it from over-reduction into the catalytically poisonous metallic copper.

A series of experiments are conducted with co-precipitated pre-catalysts with various bismuth loadings at 0 wt.%, 4 wt.%, and 8 wt.%, denoted as C0BS, C4BS, and C8BS, respectively. Their catalytic performance in the 7.5 h ethynylation process is shown in Figure 2-16.

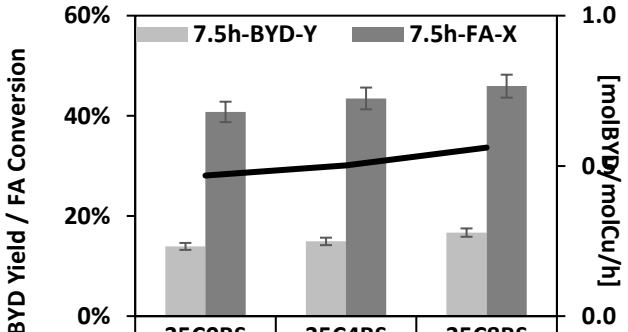

	35C0BS	35C4BS	35C8BS
7.5h-BYD-Y	13.9%	14.9%	16.7%
7.5h-FA-X	40.8%	43.5%	45.9%
7.5h-TOF	0.468	0.502	0.561

Figure 2-16. The graphs illustrate the catalytic performance in yield of BYD, conversion of FA, and TOF over 7.5 h of the one-step batch ethynylation process with CBS pre-catalysts consisting of 0 wt.%, 4 wt.%, and 8 wt.% of bismuth.

Although the roles of bismuth species in the CBS ethynylation catalyst have been established through analytic techniques like XRD and TPR, interpreting its influence on the catalytic performance in BYD yield, FA conversion, and TOF is still necessary.

The results show a generally increasing trend with higher bismuth contents that agree with the previous discussion and prove the role of bismuth as a promoter to improve the catalytic performance of the standard CBS ethynylation catalysts. However, 4 wt.% of bismuth is still preferred over 8 wt.%. This is because the findings from PXRD of the spent catalysts show that bismuth species may form highly crystalline species like $(BiO)_2CO_3$ (refer to Figure 2-32) and deposit on the catalyst surface. Although there is no direct impact of the Bi-containing crystallites on the catalytic performance, the high Bi content in the catalyst may interfere with further investigations and identifications of the formation of the catalytically active cuprous acetylide species. Thus, 35C4BS will still be used as the standard catalyst in this work.

The Promoting and Supporting Effects of Various Species

Inspired by the excellent promoting effect of the bismuth species in the ethynylation catalyst, highlighted by Reppe in the 1940s, recent studies have also explored a large variety of promoters and carriers, aiming to generate a new ethynylation catalyst showing outstanding catalytic activity and stability.

This work investigates a few specific promoters and carriers, like magnesia (MgO), alumina (Al_2O_3), and zinc oxide (ZnO). The selections are either suggested by experienced technicians and recent publications or motivated by the latest industry developments. The most promising one is magnesia, denoted as CBSM, CSM, or CM. This catalyst is already widely applied in industrial production. Magnesia in silica-magnesia carriers provides the surface basicity of the catalyst [118]. It strengthens the interaction with copper species and stabilizes the copper(I) active phase, thereby improving the catalytic activity.

A similar effect also contributes to using zinc oxide as the carrier, denoted as CBZS, CZS, or CZ. It provides moderate basic sites that form a strongly interacted CuO-ZnO interface. It enhances the adsorption of the carbonyl oxygen of formaldehyde with the electropositivity of $C^{\delta+}$, which increases the formation rate of the production of this catalytic reaction.

The introduction or the replacement with alumina into the ethynylation CBS catalyst, denoted as CBSA, CSA, or CA, in contrast, creates acidic sites [118], which may polymerize the dissolved acetylene and block the active surface of the catalyst, lowering the catalytic activity. However, the alumina species may potentially improve the catalytic stability and long-term activity, which might be a field for future work.

The abovementioned copper-based pre-catalysts with different promoters and carriers are synthesized and characterized according to the standard procedures described in Chapter 5.3.1. Their catalytic performance in ethynylation is shown in Figure 2-17.

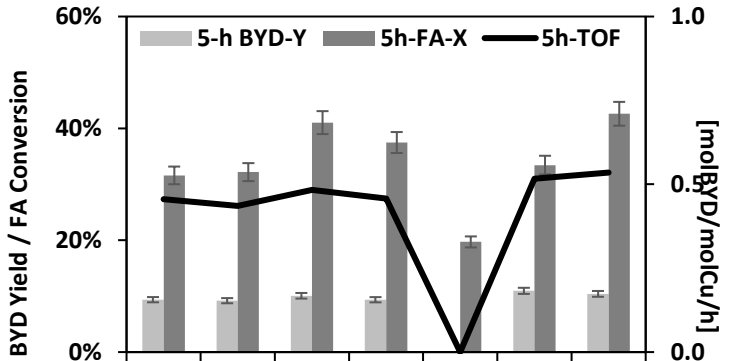

	CS	CAS	CA	CMS	CM	CZS	CZ
5-h BYD-Y	9.4%	9.2%	10.1%	9.4%	0.0%	11.0%	10.4%
5h-FA-X	31.6%	32.2%	41.0%	37.5%	19.7%	33.4%	42.6%
5h-TOF	0.456	0.436	0.483	0.457	0.000	0.517	0.535

Figure 2-17. The graphs illustrate the catalytic performance test in yield of BYD over 5 h of the one-step batch ethynylation process with copper-based pre-catalysts with silica (CS), alumina-silica (CAS), alumina (CA), magnesia-silica (CMS), magnesia (CM), zinc oxide-silica (CZS) and zinc oxide (CZ), as promoters and carriers.

The unexpected result is that the CM pre-catalyst has no initial activity. No BYD can be detected from GC-TCD analysis, which gives a 0% yield and TOF. From observation during the experiment, the CM pre-catalyst is highly viscous. It is difficult to stir during ethynylation and also challenging to filter during sampling for GC measurement. It is suspected that the BYD formed may be trapped with the viscous catalyst slurry and filtered away; thus, no signal of BYD can be detected by GC-TCD.

From the results of the other catalysts, the absolute variation is only about less than 2% in BYD yield. It is difficult to conclude since, as mentioned, only an initial activity of 5 h is shown. This also explains the failure of the DoE evaluations of a similar series of experiments with various catalyst carriers, in which the variations of the catalytic performance results are too less significant to decide whether they are caused by the catalytic activity or simply by the errors.

The influence of different promoters and carriers is not significant and cannot further enhance the catalytic performance. Hence, the standard CBS pre-catalyst will be used.

2.2.2 Catalytic Performance Based on Catalyst Synthesis Techniques

Several catalyst synthesis techniques, other than co-precipitation, are also reported in recent publications for Reppe ethynylation pre-catalysts, such as incipient wetness impregnation (IWI), ammonia evaporation (AE), and deposition precipitation (DP). Each technique has its limitations for the synthesis, such as the limited solubility of the metal salts or components in reagents like ammonia solution. In contrast, each method has its strengths in catalytic performance and may help in a deeper investigation of the reaction mechanism.

This work first studies the ethynylation pre-catalysts synthesized under different co-precipitation conditions, like the pH values and precipitating agents, their properties, and catalytic performance, and finalizes the optimal co-precipitation conditions. Then, they are compared with the pre-catalysts synthesized by IWI, AE, and DP methods with specially modified procedures and conditions. Their synthesis procedures are shown in Chapter 5.3.1, and characterizations are shown in Chapter 2.2.3. The catalytically active Cu_2C_2-containing catalysts are also synthesized, but they are discussed in Chapter 3.2.

Co-precipitation at Varied pH Values and Precipitation Agents

Co-precipitation is used as the standard method to synthesize the Reppe ethynylation pre-catalysts, like CBS and other catalysts of diverse compositions and components. This is the most applied method in research and industry since the invention of this process.

The standard co-precipitation conditions of 500 rpm stirring, 60 °C, and pH 7 using sodium carbonate as a precipitating agent to maintain the pH value are monitored by a magnetic stirring hotplate and an automatic pH titrator. The metal salt solutions are diluted depending on the respective concentration of the solutions and the water solubility of the metal salts. The solutions are added simultaneously via peristaltic pumps at about 2 mL/min.

All these parameters are influential to the catalyst formation. The stirring rate impacts the homogeneity of the catalyst. It has to be adjusted time by time to ensure sufficient mixing when the suspension of the precipitated catalysts is increasing over time. The flow rate is also decisive for the homogeneity of the catalyst and the copper dispersion on the carriers. Additionally, it affects the consistency of the pH conditions during co-precipitation. It has to be adjusted case by case, depending on the pH value of the mixed metal salt solutions, to ensure the selected precipitating agent is sufficient to maintain the pH value. This will result in different crystallinities in copper species. The pH values and the precipitating agents lead to the formation of varying copper phases and crystal structures.

A series of experiments are performed to investigate CBS pre-catalysts co-precipitated from pH 3-10, using either the 2 M nitric acid or the 2 M sodium carbonate as precipitation agent,

and correlate their catalytic performance in ethynylation with the catalyst structures and properties. The photo of the dried co-precipitated CBS-d80 catalysts synthesized at different pH values is shown in Figure 2-18. Their differences in catalytic performance in the two-step ethynylation process are shown in Figure 2-19.

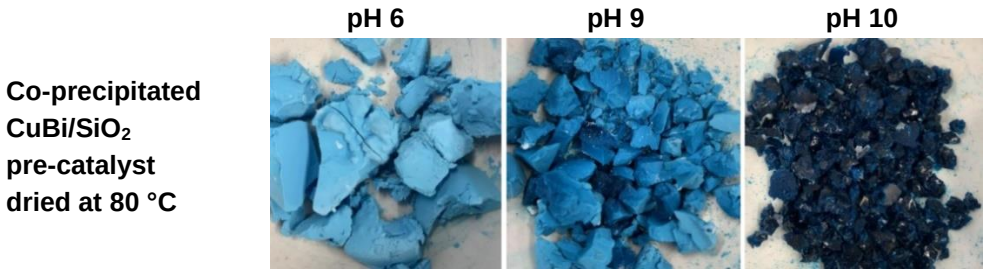

Figure 2-18. The photos show the color and the appearance of the co-precipitated CBS catalysts synthesized at pH 6, pH 9, and pH 10, with either nitric acid or sodium carbonate to maintain the pH values, and dried in an oven at 80 °C overnight.

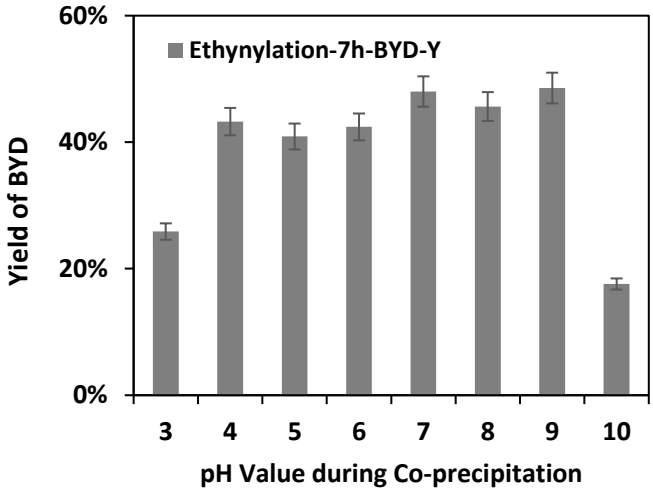

Figure 2-19. The graph depicted the catalytic performance in terms of BYD yield in % of CBS pre-catalysts co-precipitated at pH 3 to pH 10 after 7 h of the two-step Reppe ethynylation process.

From their colors, appearance, and textural properties, it can be easily concluded that they have significant influences on catalyst formation under various co-precipitation conditions. The ones at pH 9 and pH 10 are highly dense and exhibit extreme hardness that cannot be easily ground into powders for catalytic performance tests and other characterization. These series of catalysts are calcined at 450 °C. The CBS-c450 pre-catalysts are analyzed by PXRD and N_2-physisorption. Only the one co-precipitated at pH 3 shows XRD crystallites with reflexes

corresponding to CuO, and the other catalysts are XRD-amorphous. On the other hand, the BET surface area and BJH pore volume of the catalyst co-precipitated at pH 10 have much lower values of 148.7 m^2/g and 0.034 cc/g, compared to the other with an average of about 250 m^2/g and 0.50 cc/g, respectively. The different properties of CBS-pH3 in crystallinity and CBS-pH10 in porosity suggested their difference in catalytic performance.

The significantly lower yield of BYD at about 20% compared to the others at about 40% agrees with the findings from the PXRD and N_2-physisorption analysis. The formation of the crystal structure of the copper species as CuO in CBS-pH3 in one aspect represents the comparably poor copper dispersion, and on the other side, which is believed to play a more dominant role, is the poor reducibility from copper(II) oxide to the copper(I) species due to its more stable structure. The extremely low porosity of CBS-pH10 suggested the poor copper dispersion on the silica carrier and the small number of active sites that converted directly from copper(II) sites in the pre-catalysts to the activated catalyst, which resulted in the low yield.

All the other pre-catalysts, synthesized at pH values between 4 and 9, yield BYD in a similar range that is acceptable as a suitable co-precipitation condition. However, pH 6 to pH 7 is preferable when considering the operation and monitoring during the auto-titration process, the use of the precipitation agent, and the post-treatment. These practical implications of the lab work are less influential in the catalytic performance of the ethynylation process and are not worthy of elaborating in detail in this work.

Synthesis of Pre-catalyst by Various Techniques

Many catalyst synthesis techniques are proposed. In this section, CBS or CS catalysts synthesized by IWI, AE, and DP methods are tested in the ethynylation process.

The mesoporous silica carrier is self-prepared by precipitation at pH 7 with a BET surface area between 100-150 m^2/g and a BJH porous volume at 0.50 ±0.10 cc/g. Additionally, a Bi_2O_3-SiO_2 carrier is also prepared and has a BET surface area between 50-100 m^2/g and a BJH porous volume at 0.30 (±0.10) cc/g.

The pre-catalysts synthesized by various methods contain 15 wt.% copper loading, not 35 wt%. This is because, for example, the carrier's adsorption capacity of copper salt solution due to the limitation of the porous volume by the IWI method and the limited ligand removal and ion exchange efficiency in ammonia and urea solution by AE and DP methods. The pre-catalysts in this series of experiments are denoted as CBS/CS-CP/AE/IWI/DP, respectively. Their catalytic performance in ethynylation is shown in Figure 2-20. The PXRD analysis of the pre-catalyst is shown in Figure 2-23.

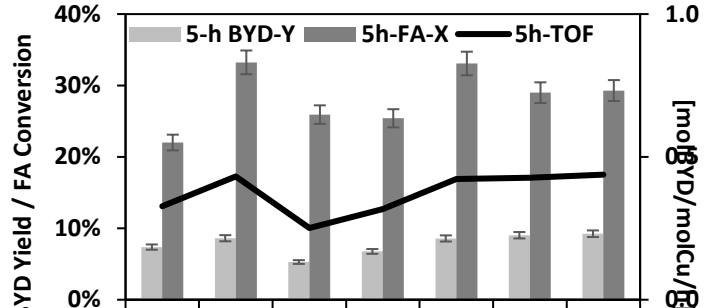

	CS-CP	CBS-CP	CS-IWI	CS-AE	CBS-AE	CS-DP	CBS-DP
5-h BYD-Y	7.4%	8.6%	5.3%	6.8%	8.6%	9.0%	9.2%
5h-FA-X	22.0%	33.2%	25.9%	25.4%	33.1%	29.0%	29.3%
5h-TOF	0.328	0.432	0.251	0.317	0.423	0.428	0.438

Figure 2-20. The graphs illustrate the catalytic performance over 5 h of the one-step ethynylation process with CBS and CS pre-catalysts synthesized by co-precipitation (CP), ammonia evaporation (AE), incipient wetness impregnation (IWI), and deposition precipitation in urea solution (DP-U).

From the results, despite the Bi species being pre-synthesized with silica in the carrier, the catalytic performances with Bi are generally better than the ones without Bi, which provides more evidence for the role of Bi as an effective and essential promoter. It is suggested that the phase transformation, not only the copper species but also the bismuth species, may take place, which creates unique interactions that enhance the catalytic performance. That may also provide a hint for the hypothesis of the catalytic activation mechanism from CuO into Cu_2C_2 involving bismuth. However, the differences in yield of BYD of pre-catalysts synthesized via different methods are not significant for CBS-CP, CBS-AE, and CBS-DP within 5 hours of ethynylation. Therefore, it is still reasonable to use co-precipitation as the standard catalyst synthesis method.

2.2.3 Catalyst Analysis and Characterization

In heterogeneous catalysis, analyzing and characterizing the catalysts is crucial to ensure the quality of the catalyst that meets the requirements for further studies and the catalytic performance. The typical analysis and characterizations of heterogeneous catalysis include structural and morphology analysis, compositional and elemental analysis, thermal and chemical properties analysis, and phase identification. The techniques include X-ray diffraction, physisorption and chemisorption, and microscopy and spectroscopy studies.

The investigation of the ethynylation catalyst is also essential to determine the structure-activity relationships and understand the reaction mechanisms. This is crucial in the development and upgrading of the catalysts, the reactors, and the reaction processes.

This chapter studies only the copper-based pre-catalyst for the ethynylation process. The discussion on the activated catalyst is shown in Chapter 3.1. The analytical parameters and procedures are described in Chapter 5.2 and Chapter 5.3.4.

Crystallinity and Phase Identification by PXRD

Powder-X-ray diffraction is a non-destructive technique used to study solid-state materials, and it is most commonly applied in heterogeneous catalysis. This method identifies the crystal formation by defining the crystallographic structure with the information on the X-ray intensity and scattering angle of diffraction. Each crystalline substance has distinct XRD reflexes and a unique X-ray diffractogram pattern, which is collected in the International Centre for Diffraction Data (ICDD) database. From the XRD diffractogram, the crystallite size, crystal structure, and the space lattice and unit cell can be identified and calculated [186-188].

In this section, PXRD is used to estimate the crystallinity of the copper species and identify the copper phases in the ethynylation catalysts prepared by varied compositions, components, and synthesis techniques.

The CBS ethynylation pre-catalysts, synthesized by co-precipitation, predominately exist as XRD-amorphous due to the excellent copper dispersion, partially promoted by the bismuth species and also benefit from the large BET surface area of the silica carrier. However, the CBS pre-catalyst, with its high copper loadings (more than 35 wt.%) and the standard 35CBS pre-catalyst co-precipitated at low pH ranges (below pH 4), exhibit a certain degree of crystallization of the copper species by the PXRD analysis.

The PXRD diffractograms shown in Figure 2-21 identify the formation of different copper phases, including $Cu_2(NO_3)(OH)_3$, $Cu_2(CO_2)(OH)_2$, and CuO, under different co-precipitation (precipitation and pH adjustment agent) and post-treatment (calcination temperature)

conditions. Notably, the proposed copper spinel phase, which is expected to be $CuSiO_3$ or $CuBi_2O_4$, is not found in PXRD. Additionally, the PXRD diffractograms illustrate the role of bismuth species, which enhances copper dispersion and reduces copper crystallite sizes. This is shown by the higher intensity of the reflexes corresponding to CuO in the CS than in the CBS pre-catalyst. The higher intensity and sharper reflexes represent a higher degree of crystallinity and larger crystallite sizes.

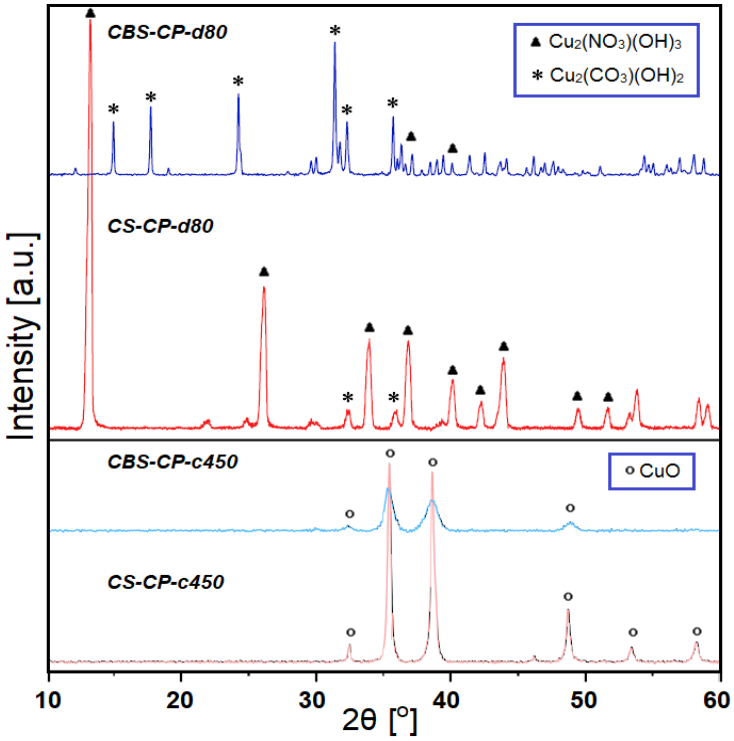

Figure 2-21. The PXRD diffractograms of X-ray intensity (a.u.) against 2θ angles in degree (°) are shown. The samples analyzed by PXRD are the copper-bismuth-silica (CBS) and copper-silica (CS) pre-catalysts synthesized by the co-precipitation (CP) method and post-treated either dried at 80 °C (d80) or calcined at 450 °C (c450). The XRD reflexes correspond to $Cu_2(NO_3)(OH)_3$, $Cu_2(CO_3)(OH)_2$, and CuO, as referred to in the ICDD database, are marked accordingly in the diffractograms.

The phase identification of the copper species provides valuable information on the influences of different copper phases in the pre-catalyst in the catalytic performance of the ethynylation process. As elaborated in Figure 2-14 and Figure 2-15, the pre-catalysts CBS/CS-CP-d80 show either $Cu_2(NO_3)(OH)_3$ or $Cu_2(CO_3)(OH)_2$ copper crystallite phases, depending on the precipitation and pH adjusting agents, whether nitric acid or sodium carbonate is used. Whereas both pre-catalysts CBS/CS-CP-c450 show CuO. The copper species have different reducibility and strength of metal-support interaction, hence affecting the transformation rate of the copper(II)-containing pre-catalyst into the Cu_2C_2-containing active phase. To achieve comparability, all the pre-catalysts mentioned below are calcined at 450 °C.

The PXRD analysis of copper-based ethynylation pre-catalysts with different carriers and synthesized by various methods are shown below:

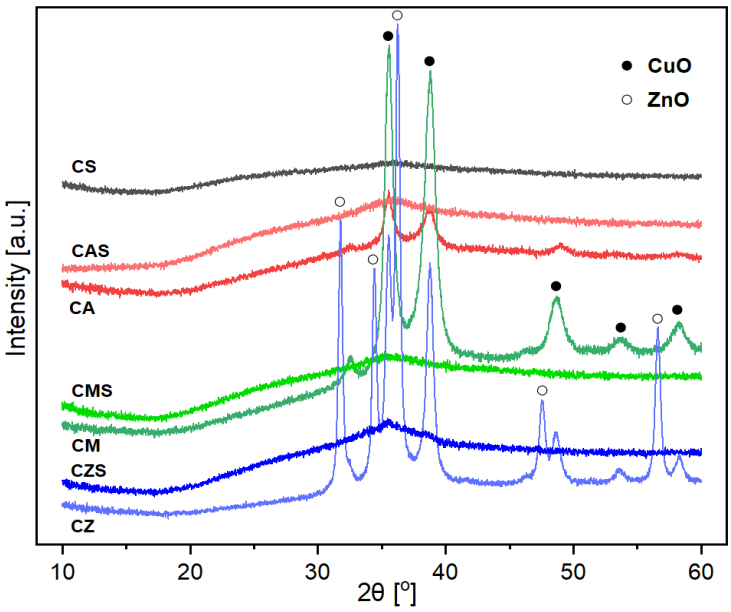

Figure 2-22. The PXRD diffractograms of X-ray intensity against 2θ angles are shown for CuO-based pre-catalysts with various carriers, including silica (CS), alumina (CA), magnesia (CM), zinc oxide (CZ), and the combinations with silica in 1-to-1 mole ratio (CAS, CMS, and CZS). The XRD reflexes corresponding to CuO and ZnO are labeled.

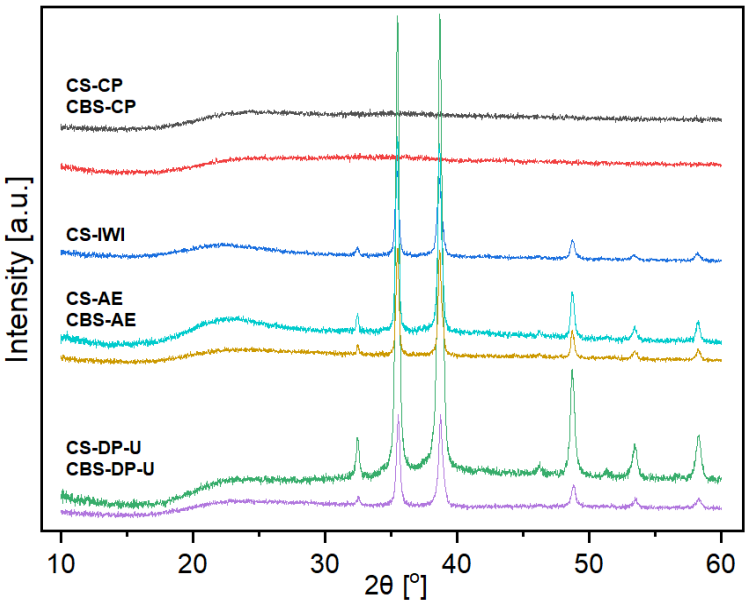

Figure 2-23. The PXRD diffractograms of X-ray intensity against 2θ angles are shown for CS and CBS pre-catalysts synthesized via various techniques, including co-precipitation (CP), incipient wetness impregnation (IWI), ammonia evaporation (AE), and deposition-precipitation in urea (DP-U).

The XRD diffractograms of the 35C0B-CP pre-catalysts with alumina, magnesia, zinc oxide, and their combination in 1-to-1 molar ratio with silica as promoters or carriers, denoted as CS, CAS, CA, CMS, CM, CZS, and CZ are shown in Figure 2-22. Their catalytic performance in 5 h ethynylation is shown in Figure 2-17. CA, CM, and CZ show reflexes corresponding to CuO. CZ also shows ZnO of high crystallinity. In contrast, all the pre-catalysts containing silica are XRD amorphous, representing better copper dispersion, lower copper crystallinity, and smaller copper particle sizes. The roles of SiO_2 in providing a large specific surface area of the catalyst and enhancing the copper dispersion are significant.

The XRD diffractograms of the 15 wt.% Cu on a pre-synthesized silica and bismuth oxide-silica catalysts are prepared by co-precipitation, incipient wetness impregnation, ammonia evaporation, and deposition precipitation in urea methods, denoted as CS/CBS-CP, CS-IWI, CS/CBS-AE, and CS/CBS-DP-U are shown in Figure 2-23. Their catalytic performance in 5 h ethynylation is shown in Figure 2-20. The co-precipitated catalysts using silica as the carrier are X-ray amorphous. The synthesis via the other methods, despite using pre-synthesized SiO_2 or Bi_2O_3-SiO_2 as the carrier, shows significant XRD reflexes corresponding to CuO. This represents that these methods do not provide a condition for a copper salt solution to diffuse efficiently through the SiO_2 carrier during synthesis. The copper tends to agglomerate and crystallize upon drying and calcining and shows poor dispersion. Again, the ones with Bi species show significantly lower crystallinity.

Thermal Properties and Phase Identification after Decomposition by TGA/DSC-MS

The copper species containing hydroxides (OH^-), nitrates (NO_3^{2-}), and carbonates (CO_3^{2-}) are identified by TGA/DSC-MS analysis. The thermogravimetric analysis (TGA) determines the mass loss due to the thermal decomposition of the sample over the ramping temperature ranges. It is coupled with differential scanning calorimetry (DSC), which measures the heat flow from the amount of heat energy absorbed or released from the sample during the same temperature profile. The decomposed gases at specific temperatures are directed to mass spectroscopy (MS) for identification by their mass-to-charge (m/z) ratio.

The TGA/DSC-MS analysis of a standard CBS-d80 pre-catalyst is shown in Figure 2-24. The mass-to-charge ratio of 17, 18, 30, 44, and 46, corresponding to OH^-, H_2O, NO, CO_2, and NO_2, respectively, are analyzed by MS. The mass loss of the sample is recorded in % by TGA with elevating temperature from room temperature to 800 °C at the ramp rate of 10 K/min under synthetic air atmosphere. The DSC data of this experiment has not been recorded. However, DSC is necessary for the evaluation of the quantitative analysis of cuprous acetylide species, which will be discussed in detail in Chapter 3.2.2.

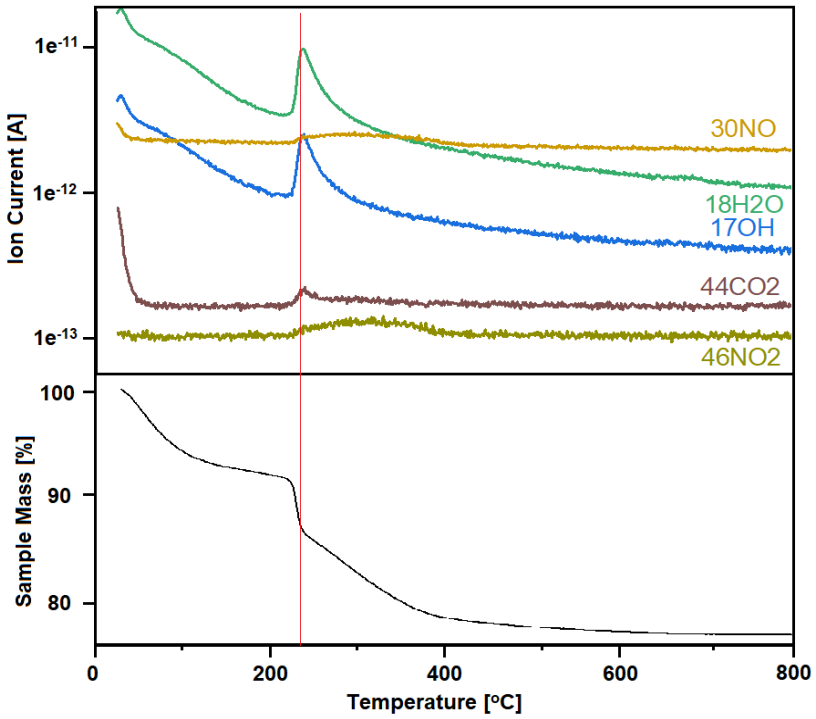

Figure 2-24. The TGA-MS analysis of a CBS-CP-d80 pre-catalyst of ion current in A of Mass Spectroscopy (top) and sample mass in % of thermogravimetric analysis (bottom) against the elevation temperature from 20 °C to 800 °C. (The m/z ratio of H_2O/OH^- signals and NO/NO_2 signals in the MS are directly correlated with each other. Hence, they can be treated as one component.)

It can be seen that there is a gradual mass loss in a general trend from 100% to approximately 78% over the entire temperature profile. This corresponds to the H_2O/OH^- signals from MS. A significant mass loss from approximately 92% to 87% is observed at a temperature of around 225 °C. This mass loss corresponds to the excess release of the H_2O/OH^- and CO_2. It is also observed that a slow release of NO/NO_2 at the same point until around 400 °C, shown by a steep decreasing curve in the mass loss plot. After that, a very gentle curve is shown, representing that no more decomposition takes place.

The TGA-MS experiment not only identifies the components, like water, hydroxides, nitrates, and carbonates, that consist in the catalyst, but it also suggests the appropriate calcination temperature of at least 400 °C that is sufficient to decompose the unwanted components. This is also the experiment that decides the calcination temperature of 450 °C for the standard ethynylation pre-catalysts as supporting evidence.

Determination of the amount of each element in the pre-catalyst by ICP-OES.

The ICP-OES technique is used to determine the amount of each element that is actually present in the pre-catalyst after synthesis. It is also used for the leaching study to analyze the amount of each component from the catalyst leached into the reaction mixture during the catalytic ethynylation process (refer to Chapter 2.4.2). This is for the investigation of the appropriate reaction conditions and the study of catalyst deactivation.

The ICP-OES is a highly sensitive elemental analysis that quantitatively determines the concentration of elements at the ppm (or ppb) level with the calibration of each analyte. Multiple ICP-OES devices are employed due to their analytical capacities and detection limits. They are selectively chosen due to the availability and requirements since the sample preparation can be highly challenging in one device but not in another.

The actual copper contents in the pre-catalysts with the catalysts of various copper loadings and carriers, as discussed in Chapter 2.2.1, and various synthesis techniques, as discussed in Chapter 2.2.2, are analyzed by ICP-OES (diluted to 30 ppm Cu) and shown in Table 2-3.

Table 2-3. The copper and bismuth content in the CBS-c450 pre-catalysts are analyzed using the ICP-OES technique. The pre-catalyst samples contain (1) the desired copper loadings of 15%, 25%, 35%, 45%, and 55% of copper and 4% of bismuth on SiO_2 by co-precipitation method; (2) the desired 0%, 4%, and 8% bismuth and 35% copper on SiO_2 by co-precipitation method; (3) 15% copper on SiO_2, by co-precipitation (CP), ammonia evaporation (AE), incipient wetness impregnation (IWI), and deposition precipitation in urea (DP-U) synthesis techniques; and (4) 35% copper and no bismuth on varies carriers of silica (S), zinc oxide (Z), alumina (A), magnesia (M) and combinations (SZ, SA, and SM). The samples are diluted to 30 ppm of copper content in the catalyst, and the analytical results of copper- and bismuth-loadings are shown in %.
Note: 15CBS is used for CBS-CP in (3), 35CBS is used for C4BS in (2), and C0BS is used for CS in (4)

	Pre-catalysts	***Copper-Loadings** [%]*		***Bismuth-Loadings** [%]*	
	Calcined at 450 °C	*Desired*	*Measured*	*Desired*	*Measured*
(1)	***15CBS***	*15*	*14.44*		*3.88*
	25CBS	*25*	*26.45*		*5.01*
	35CBS	*35*	*32.75*	*4*	*5.19*
	45CBS	*45*	*42.54*		*1.18*
	55CBS	*55*	*54.42*		*1.43*
(2)	***C0BS***	*35*	*35.33*	*0*	
	C8BS		*35.29*	*8*	*7.96*
(3)	*CS-AE*		*16.70*		
	CS-IWI	*15*	*17.61*	*0*	
	CS-DP-U		*18.39*		
(4)	*CZ*		*36.26*		
	CA		*34.81*		
	CM	*35*	*--*	*0*	
	CSZ		*38.45*		
	CSA		*39.34*		
	CSM		*--*		

This section aims to determine the loading of each component in the pre-catalyst. However, silicon (Si) is not because silica (SiO_2) is hardly soluble in diluted (about 5%) nitric acid, which is required as the solvent acidity for the ICP-OES analysis. Hence, the determination of silicon is out of the discussion, but it is involved in the leaching study where another ICP-OES device is used. Bismuth has also encountered poor accuracy in the ICP-OES analysis. Copper, as the focused species in the discussion, shows good accuracy and reproducibility in ICP-OES. The actual copper content is used for the calculation of TOF in the catalytic ethynylation process, as it is assumed that all copper can be activated into the active cuprous acetylide phase.

Catalyst's Surface and Porous Properties by N_2 Physisorption (BET and BJH methods)

The catalyst's surface and porous properties are analyzed using the N_2 physisorption technique. The adsorption isotherm models to determine the porous sizes are indicated by the amount of adsorbed gas against the relative pressure (p/p_0) of the gas, as shown in Figure 7-6. The catalyst's total surface area is determined by the BET method, calculated with mono-layer adsorption of the N_2 atom, where p/p_0 is below 0.35. The pore size is determined by the BJH method, calculated with the amount of N_2 atoms to fill the pores with p/p_0 is 0.35 to 1.00.

The specific surface area and porous size of the ethynylation pre-catalyst determined by the N_2 physisorption technique are shown in Table 2-4. Their correlations with the catalytic performance in ethynylation are shown in Figure 2-25.

Table 2-4. The N_2-physisorption technique of pre-catalysts is used to determine the specific surface using the BET method and the pore radius and pore volume using the BJH method.

	Pre-catalysts	***BET Surface Area*** *[m^2/g]*	***BJH Pore Volume*** *[mL/g]*	***BJH Pore Radius*** *[nm]*
(1)	***15CBS***	***206.2***	***0.666***	***1.681***
	25CBS	*122.5*	*0.411*	*1.678*
	35CBS	***148.8***	***0.416***	***1.688***
	45CBS	*189.3*	*0.466*	*1.683*
	55CBS	*111.5*	*0.387*	*1.685*
(2)	***C0BS***	***110.1***	***0.332***	***1.684***
	C8BS	*163.3*	*0.385*	*1.690*
(3)	*15CS-AE*	*50.3*	*0.203*	*5.844*
	15CS-IWI	*79.2*	*0.410*	*7.724*
	15CS-DP-U	*89.3*	*0.319*	*1.683*
(4)	*CZ*	*25.7*	*0.073*	*1.700*
	CA	*76.6*	*0.555*	*1.669*
	CM	*25.4*	*0.072*	*1.689*
	CSZ	*68.3*	*0.164*	*1.685*
	CSA	*137.5*	*0.530*	*1.686*
	CSM	*231.5*	*0.411*	*1.682*

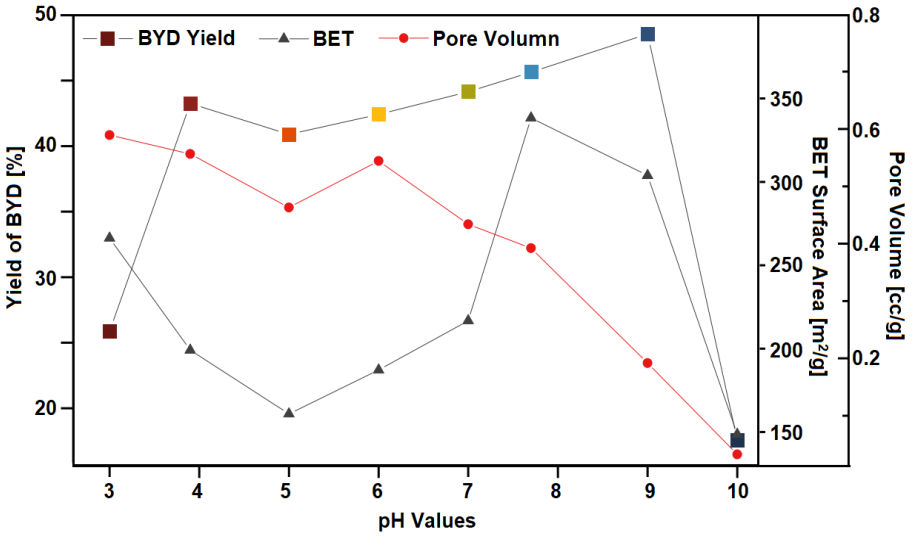

Figure 2-25. The correlation of the catalytic performance in BYD-yield after a 7 h one-step ethynylation process with the BET surface area (m^2/g), BJH pore volume (cc/g), and the pH conditions during the co-precipitation synthesis of the corresponding CBS pre-catalysts.

All of the catalysts can be classified as mesoporous based on their pore radii (pores diameter between 2 and 50 nm), which are very similar among all co-precipitated catalysts. The catalysts synthesized with different methods produce significantly large pore sizes, such as AE and IWI methods. Additionally, other carriers like magnesia and zinc oxide give significantly low pore volumes. They also produce generally low surface areas compared to the catalysts prepared by co-precipitation and using silica as the carrier. The BET surface area and the BJH pore have significant differences. Still, they are difficult to discuss one by one as no direct correlation with the catalytic performance can be observed.

The N_2 physisorption technique characterizes the properties of the entire catalyst, including the effects from the carrier and promoter, which are not involved in the catalytic reactions. The study of the active copper species can be characterized by the chemisorption techniques.

Copper Phase Properties by Temperature-Programmed Techniques

The temperature-programmed techniques include the reduction (TPR), oxidation (TPO), desorption (TPD), and pulse chemisorptions coupled with a TCD or with an MS. By introducing a gas that can be directly interacted with the targeted species, the change in phases of this species, whether been reduced, oxidized, adsorbed or desorbed, can be characterized according to the temperature profile and the phase identification by the TCD or MS.

In this work, TPO and TPD can obtain information that TGA/DSC-MS has already discovered. TPR is applied with the introduction of H_2 gas flow to the copper-containing pre-catalyst at

elevated temperature to determine the conditions when copper(II) species are being reduced, hence determining the reducibility of copper(II) with different amounts of bismuth and various carriers. It is essential to investigate the role of the bismuth species in the CBS pre-catalyst to prevent the over-reduction of copper(II) into the metallic copper and stabilize the copper(I) active phase during the catalytic Reppe ethynylation process. The TPR experiments with C0BS, C4BS, and C8BS catalysts are compared, as shown in Figure 2-26. A similar experiment with CBZ and CZ pre-catalysts, which shows a more significant effect of reducibility impacted by bismuth species, is shown in Figure 7-17 as supporting information.

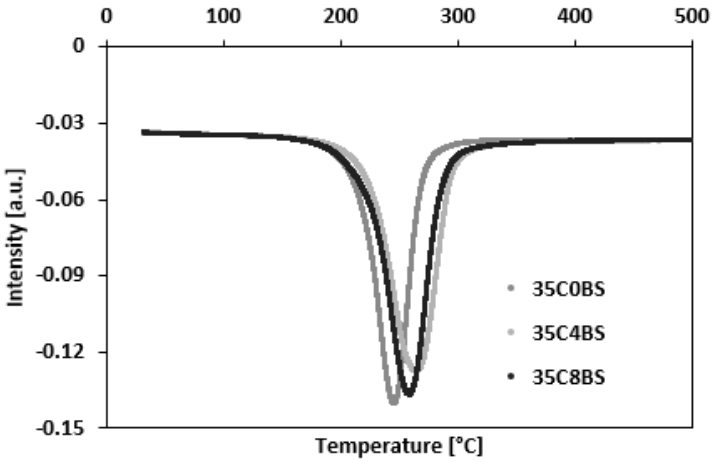

Figure 2-26. The temperature profile of Temperature-Programmed Reduction (TPR) for $CuO\text{-}SiO_2$ with 35 wt.% Cu and 0, 4, and 8wt.% Bi (35C0/4/8BS) pre-catalysts to investigate the role of bismuth species in the ethynylation catalyst, which prevents the over-reduction of Cu^{2+} from CuO to Cu(0).

It is expected that pre-catalyst containing bismuth species will stabilize the copper(I) phase by hindering the over-reduction of copper(II) into copper(0), as it may change the reducibility of copper species. The TPR experiment, however, was unable to tell the presence of copper(I) species. It is unlikely, due to the reduction potential of copper under strong reduction conditions, that copper(I) can be present. It is expected that a gentle and broader signal or a signal with a shoulder will show. However, it doesn't exist. Only a slightly broader signal for 35C4BS is present at a slightly higher temperature than 35C0BS. This indirectly indicates the effect of bismuth species that changes the reducibility of copper(II) in the standard CBS ethynylation pre-catalyst. Additionally, the signal of 35C8BS lies between 35C0BS and 35C8BS, which opposes the idea, also indirectly, that the more bismuth, the better the inhibiting effects of copper over-reduction. This may be because the excess bismuth adversely interferes with the equalized $CuO\text{-}Bi_2O_3$ interactions, thus enhancing the reducibility of CuO.

TP pulse chemisorption with N_2O gas is of high interest for the particular copper-based pre-catalyst, which is used to determine the copper(0) surface area and dispersion in the catalyst.

The N_2O pulse chemisorption with a pre-reduction step on a CBS pre-catalyst is shown in Figure 2-27 to determine the influence of bismuth on the copper dispersion. It is determined from the amount of N_2O consumption by copper(0) oxidation, with a stoichiometric ratio of Cu_s: O_{ads} at 2:1, as shown in Scheme 2-1 [189].

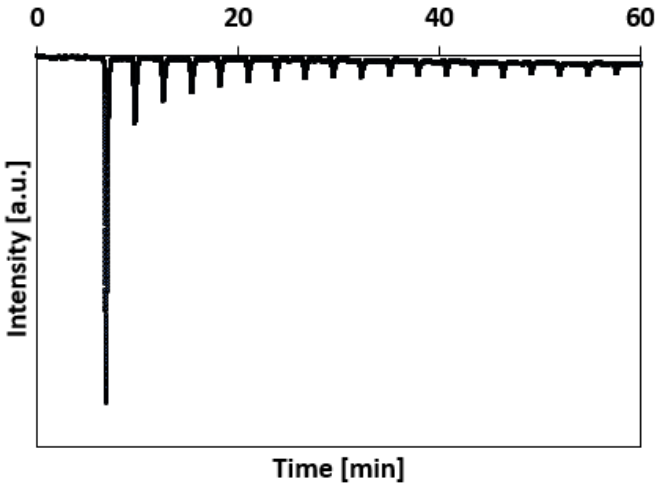

Figure 2-27. The signals of N_2O pulse chemisorption of a CBS and a CS pre-catalysts are shown by the amount of N_2 that passes through to the TCD detector. The sample catalysts first undergo a pre-reduction step under 10% H_2 in Ar gas flow at 350 °C to obtain the copper(0) phase. Twenty times of N_2O dosing is introduced with a loop size of 500 µL at 110 °C to the sample catalysts at 40 °C. A liquid nitrogen cold trap is placed to retain the leftover N_2O and allow N_2 to pass through to the detector. The copper dispersion, particle size, and particle surface area can be calculated.

$$N_2O + 2Cu_s \longrightarrow Cu_s{-}O{-}Cu_s + N_2$$

Scheme 2-1. The proposed N_2O chemisorption on exposed Cu atoms to produce N_2 gas is based on the publication by Hinrichsen *et al.* [189].

From Figure 2-27, the area under the curve is the amount of N_2 detected in 20 pulses of N_2O, indicating the amount of Cu in the sample that has been oxidized by N_2O. After integrating and evaluating the values, The copper dispersions are calculated at 5.47% on the CBS pre-catalysts. The copper particle size of 12.70 nm and surface area of 12.35 m^2/g were calculated by the number of moles of copper on the surface. The comparative CS pre-catalyst should be analyzed, but the device is out of order. It is also interesting to evaluate the activated and spent catalysts that contain Cu_2C_2. It can be helpful in predicting the mobility and transformation of copper species and possibly propose the catalytic activation mechanism in ethynylation.

N_2O pulse chemisorption is an accurate and reliable technique with high relevance to studying the catalytic activity of the catalyst when compared with the N_2-physisorption method, which analyzes the BET surface area of the entire catalyst instead of the active copper phase and the ICP-OES, which determines the total amount of copper content in the catalyst but without information on the copper dispersion and its active surface area.

The pulses of the defined amount of N_2O are dosed with a constant flow of helium, in which N_2O can be chemisorbed to the pre-reduced copper(0) species. The amount of N_2 formed is analyzed by the TCD and used to equate the theoretical amount of copper active sites (AS) as the active surface area of the catalyst.

However, in Reppe ethynylation, the catalytically active phase is *in situ* formed cuprous acetylide species under the reaction conditions, not the metallic copper that can be analyzed directly by N_2O pulse chemisorption. It is questionable whether this technique is suitable since it cannot be guaranteed that the surface area of the metallic copper is equivalent to the copper phase in the cuprous acetylide species. Despite the uncertainty, this experiment provides a step forward to correlate the catalytic performance and the AS of copper.

2.3 Influence of Aqueous Formaldehyde

The electrophilic aqueous formaldehyde (FA) is highly reactive and difficult to determine quantitatively (Chapter 1.1.3). However, the concentration, the pH value, and the buffer species of the FA solution are crucially important in the highly complex 3-phase catalytic ethynylation process. The pH values and the buffer species play a significant role in maintaining the stability of the FA solution. They also influence the rate of the *in situ* formation of the active cuprous acetylide phase during activation and the reactivity of the nucleophilic addition of the cuprous-activated acetylide anions to the electrophilic carbonyls of formaldehyde molecules during the catalytic ethynylation.

Despite the crucial role of formaldehyde, not many studies have focused on the influences of aqueous FA in the catalytic ethynylation process. This work primarily aims to determine the optimal parameters of aqueous FA in the catalytic ethynylation process to obtain a high yield and selectivity of 1,4-butynediol (BYD).

It is also interesting to prove the decisive role of formaldehyde, which is suggested to act as a reducing agent to reduce Cu^{2+} in the pre-catalyst into the Cu^{+} phase, a crucial pre-step for the catalyst activation. It also has a deprotonation effect with acetylene to form H-C≡C$^{\delta-}$ and react with Cu^{+} to catalytic active H-C≡C-Cu or in the catalyst activation step and with $C^{\delta+}$ electropositive carbonyl carbon to H-C≡C-COH in the catalytic ethynylation. This dual role of formaldehyde is significant in understanding its influence on the catalytic process.

Addressing the desired objectives of this work, the first step is to prepare a standardized and well-defined pH-buffered FA solution, as detailed in Chapter 2.3.1. Analyzing the FA concentration is another challenge due to its high reactivity and volatility and limited analytical techniques that meet the requirements for its quantitative analysis. This work investigated and evaluated the possible strategies, including titration, NMR, and GC methods. The next step involved testing different series of FA solutions, including the commercial formalin solutions, the self-prepared phosphate-buffered, and acetate-buffered formaldehyde at pH 4.0 to pH 7.5, in the catalytic Reppe ethynylation process. The influences of these solutions on the catalytic performance in terms of the yield or TOF of BYD and the conversion of FA, with respect to their roles in activating the Cu-based catalyst precursors and forming the active cuprous acetylide phase, are discussed in Chapter 2.3.2.

2.3.1 Preparation of pH-buffered Formaldehyde Solution

The preparation of the aqueous formaldehyde solution at the desired concentration and pH value is challenging due to its volatility and the highly reactive nature of formaldehyde in water. Its volatility and reactivity change the concentration and compositions of the solution over time, which lowers its consistency in the reaction, thus affecting performance and reproducibility. The lack of relevant literature on the detailed preparation of pH-buffered aqueous formaldehyde solution for the ethynylation process makes the investigation more challenging. It also highlights the uniqueness and importance of this study.

The commercial formalin or aqueous FA solution is available in a wide range of concentrations and pH values (refer to Table 5-4). However, their applications are in the fields of pathology, medication, construction, and food industries, which do not require a high concentration and a stable pH value as for the Reppe ethynylation process [190]. Most commercial formalins do not provide information on pH values and buffer species. This makes the investigation of the formaldehyde's role in ethynylation and the catalytic performance test with the commercial formaldehyde solution more challenging and unreliable.

The objectives of this section are not just to investigate the influences of different pH values and buffer species of the aqueous FA solution on catalytic ethynylation performance but also to gain deeper insights into the catalytic reaction mechanism and kinetics. Thus, preparing a standard and well-defined formaldehyde solution is crucial. The saturated aqueous formaldehyde solutions are self-prepared with acetate buffer (CH_3COONa-CH_3COOH) and sodium hydrogen phosphate buffer (Na_2HPO_4-NaH_2PO_4). For comparison, several commercial formalin solutions of different pH values and concentrations are analyzed and calibrated.

Investigation of the pH Range of Buffer System

The pH values with corresponding buffer species and buffer capacity of the standard aqueous solutions are collected in the literature [191-192]. However, these values in aqueous formaldehyde solution have to be determined experimentally, especially for the highly reactive formaldehyde species that are involved in the catalytic ethynylation reaction with a constant change in the composition and concentration.

A series of pre-tests are carried out to determine the initial pH values of the aqueous FA solutions with different conjugated base-to-acid ratios. The actual measured pH values and the molar ratios are listed in Table 2-5. Their relationships are plotted in Figure 2-28.

Table 2-5. The formaldehyde solutions are prepared with a molar ratio of the conjugated base-to-acid of acetate ($NaCH_3COO$-CH_3COOH) and phosphate (Na_2HPO_4-NaH_2PO_4) buffer systems at 1:5, 1:2, 1:1, 2:1, and 5:1, and the desired pH values from 4.0 to 7.5. The amount of the buffer species added to FA solution is equivalent to 4-6 wt.% of the total mass. The actual measured molar ratios and pH values of the aqueous formaldehyde solution are recorded at ambient conditions.

Desired Molar Ratio	*-*	*0.20*	*-*	*0.50*	*1.00*	*-*	*2.00*	*-*	*5.00*	*-*
Desired pH Value										
Acetate buffer	*4.00*	*-*	*4.50*	*-*	*-*	*5.00*	*-*	*5.50*	*-*	*5.75*
Phosphate buffer	*5.75*	*-*	*6.00*	*-*	*-*	*6.50*	*-*	*7.00*	*-*	*7.50*
Acetate Buffer										
Measured ratio	*0.11*	*0.19*	*0.36*	*0.53*	*1.01*	*1.14*	*1.90*	*3.25*	*4.50*	*6.37*
Measured pH	*3.99*	*4.20*	*4.52*	*4.69*	*5.00*	*5.01*	*5.25*	*5.57*	*5.61*	*5.80*
Phosphate Buffer										
Measured ratio	*0.19*	*0.22*	*0.37*	*0.51*	*0.97*	*1.09*	*1.86*	*3.08*	*4.90*	*8.32*
Measured pH	*5.69*	*5.70*	*5.94*	*6.19*	*6.47*	*6.57*	*6.74*	*7.03*	*7.25*	*7.39*

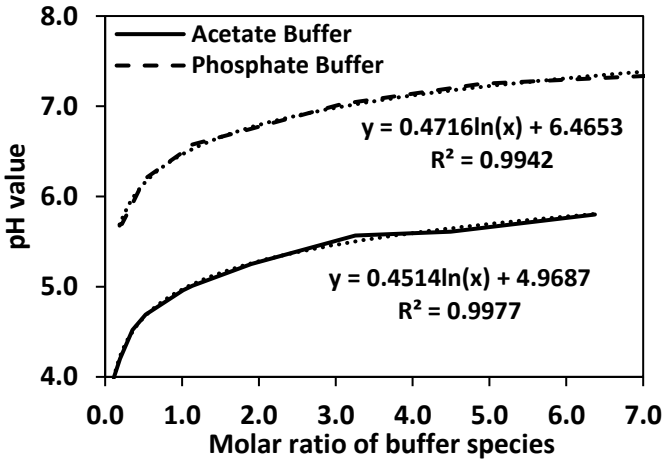

Figure 2-28. The graph illustrates the logarithmic relation between the pH values of the self-prepared pH-buffered aqueous formaldehyde solution and the molar ratio (conjugated base-to-acid) of the buffer species. Two types of buffers are tested: the acetate buffer uses sodium acetate and acetic acid, whereas the phosphate buffer uses disodium hydrogen phosphate and sodium dihydrogen phosphate.

From the results, the logarithmic relations of the conjugated base-to-acid molar ratio and the pH values of the self-prepared FA solutions are obtained with highly aligned logarithm trendlines, indicated by R_2 values. Several new tests are performed to validate and optimize these relations. The correlations are of significant importance, providing an accurate method to prepare FA solution at the desired pH values for the ethynylation process.

The suitable pH range is determined with molar ratios between 1.0 and 5.0, that is, about pH 5.0 to 5.8 for acetate buffer and pH 6.5 to 7.2 for phosphate buffer. Therefore, the aqueous FA solutions for the catalytic performance test are prepared with acetate buffer at pH 5.0, 5.5, and 6.0 (FA-A5.0/5.5/6.0) and with phosphate buffer at pH 6.0, 6.5, and 7.0 (FA-P6.0/6.5/7.0).

The experiments aim to determine the pH capacity and stability of each buffered FA solution, evaluate their influences, and select the most suitable pH-buffered FA solution for the catalytic ethynylation process. The previous standard FA solution buffered by NaOH-NaH_2PO_4 at pH 7 (FA-N7) will be tested as a reference. The evaluation of the FA influence is based on the active phase formation that is analyzed by PXRD and Raman spectroscopy, as well as the catalytic performance in the BYD yield and the FA conversion. Thus, accurately determining the FA concentration is required.

Quantitative Identification of Aqueous Formaldehyde

The quantitative identification of the self-prepared aqueous formaldehyde solution is crucial in the study of the catalytic Reppe ethynylation process. However, it is unexpectedly challenging to investigate using suitable analytical techniques.

The most commonly applied method to quantitatively identify the concentration of aqueous formaldehyde solution is titration. Iodometric (redox) back-titration with sodium thiosulfate using starch as an indicator [193-194], the acid-base titration with sodium sulfite against standard sulfuric acid [195-196] or with Schiff's reagent [197], and the formal titration with strong alkali and amino acid [198] can be found in the literature since the 1940s. Besides, ^{1}H-/^{13}C-NMR [101, 199-200], IR and UV-vis spectroscopy [201], and GC [202-203] methods have been reported since the 1960s. However, these studies mainly focus on the quantitative analysis of formaldehyde in ppm levels, such as in trace or evaporated gas. Therefore, it is necessary to adapt the available techniques to quantify formaldehyde of high concentration in its saturation and mixture solutions, as in the ethynylation process.

Recent publications in Reppe ethynylation employ titration methods to determine the FA concentration. The iodometric back-titration is one of them. However, it is not successful because iodine may react with methanol, which acts as a stabilizer in FA solution and affects the determination. The acid-base titration with sodium sulfite is a better method and successfully determines a commercial formalin solution at 40.46 wt.% (± 2.2%) and a self-prepared saturated FA solution at 38.76 wt.% (± 0.8) of formaldehyde. However, the accuracy of the results can be affected by the buffer species. The Nuclear Magnetic Resonance (^{1}H-NMR) spectroscopy method is also tested. Due to the complex components of the ethynylation samples, the characteristic spectrum of FA is hardly identified, and neither can be quantified. (details are shown in Chapter 7.1.2).

Finally, gas chromatography with a thermal conductivity detector (GC-TCD) method is introduced to quantitatively analyze the concentration of formaldehyde.

Quantitative Analysis of Formaldehyde by GC-TCD

GC-TCD, equipped with a unique Agilent J&W CP-Sil 5 CB column [204] (refer to Figure 7-3), is optimized as a practical and reliable analytical technique for formaldehyde analysis.

GC-TCD is used to quantitatively determine BYD and PA in the ethynylation process. However, it is unable to determine FA until the unique GC column is found. It is known that GC is not suitable for analyzing species with similar properties like volatility and polarity, such as formaldehyde and water. It is also not favorable for high water-containing samples. However, the J&W CP-Sil 5 CB column is specially designed for formaldehyde, water, and methanol analysis of high concentrations, which is perfect for the ethynylation process.

An example of a GC-TCD chromatogram of an ethynylation sample is illustrated in Figure 2-29. It also demonstrates the status before and after the GC troubleshooting and the common errors.

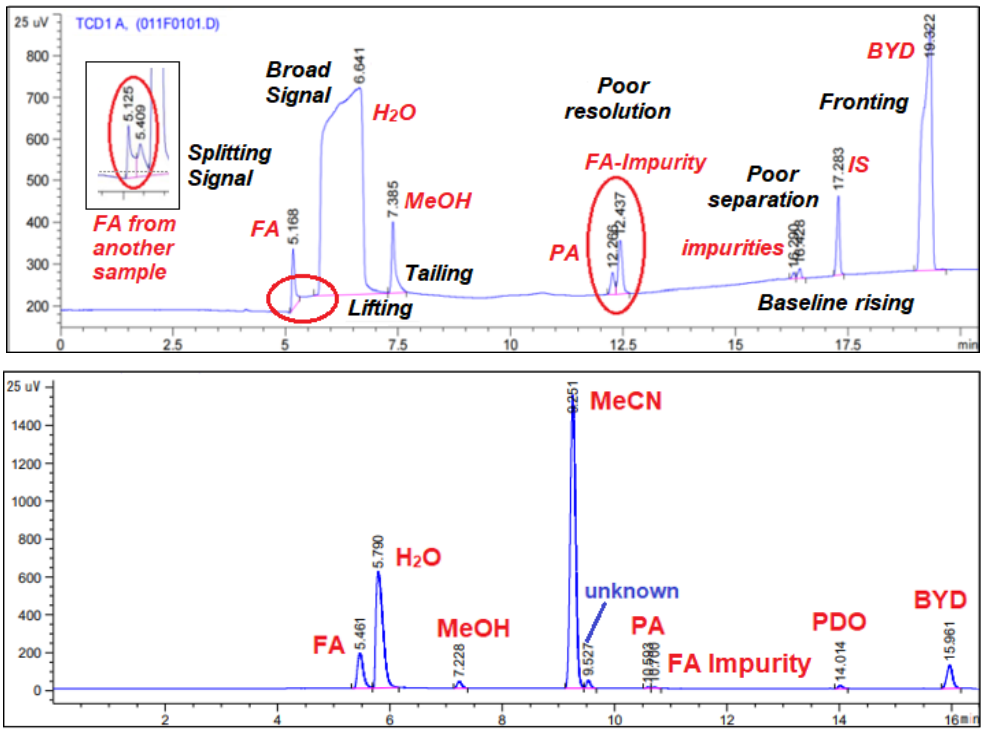

Figure 2-29. The GC-TCD chromatograms of the liquid-phase sample were prepared according to the components and compositions of the reaction mixtures from the catalytic Reppe ethynylation process. The top one is the chromatogram before the replacement of the TCD detector, and the bottom is the one after the replacement. The signals at respective retention times are formaldehyde (FA), water (H_2O), methanol (MeOH), acetonitrile (MeCN), propargyl alcohol (PA), FA impurity, 1,3-propanediol (PDO) as IS, and 1,4-butynediol (BYD), and labeled in red. The errors from the chromatogram are labeled in black.

The signals corresponding to FA, H_2O, and MeOH from the aqueous formaldehyde; MeCN as the dilution solvent, PA and BYD are the ethynylation products, unknown impurities or by-

products of the FA solution, and PDO as IS, are defined based on the respective retention times and their sequence of presence on the chromatogram due to their differences in volatility. Each analyte, including FA, BYD, and PA, has to be calibrated for its area-to-concentration relations with the IS defined by GC due to its unique thermal conductivity. These relations are used to quantify the concentration of analytes with the corresponding areas under the curve in the chromatogram and are applied to determine the catalytic ethynylation performance.

The quantitative determination of formaldehyde concentration by the GC method is a milestone that has not been reported in the literature on the Reppe ethynylation study. The detailed calibration and calculation of analytes, the selection of IS, GC troubleshooting, and GC analytical parameters are discussed in the appendix; refer to Chapter 7.1.3. The accuracy of FA concentration determined by GC is proven by the successful calibrations of FA-A4.5/5.0/6.0 and FA-P6.0/6.5/7.0 samples, as shown in Figure 2-30.

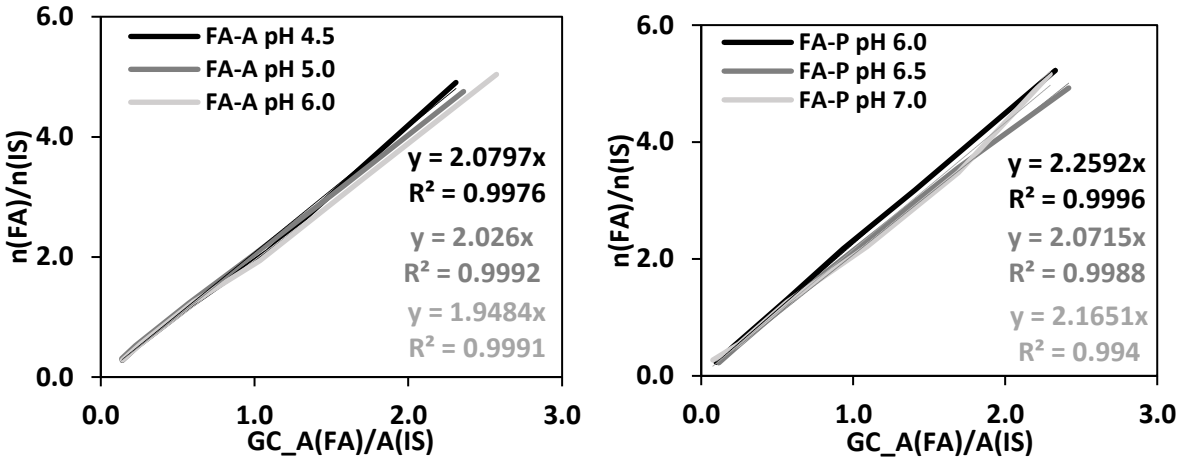

Figure 2-30. The GC-TCD calibration curve for FA solution with acetate buffer at pH 4.5, 5.0, and 6.0 and phosphate buffer at pH 6.0, 6.5, and 7.0. The plot is the ratio of the concentration of FA to IS against the ratio of the GC signal areas of FA to IS.

The linear calibration lines with high alignments, indicated by R^2 values, are achieved. The area-to-concentration relations are represented by the slopes of the calibrations, which are calculated on average at 2.018 and 2.165, with standard deviations of 5.39% and 7.66%, respectively, for acetate- and phosphate-buffered FA solutions. The consistent and reproducible chromatogram and the high degree of linearity of the calibration lines marked the successful troubleshooting of the GC-TCD for the analysis of ethynylation components. The analytical results from GC-TCD are proven reliable and accurate. Hence, it is confidently applied to the actual sample measurements from the catalytic Reppe ethynylation, as discussed in the next chapter.

2.3.2 Influences on Catalytic Performance and Active Phase Formation

The self-prepared, pH-buffered aqueous formaldehyde solutions at desired pH values are applied in the catalytic ethynylation process to study the influences of the buffer systems and pH values. This chapter focuses on the impact of the catalytic performance on BYD yield and FA conversion. Their influences on the formation of the catalytically active cuprous acetylide-containing species, analyzed by PXRD and Raman spectroscopy, which is believed to be directly related to the catalytic performance, are also discussed.

Correlation of pH Values and Buffers with BYD Yields in Catalytic Ethynylation

A trial experiment with varied pH values of the aqueous FA solution in the catalytic Reppe ethynylation is conducted before the detailed investigations. Standard CBS pre-catalysts and FA-N7 solution (NaOH-NaH_2PO_4 buffer, pH 7) are used. The pH value is adjusted to 5.0 with H_3PO_4 and to 8.0 with NaOH. The exact pH values are shown in Table 2-6. The catalytic performance in BYD yield is shown in Figure 2-31. The reaction solution after the performance tests is used to determine the copper leaching, discussed in Chapter 2.4.2.

Table 2-6. The measured pH values of NaOH-NaH_2PO_4 buffered aqueous formaldehyde solution before and after the two-step catalytic ethynylation process. The pH values are adjusted by adding phosphoric acid and sodium hydroxide. The respective catalytic performance in BYD yield is also listed.

pH of Aqueous FA Solution	*pH Before Reaction*	*Activation*		*Ethynylation*	
		pH	*BYD-Y*	*pH*	*BYD-Y*
pH 5	*4.98*	*5.13*	*11.6%*	*5.18*	*14.1%*
pH 7	*7.17*	*7.08*	*25.4%*	*7.03*	*36.3%*
pH 8	*7.98*	*7.85*	*29.9%*	*7.63*	*49.1%*

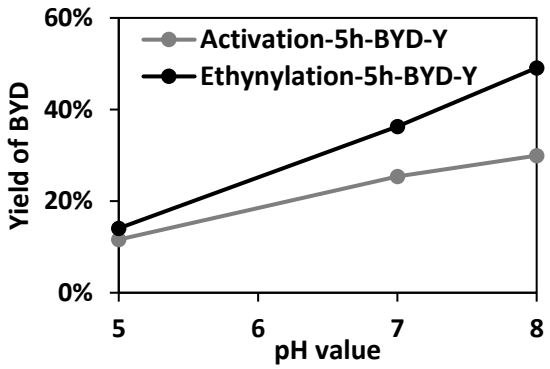

Figure 2-31. The graph illustrates the catalytic performance in yield of BYD of standard CBS pre-catalyst after 5 h activation and after 5 h ethynylation. The aqueous FA solution is buffered by NaOH-NaH_2PO_4 and adjusted to pH 5.0 (addition of H_3PO_4), 7.0, and 8.0 (addition of NaOH).

From the results, an excellent pH consistency (less than ± 0.35) is shown before and after activation and ethynylation, which marks the reliability of the performance test and conclusions. Furthermore, a linear relationship between the BYD yield and pH values from 5 to 8 is obtained. It provides a reasonable conclusion that the catalytic ethynylation performance is enhanced with the higher pH value due to the deprotonation effect of acetylene.

Further study of the pH influence of the FA solution in the formation of cuprous acetylide species and the yield of BYD is investigated. In the first series, four buffer systems, including phosphate (P), citrate (C), acetate (A), and borate (B) buffers, are applied to prepare the FA solution at pH 4 to pH 9. The detailed buffer species, the molar amount, the pH ranges, and their effects on the catalytic performance in BYD yield are listed in Table 2-7.

Table 2-7. The list of the buffer systems, buffer conjugated acid-base species, the molar amount of addition, and the desired pH values to prepare the aqueous formaldehyde solution. The differently buffered aqueous FA solution is applied in the catalytic ethynylation using the standard CBS pre-catalyst in a one-step process with a parallel test unit. The catalytic performance in BYD yield is also listed.

pH Buffer	***Conjugated Acid-Base***	***Molar Amount***	***pH Values***	***BYD Yield***
Acetate	*Acetic acid*	*~ 2.0 mmol*	*4*	*1.63*
	Sodium acetate		*5*	*3.44*
Citrate	*Citric acid*	*~ 0.2 mmol*	*5*	*2.33*
	Sodium citrate		*6*	*3.18*
Phosphate	*Sodium dihydrogen phosphate*	*~ 8.5 mmol*	*6*	*2.81*
	Sodium hydroxide		*7*	*9.47*
			8	*7.39*
Borate	*Boric acid*	*~ 4.0 mmol*	*8*	*7.27*
	Sodium hydroxide		*9*	*8.37*

The limitation of the buffer systems is the use of sodium hydroxide, which is a strong base, to adjust the pH value to the higher ranges, like pH 8 for phosphate and pH 9 for borate buffers. Additionally, the molar amount of the buffers added is inconsistent, which may be less reliable for the comparison. This leads to the modifications in the second series of experiments.

Correlation of pH Values and Buffers with Active Phase Formation

The intermediate step, which is the formation of the catalytically active species Cu_2C_2, explains the correlation of the differently-buffered aqueous FA solution with the catalytic ethynylation performance. The corresponding spent catalysts after ethynylation are analyzed by PXRD, as shown in Figure 2-32.

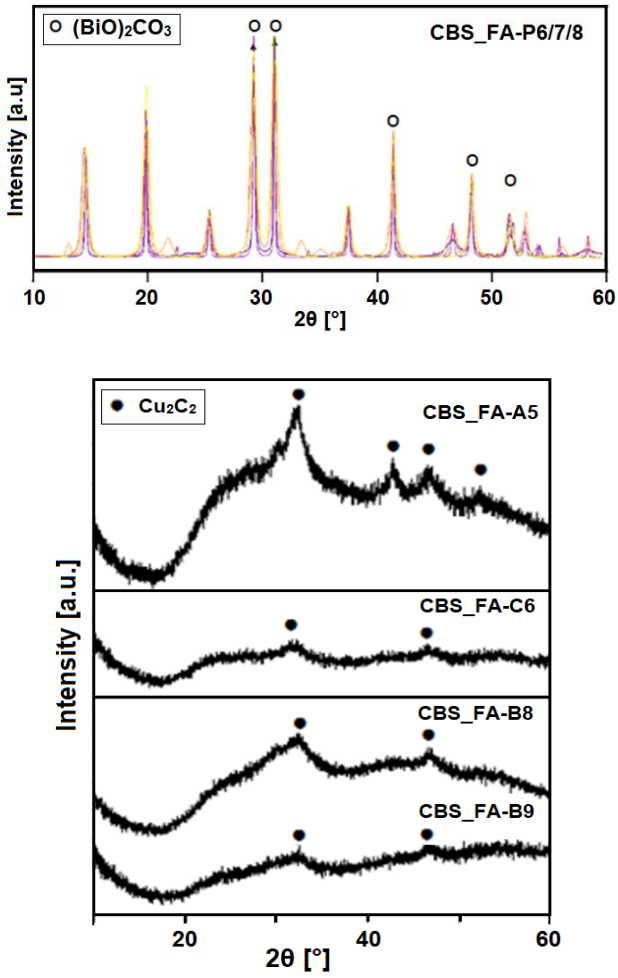

Figure 2-32. The PXRD diffractograms of the CBS catalyst were performed in differently buffered aqueous FA solution at desired pH values after 5 h of the one-step ethynylation process. The spent CBS catalyst using phosphate-buffered FA solution at pH 6, 7, and 8 (FA-P6/7/8) (top) and using acetate buffer at pH 5 (A5), citrate buffer at pH 6 (C6), and borate buffer at pH 8 and 9 (B8/9) (bottom) are shown.

From the diffractograms, the proposed 2θ angles of Cu_2C_2 are marked for all samples except the one with phosphate buffers (CBS-FA-P). It doesn't mean that Cu_2C_2 reflexes are missing, but they are probably not visible due to the high intensities of the other crystallized species.

This also suggested that different buffer systems have a dominating impact compared to the pH values on the catalyst transformation, whether it is formed in the active cuprous phase or the other crystalline structures. This is proven by the highly reproducible XRD patterns corresponding to $(BiO)_2CO_3$ of CBS_FA-P at pH 6, 7, and 8. Its characteristic XRD reflexes have very similar 2θ angles to the ones defined as Cu_2C_2 species, which may cause misinterpretations. The confusion also comes from the inaccurately determined XRD patterns of Cu_2C_2, which have no available data from the ICDD database. This excellently motivates the genesis of pure-phase cuprous acetylide species and identifies and differentiates the pure-phase from the interfering and its derivative species, as focused in the next chapter.

Modifications on the FA Solution Preparation and PXRD Analysis

This series of experiments focuses only on the acetate and phosphate buffers, which are modified from the limitations mentioned above. The newly developed standard procedures of FA preparation followed, as shown in Table 2-5 and Figure 2-28.

The pH-buffered aqueous FA solutions are prepared. The measured pH values before and after the 32-h ethynylation and the catalytic performance with standard CBS pre-catalyst in BYD yield are summarized in Table 2-8. The correlation of the BYD yield and FA conversion with the actual pH values is plotted in Figure 2-33. The PXRD diffractograms of the corresponding catalyst after ethynylation are shown in Figure 2-34.

Table 2-8. The catalytic performance test in BYD-yield and FA-conversion using standard CBS pre-catalyst with acetate (A)- and phosphate (P)-buffered aqueous FA solution at pH 4.5 to 7.5 in a two-step 5 h activation and 32 h ethynylation process with a Carousel test unit. A NaOH-NaH_2PO_4 (N)-buffered FA solution is tested as a reference.

FA solutions	***FA-A4.5***	***FA-A5.5***	***FA-A6.0***	***FA-P6.5***	***FA-P7.5***	***FA-N7.5***
Measured pH	*4.52*	*5.57*	*6.10*	*6.57*	*7.39*	*7.48*
pH after Activation	*4.49*	*5.47*	*6.14*	*6.45*	*6.84*	*6.53*
pH after Ethynylation	*4.71*	*5.71*	*6.20*	*6.40*	*6.63*	*6.52*
BYD yield [%]	*23.6%*	*27.6%*	*38.5%*	*50.7%*	*46.1%*	*52.6%*
FA conversion [%]	*55.2%*	*58.0%*	*74.1%*	*90.2%*	*93.0%*	*94.4%*

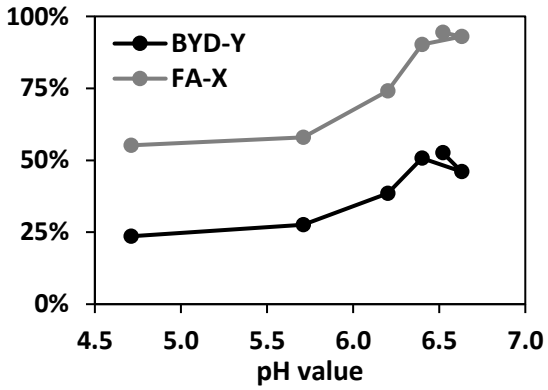

Figure 2-33. The graph illustrates the catalytic performance in BYD yield and FA conversion in a two-step ethynylation process with the actual pH values (and buffer system) of the aqueous FA solution.

The results reveal a noteworthy stability of pH values in the acidic range from pH 4.5 to 6.5, with a deviation of ±0.3. In contrast, the pH values experience a significant reduction from pH 7.5 to approximately pH 6.5, irrespective of the buffer systems. This finding aligns with the literature regarding the reactivity of the aqueous FA that favors acidic conditions.

In the plots of the BYD yield and FA conversion with the actual pH values, it can be observed that the BYD yield is directly linked to the FA conversion. It generally agrees with the trial test shown in Figure 2-31 that better catalytic performance is achieved with higher pH values.

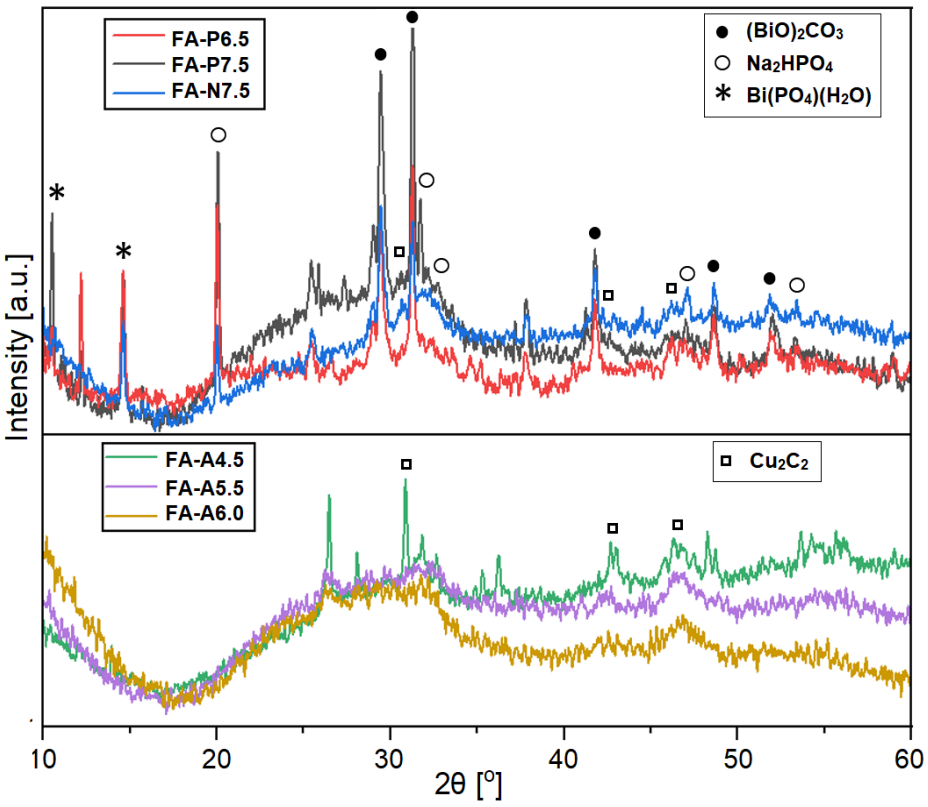

Figure 2-34. The PXRD diffractograms of the spent CBS catalysts were performed in differently buffered aqueous FA solution at respective pH values after 5 h activation and 32 h ethynylation of the two-step ethynylation process. The spent CBS catalyst using phosphate-buffered FA solution at pH 6.5 and 7.5 (FA-P6.5/7.5) and NaOH-NaH_2PO_4 buffered FA at pH 7.5 (FA-N7.5) (top) and using acetate buffer at pH 4.5, 5.5, and 6.0 (FA-A4.5/5.5/6.0) (bottom) are shown.

Based on the BYD yields and the PXRD analyses of the spent catalysts in acetate- and phosphate-buffered FA solution after the catalytic ethynylation process, the influence of the buffer species on the formation of the active phase and further catalytic performance is unclear.

The XRD reflexes corresponding to Cu_2C_2 species are estimated based on the current discovery and labeled in the diffractograms. They are easier to identify in the acetate-buffered spent catalyst because fewer crystallized impurities are presented. Compared to the phosphate-buffered one, highly crystallized $(BiO)_2CO_3$, $Bi(PO_4)(H_2O)_n$, and re-precipitated Na_2HPO_4 (or Na_2HPO_4-NaH_2PO_4) are identified in accordance with the ICDD database.

One finding worth mentioning from the PXRD analysis to identify a suitable buffer system is the presence of phosphate-containing crystallites on the purified spent catalyst's surface. The

precipitation of the phosphate species from the buffer system will significantly reduce the buffering efficiency, which provides a reasonable explanation for the decrease in pH values of FA-P7.5 and FA-N7.5.

The FA solutions buffered by acetate at pH 5.0 and by phosphate at pH 6.0 and 7.0 will be prepared and tested. It is expected to fill up the gaps and gain a better image of the pH influence of FA solutions in the catalytic ethynylation. Furthermore, FA solution at pH 6.0, which is possible to achieve by both acetate- and phosphate-buffer systems, will provide a clear conclusion, whether the buffer species or the pH values play a dominant role in the impacts on the catalytic performance in ethynylation. These could potentially lead to an improved understanding of the influence of the aqueous formaldehyde solutions and further optimization of the catalytic ethynylation process.

Impacts of Methanol Content on the Active Phase Formation and Raman Analysis

Besides the study of the influences of catalytic performance and the active phase formation by the pH and buffer of aqueous FA solution, the impact of methanol (M) content from 5% to 40% in FA solution is investigated in a trial test. The purpose of this study is to understand how the methanol content affects the FA solution, such as the formaldehyde concentration, pH values, and solubility (refer to Figure 7-2), thus affecting the catalytic performance. The spent catalysts are analyzed by Raman spectroscopy. The details will be discussed in Chapter 3.2.

2.4 Catalytic Activation and Deactivation Behavior

Studying the catalyst's activation and deactivation behaviors is one of the scopes of this project. It is beneficial not only to understand the Reppe ethynylation process, such as the identification of the catalytically active phase and the catalytic reaction mechanisms, but also to ensure working safety with this highly explosive active cuprous acetylide-containing species. However, due to the complexity of the reaction kinetics and mechanisms, the challenges in experimental handling and operations, and the difficulties and limitations in analytics, only limited experiments can be performed. The study on storage conditions is shown in Chapter 2.4.1, and the leaching study is shown in Chapter 2.4.2.

Other relevant investigations, such as the study of the catalytic activation mechanism and conditions during ethynylation, are partially merged with the genesis of the pure-phase cuprous acetylide in Chapter 3.1. This is because no carrier and promoter effect can impact the pure phase synthesis; hence, a direct influence can be observed. Another investigation aims to determine the reduction behaviors of the copper(II) phase in the pre-catalyst, which is partly tested regarding the role of bismuth as an inhibitor to stabilize the copper(I) active phase. It is also discussed during the pure phase synthesis using copper(II) precursors to determine the actual reducing agent, whether it is formaldehyde solution or acetylene gas, to effectively reduce the copper(II) phase in the ethynylation catalyst into copper(I). This topic is still an interesting argument in literature, as mentioned in Chapter 1.1.4.

This chapter only illustrates the leaching studies and effects of storage conditions. Several evaluations regarding the reaction kinetics, such as the one with respect to the number of AS of the catalyst that activates *in situ* under the ethynylation conditions and the reaction rate considering PA formation as the intermediate product to produce BYD, are investigated. It helps to understand the selectivity of PA and BYD and their favorable reaction conditions in ethynylation. The reaction orders with respect to acetylene and formaldehyde are also interesting. Part of the current results are shown in the Appendix in Chapter 7.1.4.

2.4.1 Storage Effects in Catalytic Activity

The effects on storage conditions of the activated ethynylation catalyst, which contains the highly sensitive and explosive cuprous acetylide species, are critical. The implementation of the experimental setups, procedures, and reaction parameters are compromising safety and efficiency in the catalytic performance and operation. However, the exact properties and favorable conditions for the Cu_2C_2-containing active phase, such as its formation mechanism and reducibility, are unknown. To enhance the catalytic activity for the two-step process and investigate the sample preparation procedures and conditions for reliable analyses that could accurately reflect the actual status of the Cu_2C_2 active phase, the storage and aging effects are examined. Thus, catalytic stability is studied in the long-term and the multi-cycle test.

Long-Term Tests on Catalytic Stability

The catalytic performance was focused on the initial activity of 5 to 7 hours in a one-day experiment for safety reasons. A linearly increasing trend of BYD yield over time can be achieved, which indicates the constant catalytic activity since the completion of the catalytic activation step from CuO in the pre-catalyst to the Cu_2C_2 active phase. However, the catalytic stability, the lifespan of the catalyst, the limiting reagent of the process, and the catalytic deactivation behaviors cannot be evaluated due to the limited experiment duration.

A long-term catalytic ethynylation performance test of 10 h is shown in Figure 2-35. A slight downward curve can be observed, showing a decrease in the catalytic activity. This finding motivates the determination of the rate-limiting parameters and the limiting reagent of this process to retain the catalytic performance.

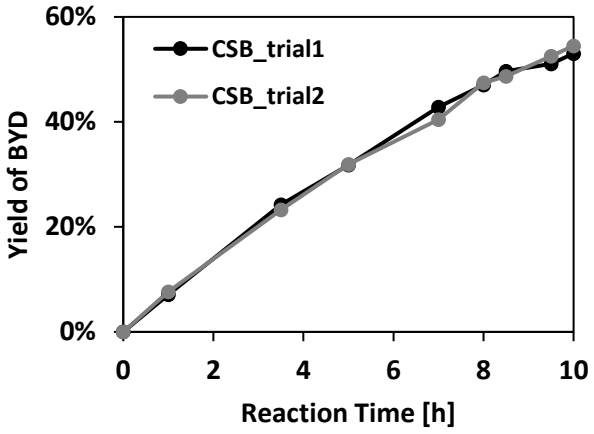

Figure 2-35. The graph illustrates two trials of the catalytic performance in BYD yield over 10 h of reaction in a two-step ethynylation process.

After a comprehensive safety inspection of the overnight experiment and modifications to the experimental procedures, like adjusting the catalyst to formaldehyde ratio to avoid the limiting reagents, a 32 h ethynylation process is performed, as shown in Figure 2-36.

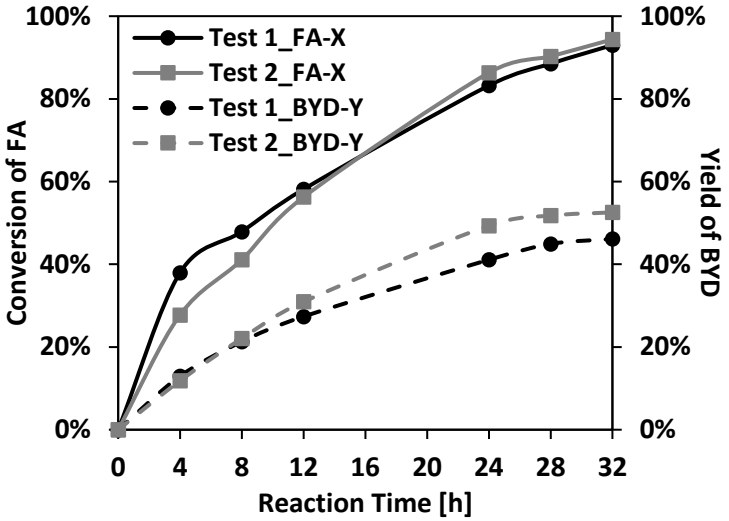

Figure 2-36. The graphs illustrate two runs of long-term catalytic performance tests with saturated aqueous formaldehyde solutions in the conversion of FA (solid lines) and the yield of BYD (dotted lines) over 32 h of reaction time with standard Cu-Bi/SiO_2 (CBS) pre-catalysts.

A more obvious trend of decreasing curve is obtained, corresponding to the high BYD yield and FA conversion that may limit the rate of reaction. The results support to a certain extent that catalysts exhibit acceptable short-term activity and long-term stability. However, they do not provide enough information for deeper investigations of the catalytic deactivation mechanism since it cannot be concluded that the catalysts start deactivated. As a result, the multi-cycle test involving the challenging transition steps of separation, purification, and storage is performed.

Multi-Cycle Tests on Catalytic Stability

Two different pre-catalysts are tested with 8 cycles of a 7 h ethynylation process, as shown in Figure 2-37. Two separation techniques, vacuum filtration and centrifugation, are used. The storage conditions, either in the reaction mixture, dried in air, or purified and stored in fresh FA solution, are applied over different cycles and days. The details are shown in Table 2-9.

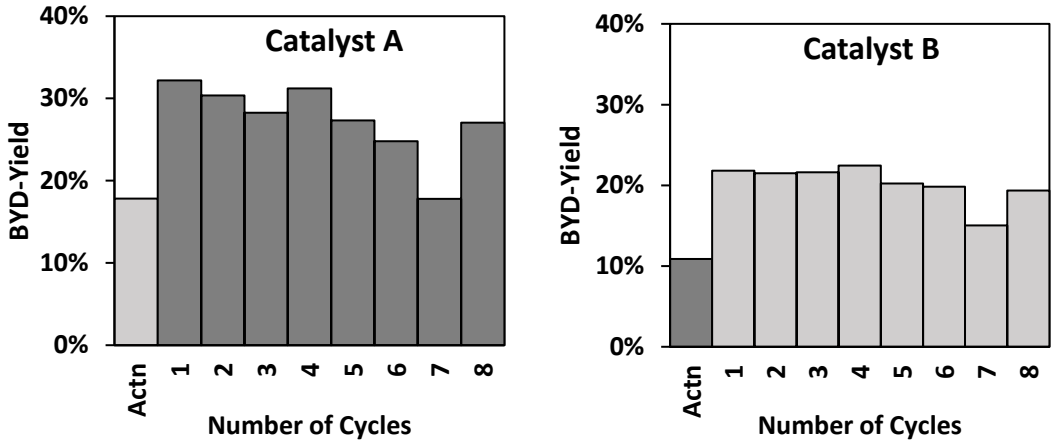

Figure 2-37. The graphs illustrate the catalytic performance in yield of BYD of two sets of activated CBS pre-catalysts, A and B, in 8 cycles of 7 h ethynylation processes over 18 days. The spent catalysts are stored under various conditions, as detailed in Table 2-9.

Table 2-9. The list of the storage conditions of the multicycle ethynylation process.

Cycle	***Day***	***Storage Conditions***	***Duration***
Activation	*1*	*(a). Stored in the original reaction solution,*	
1	*2*	*Separated and filled with fresh formaldehyde on*	*Overnight*
2	*3*	*the next day for a new cycle of ethynylation*	
3	*4*	*(b). Separated and stored dry in open air*	*4 days*
4	*8*	*Same as (a)*	*Overnight*
5	*9*		
6	*10*	*Same as (b)*	*6 days*
7	*16*	*(c). Separated and stored in fresh FA solution*	*1 day*
8	*18*	*(d). Deactivation and disposal*	*Done*

The catalytic activities in BYD yield differ cycle-by-cycle and are influenced by different storage conditions. For instance, in cycles 1 to 3 and 4 to 6, a slight decrease in BYD yield is observed. The storage conditions (a) and duration are applied. This is expected for the catalytic process, where the activity decreases over time and loses the catalysts during the transition steps. However, when different separation and storage conditions (b) and (c) and duration (1 to 6 days) apply, the catalysts exhibit different catalytic activity. In cycles 3 to 4 and cycles 7 to 8, the catalysts regained activity with a higher BYD yield. In contrast, from cycles 6 to 7, the catalysts lost activity at a faster rate with a decreased BYD yield.

These findings led to the discussion on the effects of storage conditions of the activated catalysts. A detailed investigation of its impacts is shown in the next section. Additionally, based on the current results, it is concluded that separating and purifying activated catalysts and storing them in a fresh formaldehyde solution are the optimal storage conditions.

Effects on Storage Conditions

Since the significant impacts of different storage conditions are observed from the multi-cycle tests, a series of experiments focusing on storage media and duration is performed. The catalytic performance in BYD yield of differently separated, purified, and stored activated catalysts is shown in Figure 2-38. The detailed conditions are shown in Table 2-10.

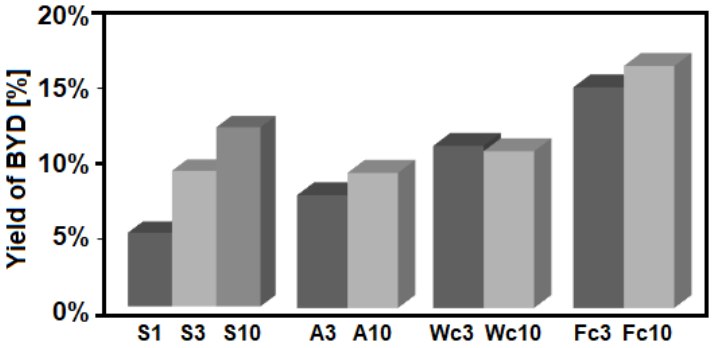

Figure 2-38. The graph illustrates the catalytic performance in BYD yield after 7 h ethynylation of an activated CBS catalyst separating and storing according to Table 2-10 after 1 day, 3 days, and 10 days.

Table 2-10. The separation, purification, and storage conditions of the activated catalysts.

Denote	***Procedures and Conditions***
S	*Store the activated catalyst in the original reaction solution overnight; separate and purify it the next day, right before the performance of the ethynylation.*
A	*Wash and purify the activated catalyst with water; separate it by vacuum filtration, and leave the separated catalyst on the filter paper in the open air.*
Wc	*Separate the activated catalyst by centrifugation; wash and decant the supernatant solution; cover the residue catalyst with water and store it.*
Fc	*Same as Wc but stored in fresh formaldehyde solution and used directly for ethynylation.*

The results show significantly higher catalytic activities in BYD yields with longer storage time, except Wc. The one store with Fc shows the best performance among all, which agrees with the experiments in cycles 7 to 8 in the multi-cycle test. This further supports the decision to use Method Fc as the standard experimental procedure for the Reppe ethynylation process.

2.4.2 Leaching of the Catalyst during Ethynylation

Copper-Leaching and Formation of Cu_2C_2 under Ethynylation Conditions

The motivation of the leaching study by the ICP-OES to determine the amount of copper leached from the CBS pre-catalyst into the reaction solution during ethynylation is to explore the unique catalyst's activation and catalytic reaction mechanisms.

A test was done with the supernatant solution after 5 h ethynylation with the initial FA solutions adjusted to pH 5 and pH 8 (refer to Chapter 2.3.2). The analytical results of copper leaching are shown in Table 2-11. The detailed calculations, the sample preparation, and the discussion on the ICP-OES devices are shown in the appendix; refer to Chapter 7.1.5.

Table 2-11. The ICP-OES analytical results of copper leaching in the ethynylation solution. About 1.90 g of 35 wt.% copper-loaded CBS is remaining in 75 mL FA solution at pH5 and pH8 after ethynylation.

Copper Leaching	***ppm***	***Mass [mg]***	***Leaching [%]***
pH 5	*0.084*	*0.126*	*0.019%*
pH 8	*0.200*	*0.300*	*0.045%*

The results show low copper leaching of 0.019% and 0.045% that can be negligible. This is expected since it is known that the active cuprous acetylide phase formed during ethynylation is sparingly soluble in aqueous solution. Any leached copper species will instantly precipitate into Cu_2C_2 under the acetylene atmosphere and leave very few dissociated copper ions.

A modified experiment tracking the changes in copper leaching under different ethynylation conditions is performed with 2 g of CBS pre-catalyst (35 wt.% Cu loading) in 50 mL of FA-P7 solution. The ICP-OES samples are taken during N_2 purging and C_2H_2 atmosphere at room temperature and elevated temperatures up to 90 °C. The ICP-OES results and corresponding conditions are shown in Figure 2-39.

The results, in general, show a low level of copper leaching in the ethynylation solution of less than 0.80 mg, equivalent to 0.11%. Nearly no copper is left in the solution when the acetylene gas is introduced with heating. This agrees with the first experiment and the literature reported by *Bruhm et al.* [159], who performed a similar copper leaching test under the ethynylation conditions, as shown in Figure 7-15. Additionally, considering the unavoidable errors during the challenging sample preparation steps, including evaporating the organic contents, re-dissolving the residues, and diluting the samples to the detectable concentrations and acidities, the results obtained are acceptable. Thus, it is confident to conclude that the amount of copper leached in the solution during ethynylation remains at a low level that can be negligible.

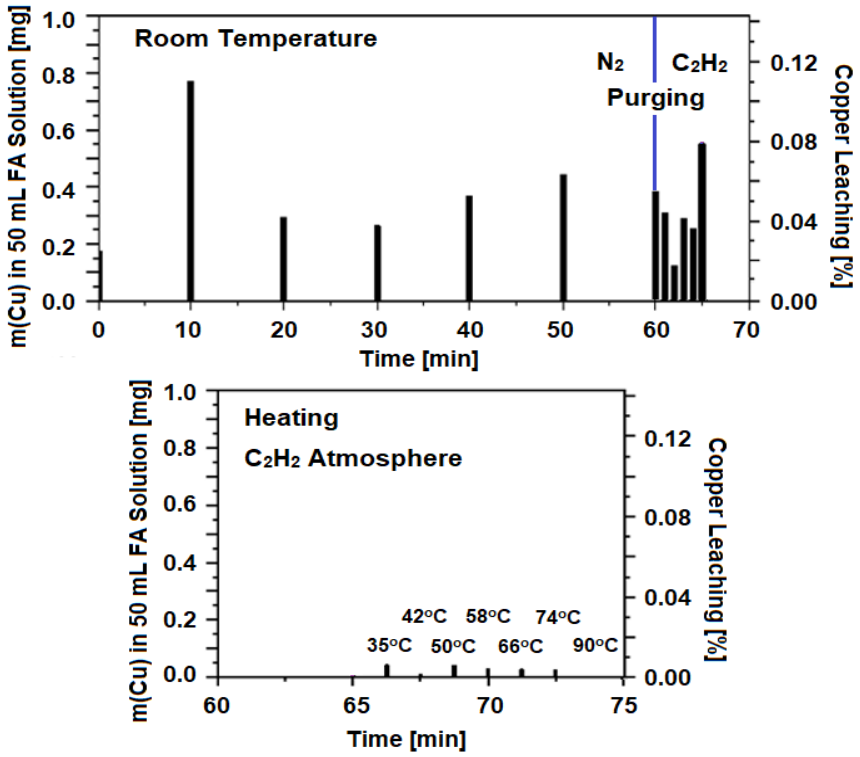

Figure 2-39. The leaching tests by the ICP-OES technique were applied to determine the amount of copper content leached in mg and converted into % from 2 g of CBS pre-catalyst into 50 mL of aqueous FA solution during the ethynylation process. The conditions analyzed were during N_2 purging and C_2H_2 atmosphere (top) at room temperature and elevated temperatures up to 90 °C at 75 min (bottom).

However, it is still debatable regarding the catalyst activation mechanism whether the copper(II) from the catalyst is leached into the solution, reduced to copper(I), and transformed into sparingly soluble cuprous acetylide active phase with dissolved acetylene gas that is instantly re-precipitated and deposited back to the catalysts, or only surface reaction on the catalyst has taken place for copper(II) to be transformed into Cu_2C_2 species. Additionally, the leached copper species, whether in copper(I)/(II) or instantly formed Cu_2C_2, can be part of the catalytic cycles. It may show different reactivity and reaction rates due to the difference in the surface reaction of the heterogeneous catalysis and with leached species that are similar to the homogeneous catalysis. This is also an interesting hypothesis reaction mechanism that needs to be proven. This will be an open question for further research and development.

Silicon-Leaching and Catalyst Stability

Another series of leaching tests, focusing on the silicon leaching to determine the catalytic stability, is performed using a different ICP-OES device. This device is more suitable for the sample preparation of the ethynylation solutions, such as allowing organic content, no requirement for acidity, and no upper detection limits but with a lower limit of 2.0 ppm. This

eliminates most of the possible errors during sample preparation and ensures the accuracy of the analytical results. The ICP-OES analytical results of sodium, bismuth, silicon, magnesium, and copper are shown in Table 2-12.

The first test is conducted with a well-defined CBS pre-catalyst, which contains 35 wt.% Cu, 4 wt.% Bi, and 24.2 wt.% Si. 15 g CBS catalyst is used in 250 mL of 37 wt.% saturated FA-P7 solution. The samples were taken at 0 h at 90 °C and 1.2 bar_{abs} pressure of acetylene, 4 h and 24 h of ethynylation reaction, and during cooling and purging with N_2 after the reaction.

The second test is conducted with a model CBMS pre-catalyst without detailed compositions. 15 g CBMS catalyst is used in 250 mL of 9 wt.% diluted FA-A5 solution. The samples are taken during N_2 purging, at times 0 h, 4 h, 20 h, and 24 h at 90 °C and 1.2 bar_{abs} pressure of acetylene during ethynylation.

Table 2-12. The theoretical values in *g* and analytical results in *ppm* (*mg/L*) by ICP-OES of sodium, bismuth, silicon, magnesium, and copper contents leached in the ethynylation reaction solution at different sampling times. Test 1 uses a standard CBS pre-catalyst in 37% phosphate-buffered FA solution at pH 7. Test 2 uses a model CBMS pre-catalyst in a 9% acetate-buffered FA solution at pH 5.

(1). CBS in 37FA-P7	***Na [ppm]***	***Cu[ppm]***	***Bi [ppm]***	***Si [ppm]***	***Mg [ppm]***
Theoretical amount	*657*	*5.25 g*	*0.90 g*	*3.63 g*	*0 g*
0 h	*1050*	*<2*	*5*	*<2*	*<2*
4 h	*1790*	*2*	*4*	*45*	*<2*
24 h	*1740*	*2*	*5*	*56*	*<2*
After	*1800*	*8*	*5*	*191*	*<2*
(2). CBMS in 9FA-A5	***Na [ppm]***	***Cu[ppm]***	***Bi [ppm]***	***Si [ppm]***	***Mg [ppm]***
Theoretical amount	*161*	*-*	*-*	*-*	*-*
N_2 purging	*280*	*<2*	*<2*	*<2*	*17*
0 h	*290*	*<2*	*<2*	*<2*	*16*
4 h	*320*	*<2*	*<2*	*93*	*27*
20 h	*320*	*5*	*<2*	*109*	*34*
24 h	*320*	*3*	*<2*	*110*	*35*

Sodium is present in the sample as a dissolved buffer species (NaOH, NaH_2PO_4, Na_2HPO_4, and $NaCH_3COO$) of FA solutions. The theoretical values of Na in the initial FA solutions are calculated at 657 ppm and 161 ppm, respectively. However, additional NaOH is added to the FA solutions of both tests to adjust the pH values, which increases the Na contents. This explains the higher analyzed Na amount. In both tests, Na contents are stabilized after 4 h.

Copper is the catalytically active species, which transforms *in situ* from CuO into Cu_2C_2 under ethynylation conditions. In Test 1, the catalyst contains 35 wt.% copper (5.25 g). The maximum leaching is 8 ppm (2 mg, 0.038%), which agrees with the experiments shown above.

Bismuth is the catalyst promoter or inhibitor at 4 wt.% in Test 1. It is calculated at 0.90 g. The maximum leaching is 5 ppm (1.25 mg, 0.139%). Bismuth itself is a less soluble species; its leaching is constant and independent of the reaction conditions. It shows good stability as part of the catalyst that exhibits excellent metal-support interaction and is catalytically inert.

Magnesium is added to the catalyst either as part of the carrier together with silicon in the form of $MgO\text{-}SiO_2$ or as the promoter to enhance the activity of the active species. The CBS catalyst in Test 1 is absent of Mg; thus, it shows <2 ppm. In Test 2, an unknown amount of Mg is added, but the amount of leached Mg is considerably constant and at a low level throughout the ethynylation process. No relevant findings or conclusions can be proposed.

Silicon is the focus of the experiment, which is used as the carrier of the ethynylation catalyst. The silica-leaching study is essential to investigate catalyst stability and activity. The leached silicon will destroy the catalyst structure, causing sintering and loss of supporting effect to the catalytically active species that deactivates the catalyst.

In Test 1, 24.2 wt.% (3.63 g) silicon is involved, while the maximum Si-leaching is 191 ppm (47.75 mg, 1.32%). No silicon is leached before heating and introducing acetylene. Most leaching happens during N_2 purging after the ethynylation in Test 1 and during the first 4 h of ethynylation in Test 2. Despite the limited data, possible explanations are proposed.

In Test 1, the release of the slight overpressure of the acetylene atmosphere and cooling down from 90 °C changes the condition in the reaction mixture, such as the equilibrium and gas solubility, which may lead to an increase in Si-leaching. In Test 2, the amount of Si leaching mainly happens when the catalyst is at the activation stage in the first 4 hours, and conditions in the reaction mixture also changed with the increase in pressure and temperature. Additionally, this is also the time when copper is actively transformed from CuO into Cu_2C_2. The metal-support interaction alters significantly with surface reactions, and potential delocalization and movement take place, which may lead to Si leaching. It is then stabilized when the equilibrium is reached; for example, the change is 109 to 110 ppm at 20 h to 24 h. It is also known that silicon is less soluble in acidic conditions. However, this is not supported by the results that Test 1 is at pH 7 and has higher silicon leaching at the ending but lower at 4 h and 24 h than Test 2 at pH 5.

Interesting results are obtained from the leaching study using the ICP-OES technique with different devices. The results and findings provide supporting information, valuable insights, and new ideas for the design of new ethynylation catalysts and a deeper understanding of the catalytic Reppe ethynylation mechanisms. However, concrete conclusions can only be drawn with evidence from further relevant and modified experiments and data. This will be an exciting direction for future investigation to produce the catalyst with enhanced stability.

3

GENESIS OF CUPROUS ACETYLIDE SPECIES

3.1 Genesis Pathways of Cuprous Acetylide

Cuprous acetylide is believed to be the catalytically active phase in the Reppe ethynylation of formaldehyde to produce 1,4-butynediol (BYD) and propargyl alcohol (PA). However, the identification of the actual active phase has been a real challenge since the discovery of this catalytic process. Up to now, limited information and properties of copper acetylide species are known in the chemical database and safety data sheets due to their highly explosive nature.①

Not many studies have focused on the identification and differentiation of cuprous acetylide from other possible structures. Several hypotheses for the copper acetylide-containing catalytically active phase are discussed in Chapter 1.1.4. A list of potential structures and compositions was proposed by Kirchner in 1972 [160] (refer to Table 7-3). An XRD diffractogram and a structure of cuprous acetylide nanoparticles were simulated from DFT calculations and reported by Judai *et al.* [162, 174] (refer to Figure 7-12).

Motivated by Bruhm *et al.* [159] (refer to Appendix in Chapter 7.1.4), who experimentally identified the presence of cuprous acetylide in the catalytic ethynylation process, this paper verified their findings and further developed the analytical processes of this explosive species using techniques like PXRD and Raman spectroscopy.

This chapter aims to genesis the pure-phase and cuprous acetylide-containing phases via various formation pathways, such as the *in situ* transformation from CuO-based catalysts under the ethynylation conditions, deposition precipitation (DP) in ammoniacal cuprous salt solution under the acetylene atmosphere, and direct precipitation and potential crystallite growth of pure-phase Cu_2C_2 in dissolved aqueous acetylene solution under inert or reductive conditions.

With the expected cuprous acetylide phases in multiple forms produced via various synthesis methods, they are washed, separated, and stored under different conditions and atmospheres. The samples are then analyzed by several suitable and safe qualitative and quantitative analytical techniques, such as PXRD, Raman spectroscopy, TGA/DSC-MS, and CHN analysis, in Chapter 3.2, to identify the unique explosive and sensitive species. Standard and optimized sample handling, processing, and analysis procedures are implemented to ensure the reliability and accuracy of the measurements.

Next, it is also necessary to differentiate the desired cuprous acetylide (pure-phase) from the other potential species, such as cupric acetylide, copper diacetylides, and copper polyynides, supported by analytical data, the catalytic performance, and their physical and chemical properties, such as the appearance, reactivity, and explosivity.

① Copper (I) acetylide, CAS No. 1117-94-8; Copper (II) acetylide, CAS No. 12540-13-5

3.1.1 Optimization of Synthesis Procedures of Cuprous Acetylide

The synthesis procedures of the cuprous acetylide, Cu_2C_2, can be found easily in the literature. However, post-treatments, such as separation, purification, drying, and storage conditions, especially the proper and reliable methods to qualitatively and quantitatively identify pure-phase Cu_2C_2, are not discussed and remain challenging. As mentioned (refer to Scheme 1-7), cupric acetylide, copper di-/polyacetylides (polyynides), and copper acetylide complexes can be formed under similar conditions, which are difficult to identify and differentiate from the cuprous acetylide phase, showing different properties and catalytic performance. Most studies of cuprous acetylide are safety inspections for industrial plants involving acetylene, which try to avoid the formation of explosive metal acetylides that may lead to severe damage and danger. Hence, the formation, especially in the pure phase, is out of focus.

This section aims to genesis and identify the pure-phase cuprous acetylide in a safe and reproducible process. Several possible synthesis pathways of cuprous acetylide species (refer to Chapter 5.3.1) are discussed, including the catalysis pathways that formed *in situ* from a silica-supported CuO catalyst via deposition precipitation (DP) methods to precipitate cuprous acetylide in ammonia solution onto the surface of a silica carrier and by direct precipitation under various conditions, like in air or oxygen-depleted atmosphere in water, formaldehyde, and ammonia solution, to precipitate pure-phase cuprous acetylide. The identification and differentiation of the Cu_2C_2 from the other phases are investigated in the following chapters.

The standard method to synthesize Cu_2C_2 is dissolving copper(I)/(II) salt precursors in basic ammoniacal solution, for example, copper(I) chloride in 25-30% ammonia solution. The acetylene gas is bubbled into the ammoniacal cuprous chloride solution and produces highly explosive reddish-brown cuprous acetylide precipitates.

This procedure raises several questions. One is the necessity to add a reducing agent into the ammoniacal solution to ensure only cuprous instead of cupric ions are present. In this experiment, hydroxylamine hydrochloride ($HONH_2 \cdot HCl$) is applied as a reducing agent. The oxidation state of copper can be easily concluded. This benefits from copper's unique property of color change in copper-ammonia solutions. The deep blue represents a copper(II)-ammonia complex, while the colorless represents a copper(I)-ammonia complex. This argument also depends on whether copper(I) or copper(II) salt precursors are used and whether the inert and oxygen-depleted atmosphere is maintained during the synthesis process.

Additionally, this is an experiment to study whether formaldehyde or acetylene acts as the RA in the catalytic ethynylation process, where CuO in the pre-catalyst is reduced and transformed into Cu_2C_2 without adding a reducing agent (RA). It is also interesting to investigate the role of ammonia solution in its synthesis since CuO can be transformed into Cu_2C_2 in formaldehyde solution under ethynylation conditions.

The proposed reaction scheme of direct synthesis of Cu_2C_2 species is shown in Scheme 3-1.

$$[Cu(NH_3)_4]^{2+} \xrightarrow{\text{Reducing Agent}} [Cu(NH_3)_4]^{+} \xrightarrow{C_2H_2} Cu^{+}{}_m(C{\equiv}C)_n$$

Scheme 3-1. The reaction scheme of copper(II) is reduced to copper(I) in a copper-ammonia complex solution by a reducing agent (RA) and then transformed into copper(I) acetylide species with the introduction of acetylene gas.

A relevant consideration is the atmosphere during synthesis and post-treatment, whether the oxygen-free, oxygen-reduced, or open condition is influencing the Cu_2C_2 formation. Theoretically, if the copper(II)-ammonia complex is present, cupric acetylide, CuC_2, will be formed when acetylene gas is introduced. Hence, it is necessary to ensure only copper(I) is present, either using the copper(I) salt precursor in the strictly oxygen-free condition or adding an RA in excess to eliminate the formation of the copper(II) phase during the synthesis under an acetylene atmosphere. The following question is then raised. That is, whether or not the precipitated Cu_2C_2 will be oxidized into CuC_2 afterward. This can happen in the wet slurry form in the suspension or during washing and purification in water or methanol. It is also possible during the separation and drying process and even during the analysis in contact with air.

Another aspect to be taken into account is the decision of the limiting reagents for the Cu_2C_2 formation. Either copper(I) or acetylene is added in excess to investigate the possibility of producing acetylene coupling reaction, polyynes/polyynides, and complex formation, as proposed by Glaser [53], Cataldo *et al.* [166-171], and Kirchner [160].

With these considerations, a series of experiments under ambient conditions to directly synthesize pure-phase Cu_2C_2 is performed. Test (1) uses copper(II) salt precursors, $CuSO_4$, dissolved in an ammonia solution with the addition of RA and saturated acetylene water.② Tests (2) and (3) use copper(I) salt precursors, CuCl, dissolved directly in saturated acetylene water, with and without the addition of RA. These tests compare the impacts of the oxidation states of copper and investigate the reduction capability of the chosen reducing agent, $HONH_2HCl$, when oxygen is present in the atmosphere. For comparison, the co-precipitated CBMS pre-catalyst containing CuO is used for Tests (4), (5), and (6). The CBMS catalyst samples are immersed in saturated acetylene water, with the addition of RA, FA, and heat to 90 °C, respectively. These tests evaluate the sole role of FA and acetylene as RA to reduce CuO into

② The saturated acetylene water is used to provide a diluted and quantitative acetylene supply. This is an alternative of a diluted gas, e.g., 10% C_2H_2 in Ar, which is not available in the market as acetylene gas is dissolved and pressurized acetone in a porous monolithic material-filled cylinder. The acetylene gas solubility of 1.20 g/L at 20 °C (Table 2-1), has an appropriate concentration for the experiments.

Cu^+ and further to Cu_2C_2. Additionally, the CBMS pre-catalysts activated in water and aqueous FA solution under the ethynylation conditions are tested and shown as Tests (i) and (ii).

The photos of these syntheses and tests under various conditions are shown in Figure 3-1. The corresponding samples ((1) – (4)) are analyzed in XRD, as shown in Figure 3-2 (refer to Figure 7-20 for supplementary data). These samples are prepared and analyzed by XRD after optimizing the synthesis, post-treatment, and analytical procedures. The details, such as the XRD evaluations on Cu_2C_2, are discussed in Chapter 3.2.

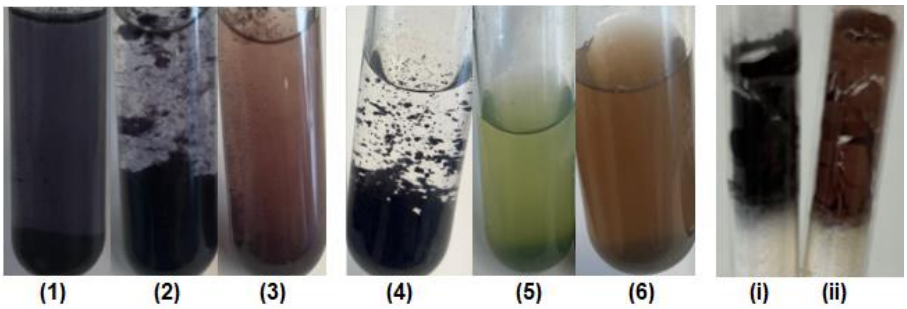

Figure 3-1. The photos of self-synthesized Cu_2C_2 under various conditions: (1) dissolve $CuSO_4$ in ammonia solution, adding RA and acetylene-water; (2) dissolve CuCl in acetylene water with dropwise addition of RA; (3) dissolve CuCl in acetylene water; (4) add CBMS catalyst in acetylene-water with dropwise addition of FA; and (6) heat (5) to 90 °C. The photo of the (i) water-activation and (ii) formaldehyde-activated CBMS catalyst in the catalytic ethynylation process.

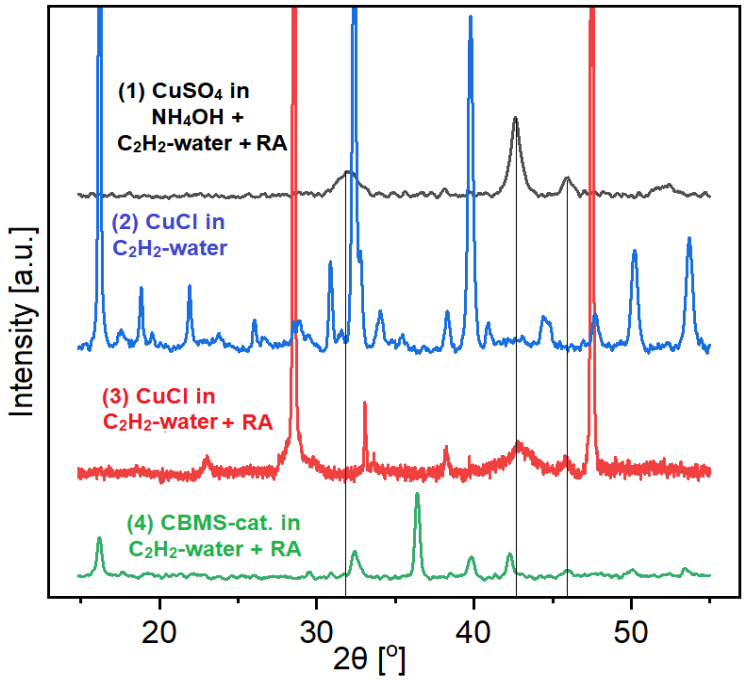

Figure 3-2. The PXRD diffractograms of pure-phase Cu_2C_2 samples were prepared via various synthesis pathways. (1) dissolve $CuSO_4$ in ammonia solution, adding RA and acetylene-water; (2) dissolve CuCl in acetylene water with dropwise addition of RA; (3) dissolve CuCl in acetylene water; (4) add CBMS catalyst in acetylene-water with dropwise addition of RA

From the XRD analysis, Test (1), with the standard Cu_2C_2 synthesis procedures, shows the characteristic XRD pattern of Cu_2C_2, indicating its successful transformation from the $CuSO_4$ precursor into Cu_2C_2. It suggested the crucial role and necessity of ammonia solution in the pure-phase Cu_2C_2 synthesis, compared to the others without ammonia. For Tests (2) and (3), both using CuCl as copper(I) precursor, Test (2) without the addition of RA has the characteristic XRD reflexes of $CuCl_2$, indicating its partial oxidation of Cu^+ to Cu^{2+}. Test (3) with RA has the reflexes of CuCl. It also suggests showing a certain degree of the Cu_2C_2 reflexes besides its highly intense CuCl reflexes. This proves the role of the reducing agent.

From the photos, different colors of the precipitates or solid particles and liquid phase solutions can be observed. From theory, the cuprous acetylide is a reddish-brown precipitate, while the cupric acetylide is a brownish-black precipitate. The CBMS catalyst is a green powder.

For Tests (1) to (3), it is obvious to tell the differences. Test (1) with ammonia solution has the darkest color, which is contributed by the dark precipitates and the deep blue color from the remaining copper(II)-ammonia complex. Test (2) has fluffy black precipitates and a clear solution, while Test (3) shows a brownish solution and precipitates. This shows the decisive role of RA during the synthesis to selectively precipitate copper(I) or copper (II) acetylides. However, it is still hard to conclude their efficiency from the supporting analytical results like PXRD, elemental analysis, and catalytic performance test. It is better to centrifuge these sample suspensions to obtain a clear solid-liquid phase separation for better observation.

For Tests (4) to (6), the differences are also significant. When RA is added in Test (4), fluffy black precipitates form in a clear solution, similar to Test (2). With the same samples but replacing RA with FA, a completely different solution and precipitates are formed in Test (5). The color is the same as the CBMS catalyst used in this test. Upon heating Test (5) to 90 °C, it turns slowly brownish and becomes similar to Test (3) over time, which has no RA added. This, again, proves the crucial role of RA in forming copper(I) acetylides instead of copper(II) acetylides. This series of tests further proves that FA, not solely and even with a limited amount of acetylene that dissolved in water, is as efficient as the RA in reducing the CuO in the pre-catalyst and transforming into the catalytically active Cu_2C_2 phase.

For Tests (i) and (ii), the CBMS pre-catalysts are activated in water and aqueous FA solution, respectively, under the ethynylation conditions at a static 90 °C and 1.2 bar absolute acetylene pressure for 5 h. From the pictures, the activated catalysts are filtered. The one activated in water is black, which is suspected to be cupric acetylide, and the one activated in FA solution is reddish brown, which is suspected to be cuprous acetylide. The catalytic performance in BYD Yield of these two differently-activated catalysts in ethynylation is shown in Figure 3-3.

From the results, the water-activated catalyst produces about one-seventh the yield of BYD compared to the formaldehyde-activated catalyst. This suggests, assuming the conclusion of

the presence of cupric and cuprous acetylides based on the color of the activated catalysts is correct, that cuprous acetylide has higher activity in the catalytic Reppe ethynylation process. Also, a formaldehyde solution only under ethynylation conditions (compared to Test (5) and (6)) can effectively transform CuO in the pre-catalyst into the active Cu_2C_2 phase but not water.

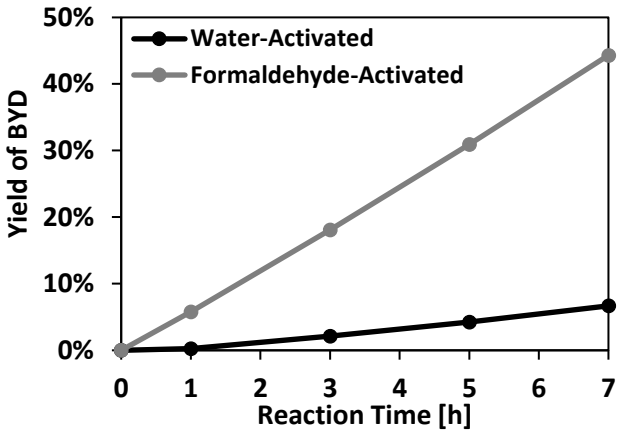

Figure 3-3. The graph illustrates the catalytic performance in yield of BYD of a water-activated and a formaldehyde-activated CBMS pre-catalyst in a 7 h two-step ethynylation process.

Besides the visual observation and in the catalytic ethynylation performance test, the direct proof of the formation of the Cu_2C_2 phase, differentiated from CuC_2 and other phases, is necessary. Beyond that, the influences of the synthesis, post-treatments, and analytical conditions also need to be investigated. The analysis, focused on PXRD and supported by Raman and TGA/DSC-MS, is evaluated and discussed in the next section.

3.1.2 Comparison of Catalytic Activity of Differently Formed Copper Acetylides

The catalytic performance in Reppe ethynylation of the catalytically active cuprous acetylide phase, formed via different pathways, is investigated. With the study of the catalytic structure-activity relationships in Chapter 2.2, it has been concluded that various promoters and carriers play a crucial role in conventional ethynylation catalysts. However, for the directly synthesized active Cu_2C_2 species, whether it is supported or in pure phase via deposition or direct precipitation, it is difficult to include an additional species and function in their respective roles. This is because of the difference in solubility, such as bismuth, which is insoluble in basic solvents like ammonia solution. This will affect the homogeneity and dispersion of the produced catalyst and largely influence the metal-promoter-carrier interactions. The differences in other properties, such as copper dispersion, particle size, and crystallinity, are also significant.

On the other hand, the directly synthesized active Cu_2C_2 phase has the advantage of avoiding a black box of the unclear catalytic activation mechanism. It eliminates the uncertainty of the phase and structural transformation from the CuO precursor to the active phase and reduces the parameters in a highly complex reaction system.

In an experiment, Cu_2C_2 on silica is prepared by deposition-precipitation; refer to Figure 3-4. Cuprous chloride is used as a copper(I) precursor that is equivalent to 5 wt.% of Cu in the model catalyst. It is dissolved in a 10% ammonia solution containing silica at ambient conditions and atmosphere. No reducing agent is added. A light blue solution and white silica suspension are formed. When acetylene gas is introduced, an instant color change is observed to brownish. The color of the suspension becomes darker over time, and water droplets condense outside the cold reaction tube, indicating an endothermic reaction during the Cu_2C_2 formation. After about two hours, the color remains unchanged, and the temperature returns to room temperature, which marks the completion of the Cu_2C_2 formation on the silica carrier.

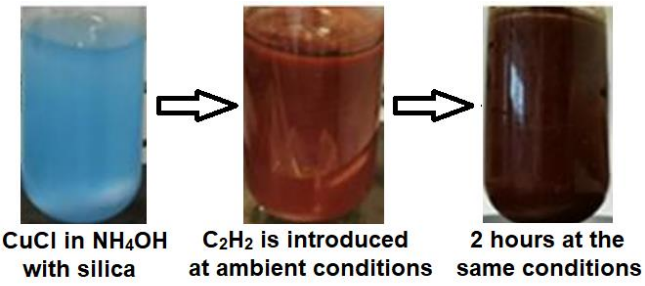

Figure 3-4. The photos of a trial test of deposition precipitation of cuprous acetylide on silica in ammonia solution under ambient conditions with the introduction of acetylene gas. The color of the suspension during different stages is shown: light blue (left) is observed before introducing acetylene, a brownish color (middle) is shown immediately when acetylene is introduced, and dark brown suspension (right) forms over time in 2 hours of reaction under flowing acetylene.

The follow-up experiments with copper loadings from 1-50 wt.% of CuCl on 2 g of silica according to the same procedures are prepared. These obtained Cu_2C_2/SiO_2 catalysts are separated from the ammoniacal solution by vacuum filtration under ambient conditions and used as model catalysts to be tested in the catalytic Reppe ethynylation. Their catalytic performance in BYD yield regarding copper content in *mmol* (converted from copper loadings) is shown in Figure 3-5. CBS and CS pre-catalysts containing 35 wt.% copper (11.0 mmol) are prepared by co-precipitation and tested in ethynylation to compare with the one with 11.0 mmol copper prepared by the deposition precipitation method.

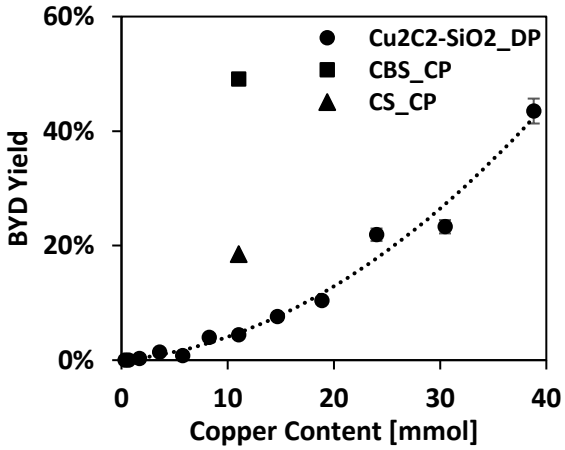

Figure 3-5. The graph illustrates the BYD yields of copper loadings from 1 to 50 wt.% that converted into 0.3-38.8 mmol of Cu_2C_2/SiO_2 model catalysts synthesized from CuCl in ammonia solution by introducing acetylene gas via deposition precipitation (DP) methods. CBS and CS pre-catalysts containing the same amount of 11.0 mmol of copper prepared by the co-precipitation (CP) method are shown for comparison.

From the results, a polynomial trendline with an order of 2 is plotted to fit the catalytic performance of the Cu_2C_2/SiO_2-DP model catalysts of different copper contents from 0.3 to 38.8 mmol. A possible explanation for this behavior is that mesoporous silica provides a relatively huge volume of pores and a large surface area. When the copper content is too low, copper species can easily diffuse into the deep pores of the silica carriers by the capillary forces, leaving the surface with few active sites of cuprous acetylide for the catalytic reaction. With increasing copper loadings, the deposition precipitation of copper species fills not only inside the pores but also the outer surfaces, creating good dispersion and a large number of active sites. Furthermore, it can be predicted that if the copper content is further increasing, blockage and agglomeration may take place, which will reduce the active sites and hinder the catalytic activity in the ethynylation reaction.

Additionally, a more significant error rate and horizontal error bar referring to the copper content are applied based on the calculation. This is because the actual copper loading is not

determined (i.e., ICP-OES). The ICP-OES method is used for the CuO-containing pre-catalyst. Since the model catalysts contain directly deposited Cu_2C_2 with relatively larger particles, indicating its low dispersion, compared to the *in situ* formed Cu_2C_2 from the co-precipitated catalyst. Their decomposition in the concentrated acids, which is required to dissolve the solid phase for the ICP-OES sample preparation, becomes even more challenging due to the vigorous and explosive reaction.③ The safe and reliable sample preparation procedures for ICP-OES measurements of copper acetylide-containing samples will be investigated. It also can be observed from the supernatant solution, after filtering away the precipitated catalysts, turns to deep blue in the air over time, marking the remaining copper(II)-ammonia complex $[Cu(NH_3)_4(H_2O)_2]^{2+}$. This means that the copper is in excess and cannot be deposited entirely on silica. Modifications are done with the pure-phase Cu_2C_2 and shown in the next chapter.

When comparing with co-precipitated CBS and CS pre-catalysts of the same amount of copper of 11.0 mmol, deposition precipitated Cu_2C_2 model catalyst shows a much lower performance. A poorer copper dispersion, less active sites, and weaker metal-support interaction can be expected. Moreover, the catalysts without bismuth also lack their promoting and inhibiting effects, as discussed above, resulting in poorer catalytic performance.

On the other side, this trial experiment has several limitations. The foremost one is the improper and inconsistent drying, purification, and storage techniques. This may lead to the deactivation of the Cu_2C_2-containing model catalyst and affect the catalytic performance. This impact on the *in situ* activated catalyst is shown in Chapter 2.4.1, and the impact on the directly formed Cu_2C_2 species will be discussed in the next chapter. The analytical data on the model catalyst, such as the actual copper loadings, the phase identifications, the specific surface area, and the pore volume of the catalyst, will be collected to support the current findings. These data and further modifications will be helpful in correlating and concluding the structure-activity investigations and catalytic performance with the catalyst synthesis methods, the structural properties, and the active phase transformation.

However, the successful direct synthesis of Cu_2C_2 on silica via the deposition precipitation provides incredible insight and motivation for the following investigations on the different synthesis and post-treatment conditions of pure-phase Cu_2C_2 and the respective analytical methods of the qualitative and quantitative identifications.

③ It is known from database that the explosivity of cupric acetylide is higher than cuprous acetylide. The explosivity is also proportionally related to the particle (or rather crystalline) size of copper acetylides.

3.2 Identification and Characterization of Cuprous Acetylide

The catalyst structure-activity relationships have to be literally discussed based on the catalytically active phase. The study of the pre-catalysts, which is presented in Chapter 2.2, provides valuable insights and knowledge for the relevant research. However, there is always a black box of unknowns and uncertainties during the transformation from the precursor phase to the activated phase, such as the activation mechanism and the catalytically active phase identification, quantification, and characterization, which is critical for further investigations.

With the objective of achieving a step forward to the actual active phase of the catalytic Reppe ethynylation of the formaldehyde process, the aim is to prove and experimentally identify the catalytically active cuprous acetylide-containing species formed *in situ* under the ethynylation conditions. However, the prerequisite step is to synthesize the pure-phase cuprous acetylide, characterize, and differentiate the pure-phase from the other mentioned interfering species based on their appearance, physical and chemical properties, and, more importantly, their characteristic crystallography, diffraction, and spectral data.

Copper acetylides are sensitive to the environment due to their highly explosive, decomposed, and easily phase-transformed nature. Hence, it is critical to determine suitable synthesis, storage, and analytical conditions to avoid the chemical transformation of cuprous acetylide before the final identification. On the other hand, it is also challenging to implement reliable analytical techniques to identify the cuprous acetylide species.

This chapter uses copper acetylide-containing samples obtained via several synthesis pathways, as modified and deviated from the previous discussions on the synthesis, post-treatment, and analysis conditions and requirements in Chapter 3.1. It employs the typical qualitative analysis techniques, like XRD and Raman spectroscopy, discussed in Chapter 3.2.1, and quantitative analysis techniques, like TGA/DSC-MS and elemental CHN analysis, discussed in Chapter 3.2.2. The copper acetylide-containing species are analyzed using specially developed sample preparation procedures under optimized analytical conditions. Cu_2C_2 and its derivations are experimentally identified and partially differentiated. Lastly, the explosion tests and catalyst deactivation elaborated in Chapter 3.2.3 provide valuable knowledge on the explosive conditions and explosivity of the copper acetylides and safeguard the successful and accurate analytical results from accidents.

3.2.1 Qualitative Analysis of Cuprous Acetylide and Influencing Parameters

The qualitative analysis of acetylide and its derivative species focuses on XRD and Raman spectroscopy techniques. In the first part of this section, XRD is applied to identify the pure-phase cuprous acetylide, the impurities that may be formed during the synthesis and sample preparation, and unknown phases that potentially form the Cu_2C_2 derivative phases. The proper handling and treatments during the pure-phase Cu_2C_2 synthesis and the influences of the respective parameters are also investigated. The second part employs Raman spectroscopy, which has several unique features for phase identifications and differentiations among the copper acetylide species that XRD cannot identify. Combining both techniques, a reliable X-ray diffractogram and Raman spectrum for pure-phase cuprous acetylide are obtained. Furthermore, the standard synthesis, post-treatment, and analytical procedures are implemented, which can ensure pure-phase cuprous acetylide formation.

XRD Analysis of Copper Acetylides

XRD determines the crystallography of a substance. However, Cu_2C_2 and its derivative species have no established XRD data and crystallography structures. The only few relevant publications are Bruhm *et al.* [159] and Judai *et al.* [162, 174] (refer to Chapter 7.1.4), which are used as the reference of this investigation. This work has successfully identified and proposed XRD patterns and the characteristic reflexes of copper acetylide pure-phase Cu_2C_2. This is done by evaluating all the possible XRD analytical data of the Cu_2C_2-containing samples, which are synthesized under different pathways, and the pure-phase Cu_2C_2 that are prepared under different synthesis, post-treatments, and analytical conditions. The XRD reflexes and patterns are compared with each other and with the references in the literature. The most characteristic ones that existed in all samples were identified and assigned to Cu_2C_2.

As an overview, Cu_2C_2 is produced in the following pathways (refer to Figure 3-1):

i. An activated $CuO(\text{-}Bi_2O_3)/SiO_2$ catalyst under ethynylation conditions (in aqueous formaldehyde solution under slight over-pressure acetylene atmosphere at 90 °C);
ii. A Cu_2C_2 on SiO_2 model catalyst synthesized by deposition precipitation (in ammoniacal cuprous chloride solution under flowing acetylene atmosphere at room temperature);
iii. A pure-phase Cu_2C_2 powder prepared via direct precipitation (to be elaborated in detail).

These Cu_2C_2-containing samples are analyzed by XRD either in a wet slurry or in a dried powder form after standard post-treatments, like washing, drying, and purification. A collection of XRD diffractograms of self-synthesized Cu_2C_2 under various pathways and conditions, including the published ones, is summarized in Figure 3-6 as an illustration. The target XRD reflexes can be identified. The stepwise development and discussion will be shown in detail.

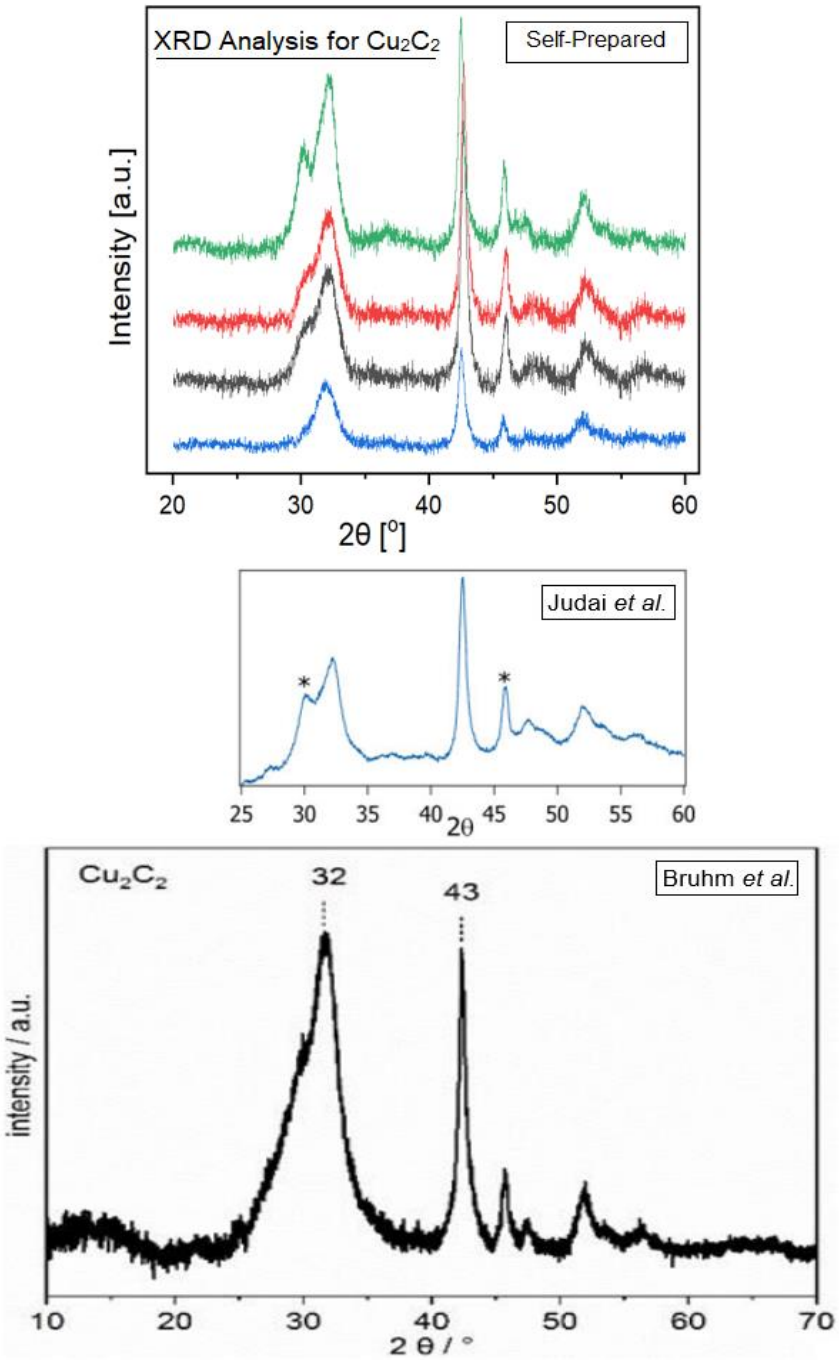

Figure 3-6. A collection of PXRD diffractograms of self-prepared Cu_2C_2 samples via different synthesis pathways and conditions are shown for illustration purposes. These XRD patterns are compared with the published ones by Bruhm *et al.* [159] and Judai *et al.* [162, 174].

From the overview XRD diffractograms in Figure 3-6, highly reproducible XRD patterns are obtained from four of the self-prepared Cu_2C_2 samples (their detailed synthesis conditions will be covered in the following discussions). The identical and most characteristic XRD reflexes are assigned at 2θ angles of 32.2°, 42.4°, 45.9°, and 52.0°. Another reflex at about 30.1° is noticed only in some samples; however, whether or not this reflex is present, the overall

patterns are highly similar to those found in the literature. The pattern in green with a significant shoulder reflex is highly aligned with the one published by Judai *et al.* [162, 174], while the red and black ones with a less significant shoulder reflex are similar to the one of Bruhm *et al.* [159]. Only the blue one does not show a shoulder, but the other reflexes are identical.

The successful analytical results with five identified XRD reflexes at 2θ = (30.1°), 32.2°, 42.4°, 45.9°, and 52.0° encourage further investigations of Cu_2C_2-containing species by XRD.

The objective is to synthesize a pure-phase cuprous acetylide. The first series of experiments aims to identify the possible impurity species that may be formed during its synthesis. This is done by tracking the *in situ* transformation of the directly precipitated Cu_2C_2 from ammoniacal cuprous chloride in acetylene-saturated water. The Cu_2C_2 precipitate samples are taken at 2, 15, and 60 min. After 60 minutes, excess C_2H_2 is introduced, and another sample is taken. These samples are filtered without purification and analyzed in XRD in a wet slurry formed in the open air. The XRD analyses of these samples are illustrated in Figure 3-7. The XRD diffractograms of CuO (from a self-prepared CuO/SiO_2 catalyst), CuCl (the chemical used to prepare the ammoniacal cuprous chloride solution), and Cu_2C_2 (a direct precipitated sample after proper purification) are shown in the figure as reference.

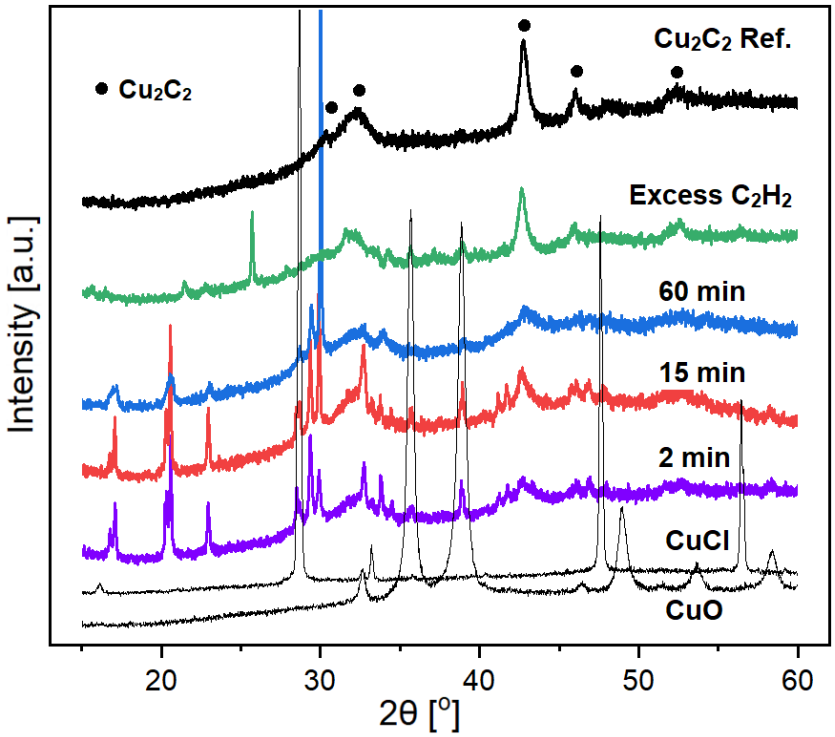

Figure 3-7. The XRD diffractograms of unwashed samples during the direct synthesis of pure-phase cuprous acetylide. The samples were taken at 2, 15, and 60 min after mixing the acetylene-saturated water and dissolved copper(I) chloride (CuCl) in ammonia solution. Another sample was taken afterward when excess C_2H_2 was added to precipitate the remaining copper ions in the solution. The references CuO, CuCl, and Cu_2C_2 are shown.

From the XRD diffractograms, the characteristic reflexes of Cu_2C_2 already appeared in the sample after 2 min in C_2H_2 (purple) and remained over 60 minutes (red and blue). The reflexes are enhanced after excess C_2H_2 is added. However, many more crystallized species, some of which are identified as CuO and CuCl and some that have yet to be determined, are present at the same time and may interfere with the investigations. Compared to the Cu_2C_2 reference, which has undergone proper purification, nearly all of the unassigned reflexes are removed. This indicates the importance of the purification procedures, as investigated in Figure 3-8.

Since the purification step of the directly precipitated Cu_2C_2 sample is highlighted, the XRD analysis of this series of experiments still uses the unwashed samples because it aims to retain the actual status and composition of the sample to study the process of Cu_2C_2 formation. It prevents the actual phases from being dissolved and removed during the washing step.

This is elaborated by the much less intense CuCl reflexes in the samples compared to the highly crystallized CuCl reference, which represents a quick transformation rate for the consumption of CuCl and the formation of Cu_2C_2. The changes in the XRD diffractograms are less significant for the samples from 2 min to 60 min but significant after excess C_2H_2 is added.

The three reflexes at 2θ between 28° to 30° possibly correspond to CuCl, $CuCl_2$, and Cu_2O, respectively, which are determined experimentally by comparing with the XRD reflexes of reference substances (refer to Figure 7-18). They disappeared entirely in excess C_2H_2, indicating the complete consumption of the copper ions as chlorides and oxides in the precursor solution and transferred into acetylides, which is reflected in its more significant XRD reflexes of Cu_2C_2 than those at 2 min to 60 min.

On the other hand, the presence of CuO/Cu_2O in all samples suggested that part of the copper(I) species in the samples is being oxidized. However, it is not clear in which step, whether it is during the synthesis, sample preparation, or the XRD analysis, oxidation takes place. This is investigated in the next part of this section.

As discussed, the purification step is critical in analyzing the pure-phase Cu_2C_2 by XRD. The Cu_2C_2 is proposed to have a layered structure that exists as less crystalline species. The XRD analysis reflects the crystallinity of the analytes by the intensity. The less crystallized Cu_2C_2 can be easily covered by highly crystallized impurities in its structure, as shown in Figure 3-8. A similar problem is also discussed in Figure 2-32, which analyzed the spent CBS catalyst after ethynylation by XRD. The spent catalyst contains highly crystallized $(BiO)_2CO_3$ that overlaps and hinders the reflexes of Cu_2C_2, making its identification challenging.

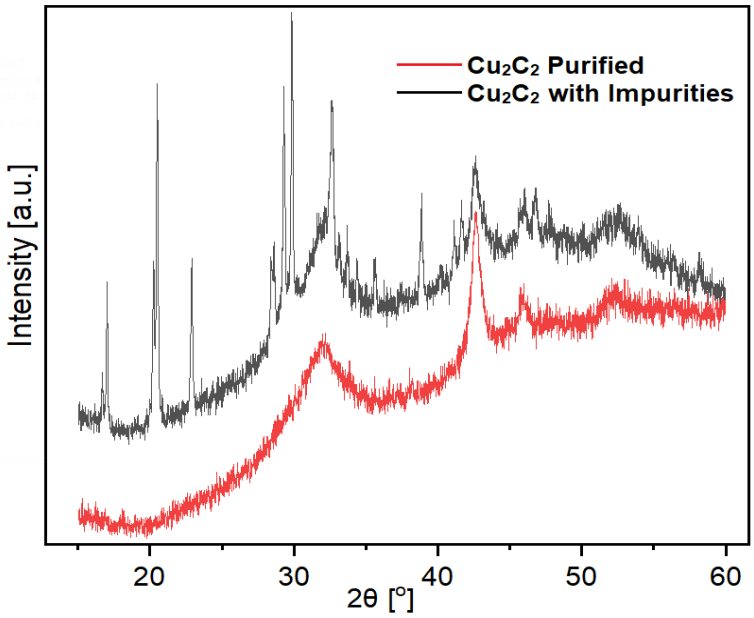

Figure 3-8. The XRD diffractograms of the sample of directly synthesized pure-phase C_2H_2 under two purification conditions. The black one contains many highly crystallized impurity species is the sample washed with methanol. The red one is the sample washed with water and then with methanol.

During the pure-phase Cu_2C_2 synthesis in the ammoniacal cuprous chloride solution with C_2H_2, ammonium chloride (NH_4Cl) and the unconverted CuCl and $CuCl_2$ are the source of impurities that may deposit on the surface of precipitated Cu_2C_2. It is also synthesized with copper(II) sulfate ($CuSO_4$) as the precursor to dissolve in aqueous ammonia and C_2H_2 solution, but the reducing agent, hydroxylamine hydrochloride ($HONH_2{\cdot}HCl$), has to be added. Ammonium sulfate ($(NH_4)_2SO_4$) is also present. As discussed in Chapter 3.1.1.

These samples are either separated directly after synthesis or rinsed with methanol before XRD analysis. Methanol is used to speed up the drying process of the pure-phase Cu_2C_2 using the Schlenk line technique due to its high volatility. However, it also enhances the crystallization of those species found in the XRD diffractogram of Cu_2C_2 with impurities in Figure 3-8. Despite many highly crystallized species, all of them are readily water-soluble and can be removed by rinsing with water, as shown in the diffractogram of purified Cu_2C_2. In conclusion, regardless of the following procedures and objectives of the study, rinsing the directly precipitated Cu_2C_2 with water (2-3 times) is necessary to obtain its pure phase.

It has been discussed in the literature that copper acetylides tend to form polymeric, ligand-complex, cluster, and non-crystalline structures (refer to Chapter 1.1.4). These refer to the proposed structures of cuprous acetylide derivatives, such as cupric acetylide and copper polyynides, and copper acetylide-containing species like $(Cu_2C_2/CuC_2)(CH_2O)_x(C_2H_2)_y(H_2O)_z$ (refer to Table 7-3). Hence, one of the objectives is to differentiate the pure-phase Cu_2C_2 from its derivative species and to identify and confirm the obtained XRD diffractograms and the

characteristic reflexes belonging to Cu_2C_2 but not any other species. It, again, emphasizes the importance of optimizing and standardizing the synthesis, post-treatment, and analytical conditions to ensure its purity. The influences of these parameters are investigated, as shown in Figure 3-9 and Table 3-1 (more are shown in Figure 7-19).

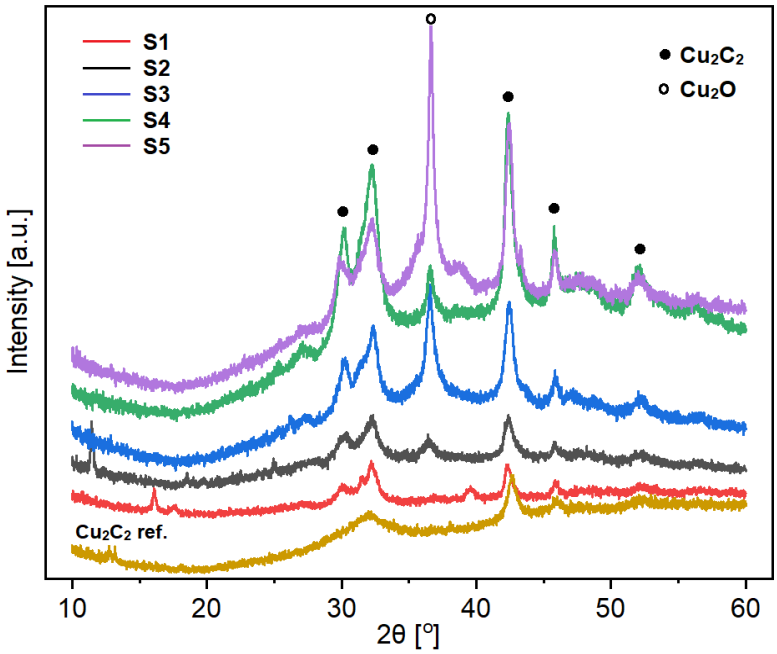

Figure 3-9. The PXRD diffractograms of the directly synthesized pure-phase cuprous acetylide under various conditions, as detailed in Table 3-1. The samples were washed three times with deionized water and one time with methanol under the respective conditions before drying and XRD measurement.

Table 3-1. The various conditions and parameters during the direct synthesis of pure-phase cuprous acetylide (Cu_2C_2) species.

Cu_2C_2	***Reducing Agent***	***Synthesis Condition***	***Drying Condition***
S1	*Yes in excess*	*Inert (Argon)*	*Vacuum (Schlenk)*
S2	*No*	*Inert (Argon)*	*Vacuum (Schlenk)*
S3	*No*	*Air Exposed*	*Oven (Air at 60 °C)*
S4	*Yes but limited*	*Inert (Argon)*	*Vacuum (Schlenk)*
S5	*Yes but limited*	*Air Exposed*	*Oven (Air at 60 °C)*

The direct precipitated pure-phase Cu_2C_2 is synthesized and dried under various conditions, as shown in Table 3-1. These samples are analyzed by XRD, as shown in Figure 3-9.

The characteristic Cu_2O XRD reflex at $2\theta = 36.4°$ can be correlated with the presence of oxygen during the Cu_2C_2 preparation process. It also illustrates the influence of oxygen at different sample preparation steps on the phase formation of Cu_2C_2 species. Additionally, it is noteworthy that no CuO is present in the XRD analysis of any samples.

S1 (red) is absolutely free of oxygen, which correlates with the absence of Cu_2O reflex in the XRD. However, it shows generally low intensity in the XRD diffractogram, which indicates the poor crystallinity of the Cu_2C_2 structure. It has several reflexes of impurity species remaining after purification. This may be due to the incomplete removal of impurities in this challenging step under absolute oxygen-free conditions, which has to be carried out very slowly.

S2 (black) and S4 (green) are under the same conditions, but one has no, and the other has a limited reducing agent. Both have the characteristic Cu_2O reflex in XRD but are less significant than S3 (blue) and S5 (purple), which are entirely air-exposed during synthesis and drying. It is suggested that a certain amount of the copper(I) ions, which are not yet precipitated as Cu_2C_2 in the synthesis solution, are partially oxidized. This is due to the insufficient amount of C_2H_2, which becomes the limiting reagent and rate-limiting step in the precipitation process since C_2H_2-saturated water is used for that synthesis. It is also because no or limited reducing agent is added, which may not be sufficient to maintain the reductive conditions that further slow down the Cu_2C_2 precipitation and lower its crystallinity. The less intense XRD diffractogram of S2 than S4 partially supports this argument.

S3 and S5 are prepared in air and show the most significant Cu_2O reflex. This can be explained by the same reason: more oxygen is involved in the Cu_2C_2 precipitation step and competitively consumes the copper(I) ions to form Cu_2O, which interferes with the formation of the crystalline structure of Cu_2C_2.

It can be concluded that oxygen has a crucial role in the synthesis and significant influence in the analysis of Cu_2C_2. The XRD characteristic reflex of Cu_2O at 36.5° has already been noticed. However, less significant Cu_2O and CuO reflexes are also observed in some pure-phase Cu_2C_2 samples that were properly purified but analyzed in wet slurry form. The XRD analysis is carried out without preventing the samples from being in contact with oxygen. The wet sample is also dried out, as shown in Figure 3-10. Hence, phase transformation and oxidation of Cu_2C_2 can be expected. It is also questionable whether the other impacts and misleadings that have not yet been identified will occur by the analytical data. Thus, analyzing the pure-phase Cu_2C_2 samples, whether in wet or dried forms, under an oxygen-free condition by XRD is evaluated.

Two tests are performed: one is to analyze the same pure-phase Cu_2C_2 samples with a layer of Kapton foil to eliminate the oxygen contact. In Figure 3-10, the XRD analysis is shown for a blank test of Kapton foil to determine its baseline as a reference (black); a real test with dried pure-phase Cu_2C_2 covered by Kapton foil, which is prepared in the glovebox that is completely free of oxygen (red); and a reference test with the same dried pure-phase Cu_2C_2 sample analyzed in the open atmosphere (blue).

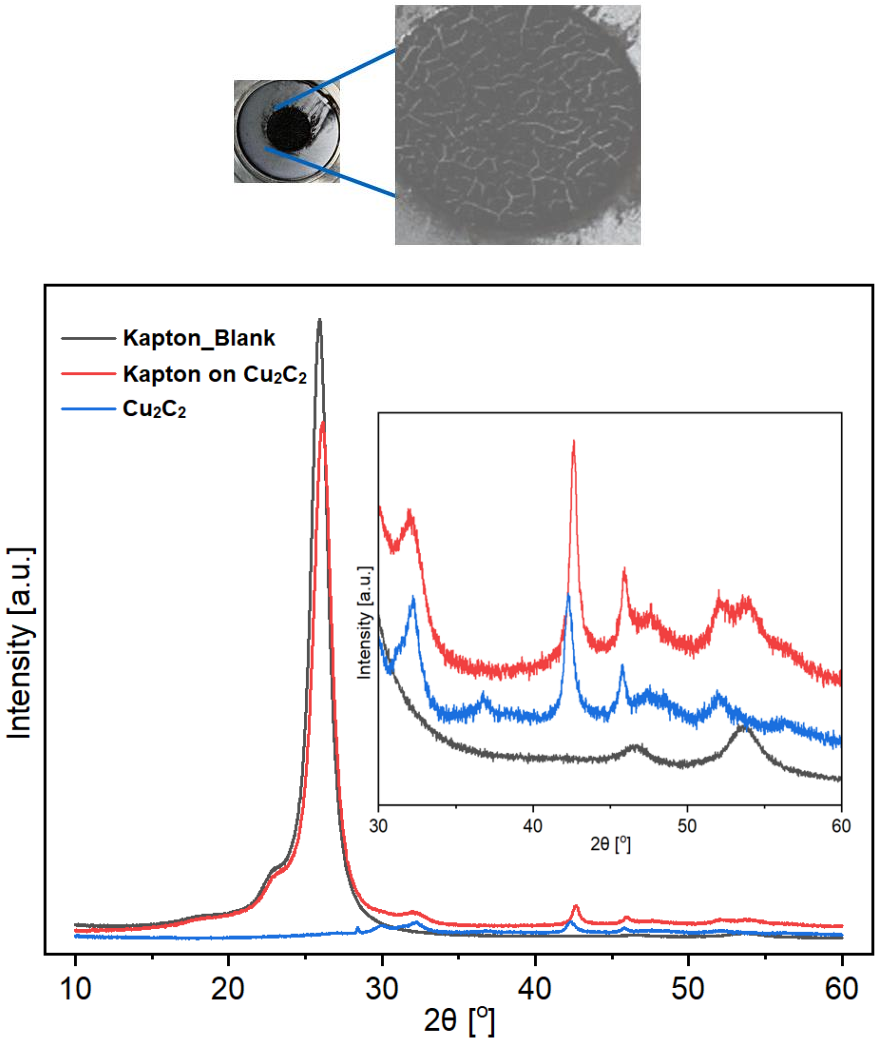

Figure 3-10. (top) The sample holder for XRD analysis was filled with a wet slurry of pure-phase Cu_2C_2 samples. It is dried out after the analysis, and the cracks can be observed. (bottom) The XRD diffractograms of a blank test of Kapton foil, a real test with dried pure-phase Cu_2C_2 covered by Kapton foil (prepared in the glovebox), and a reference test with dried pure-phase Cu_2C_2 analyzed in the open atmosphere. A zoomed-in image is shown.

The effect of the Kapton foil can be easily observed in the XRD analysis. For instance, the XRD reflex of Cu_2O at 36.5° is shown on the dried Cu_2C_2 sample analyzed in air (blue). This signal disappears in the analysis with Kapton foil (red). Of the five assigned characteristic XRD reflexes of Cu_2C_2 discovered earlier in this work, only one reflex at 30.1° is covered. The other four can be found in the sample with Kapton foil, despite the fact that two of them at 45.9° and 52.0° are partially overlapped by the broad reflexes of the Kapton foil baseline at around 46.5° and 53.4°. They can still be identified with the same XRD pattern and similar intensity as the reference sample. This result is promising as it once again verifies the accuracy of the XRD pattern with the five characteristic reflexes of Cu_2C_2.

Another verification test is shown in Figure 3-11. An XRD device using a molybdenum X-ray source and Debye-Scherrer transmission geometry is employed to analyze the dried pure-

phase Cu_2C_2 sample that is sealed in the Kapton foil. It is compared with the XRD diffractograms using a copper source and reflection geometry. The differences in the 2θ angles are converted into a scattering vector, |Q|, using the equation shown in Equation 3-1. This promising and encouraging analytical result again concludes the successful investigation of this work.

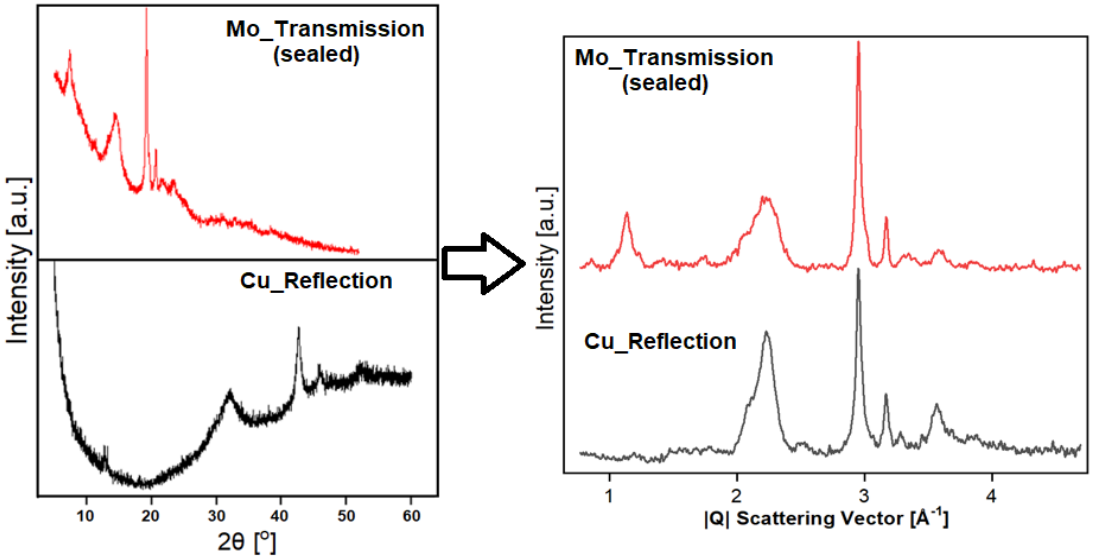

Figure 3-11. (left) The original XRD diffractograms of pure-phase Cu_2C_2 samples from two devices with X-rays using molybdenum (Mo, λ = 0 7107 Å) source and transmission (Debye-Scherrer) geometry and using copper (Cu, λ = 1 5419 Å) source and reflection (Bragg-Brentano) geometry. (right) The processed XRD diffractograms by converting radiation wavelength in λ and 2θ angles into scattering vector, |q|, according to Scheme 3-2. The sample is sealed between Kapton foil for analysis using Mo source in transmission geometry.

$$|Q| = \frac{4\pi}{\lambda} \sin(2\theta/2)$$

Equation 3-1. The conversion between the scattering vector, |Q|, and the 2θ angle degrees from XRD measurement with respect to the radiation wavelength, λ, of Debye-Scherrer geometry and Bragg-Brentano geometry. The diagram and detailed calculation are referred to in Figure 7-11.

Raman Spectroscopy Analysis for Copper Acetylides

Raman spectroscopy uses scattered light that consists of inelastic scattering photons from lasers to measure the modes of vibrational energies of the molecules. The particular chemical bonds of the molecule exhibit unique vibrational frequencies. Hence, identifying the bond vibrations at the specific wavenumber can be used as the reference for phase identification.

Similar to the XRD diffractogram, no existing database for cuprous acetylide and its derivative species is available. The reference signals and patterns for the Raman spectrum have to be self-determined. *Bruhm et al.* [159] published a reference Raman spectrum of Cu_2C_2 at wavenumbers of 430 cm^{-1} and 1710 cm^{-1}, as shown in Figure 7-13.

An example of the Raman spectra of Cu_2C_2 formed via the activation of CBS pre-catalyst under the ethynylation conditions is shown in Figure 3-12. In this measurement, a 532 nm laser with 1800 l/mm grating is applied. The maximal magnification is 50 times. The analytical parameters to be adjusted include the laser intensity and laser power (100% laser power is equivalent to 29.52 mW), exposure time, and repetitions. The optimized sample preparation and analyzing conditions are shown in Chapter 5.3.4.

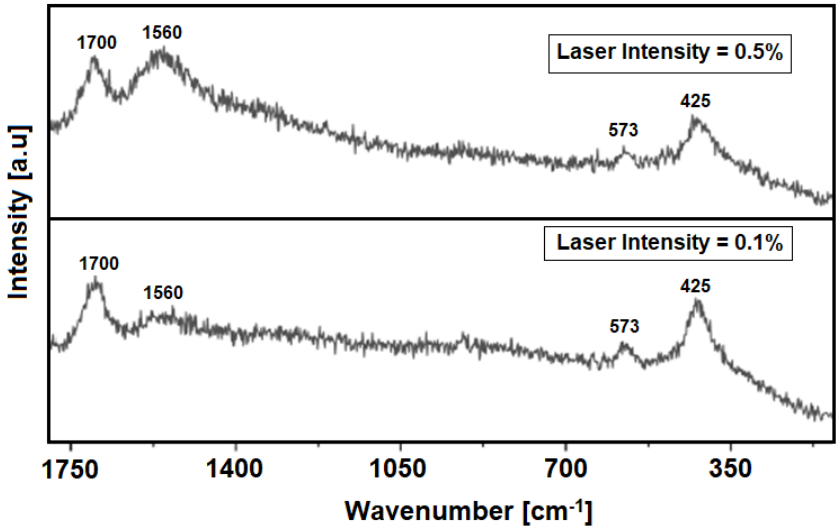

Figure 3-12. The Raman spectra using a 532 nm laser at 0.03 mW (0.1%) and 0.15 mW (0.5%) laser intensity of a standard CBS catalyst after a 7 h one-step ethynylation process.

The presence of Cu_2C_2 species is identified in Raman spectroscopy with the characteristic C≡C π-bond, which is determined by its vibrational signal at a wavenumber of 1700 cm^{-1} using calcium carbide (CaC_2) and lithium carbide (Li_2C_2) as references. Another specific bond at 425 cm^{-1} is assigned to Cu-C≡C α-bond, which is determined using copper(I) phenyl ethynyl ($(Cu\text{-}C{\equiv}C\text{-}Ph)_x$) as the reference [159].

Another vibrational signal is found at 573 cm^{-1}. This is proposed as a ≡C-C bond, which is a carbon coupled with an acetylenic carbon. This represents the formation of the carbon coupling or polymerization reactions, as introduced in Scheme 1-7. Another signal at 1560 cm^{-1} is recognized as carbon, using activated charcoal as the reference. Its formation is mainly due to the decomposition of the sensitive acetylide-containing samples by the high laser power. This is proven in Figure 3-12, where a more significant signal is formed with a laser intensity of 0.5% compared to the one of 0.1%.

Besides the signals that exist in Figure 3-12, Oxley *et al.* [133] reported a newly formed highly intense and broad signal at 1370 cm^{-1} and a small signal at 1860 cm^{-1} when exposing copper(II) salt precursors like CuO and $CuCO_3$ in acetylene. They also suggested the sp hybridized acetylide carbon's signal at 2100 cm^{-1} in Raman spectra, using phenylacetylene as the reference (refer to Figure 7-13). However, this signal doesn't appear in their samples.

This trial test with Raman spectroscopy shows both the advantages and limitations of this unique analytical technique in analyzing the copper acetylide species. The advantage is that Raman spectroscopy targets the chemical bonds of the molecules, for instance, the acetylenic carbon or the carbon-carbon coupling bonds. The identification of the specific cuprous acetylide's Cu-C≡C bond and C≡C bond, as well as the undesirable ≡C-C bonds from coupling or polymerization, allows the differentiation between the copper mono-acetylide and the di- and polyacetylides. This inspiring finding makes Raman spectroscopy an ideal technique for the step-forward investigation to qualitatively identify the actual catalytically active phase, whether the pure-phase cuprous acetylide or its derivative species, in the catalytic ethynylation process.

Additionally, the highly sensitive and explosive nature of copper acetylide species restricts the application of most of the characterization and analytical techniques. Raman spectroscopy allows the sample to be measured in solid, liquid, slurry, and suspension mixture phases. This prevents copper acetylide from exploding when dried or excited by the source of irradiation, which protects the devices and ensures operation safety. It also avoids the potential phase transformations, as shown in the PXRD measurements, during drying, exposure to the air, and contact with contaminants.

On the other hand, one of the limitations of Raman spectroscopy is the device's available laser powers. From the results, the suitable range of the laser power is below 0.1% since the signal of carbon at 1560 cm^{-1} is weakened but already present. However, the lower laser power is only possible at 0.05%, which is too low to show the desired vibrational signal-to-noise ratio. It is possible to moderate this to a certain extent by adjusting the other analytical parameters, such as the exposure time and repetitions. Still, optimal spectra cannot be expected.

This limitation also brings an argument as to whether the presence of the carbon and polymeric acetylide signals are from the original samples, which formed spontaneously during the pure-

phase cuprous acetylide synthesis or is contributed from decomposition and phase transformation due to the laser power and other improper post-treatment. Additionally, it makes the quantification of cuprous acetylide species and estimating the proportions of the Cu-C≡C bond and C≡C bond challenging.

A series of experiments for the identification of an *in situ* activated cuprous acetylide phase from CuO-based pre-catalyst (CBS) via a one-step ethynylation process is tested. Both the spent catalyst samples and the reaction mixture containing unconverted FA solution and the products of the reaction are analyzed by Raman spectroscopy, as shown in Figure 3-13. The spent catalysts and the reaction mixture are separated by centrifugation. The catalyst slurry is washed and purified under standard procedures and analyzed in the wet slurry form placed on a glass slide. The reaction mixture is filtered and placed in a transparent vial for analysis.

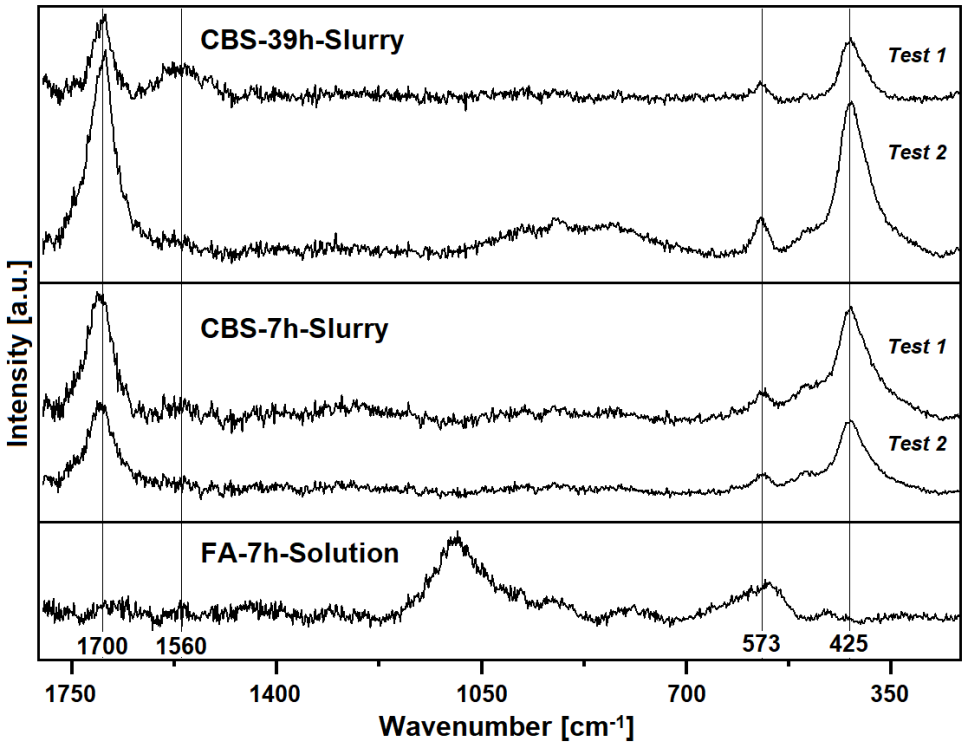

Figure 3-13. The Raman spectra using a 532 nm laser power under slightly varying analytical parameters of standard CBS catalysts via a one-step ethynylation process in aqueous FA solutions. The spent CBS catalysts after 7 h and 39 h ethynylation, labeled as CBS-7h-Slurry and CBS-39h-Slurry (two tests each at adjusted analytical conditions), are separated and analyzed in a wet slurry form placed on a glass slide. The filtered reaction mixture, labeled as FA-7h-Solution, is placed in a transparent vial and analyzed under the same condition.

From the Raman spectra in Figure 3-13, the identical characteristic vibrational spectra and signals at the specific wavenumbers are found, as shown and discussed in Figure 3-12. CBS-7h-Slurry and CBS-39h-Slurry are analyzed under slightly adjusted analytical parameters,

including the laser intensity, exposure time, and repetitions for Test 1 and Test 2. It aims to ensure the presence of the characteristic signals and to identify the signals, such as the one corresponding to carbon at 1560 cm^{-1}, whether it is originally from the sample or due to the transformation by the laser power during the analysis.

Due to these altered analytical parameters, it is difficult to draw a quantitative conclusion based on the signal intensities and the area under the curves between the spent CBS catalyst after 7 h and 39 h of ethynylation. Another explanation is due to the tendency of phase transformation and decomposition of this highly sensitive copper acetylide-containing spent catalyst. Thus, only qualitative identification is discussed for the results obtained from Raman spectroscopy. The follow-up standardization of the analytical parameters and procedures will be carried out to minimize uncertainty and variations.

In the same figure, a sample of the reaction mixture is analyzed in the liquid phase in a transparent vial for comparison. It is known that the products of ethynylation of the formaldehyde process, either BYD (HO-CH_2-C≡C-CH_2-OH) or PA (H-C≡C-CH_2-OH), contain the characteristic C≡C bond and bond at 1700 cm^{-1} and ≡C-C bond at 573 cm^{-1}, but not the Cu-C≡C bond at 425 cm^{-1}. Despite the weak signal at 1700 cm^{-1}, the presence of a signal at 573 cm^{-1} and the absence at 425 cm^{-1} agree with the hypothesis. However, there are still two limitations. One is that the concentration of BYD in the reaction mixture, as well as the other components and compositions, are not recorded. This information will be helpful in explaining the existing signals and their respective signal intensities. A follow-up analysis of the dissolved BYD solution of a higher concentration may be necessary. Another limitation is that the most intense and broad signal at around 1100 cm^{-1} has not yet been assigned.

As a relevant study of Chapter 2.3 regarding the influences of FA solutions on the active Cu_2C_2-containing phase formation, the analysis by Raman spectroscopy is shown in Figure 3-14.

The study in Chapter 2.3 focuses on the influence of the pH values and the buffer species in the FA solution and is analyzed using the PXRD technique. In this series of trial experiments, refer to the introduction and the literature shown in Chapter 1.1.3, the impact of methanol (M) content at 5%, 10%, 20%, and 40% in phosphate-buffered saturated aqueous formaldehyde solutions, labeled as FA-M5/10/20/40, on the active phase formation is investigated. The standard CBS pre-catalysts are activated in the respective FA-M solutions according to the standard experimental procedures, and the activated catalysts are analyzed by Raman spectroscopy under optimized analytical conditions.

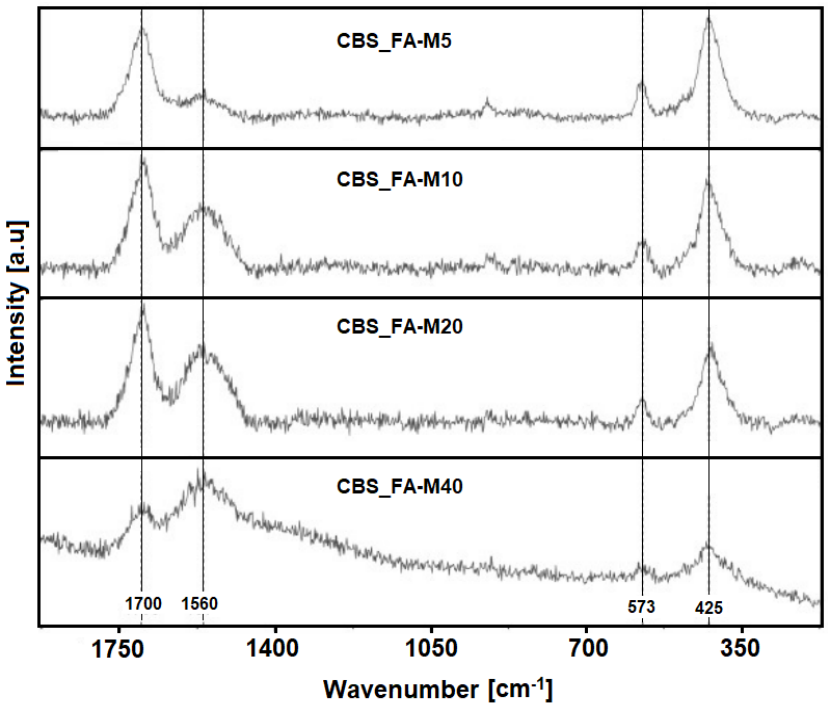

Figure 3-14. The Raman spectra using a 532 nm laser power at 0.03 mW laser intensity of standard CBS catalysts after a 7 h one-step ethynylation process in aqueous FA solutions (phosphate buffered at pH 7) containing 5%, 10%, 20%, and 40% of methanol (M5/10/20/40) as a stabilizer.

From the results shown in Figure 3-14, all four characteristic signals discussed above are shown, marking the existence of the copper acetylide phases and carbon. However, the signal at 1560 cm^{-1}, recognized as the carbon deposits, either present initially on the catalyst or lately decomposed due to the laser power, shows an inversely proportional relationship in intensities to the other three signals of respective copper acetylide bonds. This is, to some extent, logical as the total C atoms are constant. It is either shown as part of the acetylenic carbon bonds or as decomposed carbon.

On the other hand, while the methanol content increases from 5% to 40% in the formaldehyde solution, as suggested by Kiyama *et al.* [102-103], the BYD yield decreases linearly as the result of the decreasing FA concentration and conversion in the catalytic ethynylation process.

This finding agrees with the results of the catalytic performance in this series of experiments. The BYD yield for CBS_FA-M40 is only 0.36%, while the others are between 10-14%. With a step forward to explain this result, the yield is directly related to the number of active sites, which is the formation of the active cuprous acetylides. This is shown and supported by Raman spectroscopy, where the spectra for CBS_FA-M5, 10, and 20 are similar, especially for the signal intensities at 1700 cm^{-1} and 425 cm^{-1}, representing the presence of active cuprous acetylide. But this is not for CBS_FA-M40, where carbon is dominated.

3.2.2 Quantitative Analysis of Cuprous Acetylide and Structural Predictions

Despite the unsolved challenges of differentiating pure-phase cuprous acetylide from its derivatives, such as cupric acetylide and copper polyynides, and identifying the actual chemical structures and compositions, the qualitative analysis discussed in Chapter 3.2.1 of copper acetylide species via various synthesis pathways was successful using PXRD and Raman spectroscopy techniques. Furthermore, the optimal synthesis, post-treatment, and analytical parameters and conditions, which show minimal impacts on cuprous acetylide's phase stability and consistency, are implemented.

In this section, it is believed that quantitative approaches targeting the amount of copper and carbon atoms of cuprous acetylide, whether it is in the pure phase or the supported one, may provide several incredible advantages to address the same problems that qualitative measures cannot solve. The foremost one is its composition. As discussed and proven above, under similar conditions during synthesis and post-treatment, cuprous acetylide derivatives may be produced spontaneously or transformed from reactions like polymerization, oxidation, and decomposition. Regardless of their diffraction and spectroscopic properties, whether or not they are active that can be identified or differentiated, the mass balance, the atom counting, and ratios are specific. Hence, two quantitative analysis techniques, the TGA/DSC-MS and elemental (CHN) analysis, are employed.

Quantitative Analysis by TGA/DSC-MS

The quantitative analysis of cuprous acetylide regarding the copper-to-carbon ratio in the pure phase is more challenging due to the complications of the accurate calculations. Still, it is crucially helpful to identify the actual phase and chemical compositions of this species.

With the idea of mass balance, also motivated by the innovative approach by Bruhm *et al.* [159], Cataldo *et al.* [169], and Sun *et al.* [205], the thermal transformation of the highly sensitive cuprous acetylide species under oxidizing atmosphere is proposed in Scheme 3-2. The entire transformation process can be ideally recorded using the TGA/DSC-MS technique. The analytical and sample preparation procedures are shown in Chapter 5.3.4.

$$Cu\cdots C{\equiv}C\cdots Cu_{\,s} \xrightarrow{\text{heat}} (Cu + C) \xrightarrow{O_2} CuO_s + C_s \xrightarrow{O_2} CuO_s + CO_{2\,g}$$

Scheme 3-2. The proposed chemical transformation of cuprous acetylide during thermal decomposition under oxidizing conditions (synthetic air) was modified based on Bruhm *et al.* [159].

A test is carried out with a CBS pre-catalyst activated under the ethynylation conditions. The TGA/DSC-MS analysis is recorded from 25 °C (room temperature) to 700 °C at the heating rate of 10 K/min under constant synthetic air gas flow. The TGA records the mass change in % with respect to the temperature, while the DSC records the heat balance in mW simultaneously. The evolved gases, due to the thermal decomposition, are carried by the flowing gas to the coupled MS, which are identified by ion current in A for the respective mass-to-charge (m/z) ratios. The analytical results are shown in Figure 3-15.

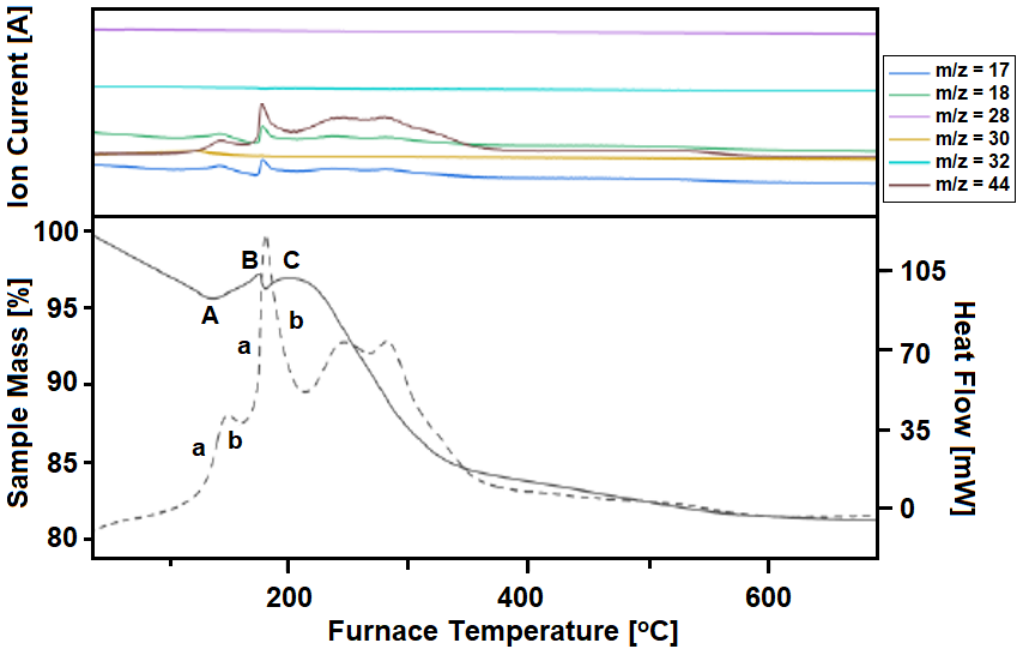

Figure 3-15. The TGA/DSC-MS analysis of the cuprous acetylide-containing sample was prepared via *in situ* activation of a CBS pre-catalyst under ethynylation conditions (the spent catalyst). The MS spectra (top) record the m/z ratio corresponding to OH (17), H_2O (18), N_2 and CO (28), NO and HCHO (30), O_2 (32), and CO_2 (44). The TG analysis with sample mass changes in % is recorded with a solid line, and the DSC measurement of heat balance in mW is recorded with a dotted line with respect to the elevated furnace temperature at a heating rate of 10 K/min (bottom). The change in the sample mass and heat flow is explained according to the proposed chemical transformation shown in Scheme 3-2.

From Figure 3-15, the solid line in the bottom graph shows the mass change of the sample. The overall mass loss is about 18%. One source of the mass loss is the consistent release of water, represented by the continuous decrease of the ion currents at m/z = 17 and 18 signals (blue and green) in the MS graph. Another source is from the evolution of the thermally transformed CO_2, shown by the m/z = 44 signal (brown). One of the limitations at this point is the missing information from the blank test and the background analysis with only bismuth oxide and bismuth oxide-silica carrier. As referred to in Figure 7-15 [159], the same trend of mass decrease is followed according to the reference signal of the pure silica carrier. It indicates that

further mass loss after the specific temperature range entirely contributed to the silica carrier, which can be neglected in the discussion focusing on copper acetylides.

The significant fluctuations in all signals happen at temperatures around 120 °C to 200 °C. It is complicated to explain these changes in mass and heat flow, as well as the signal in MS. This is because three parts of the reactions shown in Scheme 3-2, the decomposition of Cu_2C_2 into Cu and C, the oxidation of Cu to CuO, and the oxidation of C to CO_2, take place simultaneously or at a very short time interval. The mixing of these reactions confuses the analysis of mass change and heat flows. However, by combining all three sources of the corresponding signals in TGA/DSC-MS, the reasons and influences of the respective chemical transformations are explained according to the proposed reactions.

In the generally decreasing trend of the sample mass, a mass increase coupled with a sudden rise in heat balance in two regions marked with (a) is observed starting at Point (A) at 120 °C. This contributes to the exothermic thermal decomposition of Cu_2C_2 into Cu and C [205] and the simultaneous exothermal oxidation of copper(I) into CuO [159], where the mass gain is from the addition of oxygen atoms.

There is a rapid decrease in mass for a short period at point (B) at around 190 °C. The decrease is caused by the evolved CO_2 from the sample, in which decomposed carbon exothermally oxidizes immediately or simultaneously after the copper(I) oxidation. This is supported by MS, in which the releasing of CO_2 is recorded, corresponding to the sudden increase in CO_2 signals labeled by m/z ratios of 44. The same trend is followed for OH/H2O.

It is known that both copper(I) and carbon oxidation to CuO and CO_2 are exothermic reactions that release energy. However, the amount of energy released by each oxidation reaction, including the earlier decomposition of Cu_2C_2, is different. This causes interfering and accumulative effects in heat flow, whether it is gently or steeply increased or decreased.

It is worth mentioning in advance that the heat flow is calibrated with the elevated temperature. Only positive heat flow is recorded, which represents the net energy released throughout the chemical transformation in the analysis. When one exothermic reaction proceeds, the heat flow increases gently. When additional exothermic reactions take place at the same time, the increasing signal of heat flow becomes steeper. On the other hand, if an exothermic reaction is completed, depending on the amount of the total energy, the increase in heat flow becomes gentler and even decreases. The signal of heat flow goes back to net zero when all reactions are completed. Similar interfering and accumulative effects can also be applied in the explanation of mass change, which is less complicated than heat balance.

When looking at point (C) at around 200 °C, there is a little increase in mass, and soon it comes to the turning point, where only a decrease in mass is observed afterward. The slight increase is believed to be from the uncompleted Cu to CuO oxidation, which is interrupted by the

excessive C to CO_2 oxidation that starts at point (B). This results in the net loss in mass until the equilibrium in the mass change is reached. At the turning point after point (C), the copper oxidation is possibly completed, and only carbon oxidation takes place. This is supported by the continuous signal corresponding to CO_2 at an m/z ratio of 44 in MS and partially supported by the decreasing signal of heat flow, as discussed above.

It is challenging to explain these complicated partial steps from mass change, heat balance, and MS that are interconnected and influenced by each other in the diagram, especially from around 100 °C to 300 °C. Furthermore, the signals are caused by three simultaneously proceeding reactions, which are only proposed but have not been proven and well-supported by the theory.

Additionally, it is believed that other reactions and factors, such as surface adsorbed impurities other than water and sources of gas emission, may contribute to the change in mass and heat flow by the thermal side reactions. One hypothesis, especially for the Cu_2C_2 samples obtained after ethynylation, is C_2H_2 with an m/z ratio of 26. Its presence as part of the Cu_2C_2 complex structure is supported by the publications of Reppe *et al.*[41] and Kirchner [160]. The other suggestions and proposals can be referred to in Table 7-3. The C_2H_2 ion current signal with an m/z ratio of 26 was accidentally found in one pre-test in MS. However, this cannot be confirmed due to the limitation of the m/z ratio, which allows the same number to be assigned to multiple compounds. This signal needs further investigation.

In another series of modified TGA/DSC-MS experiments, freshly prepared pure-phase Cu_2C_2 is also analyzed. However, the sample explosively decomposed at slightly above 100 °C. The same sample is analyzed again after switching the analytical atmosphere from oxidative with synthetic air to the inert condition with argon. The sample exploded at around the same temperature. This agrees with the literature from Cataldo *et al.* [169], who found that Cu_2C_2 is decomposed explosively at 127 °C. To address this challenge, it is proposed that the heating rate and the sample amount should be further reduced. It is also reasonable to try reductive conditions, like 10% H_2 in argon, and vacuum conditions (possibly for DSC but not TGA and MS), if applicable, in additional experiments.

Quantitative Analysis by CHN Elemental Analysis

CHN elemental analysis accurately identifies the amount of carbon, hydrogen, nitrogen, and sulfur contents in the sample at the ppm level. This destructive analysis allows the measurement of all kinds of samples that are explosive, volatile, toxic, light sensitive, etc. The samples can also be in the solid or liquid phase and prepared under various atmospheres and conditions, such as oxygen-free or in a freezer. These properties make CNHS analysis a safe and suitable technique for studying the explosive pure-phase cuprous acetylide.

This analysis aims to identify the carbon contents in the Cu_2C_2-containing samples. It is also interesting to determine the presence of hydrogen. This is referred to the proposal by Reppe *et al.* [41] in 1955, who suggested that the $Cu_2C_2 \bullet 3C_2H_2$ complex is the actual structure. Further proposals for complex Cu_2C_2 structures containing multiple C_2H_2, H_2O, and HCHO are reported by Kirchner [160], as shown in Table 7-3. However, it is believed that the samples are adequately washed, purified, and dried to remove most of the contaminants.

Three samples containing cuprous acetylide are prepared for the CHN analysis; refer to Chapter 5.3.4 for the sample preparation procedures. Sample 1 is the CBS pre-catalyst activated under the ethynylation conditions according to the standard experimental and post-treatment procedures. Sample 2 and Sample 3 are the directly precipitated pure-phase cuprous acetylides, but one is washed with methanol, and another is washed with water. All the purified samples are dried, stored, and prepared under inert conditions. The analytical results are shown in Table 3-2.

Table 3-2. The CHN combustion analysis of the cuprous acetylide-containing samples was prepared via *in situ* activation of a CBS pre-catalyst under ethynylation conditions (Sample 1) and pure-phase cuprous acetylide via direct precipitation washed with methanol (Sample 2) and with water (Sample 3).

	"C" [%]	***"H" [%]***	***C-to-H molar ratio***	***Notes***
Sample 1	*16.6*	*1.2*	*13.8: 1*	*Contains SiO_2, Bi_2O_3*
Sample 2	*14.1*	*0.6*	*23.5: 1*	*Contains surface impurities*
Sample 3	*67.7*	*4.8*	*14.1: 1*	*Pure phase*

From the results, Sample 1, which contains SiO_2 and Bi_2O_3 as part of the spent catalyst, shows a similar C-to-H ratio to Sample 3, which is the purified pure-phase cuprous acetylide prepared via direct precipitation by the optimized synthesis and post-treatment procedures. The similarity in ratio, despite their significant differences in the absolute carbon and hydrogen contents in % in the sample, provides strong confidence and evidence to conclude the actual chemical composition of carbon and hydrogen in the pure-phase cuprous acetylide. Additionally, as a cross-reference to Reppe's proposal of the pure phase, $Cu_2C_2 \bullet 3C_2H_2$ contains 55% copper, 42% carbon, and 3% hydrogen. The C-to-H molar ratio is 14:1, which ideally agrees with the CHN analytical results of Sample 1 and Sample 3.

However, the determination of the Cu content of the same sample by ICP-OES was not possible due to the device failure. Thus, the Cu-to-C-to-H ratio is not calculated. This is expected to be able to hypothesize the actual thermodynamically stable chemical compositions and structural properties of the copper acetylide species with concrete experimental support. Further, the actual catalytically active phase in the Reppe ethynylation process can also be proposed, as referred to in the analytical results of Sample 1.

3.2.3 Explosion Test and Catalyst Deactivation

Acetylene gas and copper acetylides are well-known for their explosivity. Regrettably, there have been a number of fatal and severe accidents related to acetylene and copper acetylide explosions in recent years in the industry [205-207], which emphasizes the danger of acetylene chemistry and stops researchers from further investigating cuprous acetylides.

This work aims to identify the cuprous acetylide and its derivations, including the more explosive cupric acetylide, by appropriate analytic techniques. It is, of course, to ensure safety during the handling and operation of dangerous species and to prevent damage to the devices.

This objective, proven by the previously presented analytical results, is successfully fulfilled. However, all of the successful analytical measurements mentioned above are achieved with an abundant series of rigorous repeating experiments with blank tests, diluted and downscaled tests, and followed by stepwise upscale to the actual experimental conditions. These tests and considerations include the sample preparation, handling and storage, and the analytical parameters. Prior to all, an explosion test of the samples to be analyzed is performed.

As shown in Figure 3-16, typical explosion tests with the most significant results are presented. The photos are screenshots taken from the video clips filming the explosion test. The cuprous acetylide samples are the pure phase prepared via direct precipitation, dried under vacuum in the Schlenk line, and stored in the glove box. The samples are taken out to an open atmosphere in the fume hood right before the performance of the explosion test.

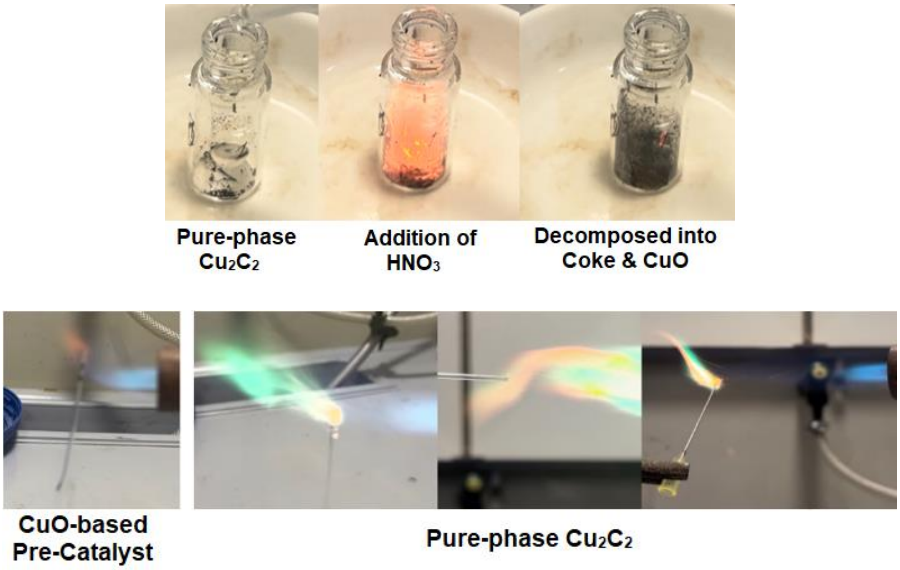

Figure 3-16. The screenshots from the video clips of the explosion tests of the directly synthesized pure-phase cuprous acetylide powders. The top shows that the cuprous acetylide samples explode when in contact with nitric acid. The bottom shows that the sample explodes when in contact with open fire, and it compares with a CuO-based catalyst.

The first test is performed when a drop of concentrated nitric acid is brought in contact with a few grains of sample powder in a glass vial. The cuprous acetylide explosively decomposed with a bright orange flame and a loud pop sound. It was left with black coke and CuO powder after the explosion. In another test, a few grains of sample powder are loaded in the tip of the glass (glass pipette) and metal (needle) tubes. They are brought into open fires or heated on the side without direct contact with fire. They exploded instantly in both cases with a mixed-colored flame (copper itself burns in a blue-green flame) and a loud pop sound. In comparison, CuO-based pre-catalyst is also burnt, but it shows a weak orange flame and black smoke.

Several explosion tests are also done with cuprous acetylide species synthesized via various pathways, like the deposition precipitation on silica and *in situ* activated from CBS catalysts. The copper acetylide-contacting samples also include the derivative phases such as cupric acetylide, the supported and unsupported ones, dried and wet ones, and different drying and storage conditions, as discussed in Chapter 3.1.1.

As summarized based on the experiments and the literature, the explosion characteristics of the pure phase or the copper acetylide-containing species, specifically in catalysis, depend on the following:

- The dryness of copper acetylides: it can be explosive only when dried;
- The copper loading as in the activated ethynylation catalyst: it is non-explosive even when dried at up to 55 wt.% Cu loaded on SiO_2(-Bi_2O_3) in the activated catalysts, determined experimentally;
- The copper acetylide grain size, surface area, and dispersion: it is non-explosive even when dried in the ethynylation catalyst for which copper acetylides are in nm scale (i.e., the crystallite size defined by XRD) that is well dispersed by SiO_2(-Bi_2O_3) carrier;
- The reducing and oxidizing conditions: reduction of CuO and oxidation of Cu_xC_2 are highly exothermic and may self-ignite and burn or explode the acetylene and acetylides;
- The dried copper acetylides in contact with oxidizing agents like oxidizing acids (conc. HNO_3) and ignition sources like sparks, fire, or high temperature (i.e., pure-phase Cu_2C_2 explosively decomposed at around 120 °C, determined experimentally).

On the other hand, the explosion tests of differently prepared cuprous acetylides provide a hint to estimate the purity. It is believed that the explosivity of the cuprous acetylide is proportionally related to its purity, which can be more directly proven by analytical results such as XRD and Raman. This not only refers to the samples with carriers but, more precisely, to the pure phases that contain surface contaminants like the ammonia-containing crystallites and carbon deposition shown in the XRD diffractograms and Raman spectra in Figure 3-7 and Figure 3-14 and partially oxidized ones, like the presence of Cu_2O in Figure 3-9.

However, due to the challenge and lack of knowledge for quantifying the explosivity, for example, using a detonator for the explosion test and the determination of the energy release during the explosion, this impact has not been further studied in this work.

The spent Cu_2C_2-containing catalysts and pure-phase cuprous acetylide have to be deactivated before disposal to avoid explosion and self-ignition. The ordinary deactivation method is shown in Chapter 5.3.3, using oxidizing acids to oxidize the copper ions to stable CuO and decompose the acetylenic C_2^{2-} ions into carbonaceous residues. Other approaches, like thermal decomposition in oxidizing conditions, are also possible. Dilute the Cu_2C_2 sample, use the diluted acids, and lower the heating rates, depending on the purity and amount of Cu_2C_2, which is necessary to avoid vigorous exothermic deactivation and explosive decomposition.

4

SUMMARY AND OUTLOOK

4.1 Summary and Outlook for Chapter 2

Chapter 2. Catalytic Ethynylation of Formaldehyde, studied the laboratory-scale catalytic Reppe ethynylation of formaldehyde to produce the desired product, 1,4-butynediol, with a supported copper-based catalyst. This chemical process involves a highly complex 3-phase catalytic reaction, using explosive acetylene gas and toxic aqueous formaldehyde as the educts and the *in situ* formed highly explosive cuprous acetylide-containing species as the catalytically active phase. Safety is the paramount concern that guides all considerations and aspects of this research. This makes the first part of this thesis, *Chapter 2.1 Implementation of Experimental Procedures*, the pre-prior and the most crucial task for the entire work.

In Chapter 2.1.1, a glassware parallel test unit and a Carousel test unit with necessary accessories were implemented to meet the requirements of flexibility and abundant catalytic performance tests of ethynylation. With safety as the top consideration, the test units were designed in the simplest but most efficient manner to allow easy access, operation, and maintenance. Additionally, a specially designed reactor is introduced for experiments with specific objectives and operation conditions with high flexibility. The appropriate reaction processes for ethynylation were discussed in Chapter 2.1.2, including the one-step or two-step process and the batch or semi-continuous process. The transition steps consisting of separation, washing, purification, and storage of the activated catalyst slurry were elaborated. Different processes and techniques were applied flexibly, with the safety and simplicity of the experimental operation as the priority. Chapter 2.1.3 investigated the influences of each experimental parameter in this complex 3-phase ethynylation process. The performances were evaluated in terms of the 1,4-butynediol yield, formaldehyde conversion, and turnover frequency to eliminate the rate-limiting parameters like the mass transport limitations and the limiting reagents of the reaction kinetics. It was essential to compromise among different parameters to influence or offset their effects.

In conclusion, with careful consideration of both experimental results and theoretical studies, the test units and reaction processes proposed have all proven safe and effective. They can be chosen flexibly depending on various research objectives of the catalytic ethynylation process. The selection of the appropriate reaction conditions was compromised at 600 rpm stirring with a magnetic stirrer bar, static 90 °C, 1.2 bar acetylene pressure, and 2 g of pre-catalyst in 40 g FA solution with the catalyst grain size of 100-300 µm.

With the successful implementation of the safe and reliable reaction test unit and the standard experimental procedures, the catalytic performance in terms of the yield of BYD and the conversion of FA were investigated in *Chapter 2.2,* Optimization of Catalyst Characteristics and Structure-Activity Relationships.

Chapter 2.2.1 discussed the CBS pre-catalyst synthesized by co-precipitation methods and thermal-treated at 80 °C, 450 °C, and 700 °C, where different copper phases like copper basic nitrate and carbonate, copper oxide, and copper-bismuth-silicon spinels were present. The CBS pre-catalysts with copper loadings from 15 wt.% to 55 wt.% and bismuth loadings from 0 wt.% to 8 wt.% were prepared to investigate the optimal active copper contents and optimal bismuth's promoting effects of the catalyst. The supporting effects of silica, alumina, magnesia, and zinc oxide and their combinations were also tested. Additionally, in Chapter 2.2.2, the silica-supported copper-based pre-catalysts, with and without bismuth content, were synthesized by co-precipitation, incipient wetness impregnation, ammonia evaporation, and deposition precipitation in urea solution. Each synthesis method gave a unique property of the pre-catalyst, like the dispersion, particle size, and active surface area. Co-precipitation catalysts with the best ethynylation performance were chosen. The rate-limiting parameters, the active metal-support interactions, the structural properties, and the role of bismuth are investigated and discussed by correlating the catalytic performances and supported with analytical and characterization data from ICP-OES, PXRD, TGA-MS, N_2 physisorption, TPR, and N_2O pulse chemisorption techniques, as illustrated in Chapter 2.2.3.

With the abundant varieties of the pre-catalysts for ethynylation, evaluated by their catalytic performances, the most suitable catalyst is 35C4BS-CP-c450, which contains 35 wt.% copper, 4 wt.% bismuth supported on silica, synthesized by co-precipitation method and calcined at 450 °C to produce $CuO\text{-}Bi_2O_3/SiO_2$ ethynylation catalyst.

With the optimal catalyst, the influences of the aqueous FA solution of different pH values and buffer systems on catalytic performance and the formation of the active cuprous acetylide species were discussed in *Chapter 2.3. Influence of Aqueous Formaldehyde*.

In Chapter 2.3.1, the FA solutions were prepared by dissolving paraformaldehyde in water, with 10% methanol as a stabilizer. The buffer systems, including acetate, borate, citrate, and phosphate, were considered with FA solution from pH 4.0 to 9.0. The acetic acid-sodium acetate at pH 4.5 – 6.0 and sodium dihydrogen phosphate-disodium hydrogen phosphate at pH 6.0 – 7.5 were finally selected and investigated in detail. The aqueous FA solution was quantitatively identified by the GC-TCD method with a unique column after a series of troubleshooting. The alternative techniques of quantitative identification, like ^{1}H-NMR and titration methods, were also investigated. However, these methods were inefficient and inaccurate for the FA analysis. In Chapter 2.3.2, the impacts of the buffer species and pH values of the aqueous FA solution on the active cuprous acetylide formation were analyzed by XRD, and the catalytic performances were evaluated in FA conversion and BYD yield. The catalytic performance increases with higher pH values, but the pH of FA solutions at a neutral or slight basic range was not stable and tended to decrease. Furthermore, the phosphate species in the buffer were likely to form crystals with bismuth species on the catalyst's surface,

which not only consumed bismuth and phosphate from their respective roles but also interfered with the identification of the active cuprous acetylide species from the XRD analysis.

Modifications on the buffer capacity were made with phosphate buffers by increasing its contents to above 6 wt.% and adjusting the washing procedure to purify the spent catalyst for XRD analysis, which are promising improvements. The experiments were performed, but the results after modification are not reported in this thesis. Follow-up analysis by Raman and TGA techniques will be arranged to support the current results. However, based on the existing findings, it is still believed that using a phosphate buffer to maintain the pH values of aqueous formaldehyde solution at pH 7 is most appropriate for catalytic Reppe ethynylation.

Chapter 2.4 Catalytic Activation and Deactivation Behavior reports a study on the storage effects of the activated catalysts and the leaching behavior of the catalyst in solution during ethynylation under different conditions and atmospheres.

Chapter 2.4.1 shows the significant changes in catalytic performance, either enhancing the activity or causing deactivation after storing the activated catalysts under various conditions, such as air, reaction mixture, water, methanol, and fresh FA solution. Furthermore, this experiment also suggests suitable storage methods for preparing analytical samples that reflect the actual status of the sample. Storage in fresh formaldehyde solution after purifying the activated catalyst and separating by centrifugation showed the best catalytic performance. Additionally, except in water, the longer the storage period, the better the performance, which proved a positive influence on the storage effect. A new series of experiments with the modified catalyst handling and purifying techniques was conducted to support the latest findings. These tests were also coupled with PXRD and Raman analysis to investigate the phase change of the catalysts after storage.

The leaching study in Chapter 2.4.2 characterizes the catalyst stability and discovers potential catalytic activation and deactivation mechanisms. Copper showed low leaching of less than 0.11% in solution under an acetylene atmosphere, which agrees with the literature that the *in situ*-formed active cuprous acetylide species is sparingly soluble. This suggested that the catalytic activation may take place via surface reaction or via leached Cu species that re-precipitate back on the catalyst surface. The silicon leaching of less than 1.3% suggests a source of deactivation via structural change or sintering. The amount of Si-leaching is also influenced by the pH values of the FA solution, which is more soluble in alkaline conditions. The leached species will also be removed during the washing and separation steps, explaining the lowered catalytic activity in the two-step and multi-cycle tests.

4.2 Summary and Outlook for Chapter 3

Chapter 3. Genesis of Cuprous Acetylide Species, aims to prove experimentally that the cuprous acetylide is the catalytically active phase in the Reppe ethynylation of formaldehyde to produce 1,4-butynediol and propargyl alcohol. By discovering the *in situ* transformation of the Cu_2C_2, it skips the black box of uncertainty and directly correlates the structural properties of the active phase, instead of the CuO-based pre-catalyst, with the catalytic ethynylation performance, to propose the catalytic activation and ethynylation mechanisms.

Cuprous acetylide is highly sensitive to and can be easily transformed into derivative phases. Its characterization is challenging and can hardly be identified by a suitable analytical technique due to its explosive decomposition nature. Thus, there is rarely an available database or publication showing its exact structure, diffraction, and spectra properties.

To achieve the objective of identifying the cuprous acetylide, Chapter 3.1 *Genesis Pathways of Cuprous Acetylide*, reports multiple synthesis pathways to produce cuprous acetylide. The *in situ* transformation from CuO-based catalyst under the ethynylation conditions, deposition precipitation of Cu_2C_2 on SiO in ammonia solution, and direct precipitation of pure-phase Cu_2C_2 in ammoniacal cuprous salt solution at oxygen-free environments are investigated in Chapter 3.1.1. The optimal synthesis conditions for the Cu_2C_2 formation are discussed. The necessity of adding a reducing agent and performing in an ammoniacal solution is confirmed by visual observations of the color change and the XRD analysis over 60 min. These conditions effectively reduce the copper(II), stabilize the copper(I), and speed up the formation of pure-phase Cu_2C_2 at higher purity compared to the ones performed in an aqueous solution of formaldehyde and acetylene. It is also proven by the catalytic ethynylation performance test that neither formaldehyde nor acetylene can solely reduce the copper(II) and transform the CuO-based catalyst into the catalytically active Cu_2C_2 phase.

In Chapter 3.1.2, the catalytic performance in the ethynylation reaction is compared between the deposition precipitated Cu_2C_2/SiO_2 model catalyst and the pre-activated CuO/SiO_2 and $CuO\text{-}Bi_2O_3/SiO_2$ co-precipitation catalyst. The performance of the model catalyst in BYD yield is only about 1/3 of the activated CuO/SiO_2 catalyst and about 1/7 of the activated $CuO\text{-}Bi_2O_3/SiO_2$ catalyst. The results are expected and can be explained by the structural properties of the model catalyst, like the poor copper dispersion, less active sites, and weaker metal-support interaction.

The experimental identification, both qualitatively and quantitatively, of the synthesized pure phase or support Cu_2C_2 via various pathways is successfully presented in Chapter 3.2 *Identification and Characterization of Cuprous Acetylide*.

Focusing on the extremely sensitive pure-phase Cu_2C_2, the qualitative analysis by X-ray diffraction and Raman spectroscopy are applied, as elaborated in Chapter 3.2.1. Five characteristic XRD reflexes at 2θ = 30.1°, 32.2°, 42.4°, 45.9°, and 52.0° are assigned to the pure-phase Cu_2C_2. Two vibrational signals at wavenumbers of 1700 cm^{-1} and 425 cm^{-1} are assigned respectively to the characteristic C≡C π-bond and Cu-C≡C α-bond of the pure-phase Cu_2C_2. The influencing parameters and optimal synthesis, post-treatment, and analytical conditions of pure-phase Cu_2C_2 are determined.

Different pure-phase Cu_2C_2 synthesis conditions, such as the addition of a reducing agent, use of solvents like ammonia, formaldehyde, and water, and exposure to air during the synthesis, purification, drying, and sample preparation and analytical conditions are systematically investigated. Partial oxidizing of the copper(I) precursor, like CuCl, into $CuCl_2$ and Cu_2O is observed by XRD, which indicates the importance of maintaining an oxygen-free environment throughout the process. The vibrational signals at a wavenumber of 573 cm^{-1}, corresponding to the ≡C-C bonds, are realized by Raman spectroscopy, indicating the formation of the undesired copper diacetylide and polyynides. These findings suggest the reactivity and sensitivity of Cu_2C_2 and explain the challenges but the desperate necessity of differentiating its pure phase from its derivatives and by-products. The experimental results also provide first-hand information to optimize its synthesis, post-treatment, and analytical conditions based on its structural properties and the implied XRD diffractograms and Raman spectra. It benefits future studies in identifying Cu_2C_2 and its relevant transformations and reaction mechanisms.

The successful qualitative analyses encourage even more challenging quantitative analyses that can further explore the actual structure and compositions of the pure-phase Cu_2C_2, which have never been assured in the literature. Chapter 3.2.2 employs the thermal analysis technique, TGA/DSC-MS, and elemental CHN analysis to gain first insight. TGA evaluates the thermal properties of pure-phase Cu_2C_2 and identified its explosive decomposition at around 120 °C. It suggests the correlation between its purity and decomposition temperature. The presence of slowly decomposed Cu_2C_2-containing samples, like the spent ethynylation catalyst, at a slightly elevated temperature can be identified by MS with respective m/z ratios. When coupling the mass change recorded by TGA and the heat change recorded by DSC, the transformation of Cu_2C_2 into CuO and CO/CO_2 under the oxidizing atmosphere can be predicted. Furthermore, the Cu-to-C ratio of the Cu_2C_2 samples can be deduced. It is helpful in predicting its actual structure and composition. Unfortunately, the TGA/DSC-MS evaluation is only performed for the Cu_2C_2-containing catalyst, which contains the catalyst promoter, carrier, and various impurities that make the calculation challenging. The evaluation of the pure-phase Cu_2C_2, which is stopped due to its explosive decomposition, must be the focus of future work. The appropriate analytical conditions, like under the inert or reductive atmosphere, precisely controlling the heating rate, and reducing or diluting the amount of Cu_2C_2, shall be

investigated to avoid or postpone the explosive decomposition. Thus, the quantitative evaluation of copper and carbon contents can be proceeded.

The CHN analysis, as a supporting technique, identifies the carbon and hydrogen contents. It determines a ratio of C-to-H at 14-to-1 for both the pure-phase Cu_2C_2 sample and the Cu_2C_2-containing spent ethynylation catalyst sample. This result is highly similar to the ratios calculated from the proposed structures in the literature, for example, $Cu_2C_2 \cdot 3C_2H_2$, reported by Reppe. The CHN analysis, on the one hand, can justify the carbon content analyzed using the TGA technique. On the other hand, it can be further correlated to the Cu-to-C ratio determined by TGA/DSC-MS with the C-to-H ratio determined by CHN analysis and propose a more precise actual structure of Cu_2C_2.

The investigations in this entire dissertation are greatly limited by the explosive nature of copper acetylide species. The performed experiments and analyses are thoroughly assessed for safety. The explanation and the explosion and decomposition tests shown in Chapter 3.2.3 adequately clarify the safe handling and operation conditions and their precautions and restrictions with copper acetylides. The explosion can be eliminated for the high dispersion of copper acetylides with crystallite or grain size in a few nm scales. It is also essential to avoid strong oxidizing environments and contact with oxidizing acids to prevent the self-ignition of copper acetylides, like the spent ethynylation catalysts. It should also be prevented from any sources of energy, including impacts, sparks, and even intensive X-ray and laser powers.

With the successful presentation of this dissertation, the safety measures regarding the explosive copper acetylides are proven appropriate and adequate. It also ensures the accuracy and reliability of the inspiring results of this fruitful research work.

5

EXPERIMENTAL

5.1 Materials and Chemicals

All chemicals were used without further purification. Detailed descriptions of the unique applications of the substances are given, along with the respective experimental procedures.①

Gases

Table 5-1: The listed gases in all experimental processes②.
Include the catalyst synthesis, catalytic reactions, analysis, and characterizations.

Substances	***Formula***	***Supplier***	***Grade***
Acetylene	*C_2H_2*	*Westfalen*	*99.600% (2.6)*
Nitrogen	*N_2*	*Westfalen*	*99.999% (5.0)*
Argon	*Ar*	*Westfalen*	*99.999% (5.0)*
Helium	*He*	*Westfalen*	*99.996% (4.6)*
Synthetic air	*N_2/O_2*	*Westfalen*	*99.999% (5.0)*
Hydrogen in Argon	*H_2/Ar (5%, 10%)*	*Westfalen*	*99.999% (5.0)*

Reppe Ethynylation Process

Table 5-2: The listed materials and chemicals for the Reppe ethynylation process.
Include calibration, safety inspection, catalyst activation, catalytic test, deactivation, and disposal.

Substances	***Formula***	***Supplier***	***Grade***
1,3-Propanediol	*$C_3H_8O_2$*	*Sigma Aldrich*	*for synthesis*
2-Butyne-1,4-diol	*$C_4H_8O_2$*	*Sigma Aldrich*	*for synthesis*
Acetonitrile	*C_2H_3N*	*VWR Chemicals*	*Technical*
Disposable Pasteur Pipette		*VWR Chemicals*	
Glass wool	*Borosilicate glass*	*Merck*	
Nitric acid 68%	*HNO_3*	*VWR Chemicals*	*Technical*
Propargyl alcohol	*C_3H_4O*	*Sigma Aldrich*	*for synthesis*
PURALOX SCCa-150/200	*γ-Al_2O_3*	*SASOL GmbH*	

① Due to the instability and highly explosive nature of copper acetylide species, especially when dried, toward heat and impacts, appropriate safety precautions and handling procedures for storage, transportation, analysis, decomposition, and disposal are crucially necessary. Proper personal protective equipment (PPE) is required. All the copper acetylide samples and contaminated apparatus must be carefully treated by deactivating them with nitric acid.

② Due to the highly reactive and unstable nature of acetylene, a specially designed compress gas cylinder is used for the acetylene gas supply. Only the specific pressure regulator, valves, and connection pipes are allowed to be used to connect with the acetylene gas cylinder.

Catalyst Synthesis

Table 5-3: The listed materials and chemicals for catalysts synthesized.
Include chemical precursors, reagents, and solvents used for different compositions in all methods.

Substances	***Formula***	***Supplier***	***Grade***
Catalyst sources			
Aluminum nitrate nonahydrate	$Al(NO_3)_3 \cdot 9H_2O$	*Merck*	*95%*
Bismuth (III) nitrate pentahydrate	$Bi(NO_3)_3 \cdot 5H_2O$	*Sigma Aldrich*	*ACS reagent 98%*
Bismuth (III) oxide	Bi_2O_3	*Grüssing GmbH*	
Bismuth (III) nitrate alkaline	$Bi_5O(OH)_9(NO_3)_4$	*Grüssing GmbH*	
Copper(I) chloride	$CuCl$	*Alfa Aesar*	*97%*
Copper(II) nitrate hemipentahydrate	$Cu(NO_3)_2 \cdot 2.5H_2O$	*VWR Chemicals*	*GPR RECTAPUR*
Copper(II) nitrate trihydrate	$Cu(NO_3)_2 \cdot 3H_2O$	*VWR Chemicals*	*GPR RECTAPUR*
Copper(II) sulfate pentahydrate	$CuSO_4 \cdot 5H_2O$	*VWR Chemicals*	*Technical 98%*
Magnesium nitrate hexahydrate	$Mg(NO_3)_2 \cdot 6H_2O$	*VWR Chemicals*	
Matrex Silica 60	SiO_2	*Fisher Scientific*	*35-70 µm*
Sodium metasilicate, anhydrous	Na_2SiO_3	*Alfa Aesar*	*Technical*
Tetraethyl orthosilicate (TEOS)	$Si(OC_2H_5)_4$	*Alfa Aesar*	*Reagent, 98%*
Zinc nitrate hexahydrate	$Zn(NO_3)_2 \cdot 6H_2O$	*Sigma Aldrich*	*ACS reagent 98%*
Reagents and solvents			
Ammonia Solution 28-30%	NH_3	*Merck*	*for analysis*
Ag/AgCl reference electrode	*Ag/AgCl*	*Merck*	
Buffer solutions, AVS TITRINORM	*pH 4, 7, 10*	*VWR Chemicals*	*AnalaR Normapur*
Hydroxylammonium chloride	$NH_2OH \cdot HCl$	*VWR Chemicals*	*Technical*
ICP multi-element standard solution IV	*23 elements in diluted* HNO_3	*Merck*	*Certipur®*
Natriumhydroxid 99%	*NaOH*	*Grüssing GmbH*	*analytische Pellets*
Nitric acid 69%	HNO_3	*VWR Chemicals*	*AnalaR Normapur*
Potassium chloride	*KCl*	*Merck*	*3 Molar*
Qualitative Filter Paper		*VWR Chemicals*	*Grade 413, 5-13 µm*
Sodium carbonate	Na_2CO_3	*VWR Chemicals*	*AnalaR Normapur*
Urea ≥95%	NH_2CONH_2	*VWR Chemicals*	*GPR Rectapur*

Aqueous Formaldehyde Solution Preparation

Table 5-4: The listed materials and chemicals for self-prepared and commercial formaldehyde solution③. Include chemical precursors, pH-buffer components, and reagents.

Substances	***Formula***	***Supplier***	***Grade***
Commercial formalin solution			
Formaldehyde 7.5% (pH 7.0 ± 0.2)	CH_2O	*VWR Chemicals*	*Technical*
Formaldehyde 10% (pH 8.2 - 8.4)	CH_2O	*VWR Chemicals*	
Formaldehyde 35%	CH_2O	*VWR Chemicals*	*Technical*
Formaldehyde 36%	CH_2O	*VWR Chemicals*	*GPR Rectapur*
Formaldehyde 36%	CH_2O	*VWR Chemicals*	*AnalaR Normapur*
Formaldehyde 37%	CH_2O	*Merck*	
Self-prepared formaldehyde solution, buffer species, and reagents			
Acetic acid	$C_2H_4O_2$	*Sigma Aldrich*	*for synthesis, 99%*
Boric acid	H_3BO_3	*Merck*	*for analysis*
Citric acid monohydrate	$C_6H_8O_7 \cdot H_2O$	*VWR Chemicals*	
di-Sodium hydrogen phosphate	Na_2HPO_4	*Merck*	*for analysis*
Formic acid	CH_2O_2	*Fluka*	*98%*
Methanol	CH_3OH	*VWR Chemicals*	*GPR RECTAPUR*
Natriumdhydrogenphosphat Monohydrat	$NaH_2PO_4 \cdot H_2O$	*Chemsolution*	*for laboratory use (99-102%)*
Natriumhydroxid 99%	*NaOH*	*Grüssing GmbH*	*analytische Pellets*
Natriumthiosulfat 97%	$Na_2S_2O_3$	*Grüssing GmbH*	
Paraformaldehyde	$(CH_2O)_n$	*VWR*	*powder*
Phosphoric acid	H_3PO_4	*Fluka*	*≥85%*
Sodium acetate (anhydrous)	$NaCH_3COO$	*Merck*	*for analysis*
Sodium borohydride	$NaBH_4$	*Sigma Aldrich*	*powder, 98%*
Sodium carbonate	Na_2CO_3	*Sigma Aldrich*	*BioXtra, ≥99.0%*
Sodium hydrogen phosphate	Na_2HPO_4	*Sigma Aldrich*	*100.00%*
Sodium perborate tetrahydrate	$NaBO_3 \cdot 4H_2O$	*Sigma Aldrich*	
Sulfuric acid (1M standard)	H_2SO_4	*Sigma Aldrich*	
Trisodium citrate dihydrate	$C_6H_5Na_3O_7 \cdot 2H_2O$	*Sigma Aldrich*	

③ Formalin refers to the saturated formaldehyde solution at 35-38 wt.% of formaldehyde, and the diluted ones refer to 8-10 wt.%. Paraformaldehyde refers to the white powder of polymeric formaldehyde with 8-100 repeating units. Formaldehyde solution contains 10-15 wt.% methanol as a stabilizer and a pH buffer system to adjust the pH value of the solution, which depends on the desired pH range and buffer capacity. The commercial formalin has to be pre-tested for the pH values as it is often not notified, and it sometimes has to be pre-filtered as the polymerization of formaldehyde to form white precipitations is possible (refer to the product specifications).

5.2 Devices, Instruments, and Experiments

Table 5-5: The list of reaction setup, devices, and analytical instruments for the ethynylation process. Include the catalyst synthesis, catalytic performance test, analysis, and characterization.

Device and Instrument	***Supplier***	***Purpose of Use***
Catalyst synthesis		
906 Titrando pH-STAT titrations	*Metrohm Germany*	*pH control*
GHM 3410-Digital Conductivity Meter	*GHM Group Greisinger*	*Electronic conductivity*
Muffle furnace	*Nabertherm GmbH*	*Catalyst calcination*
Peristaltic pump	*Medorex eK Labortechnik*	*Flowrate control*
Reax control (shaker)	*Heidolph Instruments*	*Mixing*
Reppe ethynylation process		
Carousel 6PLUS Reaction Station (with multi-position mixer)	*Radleys*	*Catalytic performance test*
Gas Chromatograph 6890N (Thermal Conductivity Detector)	*Agilent Technologies. Inc.*	*Qualitative and quantitative analysis*
Glassware parallel setup		*Reaction and testing unit*
Pipe and Instrumentation Diagram	*HiTec Zang GmbH*	*Technical drawing software*
Thermo Biofuge Primo R Centrifuge	*Heraeus Group*	*Separation*
Characterization and analysis		
Agilent 700, ICP-OES	*Agilent Technologies. Inc.*	*Elemental analysis*
AA280 Fast Sequential Atomic Absorption Spectrometer	*Varian Inc.*	*Elemental analysis*
Autochem II 2920 Analyzer	*Micromeritics Instrument*	*Chemisorption analysis*
Empyrean Multipurpose X-Ray Diffraction Instrument	*Malvern PANalytical*	*Phase identification*
Euro EA - CHN Elemental Analyzer	*HEKAtech GmbH*	*Elemental analysis*
InVia™ Qontor® Confocal Raman Microscope	*Renishaw PLC.*	*Phase identification*
MiniFlex 600-C Benchtop power X-Ray Diffractometer	*Rigaku Corporation*	*Phase identification*
NovaTouch™ LX4 Analyzer	*Quantachrome Instruments*	*Surface area and pore size analysis*
Stoe STADI P Transmission Powder Diffractometer	*STOE & Cie GmbH*	*Phase and structure identification*
Thermal Analysis STARe System TGA/DSC 3+	*Mettler Toledo GmbH*	*Thermogravimetric (mass, heat flow) analysis*
ThermoStar GSD 320 T Gas Analyzer	*Pfeiffer Vacuum GmbH*	*Gas analysis*

Catalysts Synthesis

Table 5-6: The list of synthesis techniques of the copper-based catalyst.

Catalysts	***Synthesis Technique***	***Devices***
Carriers of the catalysts	*Co-precipitation*	*pH titrations, peristaltic pump*
Supported CuO precursor	*Co-precipitation*	*pH titrations, peristaltic pump*
Supported CuO precursor	*Deposition precipitation in urea (via hydrolysis)*	*Stirring hotplate*
Supported CuO precursor	*Ammonia evaporation*	*Stirring hotplate*
Supported CuO precursor	*Incipient wetness impregnation*	*Reax shaker*
Supported Cu_2C_2 active catalyst	*Deposition precipitation in ammonia (via ligand removal)*	*Schlenk-line, stirring hotplate*
Unsupported pure phase Cu_2C_2	*Direct precipitation*	*Schlenk-line, vacuum pump*

Formaldehyde Solution

Table 5-7: The list of self-prepared formaldehyde solutions of different pH values and pH buffers.

pH Value	***pH-Buffer System***	***Conjugate Acid-Base Species***
pH 4 to 5	*Acetate*	*Acetic acid – Sodium acetate*
pH 5 to 6	*Citrate*	*Citric acid – Trisodium citrate*
pH 6 to 8	*Phosphate*	*Phosphoric acid – Sodium dihydrogen phosphate – Disodium hydrogen phosphate – Sodium hydroxide*
pH 8 to 9	*Borate*	*Boric acid – Sodium perborate*
pH 9 to 10	*Carbonate*	*Sodium bicarbonate – Sodium carbonate*

Reppe Ethynylation Process

Table 5-8: The list of different reaction types, reactors, and applications of the ethynylation process④⑤.

Process	***Reactor***	***Applications***
2-Step, Batch	*Carousel*	*Implementation of experimental procedures*
	Parallel	*Catalytic performances and reproducibility tests*
1-Step, Batch	*Single*	*Implementation of experimental procedures*
	Parallel	*Industrial-like modifications (extended, upscaled)*
1-Step, Semi-continuous	*Single*	*Catalytic deactivation tests* *Leaching, multi-cycle, long-hour experiments*

④ The 1-step reaction refers to the catalytic reaction without a separate pre-activation step, while the 2-step reaction refers to the reaction with an activation step prior to the catalytic reaction. The 2-step reaction also includes a separation, washing, and storage step of the activated catalysts. The batch process refers to the reaction without remove or refill the input and output. The semi-continuous process refers to the reaction with removal of a significant output and refilling the fresh input into the process.

⑤ A large amount of sample taken (> 10% per sampling) is considered as removal (refilling is required). The small amount of sample taken (< 2% per sampling) is negligible. Acetylene gas, as the input or the reactant, is continuously fed to keep the pressure constant in the reaction atmosphere. This is not classified as a continuous process due to the particular application of this study.

Characterization and Analysis Techniques

Table 5-9: The list of the characterization and analysis techniques in the catalytic ethynylation process. Include the qualitative and quantitative analysis of the catalyst in precursor, pure, and active phases.

Technique	***Sample***	***Applications***
Atomic Absorption Spectrometer	*Dissolved solution*	*Leaching, components loading in catalyst*
Centrifugation	*Solid-liquid suspension*	*Separation*
Chemisorption (Temperature programmed)	*Dried powder*	*Copper surface, reducibility*
CHN elemental analysis	*Dried powder*	*C and H content in catalysts*
Filtration (vacuum, filter)	*Solid-liquid suspension*	*Purification, separation*
Gas chromatograph	*Aqueous solution*	*Concentration of reaction components*
ICP-Optical Emission Spectroscopy	*Dissolved solution*	*Leaching, components loading in catalyst*
Physisorption (BET/BJH)	*Dried powder*	*Surface and pore properties*
Raman Spectroscopy	*Dried, wet, aqueous*	*Phase identification*
Thermogravimetry Mass Spectroscopy	*Dried powder*	*Mass balance, decomposition*
X-Ray Diffraction	*The dried or wet sample*	*Phase identification*

5.3 Experimental Procedures

5.3.1 Catalyst Synthesis

Conventional copper-based catalysts are commonly used in the Reppe ethynylation of the formaldehyde process. In this section, the standard catalyst precursor, $CuO\text{-}Bi_2O_3/SiO_2$ (contains 35 wt.% Cu and 4 wt.% Bi), is synthesized by co-precipitation at pH7, calcined at 450 °C for 4 h, and sieved to 100-300 µm. Different catalyst precursors are prepared with varying loadings of metal, promoters, and carrier materials, as well as synthesis and post-treatment conditions and synthesis techniques.

A list of corresponding chemicals (Table 5-3), synthesis techniques, devices, and catalyst species (Table 5-6) are shown.

Co-Precipitation (CP)

With the desired amount, components, and compositions of the catalyst precursor, the copper and other metal (Al, Mg, Zn) nitrates are dissolved in water; the bismuth (nitrate, oxide, basic) salt is dissolved in concentrated nitric acid, and the sodium silicate is dissolved in water. With the aqueous solutions, the acidic nitrate solutions are mixed, while the basic silicate solution is placed in another beaker and made to an equal volume by adding DI water.

The co-precipitation process is monitored by a Metrohm 906 Titrando titrator with a universal pH electrode (calibrated with VWR AVS buffer solution) and Tiamo 2.5 software.

A co-precipitation flask with a pH electrode, a thermometer, and 150 mL of bottom water is heated to 60 °C with 450 rpm stirring on a magnetic stirring hotplate. The two solutions are added simultaneously via a Medorex peristaltic pump at a constant volumetric flow rate of 2 mL/min. A precipitation agent, either a 2 M Na_2CO_3 or a 2 M HNO_3 solution, is added automatically by the titrator to maintain the desired pH value of the system. Upon complete addition, the titration is stopped. At the same time, the co-precipitation suspension continues aging for 60 min, then cooled down, filtered with vacuum filtration, and washed with DI water until the conductivity of the filtrate is below 4 mSm^{-1}, measured by GHM 3410-Digital Conductivity Meter. The resulting precipitate is dried in an oven at 80 °C, calcined in a Nabertherm muffle furnace with a heating rate of 2.5 $Kmin^{-1}$ at the desired temperature and duration, and sieved to the desired grain sizes. The supported catalyst precursor is obtained.

Deposition Precipitation in Urea Solution via Hydrolysis (DP-U)

The copper salt is dissolved in the urea solution to form a light blue Cu^{2+} – $(CO(NH_2)_2)_x(H_2O)_y$ complex solution. The desired amount of pre-synthesized carrier is added.⑥ The suspension is stirred at 250 rpm and heated to 90 °C with reflex until a color change from blue to colorless is observed.

An analogous post-treatment process, as in CP, is followed.

Ammonia Evaporation (AE)

The copper salt is dissolved in the ammonia solution to form a deep blue Cu^{2+} – $(NH_3)_x(H_2O)_y$ complex solution. The desired pre-synthesized carrier is added. The suspension is then stirred at 250 rpm at room temperature until the ammonia is wholly evaporated (indicated by the color change or the smell of ammonia).

An analogous post-treatment process, as in CP, is followed.

Incipient Wetness Impregnation (IWI)

The water uptake rate is pre-determined for the selected pre-synthesized carriers. The copper salt (bismuth can also be included) is then dissolved in the DI water to the same amount. The aqueous solution and carrier powders are mixed stepwise to form solid-liquid colloids while shaking with a Heidolph Reax control shaker to allow homogeneous dispersion and diffusion.

An analogous post-treatment process, as in CP, is followed.

Deposition Precipitation in Ammonia Solution via Ligand Removal (DP-A)

The supported active catalyst containing copper acetylide is expected to be obtained.

The experiment is performed in an inert condition, either in a glove box or with a Schlenk line. The solutions and the containers are degassed, purged, and vacuumed. A different post-treatment process is followed.

The pre-synthesized carrier is placed in the Schlenk tube, while the copper(I) chloride is dissolved in the ammonia solution to form a colorless Cu^{+} – $(NH_3)_x(H_2O)_y$ complex solution. The solution is stirred at 250 rpm while acetylene gas is introduced, and the reddish-brown

⑥ The carrier materials (selection of Si, Al, Mg, Zn, and combinations) are pre-synthesized following the analogous co-precipitation process. In some cases, Bi, as a promoter, is also involved as part of the carriers due to its solubility in ammonia and urea solution.

precipitates are observed immediately. The process is carried on for 2 h to allow complete precipitation. Upon completion, the acetylene is released and purged with nitrogen. The suspension is then filtered, washed with water and methanol, and dried in-vacuo in a Schlenk line. The supported active cuprous acetylide catalyst is obtained.

Direct Precipitation of Pure-Phase Active Catalysts (DP-PP)

The pure-phase cuprous acetylide, Cu_2C_2, is synthesized via controlled direct precipitation.

An analogous technique to maintain the inert or oxygen-free condition is followed.

The copper(I) chloride or copper(II) sulfate, as the copper source, is dissolved in the ammonia solution. The reducing agent, hydroxylammonium chloride, is added in excess to ensure only copper(I) is present. Acetylene gas is introduced, and immediate precipitation of reddish-brown Cu_2C_2 species is observed.

In the controlled process, the copper-ammonia solution is diluted to the desired amount; the acetylene gas is saturated in DI water (solubility = 1.20 g_{C2H2}/L_{H2O} at 25 °C) and added bit-by-bit without stirring to allow the rate-controlled formation of the well-quantified Cu_2C_2.

Then, an analogous post-treatment process, as in DP-A, is followed. The pure-phase active cuprous acetylide is obtained.

5.3.2 Preparation of Formaldehyde Solution

Formaldehyde solution is available in two ways: self-prepared from paraformaldehyde and the commercial formalin solution (Table 5-4). Since the exact concentration, the pH value, and the pH buffer species of the commercial formalin are challenging to identify and adjust. A well-defined, self-prepared formaldehyde solution will be used in most of the analysis.

Commercial Formalin (concentration and pH value modified)

Commercial formalin is used as a reference or standard solution in calibration and as a catalytic performance test of the standardized ethynylation process.

The formalin of different gradings is pre-tested. The concentration, pH ranges, and buffers are determined by GC, pH electrode, and elemental analysis.

The formalin is then diluted, purified, and pH-adjusted according to the requirements by adding DI water, heating and filtration, and corresponding acids and bases.

Self-Prepared Standard Formaldehyde Solution

The standard solution is prepared at 37 wt.% of saturated formaldehyde by dissolving paraformaldehyde in DI water, containing 10 wt.% of methanol, buffered with 4 wt.% phosphate species at pH 7 (~35 mmol of NaOH and NaH_2PO_4 each). ⑦

The paraformaldehyde is weighed in a round-bottom flask. The buffer species are dissolved with a small amount of DI water in a separate container and transferred to the flask. The desired amount of water and methanol is added to the flask and heated to 100 °C with stirring for 1 h to allow complete dissolution. The solution is cooled, filtered to remove the remaining precipitates, and stored in the clear saturated formaldehyde solution at room temperature.

Self-Prepared pH-Adjusted Formaldehyde Solution

Following the analogous preparation procedures, both saturated and diluted formaldehyde solutions⑦, with different buffer species and pH values (Table 5-7), are prepared. Various ratios of the conjugated acid-base system are added depending on the solubility of paraformaldehyde, the stability of the formaldehyde solution, and the buffer capacity.

⑦ By dissolving paraformaldehyde, bond breaking process takes place where H_2O is consumed, the solution becomes over-saturated and precipitates form upon cooling; thus, filtration is necessary to remove the excess impurities and the saturated 37 wt.% formaldehyde remains.

5.3.3 Catalytic Reppe Ethynylation Process

The process can be performed either with parallel glassware reactors, which can be connected to two or three flasks coupled with individual heating, cooling, gas connections, and the magnetic stirring hotplates, or with the Carousel 6PLUS reaction station of six flasks on a holistic system (Figure 2-1 and Figure 2-2); and can be performed via one-step or two-step batch or semi-continuous process (Table 5-8)[④⑤].

One-Step Batch Ethynylation Process

In a two- or three-necked round bottom flask, the desired amount of catalyst precursors and formaldehyde solution are weighed with the catalyst-to-solution ratio between 2 to 6 g_{cat} per 100 mL solution. About 3 wt.% of 1,3-propanediol is weighed and recorded accurately (served as the internal standard (IS) for GC analysis). The flask is inserted into the reaction system by placing a magnetic stirring bar, connecting the gas inlet and outlet pipes and the septum, the cooling water pipes and condenser, and the heating oil bath or a metallic holder. The valves are switched to allow the gas and water to flow to the desired flask positions.

After connecting all the flasks, the reactor system is purged with nitrogen for 30 min with 450 rpm stirring to remove the air, then purged with acetylene gas for 30 min while heating to 90 °C. The ethynylation reaction starts when the gas outlet valve is switched off, while the static condition is maintained at 1.2 bar of acetylene absolute pressure.

For safety reasons, a safety pressure relief valve is connected to the gas outlet, which will activate automatically when the pressure of the system accumulates above 1.2 bar.

When the reaction is finished, the acetylene gas is released, and the reaction system is cooled with nitrogen purging to room temperature (~ 40-50 °C is sufficient). The power, gas, and water are switched off, the pipes and connectors are dismounted, and the flasks are removed. The waste solution and spent catalysts are disposed of, and the flasks and accessories are cleaned.

Two-Step Batch Ethynylation Process

The two-step process consists of an activation of the catalyst precursor and a catalytic ethynylation of the activated catalyst. An additional separation step is necessary.

In the activation step, the analogous procedures are followed, except after cooling and purging, where the reaction solution and activated catalysts are separated by centrifugation or vacuum filtration, washed, and stored in a slurry form under ambient conditions.

In the ethynylation step, all the activated catalysts are transferred into the flask, the fresh formaldehyde solution and IS are filled, and the analogous procedures are followed afterward.

One-Step Semi-Continuous Ethynylation Process

The semi-continuous process involves refilling the fresh formaldehyde solution after a large sample is withdrawn using the cannula filtration technique.

The analogous procedures are followed as the one-step batch process.

Handling of the Active-Phase Catalysts

The step involves separation, washing, and storage, which applies in the two-step process, as well as the sample preparation and treatments for analysis and characterization.

The separation of the active-phase catalyst from its suspension solution can be done by either centrifugation, vacuum filtration, or Schlenk line techniques. The residual catalyst is washed with DI water two times, followed by methanol two times. The washed catalyst can be stored in slurry form in a sealed container. It can also be dried in an ambient environment in the oven or an inert atmosphere via the Schlenk line and stored in the glove box.

Deactivation and Disposal

The supernatant solution is disposed of in the organic waste tank.

The spent active-phase catalyst consists of highly concentrated explosive cuprous acetylide species, which are kept wet at all times except under careful handling and treatment for specific investigations. For safety reasons, it has to be fully deactivated before disposal.

The spent active-phase catalyst is wetted and diluted with DI water, then deactivated in excess concentrated nitric acid and stirred overnight. A vigorous reaction involves extensive heat and brownish gas release, which is a sign of catalyst deactivation. After complete deactivation, the residual catalyst is separated, collected in a sealed container, and disposed of as solid waste. The supernatant acidic solution is diluted and disposed of in an acid waste tank.

In addition, the contaminated accessories have also been rinsed with diluted nitric acid before further cleaning or disposal.

5.3.4 Sample Preparation for Analytical Techniques

The procedures of sample preparation for the listed characterization and analysis techniques (Table 5-5 and Table 5-9) are described. Some analysis can only be done by authorized co-workers; thus, the sample preparation is done partially according to the requirements.

Centrifugation

A six-position Thermo Biofuge Primo R Centrifuge machine and 15 mL or 50 mL centrifuge tubes are available and used to separate the components of different densities in a suspension.

The centrifuge tubes are filled up to the maximum label, sealed tightly, and inserted in the centrifuge machine (2, 3, 4, and 6 positions can be tested simultaneously). A counterbalance tube of the same weight is made whenever necessary. The centrifugation is set at 3000-8000 rpm for 2-10 min, depending on the separation efficiency.

Filtration (vacuum, syringe filter)

Filtration is applied frequently for the separation and purification of the solid-liquid suspension. The vacuum filtration comprises a vacuum pump, Büchner funnel and flask, and filter paper with a pore size of 5-13 µm, and it is used for large amounts of filtration.

For samples requiring free of solid and high purity, a second step of filtration with a syringe filter is then applied; the pore size is 0.45 µm.

Atomic Absorption Spectrometer

The analysis was done by authorized technicians at the Central Analytical Lab of TUM-CRC.

The Varian AA280 series Fast Sequential flame AAS, consisting of a graphite furnace and eight lamp capabilities, is used to analyze the leached and dissolved elements (e.g., copper) quantitatively from the catalyst during the ethynylation process.

15 mL of the reaction solution is extracted and filtered through a 0.45-micron syringe filter. The supernatant solution is then sealed in a centrifuge tube and sent for analysis.

CHN elemental analysis

The analysis was done by authorized technicians at the Central Analytical Lab of TUM-CRC.

The Euro EA CHN elemental analyzer, equipped with a GC-TCD, is used to quantitatively determine the content in wt.% of carbon, hydrogen, nitrogen, and sulfur in the solid sample.

Precisely weighed 1.0-2.0 mg of the air-sensitive catalyst sample is tightly sealed into two layers of the tin capsule in the glove box and sent for analysis.

Inductively Coupled Plasma -Optical Emission Spectroscopy (ICP-OES)

The analysis was done by a co-worker at the Department of Chemistry, TUM.

A unique series of analyses was done by a partner organization. The details will not be discussed.

The ICP-OES is applied for multi-elemental analysis of the solid-free aqueous sample solution to determine the content of each component in the catalyst sample and the leached content in the aqueous solution during the catalytic ethynylation process.

The Agilent 700 Series ICP-OES (at TUM) is calibrated from 0 to 50 ppm with Merck Certipur® ICP multi-element standard solution IV with 23 elements in diluted HNO_3. The elements with the corresponding wavelength were analyzed.

Determination of the catalyst loadings: The solid catalyst sample must be completely dissolved in concentrated nitric or phosphoric acid. Ultrasonic treatment and burning on a Bunsen burner in a crucible may be necessary. The solution is then diluted in volumetric flasks with bi-distilled super water to the desired concentration range (up to 50 ppm) and acidity (3 to 10% acid). 10 mL of aqueous sample is further purified with a syringe filtration (0.45 microns) for analysis.

Determination of the leaching contents: The sample is taken at the selected conditions and time frames during the catalytic ethynylation process via a syringe or by cannula technique. The sample is filtered and transferred in a crucible with the precisely measured volume to calculate the dilution factor. The organic compounds in the sample are removed by drying on heat. The analogous procedures are followed with the dried solid sample.

The samples for the analysis by the industry partner require only the filtration and purification step. The sample solution is then carefully sealed and shipped for analysis.

Chemisorption by Temperature-Programmed Techniques

The Micromeritics Autochem II 2920 Analyzer, equipped with a thermal conductivity detector (TCD) or a Pfeiffer ThermoStar GSD 320 T Gas Analyzer (MS), is used.

TP reduction (TPR) is carried out with about 45 mg catalyst sample (depending on the metal loading) at 350-800 °C with a 5-10 K/min heating rate and a 50 L/min 10% H_2/Ar gas flow. An about -90 °C cold trap is prepared with an isopropanol-liquid nitrogen mixture to freeze the decomposed gas species.

TP desorption (TPD) coupled with an MS is performed at 200-500 °C with a 2-4 K/min heating rate and a 10-20 L/min He gas flow. The sample is inserted under the inert condition, and the decomposed species is analyzed by the MS with the corresponding m/z ratio.

N_2O pulse chemisorption coupled with a TCD is used to determine the copper surface area and dispersion of the catalyst. The pre-reduced sample (using the TPR procedure) is flushed with 10-20 L/min He for 0.5 h at the reduction temperature to remove the adsorbed H_2 on the surface. The pulses of the defined amount of N_2O in a loop (50-500 µL loop size) are dosed 20 times into the constant flow of the He gas stream to adsorb on the copper surface. A liquid nitrogen cold trap is used to residual N_2O. The amount of formed N_2 is analyzed by TCD.

Gas (Liquid) Chromatograph (GC/GLC)

The Agilent 6890N GC (G1530A), equipped with a TCD (consisting of an electrically heated filament) and an EPC (for gas and pressure control), is used to qualitatively and quantitatively identify the components from a liquid-phase sample. Two Agilent J&W GC columns have been used in the analysis for different separation preferences: HP-PLOT-Q: bonded polystyrene-divinylbenzene-based column, 30 m length, 0.32 mm inner diameter, and 20 µm film thickness; and CP-Sil 5 CB for Formaldehyde: nonpolar 100% dimethylpolysiloxane phase, 60 m length, 0.32 mm inner diameter, and 8 µm film thickness.

The GC analysis is monitored by Agilent ChemStation software. The standard method is implemented and optimized with a split injection of the ratio up to 1:50, 1.25 bar at constant flow up to 50 mL/min with carrier, reference, and makeup gas by helium, 240 °C injector and detector temperature, 40 to 240 °C at a ramp rate of 25 K/min in oven.

The self-prepared filter is made by filling a bundle of glass wool and 1-2 cm of PURALOX SCCa-150/200 alumina in a 150 mm Disposable Pasteur Pipette. A minimum of 1 mL of filtrate is collected in a GC vial. Acetonitrile (ACN) is used as a dilution agent whenever necessary.

A series of standard solutions consisting of different concentrations of the desired analytes, 1,4-butynediol, propargyl alcohol, and formaldehyde, are prepared for the calibration of GC. 1,3-propanediol is used as the internal standard (IS). The pure phase analyte species are dissolved and mixed with DI water in the volumetric flask; the solution is then filtered into a GC vial and analyzed by corresponding GC Methods. A linear calibration line in a ratio-of-GC-area versus ratio-of-concentration diagram is expected for each component, and the slope (m_{GC}) of the line is used as a conversion factor in future GC analysis and calculation. The calibration is expected to be performed every six months or when any analyzing parameter changes.

The experimental samples are collected at a selected time frame during the ethynylation process. Approximately 0.7 mL of sample is extracted via a needle and syringe and diluted

with 0.7 mL of ACN. The mixture is then filtered and analyzed by GC. The unknown components are identified by comparing the retention time (t_R) of the signals in GC. At the same time, the concentration is calculated with the pre-defined values of the IS and the m_{GC}.

Physisorption (BET/BJH methods)

The Quantachrome NovaTouch™ LX4 Analyzer (4 positions) is used to determine adsorption-desorption isotherms, the total surface area by the Brunauer-Emmett-Teller method, and the pore size by Barrett-Joyner-Hallenda (BJH) method. The data evaluation is done with the Quantachrome TouchWin software.

The catalyst sample is precisely weighed in a pre-defined standard BET quartz tube and degassed under vacuum for 3 h at 120 °C to remove the surface contaminants. The sample is weighed again and recorded in the software. The BET tube, inserted with a glass rod, is loaded into the analyzer. A 40-point nitrogen isotherm at liquid nitrogen temperature (-196 °C) is analyzed over the full relative pressure range, $0 < p/p_0 < 1$. The monolayer physisorption is defined at $0 < p/p_0 \leq 0.35$ (BET method), while the multilayer is at $0.35 \leq p/p_0 < 1$ (BJH method).

Thermogravimetry Mass Spectroscopy (TGA/DSC-MS)

The Mettler Toledo Thermal Analysis STARe System TGA/DSC 3+, coupled with the Pfeiffer ThermoStar GSD 320 T Gas Analyzer, is monitored with the inter-connected STARe Software version 14.0 (TGA) and INFICON QUADERA® version 4.62 (MS). The TGA/DSC is used to analyze the decomposition of the solid sample by the changes in mass and heat flow at elevated temperatures. The MS is used to identify the gas components from the decomposition.

The sample in a TA alumina crucible is precisely weighed and recorded in the TGA device. It is heated from 25 °C up to 1200 °C with a ramp rate of up to 20 K/min under inert (Ar), oxidative (synthetic air), or reductive (H_2 in Ar) atmospheres with the gas flow of 20 mL/min. The MS then identifies the decomposed gases with the m/z ratio of 1 or 2 (H_2), 14 or 28 (N_2), 16 or 32 (O_2), 18 (H_2O), 26 (C_2H_2), 28 or 44 (CO_x), 30 (CH_2O), 30 or 46 (NO_x), and 40 (Ar).

Powder X-Ray Diffraction (PXRD)

Three PXRD devices were used for different analytical preferences and sensitivities. The PANalytical HighScore Plus software includes phase identification, crystallite size calculation with the Scherrer equation, and Rietveld refinement for data evaluation. The analytical geometries are converted with radiation wavelength, λ, and 2θ angle into scattering vector, |q|.

Malvern PANalytical Empyrean Multipurpose X-Ray Diffraction Instrument

The PXRD is performed with Kα(Cu) radiation at λ = 1 5419 Å and Ni as Kβ(Cu)-filter in a reflection mode by Bragg-Brentano geometry. The powder sample is loaded onto a flatbed silicon wafer holder and placed into the device. The X-ray diffractogram is recorded with an angular range of 5° to 70° in a step size of 0.008°.

The *in situ* XRD is measured with an Anton Paar XRK-900 reaction chamber. The analytical parameters can be set with the corresponding gas flow and heat ramp.

Rigaku MiniFlex 600-C Benchtop power X-Ray Diffractometer

The PXRD is performed with Kα(Cu) radiation at λ = 1 5419 Å in a reflection mode by Bragg-Brentano geometry. The powder or the wet slurry sample is loaded and flattened onto a silicon wafer holder and placed into the device. The wet or air-sensitive samples are covered with a layer of Kapton® foil. The X-ray diffractogram is recorded with an angular range of 10° to 60° in a step size of 0.01°, 5°/min velocity, 40 rpm spin, and 50 mA power.

STOE & Cie STADI P Transmission Powder Diffractometer

The analysis was done by a partner at the Department of Chemistry, TUM.

The PXRD is performed with Kα(Mo) radiation at λ = 0.7107 Å in a transmission mode by both Debye-Scherrer and Bragg-Brentano geometry. The sensitive powder sample is sealed between the Kapton® foil in the glove box. It is then placed in the air-tight sample holder and loaded into the device.

Raman Spectroscopy

The Renishaw InViaTM Qontor® Confocal Raman Microscope, equipped with an Andor Newton EMCCD Camera (25.6 mm width, 1600 pixels, 3 MHz), a frequency-doubled Nd: YAG crystal laser at λ = 532 nm (638 nm and 785 nm also available); and a Leica N PLAN EPI objective with 50x/0.75 magnification, is monitored with WiRE™ 5.3 software. The Raman is used to identify the components from a dried powder, wet slurry, and aqueous sample.

The solid sample is flattened on a glass slide, and the aqueous sample is dropped on a glass slide or kept in a glass vial. The analytical point is defined with the microscope. The point for analysis of the sample was selected and focused on with the microscope camera; it was then radiated with a laser intensity of 0.005 – 1.0% with 1 – 30 s exposure and 5 – 50 repetitions.⑧

⑧ The laser intensity at 100% is regarded as 29.52 mW; the applicable intensity in % depends on the availability of the device. The significant variations of the analytical parameters are related to the sensitivity of the samples. This is especially important for the powder samples to ensure the laser power does not decompose the sample. Hence, a review of the analytical point after laser radiation is necessary.

6

BIBLIOGRAPHY

[1] J. Stillman, *The Story of Early Chemistry*, D.Appleton and Co,, New York, **1924**.

[2] J. Partington, *A Short History of Chemistry*, Harper & Row, **1960**.

[3] S. Rasmussen, *Acetylene and Its Polymers – 150+ Years of History*, 1 ed., Springer Cham, USA, **2018**.

[4] J. Wisniak, *Educación Química* **2020**, *31*, 12.

[5] M. Berthelot, *Comptes Redus* **1860**, *3*, 4.

[6] E. Davy, *Journal of the Franklin Institute - Engineering and Applied Mathematics* **1837**, *19*, 3.

[7] T. Willson, J. Suckert, *Journal of the Franklin Institute* **1895**, *139*, 21.

[8] E. Davy, *The Transactions of the Royal Irish Academy* **1839**, *18*, 7.

[9] J. Nieuwland, R. Vogt, *The Chemistry of Acetylene*, Reinhold Publishing Corporation, New York, **1945**.

[10] P. Pässler, W. Hefner, K. Buckl, et al., in *Ullmann's Encyclopedia of Industrial Chemistry, Vol. 1*, 7. Edition ed., Wiley-VCH Verlag GmbH & Co. KGaA, Germany, **2012**, p. 50.

[11] M. Berthelot, in *Leçons sur les méthodes générales de synthèse en chimie organique*, professées en 1864 au Collège de France ed., Gauthier-Villars, 1864, Paris, **1864**, p. 19.

[12] M. Berthelot, *Comptes rendus de l'Académie des sciences* **1866**, *63*, 7.

[13] B. Bensaude-Vincent, I. Stengers, in *A History of Chemistry*, Harvard University Press, England, **1996**, p. 67.

[14] T. Willson*, Vol. US 492377*, US, **1893**, p. 6.

[15] in *A National Historic Chemical Landmark*, The American Chemical Society, North Carolina, **1998**.

[16] R. Stief, *A History of Union Carbide Corporation (From the 1890s to the 1990s)*, Carbide Retiree Corp. Inc., United States, **1998**.

[17] H. Schobert, *Chemical Reviews* **2014**, *114*, 18.

[18] R. Tedeschi, *Acetelyne-Based Chemicals from Coal and Other Natural Resources*, Marcel Dekker Inc, **1982**.

[19] D. Bittner, W. Wanzl, *Fuel Processing Technology* **1990**, *24*, 6.

[20] F. Diederich, R. Tykwinski, P. Stang, *Acetylene Chemistry: Chemistry, Biology and Material Science*, Wiley-VCH Verlag GmbH & Co. KGaA, Weinheim, Germany, **2006**.

[21] P. Stang, F. Diederich, *Modern Acetylene Chemistry*, Wiley-VCH Verlag GmbH & Co. KGaA, Weinheim, **2008**.

[22] R. Gannon, R. Manyik, C. Dietz, et al., in *Kirk-Othmer Encyclopedia of Chemical Technology, Vol. 1*, John Wiley & Sons, Inc., **2003**, p. 51.

[23] L. Bartholoméa, *Chemie Ingenieur Technik* **1954**, *26*, 6.

[24] H. Sachsse, *Chemie Ingenieur Technik* **1954**, *26*, 9.

[25] M. Vicar, in *DGMK Conference: New Technologies and Alternative Feedstocks in Petrochemistry and Refining*, BASF SE, Ludwigshafen, Germany, **2013**, p. 4.

[26] J. Haworth, W. Grant, in *Introduction to Petroleum Chemicals*, Pergamon Press, **1962**, p. 29.

[27] D. McIntosh, *The Journal of Physical Chemistry* **1907**, *11*, 12.

[28] D. Begany, A. Cowen, Degree of Bachelor of Science thesis, Massachusetts Institute of Technology **1957**.

[29] W. Hanford, D. Fuller, *Industrial & Engineering Chemistry* **1948**, *40*, 7.

[30] A. Travis*, Vol. 32*, Bulletin for the History of Chemistry, Hebrew University, **2007**, p. 8.

[31] S. Díez-González, in *Advances in Organometallic Chemistry, Vol. 66*, **2016**, p. 49.

[32] S. Rasmussen, *Bulletin for the History of Chemistry* **2017**, *42*, 16.

[33] H. von Pechmann, *Deutschen chemischen Gesellschaft zu Berlin* **1898**, *31*, 7.

[34] E. Weaver, *Journal of the Franklin Institute* **1916**, *181*, 3.

[35] N. Scott, C. Roberts, du Pont de Nemours & Co, US, **1939**, p. 3.

[36] A. Akhrem, T. Ustynyuk, Y. Titov, *Russian Chemical Reviews* **1970**, *39*, 732.

[37] N. Danilkina, A. Vasileva, I. Balova, *Russian Chemical Reviews* **2020**, *89*.

[38] J. Nieuwland, Notre Dame University Press Notre Dame, Ind. (Notre Dame, Ind.), **1904**.

[39] W. Reppe, *Neue Entwicklungen auf dem Gebiete der Chemie des Acetylens und Kohlenoxyds* Springer, Berlin, Berlin, Germany, **1949**.

[40] W. Reppe, *Chemie Ingenieur Technik* **1950**, *22*.

[41] W. Reppe, *Justus Liebigs Annalen der Chemie* **1955**, *596*.

[42] W. Reppe, *Justus Liebigs Annalen der Chemie* **1956**, *601*, 58.

[43] J. Kent, *Riegel's Handbook of Industrial Chemistry* Springer US, **2003**.

[44] I.-T. Trotuş, T. Zimmermann, F. Schüth, *Chemical Reviews* **2014**, *114*, 12.

[45] B. Dana, University of Illinois **1917**.

[46] V. Brameld, M. Clark, A. Seyfang, *Journal of the Society of Chemical Industry* **1947**, *66*, 8.

[47] T. Nosetani, S. Sato, in *Spring Conference of Japan Institute of Metals, Vol. 12*, Sumitomo Light Metal Technical Reports, Japan, **1969**, p. 5.

[48] C. Castro, R. Havlin, V. Honwad, et al., *Journal of the American Chemical Society* **1969**, *91*, 7.

[49] T. Rutledge, *The Journal of Organic Chemistry* **1957**, *22*, 4.

[50] T. Rutledge, *The Journal of Organic Chemistry* **1959**, *24*, 3.

[51] V. Aleksanyan, I. Garbuzova, I. Gol'ding, et al., *Spectrochimica Acta Part A: Molecular Spectroscopy* **1975**, *31*, 8.

[52] O. M. Abu-Salah, *Journal of Organometallic Chemistry* **1998**, *565*, 6.

[53] C. Glaser, *Berichte der Deutschen Chemischen Gesellschaft* **1869**, *2*, 3.

[54] G. Eglinton, A. Galbraith, *Journal of the Chemical Society* **1959**, 7.

[55] A. Hay, *Journal of Organic Chemistry* **1962**, *27*, 2.

[56] S. Miller, E. Penny, in *Institution of Chemical Engineers - Symposium on Chemical Process Hazards*, **1960**.

[57] I. Gay, G. Kistiakowsky, J. Michael, et al., *The Journal of Chemical Physics* **1965**, *43*, 7.

[58] F. Carver, C. Smith, G. Webster, *Institution of Chemical Engineers Symposium* **1972**, *33*, 6.

[59] J. Copenhaver, M. Bigelow, Reinhold Pub. Corp. New York, New York, **1949**, pp. XVI, 357.

[60] M. Chiddix, *Annals of the New York Academy of Sciences* **1967**, *145*, 11.

[61] R. Fredericks, D. Lynch, W. Daniels, *Polymer Letters* **1964**, *2*, 6.

[62] The Engineering ToolBox_Acetylene – Thermophysical Properties, **2008**.

[63] in *Working Safely with Acetylene*, BCGA, **2014**, p. 5.

[64] Chemical Book_Acetylene_Chemical Safety Data Sheet, **2023**, p. 10.

[65] R. Stokes, *Cambridge Books* **1994**.

[66] P. Luo, X. Li, *American Journal of Chemical Engineering* **2021**, *9*, 34.

[67] C. Wu, J. Chen, Y. Cheng, *Fuel Processing Technology* **2010**, *91*, 8.

[68] University of Pennsylvania, Office of Environmental Health and Radiation Safety (EHRS).

[69] T. O'Lenick, K. O'Lenick, Siltech LLC, SurfaTech Corporation, **2008**.

[70] Technische Regeln für Acetylenanlagen and Calciumcarbidlager

[71] Bundesministerium für Wirtschaft und Klimaschutz.

[72] W. Reppe, *Justus Liebigs Annalen der Chemie* **1953**, *582*.

[73] W. Reppe, O. Schlichting, K. Klager, et al., *Justus Liebigs Annalen der Chemie* **1948**, *560*, 92.

[74] W. Reppe, A. Steinhofer, H. Spaenig, et al., GAF Corp., US, **1942**, p. 2.

[75] E. Evans, in *Introduction to Petroleum Chemicals*, Pergamon Press, **1961**, p. 18.

[76] C. Rode, *Journal of The Japan Petroleum Institute* **2008**, *51*, 119-133.

[77] I.-T. Trotuș, Ruhr-Universität Bochum **2016**.

[78] S. Tanielyan, S. More, R. Augustine, et al., *Organic Process Research & Development* **2017**, *21*, 9.

[79] X. Gao, W. Mo, F. Ma, et al., *RSC Advances* **2020**, *10*, 9.

[80] in *Material Safety Data Sheet*, p. 11.

[81] Federal Institute for Occupational Safety and Health Notification Unit, Germany, **2005**, p. 29.

[82] V. Voronin, M. Ledovskaya, A. Bogachenkov, et al., *Molecules* **2018**, *23*.

[83] N. Sitte, F. Ghiringhelli, G. Shevchenko, et al., *Advanced Synthesis & Catalysis* **2022**, *364*, 8.

[84] K. Suzuki, *The Review of Physical Chemistry of Japan* **1954**, *23*, 10.

[85] K. Suzuki, *The Review of Physical Chemistry of Japan* **1954**, *23*, 8.

[86] P. Shull, (Ed.: G. A. F. Corporation), GAF Corp., US, **1964**, p. 2.

[87] D. Graham, W. Craig, E. Hort, GAF Corp., US, **1966**, p. 3.

[88] M. E. Chiddix, O. F. Hecht*, Vol. DE 1191364B*, GAF Corp., DE, **1965**.

[89] D. Zak, (Ed.: d. P. d. N. a. Co), US, **1978**, p. 5.

[90] W. Reiss, S. Winderl, W. Schroeder, et al., BASF Aktiengesellschaft, DE, **1978**, p. 6.

[91] W. Moore, C. County, R. MacGregor, Allied Chemical Corp., US, **1963**, p. 5.

[92] G. Moore, Cumberland Chemical Corp., US, **1965**, p. 4.

[93] J. Kiernan, *Microscopy Today* **2000**, *8*, 6.

[94] R. Thavarajah, V. Mudimbaimannar, J. Elizabeth, et al., *Journal of Oral and Maxillofacial Pathology* **2012**, *16*, 6.

[95] National Center for Biotechnology Information US, **2024**.

[96] M. Barret, S. Houdier, F. Domine, *The Journal of Physical Chemistry A* **2011**, *115*, 11.

[97] Alonso-Buenaposada, N. Rey-Raap, E. Calvo, et al., *Journal of Non-Crystalline Solids* **2015**, *426*, 6.

[98] R. Prinz, B. Kerr, Celanese Corp., US, **1964**, p. 6.

[99] Y. Liu, F. Kirchberger, S. Müller, et al., *Nature Communications* **2019**, *10*, 9.

[100] J. Salamanca, I. Munhenzva, J. Escobedo, et al., *Scientific Reports* **2017**, *7*, 8.

[101] I. Hahnenstein, H. Hasse, C. G. Kreiter, et al., *Industrial & Engineering Chemistry Research* **1994**, *33*, 1022-1029.

[102] R. Kiyama, J. Osugi, K. Suzuki, *Review of Physical Chemistry of Japan* **1952**, *22*, 12.

[103] R. Kiyama, J. Osugi, K. Suzuki, et al., *Review of Physical Chemistry of Japan* **1954**, *23*, 8.

[104] S. Kale, R. Chaudhari, P. Ramachandran, *Industrial & Engineering Chemistry Product Research and Development* **1981**, *20*, 7.

[105] S. Gupte, P. Jadkar, R. Chaudhari, *Reaction Kinetics and Catalysis Letters* **1984**, *24*, 5.

[106] F.-W. Chang, J.-M. Chen, J.-C. Guo, *Chemical Engineering Science* **1992**, *47*, 8.

[107] X. Hu, Q. Bo, L. Cheng, et al., *Natural Gas Chemical Industry* **2020**, *45*, 5.

[108] T. Punniyamurthy, L. Rout, *Coordination Chemistry Reviews* **2008**, *252*, 21.

[109] S. Chemler, *Beilstein Journal of Organic Chemistry* **2015**, *11*, 2.

[110] M. Gawande, A. Goswami, F.-X. Felpin, et al., *Chemical Reviews* **2016**, *116*, 90.

[111] S. Zhang, L. Zhao, *Nature Communications* **2019**, *10*, 10.

[112] C. Bartholomew, R. Farrauto, *Fundamentals of Industrial Catalytic Processes*, Second ed., John Wiley & Sons, Inc, **2006**.

[113] J. Le Page, in *Preparation of Solid Catalysts*, **1999**, p. 8.

[114] K. de Jong, *Synthesis of Solid Catalysts*, John Wiley & Sons, Ltd, Germany, **2009**.

[115] M. A. El-Okazy, T. M. Zewail, H. A.-M. Farag, *Alexandria Engineering Journal* **2018**, *57*, 10.

[116] X. Dong, X. Ma, H. Xu, et al., *Catalysis Science & Technology* **2016**, *6*, 8.

[117] H. Li, L. Ban, Z. Wang, et al., *Nanomaterials* **2019**, *9*, 16.

[118] Z. Wang, L. Ban, P. Meng, et al., *Nanomaterials* **2019**, *9*, 21.

[119] R. Madon, P. Nagel, S. Hedrick, et al., BASF Corp., US, **2014**, p. 6.

[120] H. Yue, Y. Zhao, S. Zhao, et al., *Nature Communications* **2013**, *4*, 7.

[121] C. Xu, G. Chen, Y. Zhao, et al., *Nature Communications* **2018**, *9*, 10.

[122] C. Pompe, M. Slagter, P. de Jongh, et al., *Journal of Catalysis* **2018**, *365*, 9.

[123] Z. Bian, S. Kawi, *Catalysis Today* **2020**, *339*, 21.

[124] G. Yang, F. Gao, L. Yang, *Reaction Chemistry & Engineering* **2023**.

[125] H. Li, P. Meng, Y. Zhang, et al., *CIESC Journal* **2021**, *72*, 10.

[126] Z. Ma, H. Zhang, H. Li, et al., *Industrial Catalysis* **2015**, *23*, 5.

[127] E. Hort, GAF Corp., US, **1975**, p. 7.

[128] E. Hort, GAF Corp., US, **1977**, p. 9.

[129] H. Guo, B. Sun, Shanghai Xunkai New Material Technology Co., Ltd., **2017**, p. 8.

[130] G. Yang, Y. Yu, M. U. Tahir, et al., *Reaction Kinetics, Mechanisms and Catalysis* **2019**, *127*, 12.

[131] Z. Wang, Z. Niu, Q. Hao, et al., *Catalysts* **2019**, *9*, 35.

[132] J. Gao, G. Yang, H. Li, et al., *Processes* **2019**, *7*.

[133] J. C. Oxley, J. L. Smith, F. L. Steinkamp, et al., *Journal of Chemical Health & Safety* **2017**, *24*, 26-33.

[134] G. Yang, Y. Xu, X. Su, et al., *Ceramics International* **2014**, *40*, 5.

[135] G. Yang, L. Yang, J. Chen, *Industrial & Engineering Chemistry Research* **2023**.

[136] Z. Wang, L. Ban, P. Meng, et al., *Nanomaterials* **2019**, *9*, 21.

[137] L. Ban, H. Li, Y. Zhang, et al., *The Journal of Physical Chemistry C* **2021**, *125*, 14.

[138] X. Wang, K. Ma, L. Guo, et al., *Applied Catalysis A* **2017**, *540*, 10.

[139] L. Ban, H. Li, J. Zhao, et al., *Applied Surface Science* **2023**, *640*, 13.

[140] M. Hiller, K. Köhler, *Chemie Ingenieur Technik* **2022**, *94*.

[141] J. Wang, H. Zhang, H. Li, et al., *Industrial Catalysis* **2015**, *23*, 4.

[142] J. Wang, H. Li, Z. Ma, et al., *CIESC Journal* **2015**, *66*, 7.

[143] H. Li, L. Ban, Z. Niu, et al., *Nanomaterials* **2019**, *9*, 15.

[144] H. Li, Z. Niu, G. Yang, et al., *CIESC Journal* **2018**, *69*, 7.

[145] Z. Wang, Z. Niu, L. Ban, et al., *Chemical Journal of Chinese Universities* **2019**, *40*, 8.

[146] V. Zakharov, B. Kalyuzhnyi, V. Ovchinnikov, et al., Novocherkasskii Zavod Sinteticheskikh Produktov, RU, **2000**, p. 12.

[147] S. Lin, Q. Huang, G. Yan, et al., Fujian Normal University, CN, **2007**, p. 8.

[148] S.-A. Madhukar, S.-B. Sidram, Hindustan Organic Chemicals Ltd., IN, **2008**, p. 8.

[149] S.-B. Sidram, S.-A. Madhukar, Hindustan Organic Chemicals Ltd., IN, **2009**, p. 31.

[150] B. Dai, S. Liu, W. Peng, Shihezi University, CN, **2018**, p. 7.

[151] S. Liu, W. Peng, J. Zhang, et al., *Energy Sources, Part A: Recovery, Utilization, and Environmental Effects* **2018**, *40*, 7.

[152] R. Madon, P. Nagel, K. L. Deutsch, et al., BASF Corp., US, **2017**, p. 16.

[153] M. Zhang, *Liaoning Chemical Industry* **2017**, *46*, 3.

[154] G. Li, *Liaoning Chemical Industry* **2020**, *49*, 4.

[155] Z. Jusys, A. Vaskelis, *Langmuir* **1992**, *8*, 2.

[156] S. Rana, A. Prasoon, P. Sadhukhan, et al., *The Journal of Physical Chemistry Letters* **2018**, *9*, 8.

[157] S. Liang, S. Chen, Z. Guo, et al., *Catalysis Science & Technology* **2019**, *9*, 9.

[158] M. Luo, H. Li, Z. Ma, et al., *Industrial Catalysis* **2014**, *22*, 6.

[159] T. Bruhm, A. Abram, J. Häusler, et al., *Chemistry – A European Journal* **2021**, *27*, 16834-16839.

[160] J. Kirchner, (Ed.: d. P. d. N. a. Company), du Pont de Nemours and Co, US, **1972**, p. 8.

[161] A. Stock, J. Verbsky, (Ed.: d. P. d. N. a. Co), du Pont de Nemours and Co, US, **1981**, p. 5.

[162] K. Judai, J. Nishijo, N. Nishi, *Advanced Materials* **2006**, *18*, 5.

[163] G. Evano, K. Jouvin, C. Theunissen, et al., *Chemical Communications* **2014**, *50*.

[164] A. Makarem, R. Berg, F. Rominger, et al., *Angewandte Chemie International Edition* **2015**, *54*, 7431-7435.

[165] U. Rosenthal, *Angewandte Chemie International Edition* **2003**, *42*, 1794-1798.

[166] F. Cataldo, *European Journal of Solid State and Inorganic Chemistry* **1998**, *35*, 11.

[167] F. Cataldo, *Polymer International* **1999**, *48*, 8.

[168] F. Cataldo, *Carbon* **2005**, *43*, 9.

[169] F. Cataldo, C. Casari, *Journal of Inorganic and Organometallic Polymers and Materials* **2007**, *17*, 11.

[170] F. Cataldo, G. Compagnini, A. Scandurra, et al., *Fullerenes, Nanotubes and Carbon Nanostructures* **2008**, *16*, 16.

[171] F. Cataldo, *Journal of Raman Spectroscopy* **2008**, *39*, 8.

[172] B. Hudson, *Materials* **2018**, *11*, 242.

[173] R. Singh, P. Tiwari, B. Sharma, et al., in *Recent Advances in Natural Products Analysis*, Elsevier, **2020**, p. 16.

[174] K. Judai, S. Numao, J. Nishijo, et al., *Journal of Molecular Catalysis A: Chemical* **2011**, *347*, 6.

[175] J. Liu, J. Lam, B. Zhong Tang, in *Design and Synthesis of Conjugated Polymers*, **2010**, p. 43.

[176] P. Seavill, K. Holt, J. Wilden, *RSC Advances* **2019**, *9*, 5.

[177] P. Seavill, K. Holt, J. Wilden, *Green Chemistry* **2018**, *20*, 5.

[178] J. Kirchner, du Pont de Nemours & Co, **1971**, p. 8.

[179] Y. Archakov, A. Bulatova, L. Gorchakov, et al., *Khimiya i Tekhnologiya Topliv i Masel* **1985**, *9*, 2.

[180] *Aqueous Solutions / Wässrige Lösungen*, De Gruyter, Berlin, New York, **1976**.

[181] S. H. Yalkowsky, Y. He, P. Jain, *Handbook of Aqueous Solubility Data*, 2 ed., Taylor & Francis Group, **2010**.

[182] A. C. McKinnis, *Industrial & Engineering Chemistry* **1955**, *47*, 850-853.

[183] Y. Miyano, W. Hayduk, *The Canadian Journal of Chemical Engineering* **1981**, *59*, 6.

[184] X. Huang, S. Li, *Journal of Chemical & Engineering Data* **2018**, *63*, 8.

[185] P. B. Jadkar, R. V. Chaudhari, *Journal of Chemical & Engineering Data* **1980**, *25*, 3.

[186] P. D. MIT_Scott A Speakman, Massachusetts Institute of Technology, p. 97.

[187] R. Caliandro, C. Giacovazzo, R. Rizzi, in *Powder Diffraction: Theory and Practice*, The Royal Society of Chemistry, **2008**, p. 39.

[188] R. E. Dinnebier, S. J. L. Billinge, in *Powder Diffraction: Theory and Practice*, The Royal Society of Chemistry, **2008**, p. 19.

[189] O. Hinrichsen, T. Genger, M. Muhler, *Chemical Engineering & Technology* **2000**, *23*, 956-959.

[190] in *Formaldehyde* American Chemistry Council.

[191] M. De Villiers, in *A Practical Guide to Contemporary Pharmacy Practice*, 3 ed., Lippincott Williams & Wilkins, **2009**, pp. 224-230.

[192] J. Plátenník, University of California, **2018**, p. 3.

[193] W. Supassorn, C. Salinee, S. Theeranat, *Research Journal of Applied Sciences* **2019**, *14*, 235-238.

[194] IGNOU*, Vol. 03. School of Sciences (SOS)*, IGNOU, eGyanKosh IGNOU Self Learning Material (SLM) **2017**, pp. 73-76.

[195] R. J. Carrico*, Vol. B1*, C12O 1/00; G01N 33/53 ed. (Ed.: S. R. Corp.), US, **2002**, p. 13.

[196] I. Finkelde, R. R. Waller, *Collection Forum* **2021**, *34*, 32-52.

[197] I. Sigma-Aldrich, in *Product Information*, USA, **1999**.

[198] M. Levy, *Journal of Biological Chemistry* **1934**, *105*, 157-165.

[199] M. Rivlin, U. Eliav, G. Navon, *The Journal of Physical Chemistry B* **2015**, *119*, 4479-4487.

[200] J. Berje, J. Burger, H. Hasse, et al., *AIChE Journal* **2017**, *63*, 4442-4450.

[201] A. Gratien, B. Picquet-Varrault, J. Orphal, et al., *Journal of Geophysical Research: Atmospheres* **2007**, *112*.

[202] S. Sandler, R. Strom, *Analytical Chemistry* **1960**, *32*, 1890-1891.

[203] J. G. Dojahn, W. E. Wentworth, S. D. Stearns, *Journal of Chromatographic Science* **2001**, *39*, 54-58.

[204] Agilent, in *Agilent J&W CP-Sil 5 CB*, **2014**, p. 7.

[205] F. Sun, G. Wang, *Journal of Loss Prevention in the Process Industries* **2019**, *62*, 103967.

[206] M. PÓŁKA, Z. Salamonowicz, P. Batko, European Sensor System for CBRN Applications, **2012**.

[207] F. L. Steinkamp, University of Rhode Island **2013**.

[208] Agilent, in *Agilent 6890 Series Gas Chromatograph - Operating Manual-Service Manual*, p. 286.

[209] Agilent, in *Agilent 6890N Series Gas Chromatograph - User Information*, **2001**, p. 758.

[210] Agilent, in *Agilent 7683B Automatic Liquid Sampler*, **2004**, p. 202.

[211] Agilent, in *Fundamentals of Gas Chromatography: Hardware*, **2016**.

[212] Agilent, in *Installation, Care and Maintenance of Capillary Gas Chromatography Columns*.

[213] R. Birney, A. Ucci, in *Keep your GC Column Alive* **2023**.

[214] Agilent, in *Installation Guide_Thermal Conductivity Detector on a 6890 GC*, p. 28.

[215] Agilent, in *Maintaining your Agilent GC and GC/MS Systems*, **2005**, p. 121.

[216] Agilent, in *GC Troubleshooting Guide*, **2019**, p. 1.

[217] B. Pierson, J. Humpula, Activated Research Company, LLC **2020**, p. 3.

[218] K. Kriechbaum, TU Graz, **2014**.

7

APPENDIX

7.1 Supporting Information

7.1.1 Theory, Instructions, and Photo Demonstrations

Figure 7-1.The photos of some proposed test units and accessories for the catalytic ethynylation process. The trial-tested autoclave reactor was equipped with a digital temperature controller and a pneumatic agitator for the catalytic performance test of Reppe ethynylation (left). The rotameters control the acetylene gas flow rate (middle). The overhead mechanical stirrer to agitate the reaction mixture (right).

Self-prepared Formaldehyde Solutions with Varied Buffer, Methonal, and Paraformaldehyde

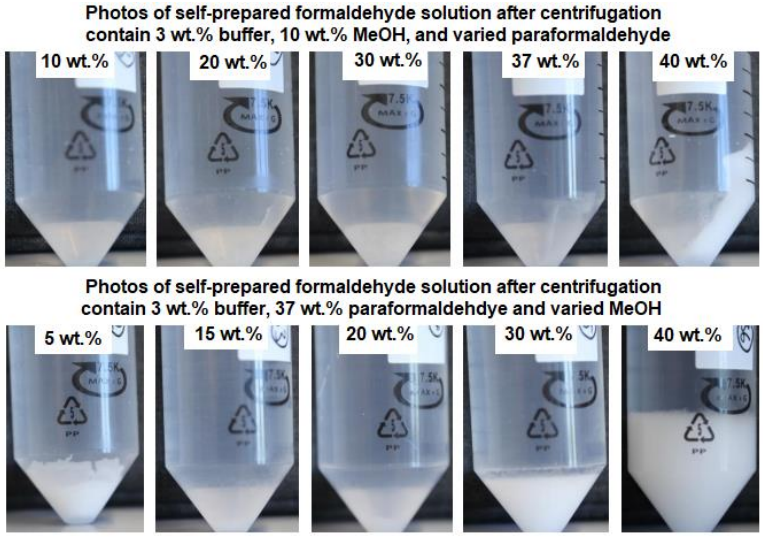

Figure 7-2. The photo of self-prepared formaldehyde solutions of 3 wt.% buffer, 10 wt.% methanol, and varied paraformaldehyde of 10, 20, 30, 37, and 40 wt.% (top); and 3 wt.% buffer, 37 wt.% paraformaldehyde and varied methanol of 5, 15, 20, 30, and 40 wt.% (bottom).

Gas Chromatography – Selection and Installation of GC Accessaries [204, 208-213]

(a)

(b)

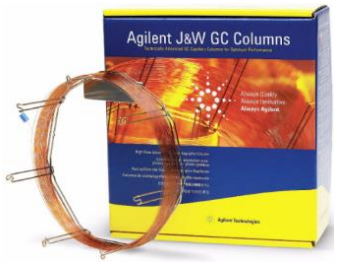

(c)

(d)

Figure 7-3. (a) Agilent 6890N Liquid Gas Chromatography for the quantitative analysis of formaldehyde, 1,4-butynediol, and the other components in the mixture solution of the catalytic Reppe ethynylation process. The GC contains two detectors, TCD and FID. It is equipped with Agilent 7683 Automatic Liquid Sampler, Split/Splitless G 1530N Injector, and Electronic Pneumatics Controller. It is monitored by the built-in control panel and Agilent Chemstation Software from a PC. (b) Agilent J&W CP-Sil 5 CB for Formaldehyde Columns. (c) Agilent Gold Standard Syringe (10 µL) with a specially designed end, which can be attached to the Agilent 7683 Automatic Liquid Sampler. (d) Agilent split inlet liner of 4 mm inner diameter, 6.25 mm outer diameter, and 78.5 mm length with a total volume of 870 µL. It contains a single taper LPD and glass wool that undergoes standard deactivation.

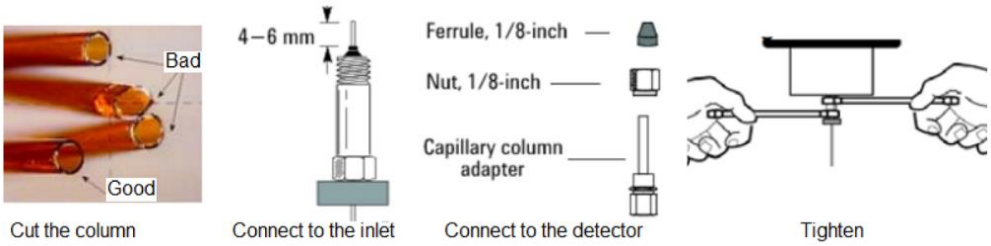

Figure 7-4. The photos of the conditions of column cutting and the demonstration of the column installation are in the installation manual. The instructions shown in the figure are specifically for the connection of the column to the split/splitless inlet of one end and the TCD detectors of the other end.

Troubleshooting and Repairing of the GC-TCD [214-216]

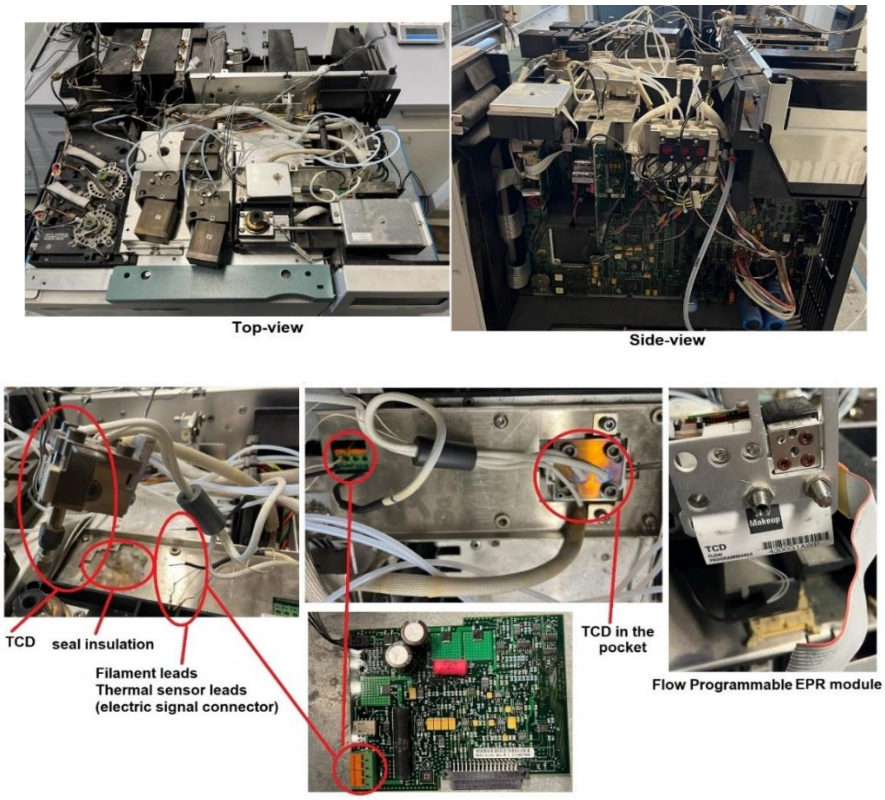

Figure 7-5. Troubleshooting and replacement of the GC-TCD. The top view and the side view of the GC device after removing the protection covers (top). The replacement of the TCD and the coupled EPC, reconnection of the filament and temperature sensor leads, and printed circuit board (PCB).

Adsorption Isotherms

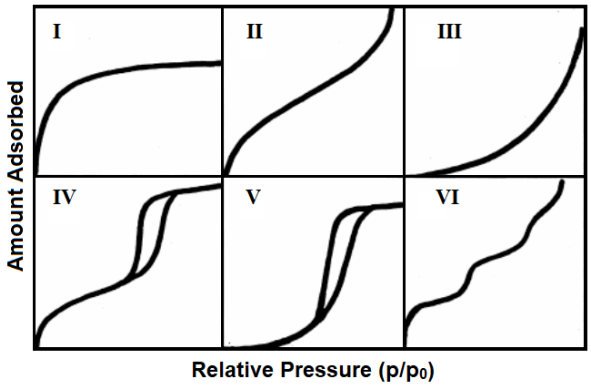

Figure 7-6. Adsorption Isotherms for Gas by IUPAC Classification. Type I is microporous; Type II is non-porous or macroporous; Type III is non-porous or microporous with weak adsorbent-adsorbate interaction; Type IV is mesoporous; Type V is Type III with pore-filling; Type VI is layer-by-layer sorption on uniform non-porous surface.

7.1.2 Qualitative and Quantitative Analysis of Formaldehyde

Formaldehyde Identification by Acid-Base Titration with Sodium Sulfite

The iodometric back-titration is a well-known method that involves the addition of a known amount of excess iodine into the alkaline FA solution to oxidize formaldehyde into formate($HCOO^-$)/sodium formate. The remaining iodine in the solution is quantified by titrating against sodium thiosulfate, using starch as the indicator. This allows the calculation of the amount of iodine that reacts with formaldehyde in the redox reaction, as shown in Scheme 7-1, thereby determining the concentration of the FA solution.

This method is not successful with both the self-prepared and commercial FA solutions. The reason proposed is that both FA solutions contain approximately 10-15 wt.% methanol as the stabilizer (refer to Chapter 1.1.3 and Scheme 1-4). Iodine may also react with methanol to form methyl iodide (CH_3I), thus affecting the determination of formaldehyde.

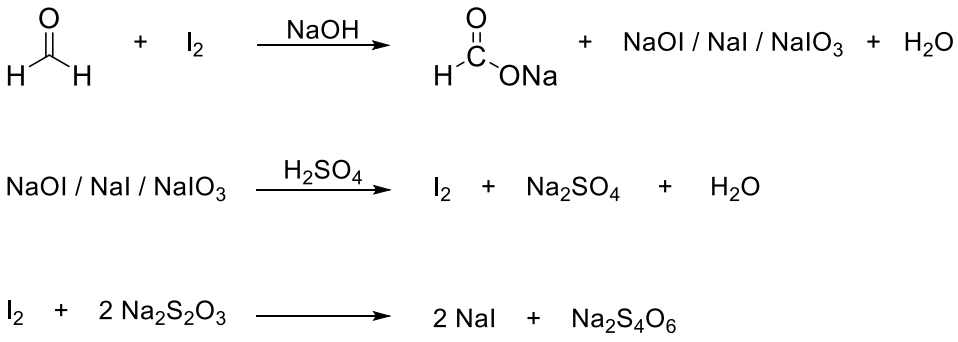

Scheme 7-1. The chemical reactions of the iodometric (redox) back-titration against sodium thiosulfate using starch as an indicator to determine the concentration of FA solution.

Formaldehyde Identification by Acid-Base Titration with Sodium Sulfite

The acid-base titration with sodium sulfite, on the other hand, generates sodium hydroxide in the FA solution, which can be titrated against a standard solution of sulfuric acid to identify the concentration of formaldehyde. The reaction equation is shown in Scheme 7-2.

This method is successful once in identifying a commercial formalin solution with 40.46 wt.% (± 2.2%) and a self-prepared saturated FA solution with 38.76 wt.% (± 0.8). The detailed calculations are shown in Equation 7-1. However, there is still a theoretical limitation as the FA solutions contain pH-buffer species that are required in the ethynylation process, which partially resist the change when a small amount of acid and base is added, hence creating a significant titration error.

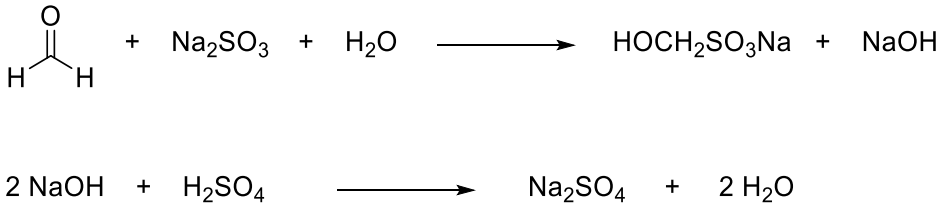

Scheme 7-2. The chemical reactions of the acid-base titration with sodium sulfite against standard sulfuric acid to determine the concentration of FA solution.

The procedures for the acid-base titration are shown as follows:

- *Taken 25 mL of diluted commercial formalin solution of self-prepared FA solution at 3 g/100 mL.*
- *Titrate against 0.10525 M H_2SO_4 solution.*
- *The Stoichiometry ratio of H_2SO_4 to HCHO (NaOH) is 1:2.*

$$c(HCHO) = \frac{V(H_2SO_4) * c(H_2SO_4) * 2 * M(HCHO)}{c(HCHO) * V(HCHO)}$$

Equation 7-1. The calculation to determine the concentration of formaldehyde by acid-base titration method with sodium sulfite against standard sulfuric acid, according to the chemical reactions shown in Scheme 7-2. In the equation, *c* is the concentration in *mol/L*, *V* is the volume in *mL*, *n* is the mole in *mol*, and *M* is the molar mass in *g/mol*.

<u>^{1}H-NMR Spectroscopy References of Ethynylation Components</u>

Titration methods cannot provide reliable results, and it is time-consuming. Hence, the Nuclear Magnetic Resonance (^{1}H-NMR) spectroscopy method is tested, as shown in Figure 7-7. It is, again, challenging to integrate and calculate quantitatively due to the complexity of the components. The self-prepared, pH-buffered, saturated aqueous formaldehyde solution contains 10-12 wt.% methanol as a stabilizer, 3-4 wt.% of sodium hydroxide-sodium dihydrogen phosphate as a pH buffer system. It is also believed that, due to the high formaldehyde concentration, many of its by-products formed in equilibria, like methylene glycol and trioxane, as shown in Scheme 1-4, are present.

It can be observed from the spectrum that a complex group of formaldehyde-derived species, water, and CD_3CN deuterated solvent is present, which makes the quantification challenging. The single species that are present in the ethynylation samples, such as BYD, MeOH, and PDO (IS), are also analyzed by NMR as references.

(a) Self-prepared, pH-buffered, saturated aqueous formaldehyde

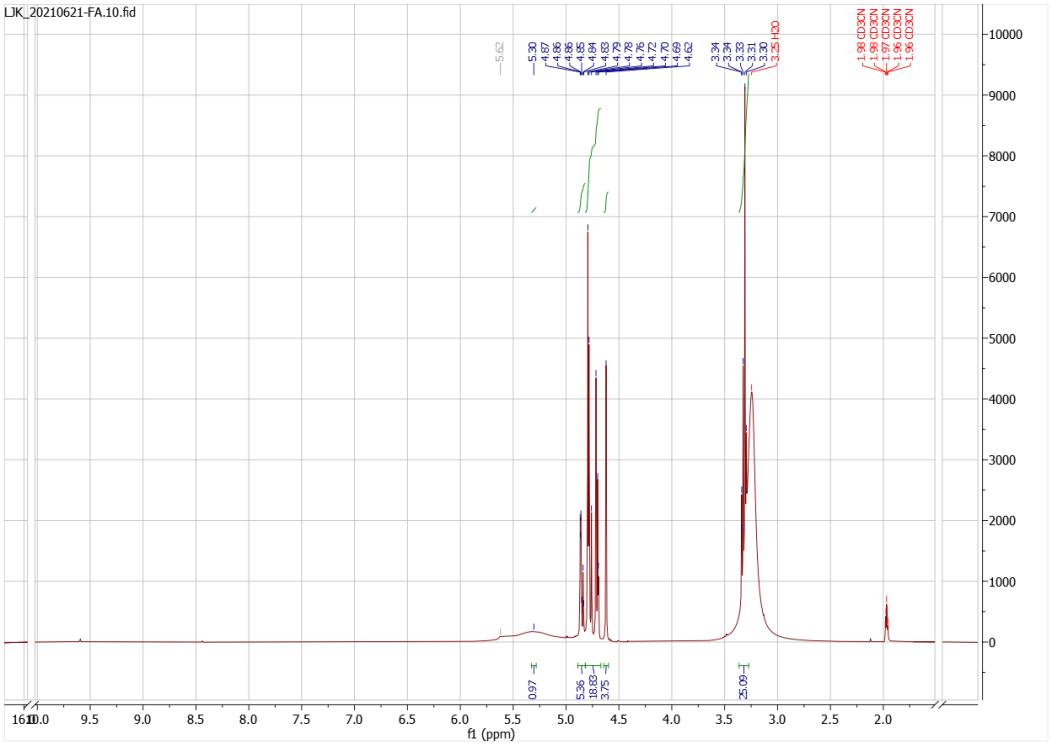

(b) an actual sample from ethynylation that contains all components

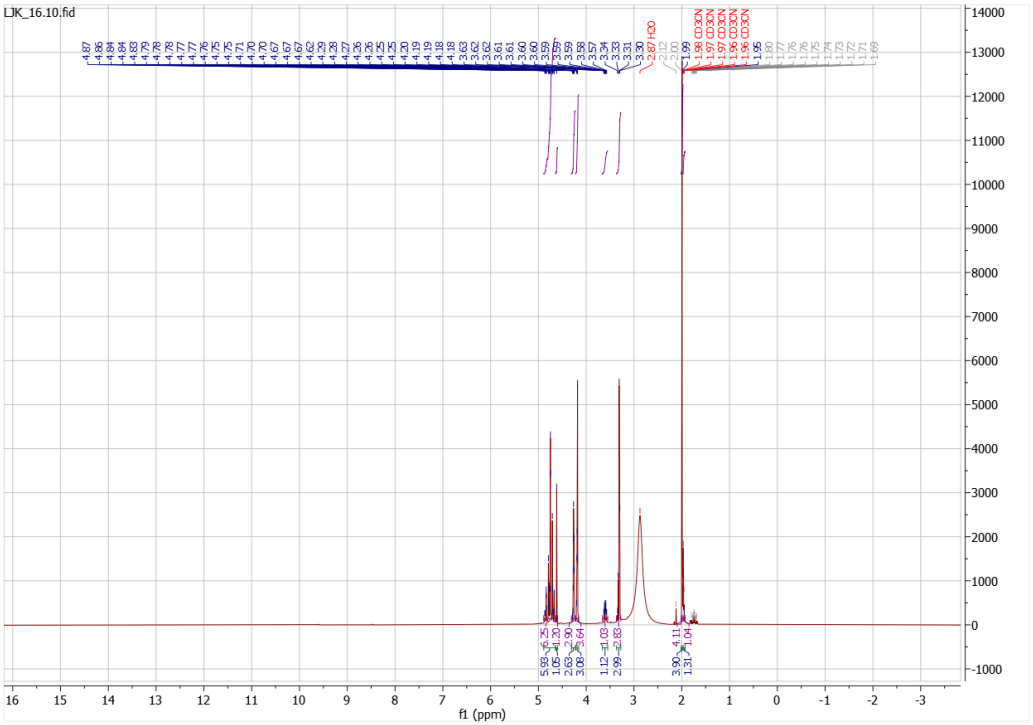

(c) BYD

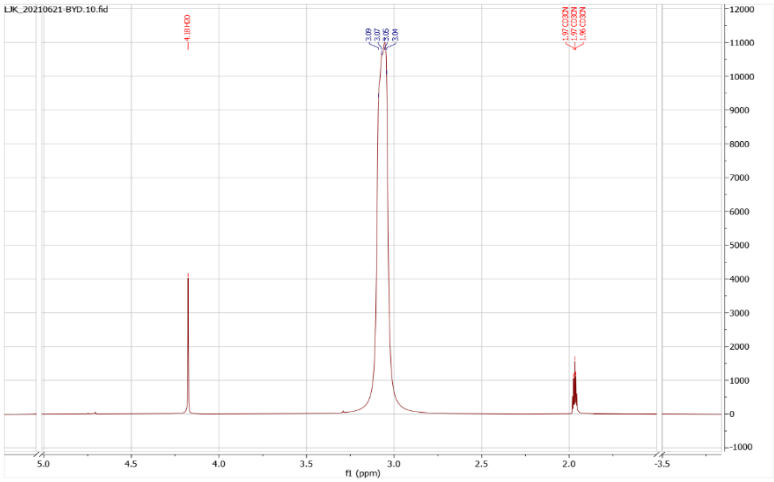

(d) MeOH

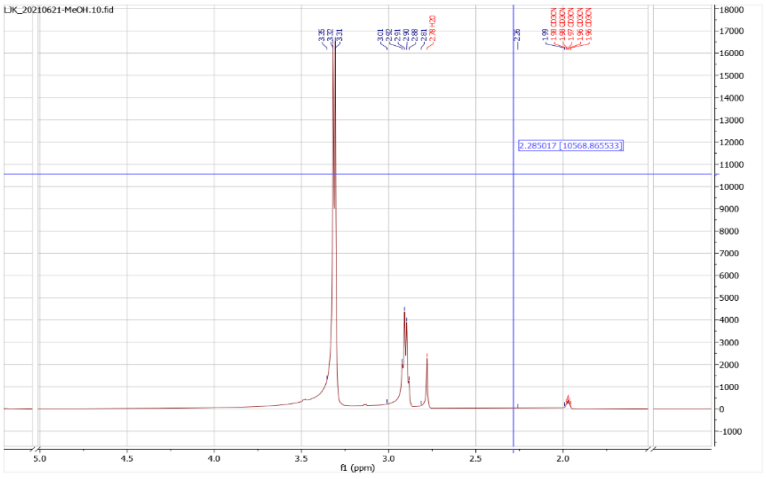

(e) PDO (IS)

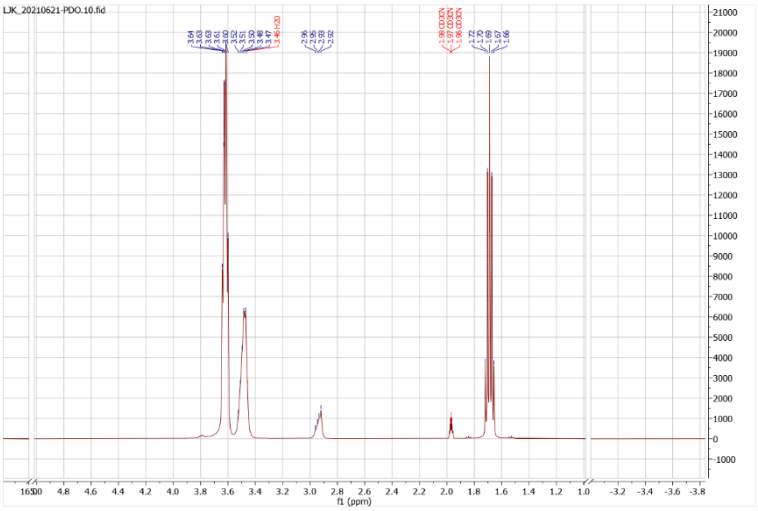

Figure 7-7. The ^{1}H-NMR spectroscopy of (a) self-prepared, pH-buffered, saturated aqueous formaldehyde containing 10-12 wt.% methanol as a stabilizer, 3-4 wt.% of sodium hydroxide-sodium dihydrogen phosphate as a pH buffer system; (b) an actual sample from ethynylation that contains all components; (c) a reference of BYD; (d) a reference MeOH, and (e) a reference of PDO (IS). Acetonitrile-d3 (CD_3CN) is used as the deuterated NMR solvent.

7.1.3 GC Troubleshooting and Analysis for Formaldehyde

Development of GC method

FA has low sensitivity and easily interacts with the column's stationary phase. It is unlikely to be separated from water by GC analysis (FID and TCD detectors) due to their similar properties.

New technologies were developed based on the GC method to identify formaldehyde. One is the installation of a new detector, like the multiple pulsed-discharge photoionization detectors (PDPIDs) [203]. However, an upgrade of the entire GC system and the corresponding gas supply is required since three PDPIDs need to be installed, and each is connected to helium, argon, and krypton gas flow for the successful measurement. Another is the installation of the Polyarc system, which acts as a microreactor [217], coupled with an FID and an ultra-inert line. It catalytically converts organic compounds into methane for analysis. It is also challenging to differentiate the mixture of formaldehyde-derived phases.

The practical possibility is the Agilent J&W CP-Sil 5 CB column, which is optimized for the analysis of formaldehyde, water, and methanol. The column is composed of 100% non-polar dimethylpolysiloxane as the stationary phase, which resists interaction with the reactive FA and separates the analytes based on volatility instead of boiling points and polarities, making it highly sensitive and efficient. The detailed specifications and the configurations of the GC-TCD, the GC column, and the GC program are shown in Chapter 5.3.4.

Calibration of GC-TCD

Regular and periodic GC-TCD calibration of each analyte is necessary to maintain reliable and accurate measurements. GC-TCD detector depends on the thermal conductivity of the respective analytes. The calibration correlates the analytical data in the area under the chromatogram curves to the amount of analyte in concentration at the specific retention time (t_R). t_R is defined experimentally. The conversion from the signal area to the concentration is calculated with respect to a defined internal standard (IS). IS must be chemically inert in the desired reactions that have similar but significantly different properties, like volatility and boiling points of the targeted analytes, to avoid overlapping signals. The slopes of the calibrations indicate the signal area-to-concentration correlations of the analytes.

In Reppe ethynylation, the targeted analytes are FA and BYD. The BYD calibration is shown in Figure 7-8, with Equation 7-2 demonstrating their linear correlations. The pure BYD is dissolved in water at the desired concentrations with the addition of 3 wt.% PDO as IS.

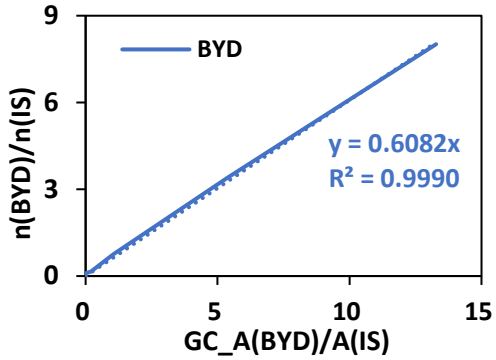

Figure 7-8. The GC-TCD calibration curve for BYD from 0.5% to 50% in yield according to the ethynylation process. The plot is the ratio of the concentration of BYD to IS against the ratio of the GC signal areas of BYD to IS.

$$\frac{n_{BYD}}{n_{IS}} = m * \frac{A_{BYD}}{A_{IS}} + c$$

Equation 7-2. The equation is used to determine the slope of the calibration curve of the analyte (e.g., BYD) and to calculate the unknown concentration of the analyte based on the defined slope and internal standard (IS) of the GC-TCD analysis. *n* is concentration in mol; *m* is the slope of the calibration curve; *A* is the area of the GC signal; and *c* is the interception point to the y-axis.

Calibration for FA Solutions

Calibration of the standard 37 wt.% FA solution is performed. Unfortunately, it is not successful, as shown in Table 7-1, with poor accuracy; in Figure 7-9, poor reproducibility and no relations can be found; and in Figure 7-10, with several errors and mistakes in the GC chromatograms. Hence, troubleshooting is carried out.

Table 7-1. The theoretical concentration of the FA solutions and the calculated concentration based on the GC-TCD measurements during the troubleshooting of GC-TCD calibration for FA solutions. (1). The reproducibility of the GC-TCD measurements of a standard 37 wt.% FA solution; (2). The reproducibility of the GC-TCD measurements of a diluted FA solution from different saturated FA stock solutions.

(1)	***Theoretical [wt.%]***	***GC-TCD Measurement [wt.%]***					
	37.0	*42.0*	*33.6*	*21.0*	*32.5*	*36.1*	*35.9*
(2)	***Theoretical [wt.%]***	*8.00*	*8.00*	*8.75*	*9.00*	*9.00*	*9.25*
	Measurement 1 [wt.%]	*17.1*	*14.4*	*13.2*	*14.2*	*11.8*	*20.0*
	Measurement 2 [wt.%]	*13.8*	*11.6*	*10.5*	*11.2*	*9.5*	*16.0*

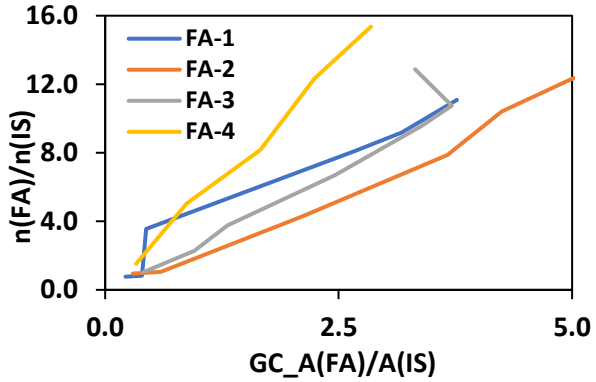

Figure 7-9. The calibration curves of the FA solutions diluted from 1.0 wt.% to 37 wt.% by GC-TCD.

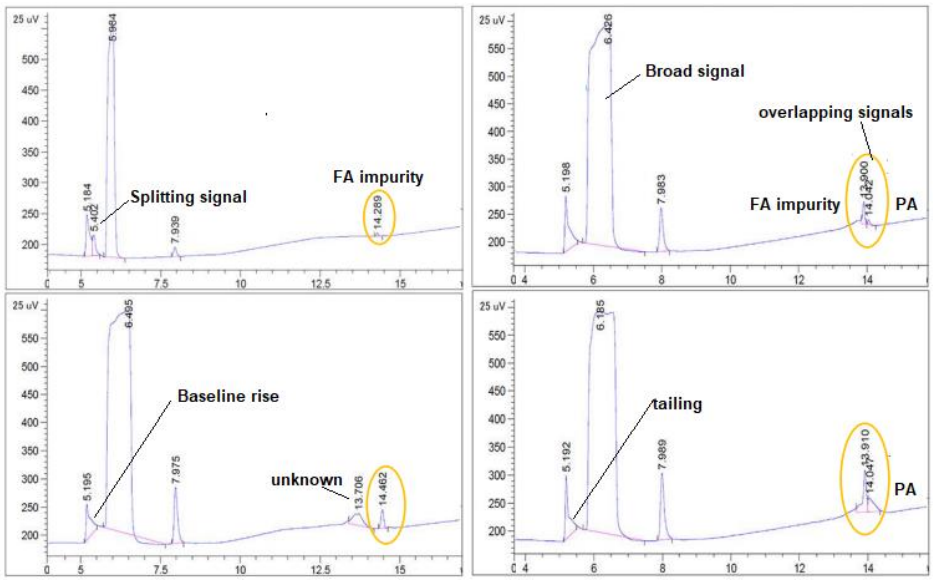

Figure 7-10. The GC-TCD chromatograms after stepwise modifications according to a self-developed DoE technique by changing the GC-TCD analyzing conditions and parameters, such as the temperature, pressure, flow rate, split ratio, etc. (*only a few examples with significant changes are shown*)

Troubleshooting of GC-TCD for Formaldehyde Analysis

Several problems of the GC-TCD analysis have been pointed out. The issues are not only limited to formaldehyde but the entire GC measurement. Luckily, the troubleshooting of GC-TCD and quantitative analysis of formaldehyde are successful. The demonstrations and instructions for selecting appropriate accessories (inlet liner, needle syringe) in Figure 7-3, column installation in Figure 7-4, TCD replacement (detector with coupled electronic, pneumatic controller (EPC), the filament and temperature sensors, and the printed circuit board (PCB)) in Figure 7-5, and analytical conditions and parameters in Table 7-2.

Table 7-2. A list of GC-TCD analyzing conditions and parameters and the appropriate range of the values adjusted according to a series of self-developed DoE techniques.

GC-TCD Parameters and Conditions	***Range***
Inlet Temperature [^{o}C]	*240 [a] – 280 [b]*
Detector Temperature [^{o}C]	*240 – 280*
Oven Starting Temperature [c] [^{o}C]	*40 – 80*
Oven Ending Temperature [^{o}C]	*240 – 280*
Oven Temperature Ramp [K/min]	*0 – 50*
Split ratio [d]	*1 to 20 – 80 [f]*
Inlet Pressure [e] [bar] (Acerage Velocity [cm/s])	*1.10 – 2.25*
Reference flow and makeup gas flow [mL/min]	*10 – 30*

Notes:

a. *BYD has the highest boiling point of 238 °C among all analytes in the samples; the temperature in the inlet and detector has to be higher than its boiling point.*
b. *The maximum temperature of the GC column is 300 °C, and the operation temperature is preferred at about 15 °C lower than the maximum temperature*
c. *The starting temperature in the oven lower than the boiling points of aqueous formaldehyde (93-98 °C) and water (100 °C) improves the signal separation and resolution in the chromatograms; this is because it allows slow vaporization due to their volatilities instead of rapid boiling where they may immerse with each other.*
d. *The split ratio decides the amount of volume of the sample after injection to be directed to the GC column and detector for analysis or discharged to the waste. A sample that is too large for analysis may cause broad signal, signal overlapping, and tailing problems. On the other hand, a sample that is too small may not be enough to be detected due to the detection limits. Additionally, the amount of sample in volume must also fit into the inlet liner (870 µL) to prevent backflash.*
e. *Sufficient inlet pressure is required to allow the sample to be introduced all at once into the GC column to avoid overlapping signals and signal broadening. It is correlated to the average velocity.*
f. *The maximum suggested inlet pressure for the particular GC column. It depends on the column's material, length, inner diameter, and wall thickness. This avoids the pressure built-up that may damage the column or shorten the lifespan.*

7.1.4 Qualitative and Quantitative Analysis of Copper Acetylides

Copper Acetylide-containing Species

Table 7-3. The list of copper acetylide-containing species, their compositions, and atomic ratios in the ethynylation catalyst, as proposed and patented by Kirchner from du Pont in 1972 [160].

No.	Formula	Weight percent copper	Atomic ratios C/Cu	C/H	C/O
1	$Cu_2C_2 \cdot H_2O$	75.2	1.0	1.0	2.0
2	$Cu_2C_2 \cdot C_2H_2 \cdot H_2O$	65.1	2.0	1.0	4.0
3	$Cu_2C_2 \cdot (C_2H_2)_2 \cdot H_2O$	57.5	3.0	1.0	6.0
4	$Cu_2C_2 \cdot (C_2H_2)_3 \cdot H_2O$	51.4	4.0	1.0	8.0
5	$Cu_2C_2 \cdot CH_2O$	70.1	1.5	1.5	3.0
6	$Cu_2C_2 \cdot CH_2O \cdot C_2H_2$	61.3	2.5	1.3	5.0
7	$Cu_2C_2 \cdot (CH_2O)_2 \cdot C_2H_2$	33.6	3.0	1.0	3.0
8	$Cu_2C_2 \cdot (CH_2O)_3 \cdot C_2H_2$	48.3	4.0	1.0	2.3
9	$(CuC_2)_4 \cdot H_2O$	69.0	2.0	4.0	8.0
10	$(CuC_2)_4 \cdot CH_2O \cdot C_2H_2$	62.6	2.8	2.8	11.0
11	$(CuC_2)_4 \cdot CH_2O \cdot C_2H_2 \cdot H_2O$	59.9	2.8	1.8	5.5
12	$(CuC_2)_4 \cdot (CH_2O)_2 \cdot C_2H_2 \cdot H_2O$	56.0	3.0	1.5	4.0
13	$(CuC_2)_4 \cdot (CH_2O)_2 \cdot (C_2H_2)_2 \cdot H_2O$	52.9	3.5	1.4	4.7
14	$(CuC_2)_4 \cdot (CH_2O)_3 \cdot (C_2H_2)_2 \cdot H_2O$	49.8	3.8	1.3	3.8
15	$(CuC_2)_4 \cdot (CH_2O)_4 \cdot (C_2H_2)_2 \cdot H_2O$	47.0	4.0	1.1	3.2
16	$(CuC_2)_4 \cdot (CH_2O)_4 \cdot (C_2H_2)_3 \cdot H_2O$	44.9	4.5	1.1	3.6
17	$(CuC_2)_4 \cdot (CH_2O)_4 \cdot (C_2H_2)_4 \cdot H_2O$	42.9	5.0	1.1	4.0
18	$(CuC_2)_6 \cdot (CH_2O)_{20} \cdot (C_2H_2)_{19} \cdot H_2O$	23.3	11.7	0.9	3.3

The PXRD 2θ Reflexes of Self-determined Cu_2C_2 and Other Species from Database

Table 7-4. The list of typical PXRD 2θ angle reflexes corresponds to the self-determined pure-phase Cu2C2 species and the other relevant species with similar reflexes. The presence of the interfering species that may be present from sources including (i) the activation via ethynylation conditions from CBS catalyst, such as $(BiO)_2CO_3$, $(BiPO_4)H_2O$, and Na_2HPO_4; (ii) incomplete reduction and transformation to Cu_2C_2 or re-oxidation of Cu_2C_2 into CuO and Cu_2O; (iii) incomplete conversion from copper salt precursors, like $CuCl_2$, $CuSO_4$; and (iv) the precipitates on the Cu_2C_2 surface from the ammonia solvent for the direct synthesis, such as NH_3H_2O, NH_4Cl, and $(NH_4)_2SO_4$.

[°]	*PXRD 2θ Angle with Cu-Kα Filter and Reflection Geometry*					
Cu_2C_2	***30.1***	***32.2***	***42.4***	***45.9***	***52.0***	
$(BiO)_2CO_3$	*30.0*	*32.8*	*42.0*	*46.8*	*52.2*	
$(BiPO_4)H_2O$	*29.5*	*31.3*	*41.8*			*20.0, 37.8, 41.8, 48.7*
Na_2HPO_4		*31.9*				*23.1, 32.8*
$Cu_3(PO_4)_23H_2O$	*29.6*	*31.4*				
Cu_2O	*29.8*		*42.6*			*36.6*
CuO		*32.4*				*35.5, 38.8, 53.8, 58.4*
$CuCl_2$	*29.6*		*41.7*	*45.8*	*52.4*	*27.4, 34.4, 50.0, 58.0*
$CuSO_4$				*46.2*	*51.6*	*25.1, 34.2, 36.2*
NH_3H_2O	*30.7*	*31.6*	*42.0*	*46.0*		*25.0, 26.9, 28.0*
NH_4Cl		*32.7*		*46.3*		*27.0, 38.9, 56.4*
$(NH_4)_2SO_4$	*29.5*					*33.5, 35.7, 38.8, 41.4*

Angular Conversion between 2θ Degrees and Scattering Vector |Q| [218]

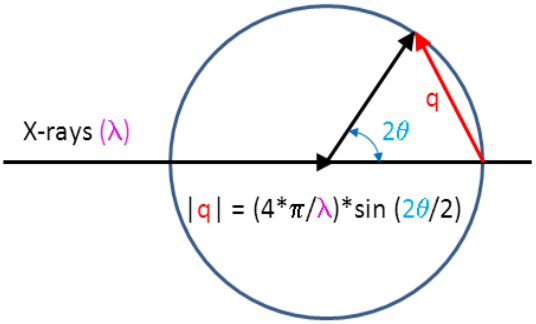

Figure 7-11. The angular conversion between the scattering between the scattering vector, |Q|, and the 2θ angle degrees from XRD measurement with respect to the radiation wavelength, λ, of Debye-Scherrer geometry and Bragg-Brentano geometry.

Identification of Cu_2C_2 by XRD

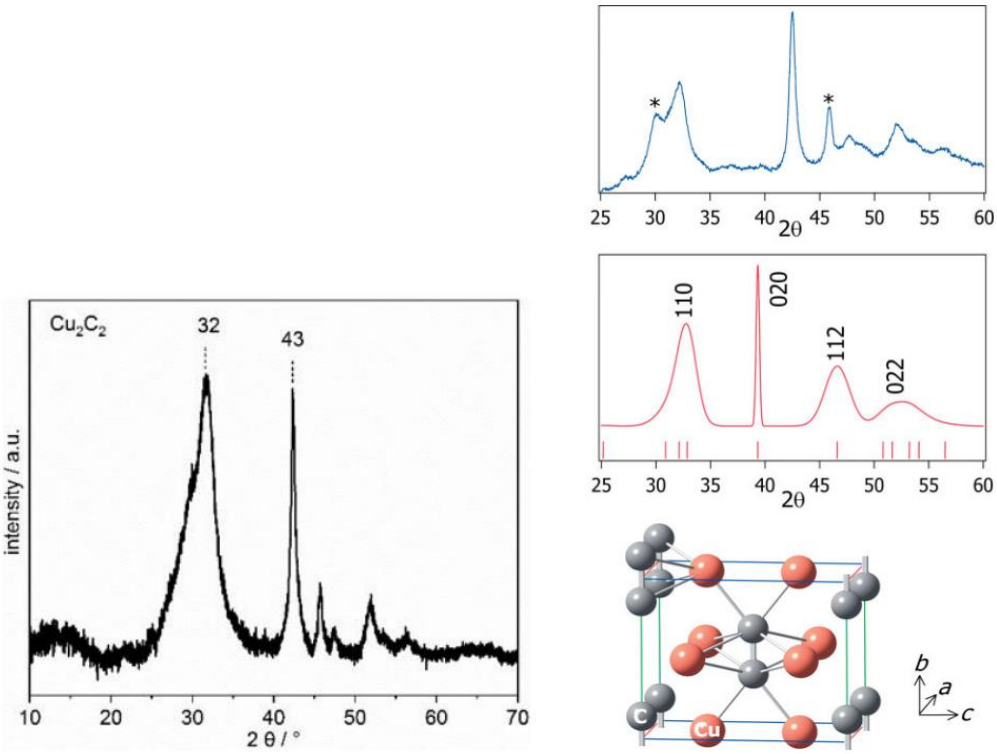

Figure 7-12. Left: The XRD diffractogram of Cu_2C_2 with the most characteristic reflexes at 2θ = 32° and 43° was published by *Bruhm et al.* [159].
Right: The crystal structure of Cu_2C_2-containing nanowire was analyzed by PXRD (top), and the XRD diffractogram simulated from DFT calculations (bottom), as well as the simulated structure (right), reported by *Judai et al.* [162, 174].

Identification of Cu_2C_2 by Raman Spectroscopy

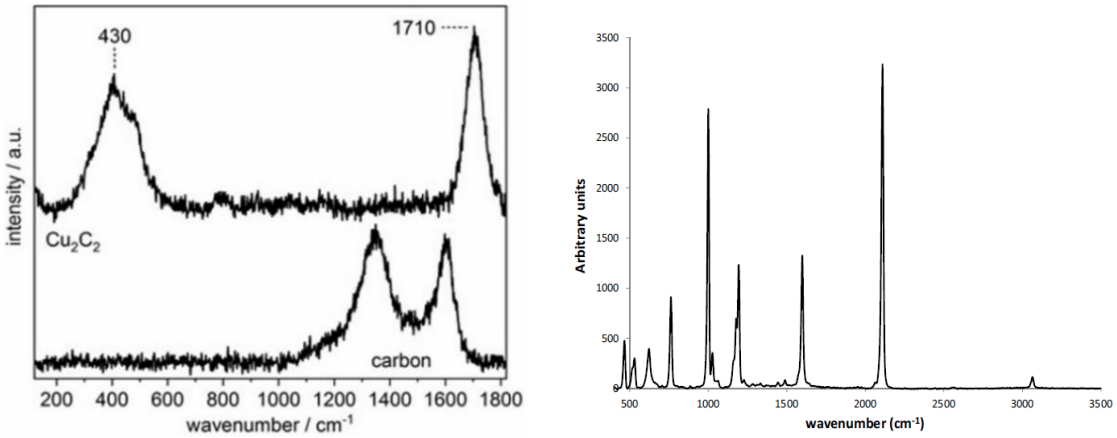

Figure 7-13. Left: The reference Raman signals of Cu_2C_2 at a wavenumber of 430 cm^{-1} and 1710 cm^{-1} and compared to the signals of carbon were published by *Bruhm et al.* [159].
Right: The Raman spectroscopy of phenylacetylene was published by *Oxley et al.* [133].

ICP-OES Analysis of Copper(II) Content

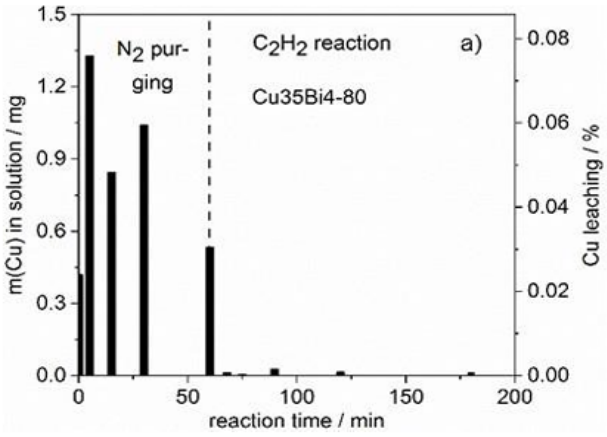

Figure 7-14. The ICP-OES analysis of copper(II) content in the formaldehyde solution for ethynylation process under N_2 and C_2H_2 atmosphere.

Thermal Analysis of Cu_2C_2-containing Species by TGA/DSC-MS

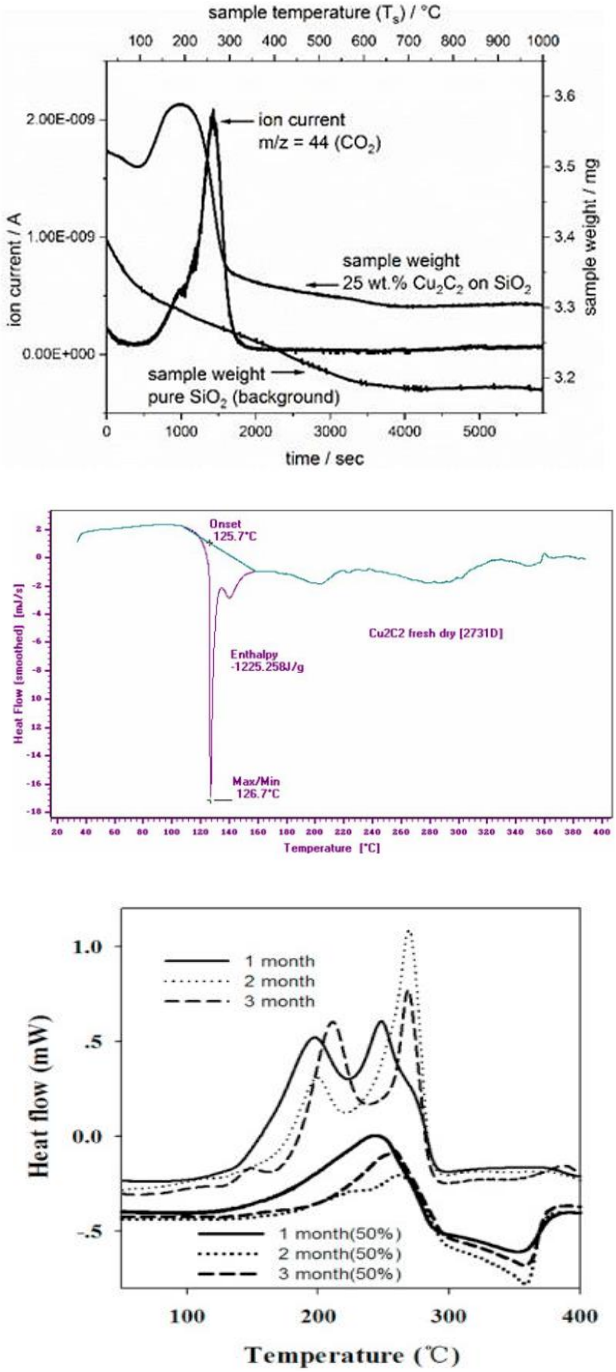

Figure 7-15. The references to TG-MS signals of Cu_2C_2-containing spent catalyst sample after ethynylation and a pure SiO_2-support were published by Bruhm et al. [159] (top), and the reference to the DSC signal of fresh-prepared Cu_2C_2 was published by Cataldo et al. [169] (middle) and of spent catalyst by Sun *et al.* [205] (bottom).

7.1.5 Supporting Analytical Data and Evaluation

Leaching Study by ICP-OES

After evaporation Dissolved in H_3PO_4

Figure 7-16. The sample preparation for ICP-OES analysis of the copper leaching in the solution after ethynylation. The defined amount of the solution is added to the tube; it has to be burnt on fire to remove the organic contents; the residue is then redissolved in the concentration acids and lastly diluted and filtered to the desired concentration.

$$pH\ 5: \quad 0.084\ ppm \times 10mL \times 150 = 0.126\ mg \qquad \frac{0.126\ mg}{35\ \% \times 1.90\ g} \times 100\% = 0.0189\%$$

$$pH\ 8: \quad 0.200\ ppm \times 10mL \times 150 = 0.300\ mg \qquad \frac{0.300\ mg}{35\ \% \times 1.90\ g} \times 100\% = 0.0451\%$$

Equation 7-3. The calculation from the ICP-OES analytical results in ppm to mg and % of the copper content in the sample solution (10 mL), with a dilution factor of 150. 1.90 g of CBS catalyst with 35 wt.% copper is used in 75 mL FA solution at pH 5 and pH 8 in the reaction.

Two ICP-OES devices are employed in this work, and each has its advantages and limitations.

The first device has excellent sensitivity to detect the concentration at the ppb level but not higher than 50 ppm. It is especially sensitive to Na, which may burn vigorously and interfere with the detection of the other components. In the ethynylation sample, a significant amount of Na is present as the buffer species. Diluting the sample based on the Na concentration may cause a concentration of the other target species to be too low. It also requires the samples to be free of organic solvents and have an acidity of about 5%. The ethynylation sample contains FA, MeOH, PA, and BYD with boiling points for PA at 115 °C, IS at 210 °C, and BYD at 238 °C. The sample has to be boiled to evaporate all the organic contents and re-dissolve the remaining residues that contain the metal salts in concentrated acids, as shown in Figure 7-16. The amount of acid and dilution factor has to be calculated carefully to meet the required acidity and concentration for analysis. Many sources of errors may happen during the preparation.

Another device does not have these requirements for samples that allow organic content and have no upper limit in concentrations. However, its sensitivity is up to 2 ppm. This can be critical and not helpful in analyzing the ethynylation samples that have concentrations below 2 ppm.

TPR Investigation of the Role of Bismuth Species

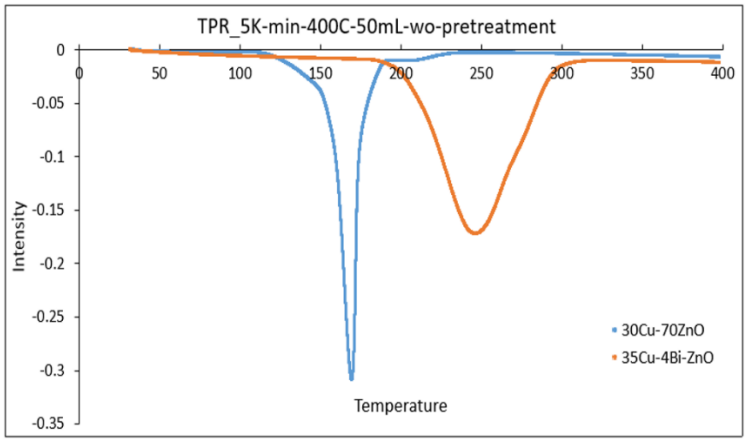

Figure 7-17. The temperature profile of Temperature-Programmed Reduction (TPR) for CuO-ZnO (30 wt.% CuO and 70 wt.% ZnO) and CuO-Bi_2O_3-ZnO (30 wt.% Cu, 4 wt.% Bi) pre-catalyst as a side proof of the bismuth role in the ethynylation catalyst, which prevent over-reduction of Cu^{2+} into CuO.

X-ray Diffractograms of the Interfering Species as the Reference

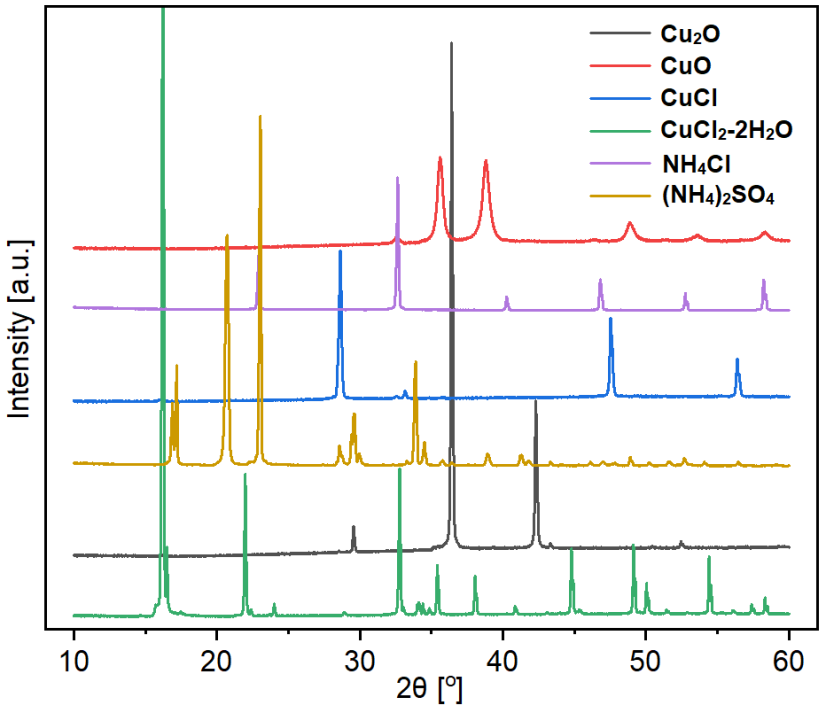

Figure 7-18. The XRD diffractograms of the chemicals used as precursors may be formed during the direct synthesis of the pure-phase cuprous acetylide species, which may interfere with the XRD analysis as the reference.

Phase Identification on Cuprous-Acetylide Cu_2C_2 Species by PXRD

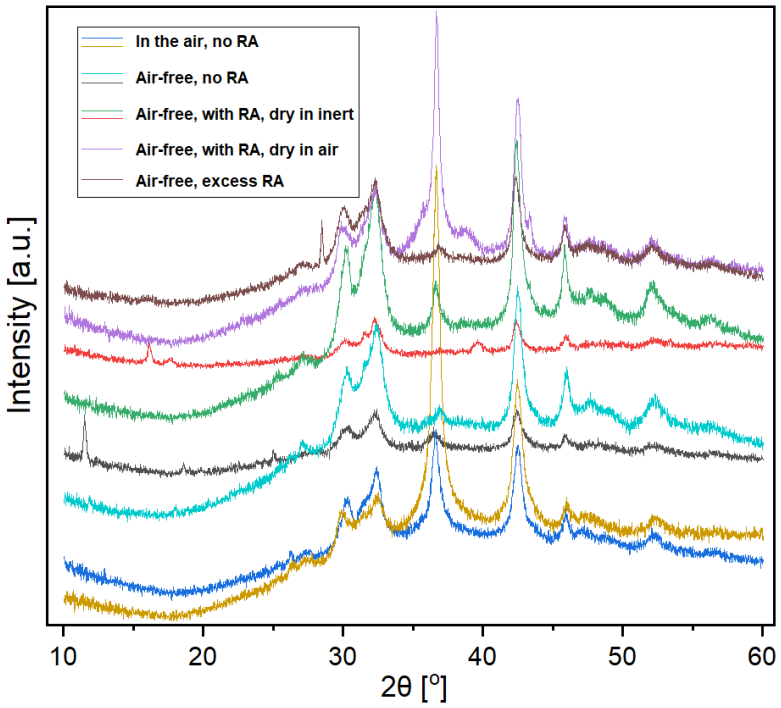

Figure 7-19. The PXRD diffractograms of various synthesis pathways to produce Cu_2C_2 species. The direct precipitated pure-phase cuprous acetylide samples were prepared under various conditions with and without air and reducing agents, as the supplementary for Figure 3-9.

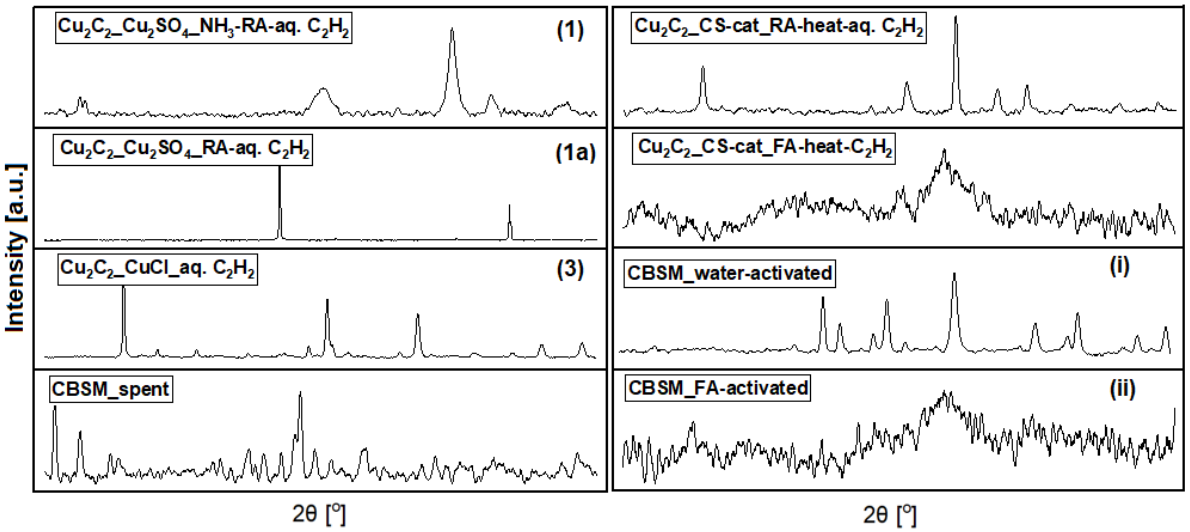

Figure 7-20. The PXRD diffractograms of various synthesis pathways to produce Cu_2C_2 species. The CBSM pre-catalysts activated in water, in formaldehyde solution, and after a complete catalytic ethynylation process; the CS pre-catalysts heated in dissolved acetylene water with reducing agent (RA) or with FA solution as RA; and CuCl as copper(I) source and $CuSO_4$ as copper(II) source to transfer in dissolved acetylene water directly or with RA and ammonia solution, respectively.

7.2 List of Publications and Conference Contributions

55. Jahrestreffen Deutscher Katalytiker_Weimar, Germany, 27 – 29 June, 2022

Deposition Precipitation of Copper Acetylide Cu_2C_2 as Catalyst for the Ethynylation of Formaldehyde to 1,4-Butynediol

- Lingdi Kong, Franz Bannert, Klaus Köhler

15th European Congress on Catalysis_Prague, Czech Republic, 27 August – 01 September, 2023

Genesis of Cuprous Acetylide Cu_2C_2 as Active Species for Reppe Ethynylation of Formaldehyde

- Lingdi Kong, Franz Bannert, Klaus Köhler, Andreas Reitzmann, Roman Bobka, Dennis Beierlein

57. Jahrestreffen Deutscher Katalytiker_Weimar, Germany, 13 – 15 March, 2024

Genesis of Catalytically Active Cuprous Acetylide in Ethynylation: The Importance of Formaldehyde

- *Lingdi Kong, Klaus Köhler, Dennis Beierlein, Frank Großmann*

18th International Congress on Catalysis_Lyon, France, 14 – 19 July, 2024

Genesis of Catalytically Active Cuprous Acetylide in Ethynylation: The Importance of Formaldehyde

- Lingdi Kong, Klaus Köhler, Dennis Beierlein